UNIVERSITÉ DE LILLE

ÉCOLE DOCTORALE BIOLOGIE-SANTE DE LILLE (ED446)

Année : 2022

THÈSE

Pour l'obtention du grade de
DOCTEUR DE L'UNIVERSITÉ DE LILLE
Spécialité : Neuroscience

Présentée par
Hamza BENDERRADJI

Uncovering the role of Tau protein in the regulation of glucose homeostasis

Soutenue publiquement le 16 septembre 2022 devant le Jury composé de :

Présidente du Jury :
Madame le Professeur Anne Muhr-Tailleux

Rapporteurs :
Monsieur le Docteur Bertrand Blondeau
Monsieur le Professeur Emmanuel Planel

Examinateurs :
Monsieur le Docteur Luc Buée
Madame le Docteur Stephanie Bombois

Membre invitée :
Madame le Docteur Julie Dumont

Directeur de thèse :
Monsieur le Docteur David Blum

Remerciements

Je tiens tout d'abord à remercier les différents membres de mon jury, le **Dr. Luc Buée,** le **Pr. Anne Muhr-Tailleux**, le **Dr. Stephanie Bombois,** et le **Dr. Julie Dumont** pour l'honneur qu'ils m'ont fait d'accepter de faire partie de mon jury de thèse et d'examiner ce travail. Je remercie en particulier le **Dr. Bertrand Blondeau** et le **Dr. Emmanuel Planel** d'avoir accepté de faire partie de mon comité de suivi de thèse, de lire avec minutie mon manuscrit de thèse et d'évaluer le travail effectué durant ces trois années de thèse de science.

Je tiens à remercier également la **Société Francophone du Diabète (SFD)** et l'**Inserm** d'avoir financé ma thèse de science.

Je tiens ensuite naturellement à remercier le **Dr. Luc Buée** pour m'avoir accueilli au sein de son équipe « Alzheimer & Tauopathies » et du centre de recherche « Lille Neurosciences et cognition » dès mon Master 2. Je vous remercie de m'avoir soutenu tout au long de ce parcours, d'avoir été disponible malgré vos responsabilités croissantes au fil des années, et de m'avoir apporté votre soutien pour développer des travaux de recherche originaux avec une approche translationelle en neuroendocrinologie conciliant la clinique et la recherche fondamentale. Merci pour tous les bons moments passés dans votre équipe !

J'adresse un immense merci à mon directeur de thèse le **Dr. David Blum**. Je me souviens encore du premier entretien que j'ai passé avec toi. Ça a été la porte qui m'a fait découvrir la recherche fondamentale. Tout a été fluide et simple avec toi depuis le début. Tu as vu en moi un vrai professionnel dès le départ, pas seulement le jeune interne débutant la recherche que j'étais. Tes conseils ont toujours été pertinents. Tu arrives systématiquement à relever le positif du travail qui a été fait, malgré toutes les difficultés et les imprévus impactant le bon déroulement du projet. Outre ta présence scientifique, tu as aussi su me soutenir dans les moments de doute. Le domaine de la recherche est un monde complexe, mais en peu de temps tu m'as transmis toute la passion que tu développes au quotidien. Ce fut un réel plaisir de réaliser ces quatre années de recherche avec toi. Grâce à ton aide et tes précieux conseils, j'ai pu décrocher sans trop de difficultés plusieurs bourses. En plus de tes qualités humaines, tu es toujours disponible, physiquement ou par mail, si bien qu'on sait qu'on peut toujours compter sur toi. Chaque année à tes côtés a apporté son lot de leçons et de découvertes. Mes travaux de publication sont le fruit de tout ce que j'ai appris à tes côtés et de mon immersion dans le monde de la recherche fondamentale.

Je voudrais communiquer ma gratitude aux **Pr. Didier Vieau**, au **Dr. Jean-Sébastien Annicotte**, au **Dr. Kadiombo Bantubungi-Blum**, au **Dr. Nicolas Sergeant**, au **Dr. Paolo Giacobini**, au **Pr. Claude-Alain Maurage**, au **Dr. Vincent Prévot**, et au **Pr. Pascal Pigny**. Bien que constamment sollicités, vos disponibilités, par mail ou de vive voix, vos conseils, scientifiques ou autres, m'ont permis de progresser au jour le jour. Merci encore **Paolo** et **Nicolas**, vous étiez parmi les rares personnes à croire à mes hypothèses. Grace à votre soutien, j'ai pu finaliser le travail sur le rôle de l'Hormone Anti-Müllerienne chez l'homme, et ce dernier a été valorisé par une publication dans la célèbre revue « The Journal of Clinical Endocrinology and Metabolism ».

Un grand merci à mes maîtres, **Pr. Wemeau**, **Pr. Fontaine**, **Pr. Vantyghem** et **Pr. Vambergue**, qui dès le début de mon internat m'ont toujours poussé à atteindre l'excellence grâce à leur expertise inestimable. Merci encore **Pr. Vantyghem**, vous m'avez toujours poussé à sortir de mes retranchements pour donner le meilleur de moi-même. En plus de vos qualités humaines, vous êtes toujours disponible, physiquement ou par mail, si bien qu'on sait qu'on peut toujours compter sur vous.

A ma première chef de clinique le **Dr. Clara Leroy**, merci pour ta formation excellente, tes précieux conseils, ta rigueur qui sont un exemple pour moi, mais surtout ta gentillesse et ta patience. Tu m'as fait découvrir et aimer l'Andrologie, et c'est grâce à ton aide que j'ai pu valider le DESC d'andrologie. Je suis content qu'on ait pu développer plusieurs projets de recherche originaux.

Un grand merci aux **Dr. Christine Cortet** et **Dr. Emilie Merlen**. Vous m'avez formé et donné l'occasion de développer des projets de recherche dans le domaine de la pathologie hypothalamo-hypophysaire. Un premier projet d'une grande utilité dans la pratique clinique a pu voir le jour et a été publié récemment dans la revue « Clinical Endocrinology ».

A l'ensemble de l'équipe du service d'Endocrinologie, Diabétologie et Maladies du métabolisme à Lille : **Dr. Claire Douillard**, **Dr. Christine Do Cao**, **Dr. Christine Cortet**, **Dr. Emilie Merlen**, **Dr. Florence Baudoux**, **Dr. Wassila Karrouz**, **Dr. Catherine Cardot Bauters**, **Dr. Stéphanie Espiard**, de l'équipe du service d'Andrologie : **Dr. Jean-Marc Rigot**, **Dr. Julie Prasivoravong**, **Dr. François Marcelli, Pr. Arnauld Villers** et encore une fois **Clara Leroy**, et aussi à l'équipe du service de gynécologie endocrinienne et médecine de la reproduction : **Pr. Sophie Catteau-Jonard**, **Dr. Maryse Leroy-Billiard**, **Dr. Christine Decanther**, et **Dr. Geoffroy Robin**. Vous m'avez tout appris sans jamais compter votre temps. Travailler avec vous fut un honneur et un plaisir.

Je ne pourrai jamais assez remercier **Kevin Carvalho**, qui m'a beaucoup aidé et m'a encadré depuis mes premiers jours au laboratoire. Par tes qualités humaines, scientifiques et techniques, tu as su me pousser à donner le meilleur de moi-même et à pouvoir surmonter les difficultés du monde de la recherche fondamentale. Je suis très content pour les dernières bonnes nouvelles. Avec ton bon cœur tu mérites le meilleur.

Merci au **Dr. Valérie Buée-Scherrer** pour avoir pris le temps de m'expliquer les techniques de biochimie, de m'avoir aidé à résoudre certaines difficultés techniques, et surtout pour sa bonne humeur quotidienne.

Je tiens à adresser mes remerciements au **Dr. Malika Hamdane**, merci à toi pour les remarques pertinentes lors de la préparation des oraux de bourses et aussi ta disponibilité et ton aide pour résoudre certaines difficultés techniques.

A l'UMR-S 1172 et en particulier aux équipes « Alzheimer et Tauopathies » et « Développement et plasticité du cerveau neuroendocrine ».

L'environnement scientifique de qualité et la constante émulation intellectuelle ont beaucoup contribué à rendre ma présence au centre très enrichissante.

Merci pour votre collaboration, votre formation, votre encadrement pendant ces quatre années de M2R et de thèse d'Université. J'adresse une salve de remerciements à **Sabiha Eddarkaoui**, **Émilie Faivre**, **Raphaelle Caillierez**, **Émilie Caron**, **Nour El Houda Mimouni**, **Sebastien Carrier**, **Victoria Gomez**, **Coline Leghay**, **Florent Sauvé**, et **Jhen**, pour leur gentillesse et leur aide tout au long du projet. Sans vous il aurait été difficile d'achever ce travail, grâce à votre expertise et vos conseils, nous y sommes parvenus !

J'adresse ensuite mes sincères remerciements à **Anna Bogdanova** pour m'avoir aidé lors des croisements et du suivi d'animaux à l'animalerie, surtout pendant les poussées d'asthme allergique !

Je tiens à remercier **Emilie Crouty**, **Laure Rolland, Florine Bornaque** et **Cyril Bourouh** pour m'avoir aidé à finaliser les expériences animales ainsi que les analyses in-vivo.

Je remercie l'ensemble du personnel des animaleries EOPS1 et EOPS2, tout particulièrement **Mélanie**.

Un grand merci au **Dr. Bruno Lefebvre** et au **Dr. Anne-Laure Barbotin**, pour leurs

qualités humaines, leur disponibilité chaque fois que cela a été nécessaire et pour m'avoir permis d'amorcer le développement de projets de recherche ambitieux.

Une dédicace particulière à **Antonino** et **Meryem**, qui ont découvert le monde secret du spermatozoïde en m'aidant dans mes travaux sur la plateforme de microscopie, et surtout à mes co-Thésards ou ex- co-Thésards **Thibaut**, **Agathe**, **Marine, Elodie, Thomas, Sarra, Sarah, Antoine, Marie**: au top, tout simplement. Toujours contents, motivés, disponibles !

Merci au personnel administratif du centre de recherche « Lille Neurosciences et Cognition », et je pense particulièrement à **Céline** pour ta disponibilité, ton écoute et tes précieux conseils.

Je souhaite également remercier tout particulièrement les **Pr. Jacques Young, Pr. Gerald Raverot, Pr. Hervé Lefebvre, Pr. Yves Reznik et Pr. Frederic Castinetti** d'être des PU-PH formidables et captivants, j'ai beaucoup appris à travers votre enseignement et si je suis ici aujourd'hui, vous y êtes probablement pour beaucoup.

Enfin, cette expérience en recherche fondamentale aura été avant tout une très belle aventure humaine. J'y ai rencontré des personnes formidables parmi les autres Doctorants, Post-Doctorants et Ingénieurs. Merci du fond du cœur à ces personnes, pour avoir partagé mes peines et mes joies.

A mon père, j'espère que tu es fier de moi, de là-haut où tu veilles sur moi, tu me manques tous les jours et particulièrement ce jour.

A ma mère, merci pour tous tes sacrifices et ton soutien depuis le tout début.

A ma grand-mère, tu me manques énormément. C'est très dur de te voir s'éteindre progressivement à cause de la maladie d'Alzheimer.

A toute ma famille, mes frères et sœurs, mes oncles et tantes, mes cousins et cousines, qui me disent souvent combien ils sont fiers de mon parcours.

A tous mes amis, il faudrait une Thèse entière pour à peine survoler tous les moments heureux auxquels vous avez contribués et qui ont enrichi ma vie. Merci pour votre gentillesse, votre présence, votre simplicité.

Particulièrement à ma fille chérie Leïla, mon plus beau cadeau, tous les jours pouvoir t'aimer et te voir grandir est ma plus grande fierté.

Enfin, à ma femme, ma chère Samira, merci pour ton soutien. Tu as changé ma vie et tu sais bien tout l'amour que j'ai pour toi.

Résumé

Tau est une protéine associée au microtubule, bien caractérisée pour son rôle dans le trafic neuronal. Ses modifications (hyperphosphorylation, agrégation) sont impliquées dans la physiopathologie de la Maladie d'Alzheimer (MA). En effet, une altération de l'homéostasie glucidique est connue pour augmenter le risque de MA. Cependant, il a été rapporté que des lésions de MA pourraient favoriser l'émergence de perturbations de l'homéostasie glucidique.

Une étude du laboratoire a montré que les souris tau-knock-out (tau KO) présentaient des altérations de l'homéostasie glucidique. Inversement, la surexpression neuronale d'une protéine tau humaine mutée a été associée à une meilleure tolérance au glucose. Néanmoins, les liens entre la perte de fonction de tau et l'homéostasie du glucose restent flous.

Dans ce contexte, le premier objectif de ma thèse de science est d'évaluer le phénotype métabolique d'un modèle original de souris tau Knock-in (KI) exprimant, sous le contrôle du promoteur tau murin, une protéine tau humaine mutée. Ce modèle de souris a permis d'évaluer l'impact de l'expression d'une protéine tau dysfonctionnelle à un niveau physiologique, dans les mêmes tissus que la protéine tau native, sans biais de surexpression. Bien que les souris tau KI sous un régime contrôle ne présentent pas de troubles métaboliques significatifs, les évaluations métaboliques ont révélé qu'uniquement les animaux tau KI mâles nourris par un régime riche en graisses (HFD) présentaient une intolérance au glucose, une augmentation de la prise alimentaire, et de la masse pondérale par rapport aux témoins.

De plus, des îlots isolés de souris tau KI et tau KO présentaient une altération de la sécrétion d'insuline en réponse à une stimulation par du glucose, un effet reproduit par la réduction de l'expression de tau dans une lignée de cellules β pancréatiques à l'aide d'un tau siRNA. Sur la base de ces données, la perte de fonction de tau est associée à une altération de l'homéostasie du glucose, qui correspond au phénotype métabolique observé chez les souris tau KO. Cependant, deux mécanismes mutuellement non exclusifs pourraient expliquer les altérations

métaboliques observées chez les souris tau KO et tau KI : tau pourrait contrôler la régulation périphérique du glucose via une action centrale, en particulier hypothalamique ; ou bien, elle pourrait contrôler directement la fonction de la cellule ß pancréatique.

Le deuxième objectif de mon projet thèse est donc de comprendre la base de la régulation de l'homéostasie glucidique par tau en étudiant les mécanismes centraux et périphériques. Pour atteindre cet objectif, une souris transgénique innovante tau floxée combinée avec différents modèles/virus exprimant la CRE recombinase, a été caractérisée et utilisée. La caractérisation initiale a révélé une réduction de l'expression de tau dans les souris tau flox homozygotes en l'absence de CRE. Nous avons donc utilisé des animaux tau flox hétérozygotes qui ont été combinés avec des approches CRE pour réduire l'expression de tau dans l'hypothalamus médiobasal (cKO-Tau^{hyp}) ou les cellules ß pancréatiques (cKO-Tau$^{\beta}$).

Dans ces modèles, un phénotypage métabolique complet a été réalisé sous un régime contrôle et un HFD. Sous les deux régimes, les animaux cKO-Tau^{hyp} présentaient des altérations métaboliques importantes en comparaison aux animaux témoins. La délétion conditionnelle de tau chez les cKO-Tau$^{\beta}$ n'a toutefois pas été associée à l'apparition d'altérations métaboliques significatives.

En résumé, malgré certaines limites, mon projet de thèse souligne que la perte de fonction de tau favorise le développement de perturbations de l'homéostasie glucidique et aussi l'altération du fonctionnement des cellules ß, fournissant ainsi de nouvelles informations sur le rôle physiologique de tau dans le contrôle du métabolisme périphérique en agissant dans les cellules ß pancréatiques et l'hypothalamus.

Mots clés : Hypothalamus, pancréas, tau, homéostasie glucidique, et modèles murins.

Abstract

Tau is a microtubule-associated protein that plays a role in neuronal trafficking. Its dysfunctions (hyperphosphorylation, aggregation) have been involved in Alzheimer's Disease pathophysiology. Indeed, impaired glucose homeostasis was suggested to increase AD risk and a pathological loss of tau function. However, AD lesions were also suggested to favor the emergence of glucose homeostasis alterations. A study from the laboratory showed that constitutive tau knock-out (tau KO) mice exhibited glucose homeostasis impairments, characterized by hyperinsulinemia and impaired glucose tolerance. Conversely, neuronal overexpression of a human mutated tau protein was associated with improved glucose tolerance. Nonetheless, the links between tau loss of function and glucose homeostasis remain unclear. Tau is largely considered as a neuronal protein but is also expressed by other tissues, particularly pancreatic ß-cells. But again, its peripheral functions have been overlooked.

In this context, the first aim of my PhD was to evaluate the metabolic phenotype of an original knock-in (KI) mice model expressing a human tau protein bearing a mutation, under the control of the murine tau promoter. This mouse model allowed us to evaluate the impact of expressing dysfunctional tau proteins at a physiological level, in the same tissues than native tau protein, without any bias of overexpression. Metabolic investigations revealed that, while under chow diet tau KI mice do not exhibit significant metabolic impairments, male but not female tau KI animals under High-Fat Diet (HFD) exhibited higher insulinemia as well as glucose intolerance, increased food intake, and body weight gain as compared to control littermates. Further, isolated islets from tau KI but also KO mice exhibited impaired glucose-stimulated insulin secretion (GSIS), an effect recapitulated by tau knockdown in a β pancreatic cell line using tau siRNA. Based on these data, tau loss of function is associated with impaired glucose homeostasis, which fits with the initial metabolic phenotype observed in tau KO mice.

However, two mutually non-exclusive mechanisms could explain the metabolic alterations observed in both tau KO and tau KI mice: tau impacts peripheral glucose homeostasis by a central-based regulation possibly involving the hypothalamus; or, in non-mutually manner, tau regulates ß-cell function in the pancreas.

The second main goal of my project was therefore to understand the basis of glucose homeostasis regulation by tau by investigating central (hypothalamus) and peripheral (pancreatic) mechanisms. To achieve this objective, an innovative transgenic tau floxed mice combined with different models/virus expressing CRE recombinase, was characterized and used. Our data revealed a hypomorphic status of homozygous tau flox mice in the absence of CRE. We thus used heterozygous tau flox animals that were combined with CRE approaches to knock-down tau from the mediobasal hypothalamus (cKO-Tau^{hyp}) or pancreatic ß-cells (cKO-Tau$^{\beta}$ animals). In these models, complete metabolic phenotyping was carried out under chow diet and HFD. Under both diets, cKO-Tau^{hyp} animals exhibited significant metabolic impairments vs. controls. However, the conditional deletion of tau in cKO-Tau$^{\beta}$ animals using tamoxifen was not associated significant metabolic impairments.

In summary, despite some limitations of the different approaches used, my project thesis highlights that tau loss of function favors the development of glucose homeostasis impairments and also pancreatic ß-cell dysfunction, supporting not only a role of central tau pathology in the development of metabolic disturbances in AD patients but also providing new insights on the physiological role of tau in the control of peripheral metabolism by acting in pancreatic ß-cell and the hypothalamus.

Keywords : Hypothalamus, pancreas, tau, glucose homeostasis, and mouse models.

Index

List of Abbreviations

AD: Alzheimer disease

Akt : *Protein kinase B*

ARC: arcuate nucleus

AgRP: Agouti-related peptide

DNA: Deoxyribonucleic acid

FTLD: Frontotemporal lobar degeneration

GFAP: Glial fibrillary acidic protein

GFP: Green Fluorescent Protein

GLP-1: Glucagon-like peptide 1

GnRH: Gonadotropin-Releasing Hormone

GSIS: Glucose-stimulated insulin secretion

GSK3β: glycogen synthase kinase 3 β

GWAS: Genome-Wide Association Study

IR: Insulin receptor

IRS-1/2: insulin receptor substrate 1/2

IPGTT Intraperitoneal glucose tolerance test

MAP: Microtubule-associated protein

MAPT: Microtubule-associated protein tau

NPY: Neuropeptide Y

OGTT: Oral glucose tolerance test

POMC: Pro-opiomelanocortin

PI3K: Phosphatidylinositol-3-kinases

PIP2: Phosphatidylinositol 4,5-bisphosphate

PIP: Phosphatidylinositol (3,4,5)-trisphosphate

PTEN: phosphatase and tensin homolog

PDK1: 3-phosphoinositide-dependent protein kinase-1

RNA: Ribonucleic Acid

rRNA: ribosomal Ribonucleic Acid

shRNA: Short Hairpin Ribonucleic Acid

siRNA: small interfering Ribonucleic Acid

T2DM: Type 2 diabetes mellitus

UTR: Untranslated Region

List of figures

List of tables

Vue d’ensemble sur le projet de thèse

Compte tenu du vieillissement de la population notamment dans les pays développés, un nombre croissant de patients âgés développent l’association diabète et troubles cognitifs. Le diabète de type 2 est le type le plus prévalent de diabète, il s’agit d’un trouble métabolique favorisé par une mauvaise hygiène de vie et sous-tendu par une prédisposition génétique. L'OMS considère le diabète comme un sérieux problème de santé publique. La Fédération internationale du diabète (FID) estime que dans le monde 463 millions d'adultes vivaient avec le diabète en 2019 et que ce nombre a plus que triplé au cours des deux dernières décennies (Organisation mondiale de la santé, 2019). Le diabète de type 2 est une maladie métabolique complexe caractérisée par une hyperglycémie chronique liée à une résistance périphérique à l'insuline et à une altération de la sécrétion d'insuline par les cellules β pancréatiques (Tomic et al., 2022).

Parallèlement, la prévalence de la démence, toutes étiologies confondues, augmente de manière exponentielle avec l'âge et représente un problème majeur de santé publique. Elle est estimée entre 2 et 5 % chez les 65-74 ans et atteint 30 à 40 % chez les plus de 85 ans. Encore une fois, les projections suggèrent que le nombre total de patients diagnostiqués dans le monde devrait augmenter massivement de 24 millions (2001) à 74,7 millions en 2030 (Herrera et al., 2016).

Un nombre croissant d'études indiquent que les patients adultes atteints de diabète de type 2 sont entre 1,5 et 3 fois plus susceptibles de développer une démence de type Alzheimer (risque relatif (RR) : 1,5 ; IC à 95 % : [1,2-1,8]) ou une démence vasculaire (RR : 2,5 ; IC à 95 % : [2,1-3]). En cumulant les risques liés au diabète et aux troubles cognitifs, ces patients présentent un risque particulièrement accru de mortalité, de perte d’autonomie et d'institutionnalisation dès qu'ils progressent en âge. Ces effets indésirables résultent non seulement de l'impact négatif de chacune de

ces pathologies sur l'autre, mais aussi des interactions entre elles et leurs traitements respectifs (Sue Kirkman et al., 2012).

A l'heure actuelle, plusieurs équipes de recherche travaillent sur les mécanismes moléculaires associant ces deux maladies. Un certain nombre d'études précliniques sur des modèles d'animaux transgéniques ont suggéré que le diabète pourrait aggraver les lésions pathologiques cérébrales de la maladie d'Alzheimer. Il a été rapporté que les souris diabétiques présentaient des altérations morphologiques et moléculaires similaires à celles des modèles murins développant spontanément des troubles neurodégénératifs (Ernst et al., 2013; Ramos-Rodriguez et al., 2013). De plus, un modèle murin de vieillissement accéléré (SAMP8), nourri avec un régime riche en graisses diabétogène, a développé des modifications cérébrales semblables à celles observées dans la maladie d'Alzheimer, notamment une augmentation du taux de protéines tau hyperphosphorylées, des dépôts amyloïdes ainsi que des déficits d'apprentissage et de mémoire, par rapport au groupe d'animaux nourris avec un régime contrôle (Mehla et al., 2014). En outre, il a été rapporté que des souris transgéniques APP, qui développent spontanément des troubles neurodégénératifs de type Alzheimer, une fois nourries avec un régime riche en graisses, ces dernières ont développé rapidement des troubles de la mémoire, associés à des lésions pathologiques cérébrales (Maesako et al., 2012). D'autres équipes ont rapporté aussi des résultats similaires (Hiltunen et al., 2012; Ho et al., 2004; Kohjima et al., 2010).

Il est particulièrement intéressant de noter qu'en plus du déficit cognitif, il a été rapporté que les patients atteints de la maladie d'Alzheimer présentaient une altération de l'homéostasie glucidique (Bucht et al., 1983; Calsolaro and Edison, 2016; Craft et al., 1992, 1998; Fujisawa et al., 1991; Matsuzaki et al., 2010a; Tortelli et al., 2017). De plus, il a été rapporté que l'hyperglycémie et l'hyperinsulinémie sont positivement corrélées aux lésions pathologiques cérébrales de la maladie d'Alzheimer (Matsuzaki et al., 2010a). En effet, l'hyperglycémie, même sans développement de diabète, représente un facteur de risque du déclin cognitif et de la maladie d'Alzheimer (Crane et al., 2013; Kim et al., 2022; Zhang et al., 2022). Dans une étude observationnelle prospective avec un

suivi médian de 6,8 ans, 524 participants ont développé une démence, dont 74 avec diabète. En effet, chez les participants non diabétiques, des taux moyens de glycémie plus élevés au cours des 5 années précédentes étaient significativement associés à un risque accru de développement de troubles cognitifs (Crane et al., 2013). Une autre étude a suggéré que la maladie d'Alzheimer pourrait augmenter le risque de développer une intolérance au glucose ou un diabète (Janson et al., 2004). Dans cette dernière étude, un suivi moyen à long terme de 10 ans a été réalisé dans une cohorte de 100 personnes atteintes de la maladie d'Alzheimer et 138 sujets témoins. Tous les participants n'avaient pas de diabète ou d'intolérance au glucose au début de l'étude. De manière intéressante, la prévalence du diabète (35 % contre 18 % ; $P < 0,05$) et de l'intolérance au glucose à jeun (46 % contre 24 % ; $P < 0,01$) étaient significativement plus élevée chez les patients atteints de la maladie d'Alzheimer que chez les sujets témoins. En accord avec la dernière étude, des données non publiées de la cohorte nationale prospective BALTAZAR (NCT01315639), dont notre laboratoire est partenaire, indiquent que la glycémie des patients atteints d'une maladie d'Alzheimer est significativement plus élevée que celle des individus du même âge atteints de troubles cognitifs légers, alors qu'aucune différence n'a été observée en ce qui concerne le diabète ou la dyslipidémie.

En outre, de nombreuses études sur des modèles murins transgéniques ont suggéré que la susceptibilité de troubles neurodégénératifs semblables à ceux d'une maladie d'Alzheimer pourrait augmenter le risque d'apparition des altérations métaboliques. En fait, une susceptibilité accrue à l'apparition de troubles métaboliques caractérisés par une glycémie à jeun élevée, une intolérance au glucose lors du test de tolérance au glucose et un gain de masse corporelle induit par l'alimentation ont été observés dans un modèle murin transgénique APP/PS1 nourri avec un régime riche en graisses par rapport aux animaux témoins non transgéniques (Mody et al., 2011; Ruiz et al., 2016). Des manifestations proches ont été rapportées chez des souris APP/PS1 obtenues suite à un croisement sur un fond génétique de souris présentant un déficit partiel en récepteur de leptine (db/+). Ces animaux ont développé une intolérance au glucose, une résistance périphérique à l'insuline et une altération de la signalisation de l'insuline par rapport aux souris db/+ développées sur fond de type

sauvage (Jiménez-Palomares et al., 2012). Des observations proches ont été également rapportées par une autre équipe (Takeda et al., 2010).

Tau est une protéine associée aux microtubules bien décrite pour jouer un rôle dans le trafic neuronal. Son dysfonctionnement (hyperphosphorylation, agrégation) est largement impliqué dans la physiopathologie de la maladie d'Alzheimer ainsi que d'autres démences (Sergeant et al., 2008a). Actuellement, tau est connue pour exercer plusieurs fonctions, au niveau neuronal, telles qu'au niveau des synapses et des noyaux par exemple (Sotiropoulos et al., 2017), mais malgré les progrès récents, les fonctions physiologiques de tau dans les neurones restent largement inconnues.

De plus, bien que la protéine Tau soit largement considérée comme une protéine neuronale, elle est également exprimée par d'autres tissus, notamment les cellules β-des îlots pancréatiques (Martinez-Valbuena et al., 2019a; Miklossy et al., 2010a). Cependant, ses fonctions périphériques ont été négligées. A l'état physiologique, chez l'homme comme chez la souris, tau est exprimée par les cellules β des îlots pancréatiques (Benderradji et al., 2022; Wijesekara et al., 2018a). D'ailleurs, une étude récente montre la présence d'agrégats de tau dans les îlots β pancréatiques de patients atteints d'une maladie d'Alzheimer (Martinez-Valbuena et al., 2021), suggérant ainsi une contribution de cette dernière aux changements métaboliques observés dans la maladie d'Alzheimer.

Les récents résultats du laboratoire d'accueil soulignent clairement que tau régule physiologiquement l'homéostasie périphérique du glucose. En effet, les études pan-génomiques (GWAS) chez l'homme montrent qu'il y a un lien entre l'Haplotype H1 de Tau et les perturbations de l'homéostasie glucidique observées lors d'une hyperglycémie provoquée par voie orale (Marciniak et al., 2017). De manière intéressante dans le modèle murin tau knock-out, la délétion constitutive de tau (Marciniak et al., 2017) favorise l'apparition d'un phénotype de perte de fonction de Tau caractérisé par des altérations de l'homéostasie du glucose à type d'hyperinsulinémie et une hyperglycémie à jeun, ainsi que d'altération de la tolérance au glucose (Marciniak et al., 2017). Il convient de noter que ces observations ont été confirmées ultérieurement par un autre groupe utilisant d'autres souris tau knock-out (Wijesekara et al., 2018a). À l'inverse, dans une autre étude du laboratoire, la surexpression neuronale d'une protéine

tau humaine mutée a été associée à une meilleure tolérance au glucose dans le modèle de souris transgéniques THY-Tau22 par rapport à WT (Leboucher et al., 2019).

Les mécanismes à l'origine de la dérégulation de l'homéostasie glucidique chez les patients atteints de maladie d'Alzheimer sont actuellement inconnus. Cependant, un ensemble convergent de données suggère que tau pourrait jouer un rôle dans de tels changements. Dans la maladie d'Alzheimer, en plus d'une localisation de la pathologie de tau principalement dans l'hippocampe, une accumulation de protéines tau hyperphosphorylées et agrégées a été bien décrite dans l'hypothalamus, une structure cérébrale impliquée dans l'interaction entre le cerveau et les organes périphériques (Gratuze et al., 2018; Ishii and Iadecola, 2015; Vercruysse et al., 2018). Il est toutefois essentiel de mieux comprendre l'origine de ces altérations métaboliques chez les patients atteints d'une maladie d'Alzheimer, d'autant plus que les modifications chroniques de l'homéostasie glucidique sont elles-mêmes susceptibles de favoriser le développement de troubles cognitifs et de lésions d'agrégats de protéines tau. L'ensemble de ces résultats suggèrent qu'une prédisposition à la maladie d'Alzheimer peut favoriser l'apparition d'un diabète. Néanmoins, les liens entre la perte de fonction de la protéine tau et l'homéostasie du glucose restent flous.

L'ensemble de ces données soulèvent l'hypothèse qu'une perte de fonction physiologique de Tau rencontrée dans le système nerveux central, mais aussi dans les îlots pancréatiques des patients atteints de maladie d'Alzheimer est suffisante pour entrainer une altération de l'homéostasie glucidique. Cependant, les mécanismes à l'origine de ces troubles ne sont pas connus.

Dans ce contexte, les principaux objectifs du projet de thèse sont d'une part, 1) d'évaluer l'impact métabolique d'une potentielle perte de fonction de la protéine tau suite à une expression constitutive d'une protéine tau humaine mutée, qui remplace la tau murine dans le modèle tau knock-in, et d'autre part 2) de comprendre les fondements physiologiques (et pathologiques) de la régulation de l'homéostasie du glucose par tau en explorant les mécanismes centraux (hypothalamus) et périphériques (pancréatiques). Afin d'atteindre cet objectif, différentes approches de délétion

conditionnelle ou d'une réduction de l'expression de la protéine tau dans l'hypothalamus médiobasal et dans les îlots pancréatiques ont été adoptées.

A. Évaluation du phénotype métabolique des souris tau knock-in :

Cette partie du projet s'intègre dans la continuité de mon travail durant l'année recherche (Master 2 en 2017/2018). Le modèle tau KiV5 est un modèle original, dont une tau humaine mutée est exprimée de manière physiologique sous le promoteur Mapt murin, à l'inverse des autres modèles murins basés sur la surexpression de transgènes. Il a été conçu par l'insertion, de manière ciblée par KI, dans le locus murin Mapt de l'ADNc humain du gène Mapt codant l'isoforme 1N4R mutée en P301L et étiquetée par un épitope V5 (GKPIPNPLLGLDST ; cet épitope permet de suivre l'expression du transgène) au niveau de l'exon 1 qui comporte le codon d'initiation de la traduction protéique (ATG). Un codon Stop est présent en terminaison du transgène humain. La mutation P301L entraine une perte de l'affinité de Tau pour les microtubules et ainsi favorise une probable perte de fonction.

L'évaluation initiale du phénotype métabolique s'est faite sous la nourriture contrôle de l'animalerie. En revanche, en comparaison aux souris contrôles de la même portée, aucune modification métabolique n'a été observée à l'âge de 5 mois.

Durant ma première année de thèse, j'ai poursuivi l'exploration du phénotype métabolique du modèle tau KiV5. Étant donné que d'après les données de la littérature ainsi que l'expérience du laboratoire, une nourriture riche en graisse (HFD) peut favoriser l'apparition d'un phénotype latent, les animaux tau KiV5 et leurs contrôles de portée (WT) ont été mis sous un régime riche en graisse (Gallou-Kabani et al., 2007). Afin d'évaluer l'existence ou non d'un dimorphisme sexuel, des mâles et des femelles ont été utilisés. De manière intéressante, sous l'effet d'une nourriture HFD, les souris mâles tau KiV5 ont présenté une augmentation de la prise alimentaire, et de la masse pondérale, et ont développé des altérations de l'homéostasie glucidique et de la sécrétion d'insuline au test de

tolérance au glucose, une hyperglycémie après un jeûne prolongé la nuit ainsi qu'une augmentation de l'insulinémie basale à jeun.

En effet, le phénotype d'altérations métaboliques observé sous la nourriture HFD dans le modèle tau KiV5 est similaire à celui observé chez les souris tau KO. Si bien que ces altérations de l'homéostasie du glucose dans les deux modèles murins sont la traduction d'une perte de fonction physiologique de tau. L'ensemble de ces données encourageantes nous ont poussé à aller plus loin dans l'exploration de l'origine des mécanismes physiopathologiques responsables d'une perte de fonction de tau. En effet, les fonctions de l'hypothalamus et de la cellule β pancréatique sont toutes susceptibles d'avoir un impact sur la régulation périphérique de l'homéostasie du glucose. Néanmoins, ces deux modèles murins ont des limites et ne peuvent pas nous guider avec précision vers l'origine des troubles observés.

B. Évaluation de l'impact phénotype métabolique d'une perte de fonction de tau dans l'hypothalamus médiobasal et dans les cellules β des îlots pancréatiques :

C'est ainsi grâce à l'utilisation de différentes approches de délétion conditionnelle ou de réduction de l'expression de la protéine tau dans l'hypothalamus médiobasal et dans les îlots pancréatiques que nous avons pu explorer l'impact métabolique d'une perte de fonction de tau dans l'hypothalamus et les cellules β des îlots pancréatiques.

Dans un premier temps, nous avons réalisé des tests de tolérance au glucose sur des îlots isolés de souris tau KI et tau KO. En effet, ces îlots isolés présentaient une altération de la sécrétion d'insuline en réponse à une stimulation par du glucose, un effet reproduit par la réduction de l'expression de tau dans une lignée de cellules β pancréatiques d'origine murine à l'aide d'un tau siRNA.

Par la suite, et afin de mieux comprendre la base de la régulation de l'homéostasie glucidique par tau en étudiant les mécanismes centraux et périphériques, nous avons caractérisé et utilisé une souris transgénique innovante tau floxée combinée avec différents modèles/virus exprimant la CRE recombinase. La caractérisation initiale a révélé une réduction de l'expression de tau dans les souris tau flox homozygotes en l'absence de CRE. Nous avons donc utilisé des animaux tau flox hétérozygotes qui ont été combinés avec des approches CRE pour réduire l'expression de tau dans l'hypothalamus médiobasal (cKO-Tau^{hyp}) ou les cellules ß pancréatiques (cKO-Tau$^{\beta}$).

Dans ces modèles, un phénotypage métabolique complet a été réalisé sous un régime contrôle et un HFD. Sous les deux régimes, les animaux cKO-Tau^{hyp} présentaient des altérations métaboliques importantes en comparaison aux animaux témoins. La délétion conditionnelle de tau chez les cKO-Tau$^{\beta}$ n'a toutefois pas été associée à l'apparition d'altérations métaboliques significatives.

En résumé, malgré certaines limites, mon projet de thèse souligne que la perte de fonction de tau favorise le développement de perturbations de l'homéostasie glucidique et aussi l'altération du fonctionnement des cellules ß, fournissant ainsi de nouvelles informations sur le rôle physiologique de tau dans le contrôle du métabolisme périphérique en agissant dans les cellules ß pancréatiques et l'hypothalamus.

En plus, nos résultats sont d'une grande importance pour la pratique clinique. En effet, une telle relation mutuelle entre les perturbations de l'homéostasie glucidique et la maladie d'Alzheimer, avec des mécanismes physiopathologiques probablement communs, nécessite un changement des politiques de santé publique en se concentrant davantage sur la prévention primaire des facteurs de risque communs au diabète et à la maladie d'Alzheimer. Il est nécessaire de sensibiliser le grand public au risque de développer ces deux maladies et à l'importance de corriger les facteurs de risque modifiables, tels qu'une alimentation plus saine, une perte de poids et une activité physique régulière. De plus, il est indispensable de réaliser une exploration métabolique incluant au moins une hémoglobine glyquée, une glycémie à jeun et une insulinémie afin de dépister les troubles de

l'homéostasie glucidique, dans le but d'une prise en charge adaptée à un stade pathologique précoce des patients porteurs d'une maladie d'Alzheimer.

Introduction

Introduction

Chapter I: The relationship between Alzheimer's disease and diabetes

In view of the population ageing especially in developed countries, an increasing number of elderly patients presents the specific constellation diabetes and dementia.

Type 2 diabetes mellitus (T2DM) is a common lifestyle disorder which is favorized by a sedentary and unhealthy lifestyle. WHO considers diabetes as a serious public health problem. The International Diabetes Federation (IDF) estimates that 463 million adults were living with diabetes in 2019 worldwide and the number has more than tripled in the last two decades (World Health Organization, 2019). T2DM is a complex metabolic condition characterized by chronic hyperglycemia related to peripheral insulin resistance and impaired insulin secretion by pancreatic β-cells. Furthermore, diabetes is associated with a specific organic complications, and cardiovascular disorders (Tomic et al., 2022).

In non-diabetic individuals with insulin-resistant and normal glucose tolerance states, pancreatic islets usually respond by increasing insulin secretion to maintain normoglycemia, a process termed β cells compensation (Kahn, 2003; Prentki, 2006). In the presence of genetic or acquired factors that make β-cells susceptible, β-cell compensation fails causing a deterioration of β-cells function with a loss of β-cells mass by apoptosis.

At the same time, the prevalence of dementia across all etiologies, increases exponentially with age and represents a major public health problem. It is estimated to be between 2 and 5% among 65-74 years old and reaches 30 to 40% among those over 85 years. Again, projections suggest that the total number of patients diagnosed globally is expected to increase massively from 24 million (2001) to 74.7 million in 2030 (Herrera et al., 2016).

1. The Link between Type 2 Diabetes and Alzheimer's disease:

A growing number of studies indicate that adult patients with type 2 diabetes are between 1.5 and 3 times more likely to develop Alzheimer's dementia (relative risk (RR) 1.5; 95% CI: 1.2-1.8) or vascular dementia [RR: 2.5; 95% CI: 2.1-3]. By combining the risks associated with diabetes and dementia, these patients present a particularly increased risk of mortality, functional dependence and institutionalization as soon as they progress in age. These adverse effects result not only from the negative impact of each of these pathologies on the other, but also from the interactions between them and their respective treatments (Sue Kirkman et al., 2012).

Currently there is an important search for the molecular mechanisms associating these two diseases. A number of preclinic studies in transgenic animal models suggested that diabetes could enhance brain AD pathology. It was reported that Diabetic mice exhibited morphological and molecular alterations similar to neurodegenerative disorders (Ernst et al., 2013; Ramos-Rodriguez et al., 2013). Interestingly, a mouse model of accelerated aging (SAMP8) fed with high fat diet, which induces diabetes, developed brain AD-like modifications including increased hyperphosphorylated tau, amyloidosis, and both learning and memory deficits, compared to the nondiabetic animals group (Mehla et al., 2014). Also, it was reported that APP transgenic AD mice fed with high fat diet exhibited memory impairment and increasing Ab oligomers and plaques in the brain (Maesako et al., 2012). Furthermore, on a diabetic background, AD transgenic mice model shown early onset of AD-like cognitive dysfunction with learning and memory deficits in the accompanied by defective brain insulin signaling and neuroinflammation (Takeda et al., 2010). Diet-induced obesity and insulin resistance supported brain amyloidosis, impaired neuronal insulin signaling, and defective learning and memory performance in the Tg2576 mice model of AD (Hiltunen et al., 2012; Ho et al., 2004; Kohjima et al., 2010).

2. Impaired peripheral glucose homeostasis in Alzheimer's disease:

It is particularly noteworthy that, besides cognitive deficits, AD patients have been reported to exhibit altered glucose metabolism (Bucht et al., 1983; Calsolaro and Edison, 2016; Craft et al., 1998, 1992; Fujisawa et al., 1991; Matsuzaki et al., 2010b; Tortelli et al., 2017). Additionally, it was reported that hyperglycemia and hyperinsulinemia correlate positively with AD pathology (Matsuzaki et al., 2010a). Furthermore, hyperglycemia, even without the development of diabetes, represents a risk factor for memory decline and AD (Crane et al., 2013; Kim et al., 2022; Zhang et al., 2022). In a prospective observational study with a median follow-up of 6.8 years, 524 participants developed dementia, whose 74 with diabetes and 450 without. Among participants without diabetes, higher average glucose levels within the preceding 5 years were related to an increased risk of dementia (Crane et al., 2013). Interestingly, another study reported that AD can increase the risk of developing impaired glucose tolerance or diabetes (Janson et al., 2004). In the former study, an average 10-year long-term follow-up was carried off in a cohort of 100 individuals with AD and 138 controls with AD. Interestingly, both diabetes (35% vs. 18%; $P < 0.05$) and impaired fasting glucose (46% vs. 24%; $P < 0.01$) were significantly more prevalent in patients with AD than in control subjects. In agreement with the last study, unpublished data from the BALTAZAR prospective cohort (NCT01315639), of which our laboratory is a partner, indicates that glycemia from cognitively-impaired AD patients is significantly higher than aged-matched individuals with mild cognitive impairments, while no difference is seen regarding diabetes or dyslipidemia (Table 1).

Furthermore, many studies in transgenic animal models suggested that AD susceptibility may increase metabolic dysfunction. In fact, an increased susceptibility to metabolic impairment characterized by high fasting blood glucose, peripheral glucose intolerance and diet-induced body weight gain was observed in transgenic AD mouse model APP/PS1 fed on high fat diet compared to non-transgenic controls (Mody et al., 2011; Ruiz et al., 2016). Close manifestations were reported in APP/PS1mice on a partially deficient leptin receptor background (db/+). The former animals developed glucose intolerance, insulin resistance and impaired insulin signaling when compared to db/+ mice on wildtype background (Jiménez-Palomares et al., 2012).

	MCI	AD	p
N	552	508	-
Age (year)	77.8 (±5.5)	77.3 (±7.7)	0.18
Gender (% women)	59.2 (327)	56.7 (288)	0.44
MMSE (/30)	26.3 (±2.6)	21.7 (±3.7)	**<0.0001**
Fluency score	17.3 (±7.2)	12.9 (±7.7)	**<0.0001**
Body weight (kg)	67.4 (±14.7)	66.1 (±13.2)	0.16
Size (cm)	163 (±9)	162 (±10)	0.27
Hypertension (%)	47.3 (259)	47.3 (207)	0.99
Diabetes (%)	10.8 (59)	11.2 (49)	0.89
Chlolesterol (mmol/L)	5.51 (±1.17)	5.42 (±1.21)	0.32
Triglycerides (mmol/L)	1.22 (±0.58)	1.27 (±0.63)	0.25
Glycemia (mmol/L)	5.31 (±1.14)	5.56 (±1.77)	**0.01**

Table 1. Increased glycemia in Alzheimer disease patients vs. MCI at baseline in the BALTAZAR cohort (unpublished data).

Abbreviations: AD: Alzheimer disease, MCI: Mild Cognitive Impairments, MMSE: Mini-Mental State Examination

Furthermore, the APP23 transgenic mouse model of AD amyloid pathology crossed with mouse models of diabetes, a leptin deficient ob/ob or a polygenic Nagoya-Shibata-Yasuda, the resulting transgenic mice developed severe hyperglycemia, hyperinsulinemia, glucose intolerance and insulin resistance and compared to APP23 or diabetic models alone (Takeda et al., 2010). In the former study, impaired insulin signaling in skeletal muscle and liver was also observed.

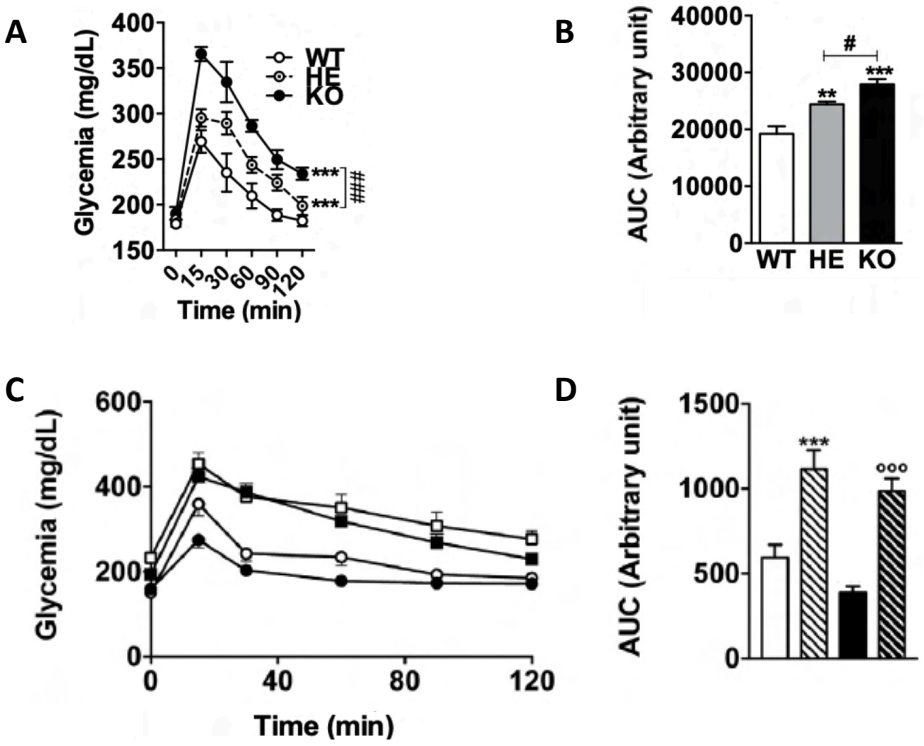

Figure 1. **Tau and glucose homeostasis (adapted from Marciniak et al., 2017 and Leboucher et al., 2019).**

(A & B) Intraperitoneal glucose tolerance test and resulting AUC in constitutive Tau knock-out (KO; black circle/bars), littermate heterozygous (HE; grey bars/dashed line) and wild-type (WT; open circles/bars) animals.

(C & D) Intraperitoneal glucose tolerance test and resulting AUC in THY-Tau22 and WT fed in Chow and high fat diet (HFD). (n=9–11/group; ***p < .001 vs WT Chow, °°°p < .001 vs THY-Tau22 Chow, One-Way ANOVA followed by LSD Fisher post-hoc test). Results are expressed as mean ± SEM. WT mice are indicated as open circles/bars, THY-Tau22 mice as black circles/bars. HFD groups are represented by squares or dashed bars. WT and THY-Tau22 mice were treated with HFD from 4 to 9m of age.

A study from the laboratory showed that constitutive tau knock-out (tau KO) mice exhibited glucose homeostasis impairments, characterized by hyperinsulinemia and impaired glucose tolerance [Figures 1A and 1B; (Marciniak et al., 2017)]. Of note, these observations have been later confirmed by another group using other knock-out mice (Wijesekara et al., 2018a). Conversely, neuronal

overexpression of a human mutated tau protein was associated with improved glucose tolerance in THY-Tau22 mouse model compared to WT [Figures 1C and D; (Leboucher et al., 2019)].

Variable	N	Beta	SE	p
Fasting glucose (mmol/liter)	46,186	0.004	0.005	0.42
Fasting insulin (pmol/liter)	46,186	−0.001	0.005	0.79
2-h glucose (after OGTT) adjusted for BMI (mmol/liter)	15,234	0.096	0.024	**5.9E-^{05}**
30-min insulin secretion (after OGTT, ln) adjusted for BMI (pmol/liter)	5,318	−0.063	0.030	**0.035**

Tableau 2. Tau and glucose homeostasis (from Marciniak et al., 2017). GWAS meta-analysis assessing the impact of MAPT haplotypes on glycemic traits in European individuals. Data were downloaded from www.magicinvestigators.org. Specific regression coefficients (beta) and standard error (SE) represent changes in the variable per copy of the rs1052553 A major allele (H1 haplotype, frequency = 0.79). Trait values for fasting insulin and insulin secretion 30 min after an oral glucose tolerance test (OGTT) were naturally log transformed (ln). Results are adjusted for age, sex, study-specific covariates, and body mass index (BMI) where indicated. N, sample size.

Recently, our laboratory had explored the potential association between tau haplotypes and metabolic traits using published genome-wide association study (GWAS) data (Marciniak et al., 2017). Interestingly, we observed that Tau H1 haplotype in human was associated with a higher 2-hours glucose level and a lower 30-minutes insulin secretion after an oral glucose tolerance test (Table 2).

Yet, mechanisms that trigger and govern metabolic and glucose dyshomeostasis in AD patients are currently unknown. It is however critical to better understand the origin of such metabolic alterations in AD patients considering that, particularly, chronic changes of glucose homeostasis, are themselves prone to favor the development of cognitive impairments and tau lesions, in a presumable detrimental loop.

Taken together, these results suggest predisposition to AD may prompt the onset of diabetes. Nonetheless, the links between tau loss of function and glucose homeostasis remain unclear. Tau is largely considered as a neuronal protein but is also expressed by other tissues, particularly pancreatic ß-cells. But again, its peripheral functions have been overlooked.

Chapter II: Alzheimer's disease and tauopathies

There are currently 50 million cases of dementia worldwide, with more than 10 million new cases per year. Almost 70% of cases are attributed to Alzheimer's disease, making it the most common form of dementia and cognitive impairment (Scheltens *et al.*, 2016), being more prevalent than vascular dementia, mixed dementia, Lewy body dementia (LBD) and frontotemporal dementia (FTD).

1. Alzheimer's disease and tauopathies:

Alzheimer's disease (AD) is a progressive neurodegenerative disease first reported by Dr. Alois Alzheimer in a patient who experienced dementia, memory loss, and delusions (Stelzmann et al., 1995). Postmortem analysis of the brain revealed mature neurofibrillary tangles and Aβ plaques (Stelzmann et al., 1995), which became the recommended neuropathological hallmarks for the eponymous disorder, as first discussed by Khachaturian criteria in 1985 (Khachaturian, 1985).

AD is implicated in a half of the deaths occurring after 85 years (Graham et al., 2017; Vinters, 2015). The international federation of Alzheimer and dementia "Alzheimer's Disease International" had estimated that cases of dementia will increase to 80 million in 2030 and 150 million by 2050 (World Alzheimer Report 2018), which will make it one of the biggest public health issues with an important economic cost for society. Symptoms of AD include progressive cognitive decline and memory loss, as well as a failure to perform routine daily activities. The immense majority of AD cases are sporadic, and less than 1% of AD cases are caused by rare genetic mutations found in a small number of families, involving chromosome 14 on the gene for the presenilin-1 (PS-1), chromosome 1 on the gene for presenilin-2 (PS-2), and chromosome 21 on the gene for amyloid precursor protein (APP). In these inherited forms of AD symptoms tend to develop before the age of 65, and it is known as young onset dementia. Nevertheless, both inherited forms of AD and sporadic AD share similar behavioral symptoms and pathophysiological mechanisms.

2. Characteristic lesions:

At the macroscopic level, the brains of AD patients exhibit severe brain tissue atrophy and increased cerebral ventricles' volume and cortical cerebral grooves (DeTure and Dickson, 2019) (Figure 2A). AD neuropathology is characterized by aggregation of the β-amyloid (Aβ) peptide in plaques and the hyperphosphorylated tau protein in neurofibrillary tangles (NFTs) (Schellenberg and Montine, 2012). Although AD plaques are extracellular Aβ peptides aggregates (from 37 to 43 amino acids, deriving from the successive cleavage of the amyloid precursor protein (APP), Figure 2B), known as plaques. NFTs are characterized by the intraneuronal accumulation of hyper- and abnormally phosphorylated Tau proteins [Figure 2B (Sergeant et al., 2008a)].

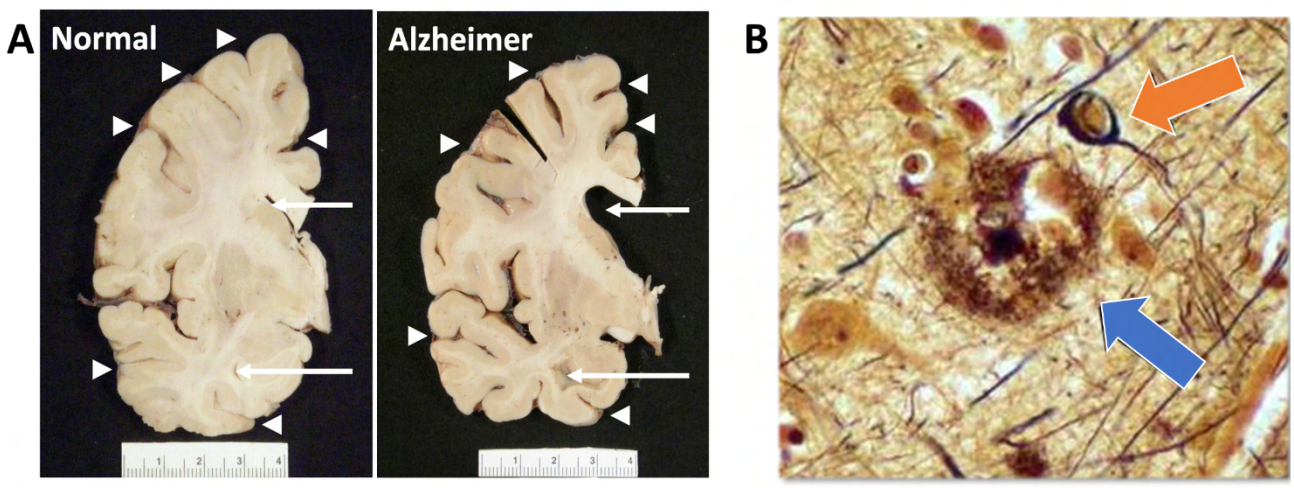

Figure 2. **Characteristic lesions of Alzheimer's disease**. **(A)** Picture of coronal sections from a healthy individual brain and a patient with Alzheimer's disease highlight severe cortical atrophy and increased cerebral grooves (arrowheads), and this atrophy is often accompanied by enlargement of the frontal and temporal horns of the lateral ventricles as highlighted by the arrows. Image adapted from DeTure & Dickson 2019.
(B) The pathological hallmarks of Alzheimer's disease. Neurofibrillary tangles (black semi-circle; orange arrow) and amyloid plaques (dark brown, fibrous mass; blue arrow) are the two major neuropathological hallmarks of Alzheimer's disease. Image adapted from Schellenberg and Montine, 2012).

The main brain areas affected are the medial temporal lobe (hippocampus, transentorhinal and amygdala cortex) and frontal lobe. This atrophy is partly a related to a large neuronal loss causing a decrease in cortical ribbon and brain convolutions.

2.1. Accumulation of beta-amyloid (Aβ) peptides:

Studies on post-mortem tissue revealed that **Aβ** deposits appeared early in AD in the neocortex (frontal, parietal, temporal and occipital cortex) and extend into more internal regions (entorhinal cortex, striatum) to reach the cerebellum and brainstem (LaFerla et al., 2007). The observation of amyloid deposits is possible through a technique of argentic impregnation or by coloration with the red congo and the thioflavine S.

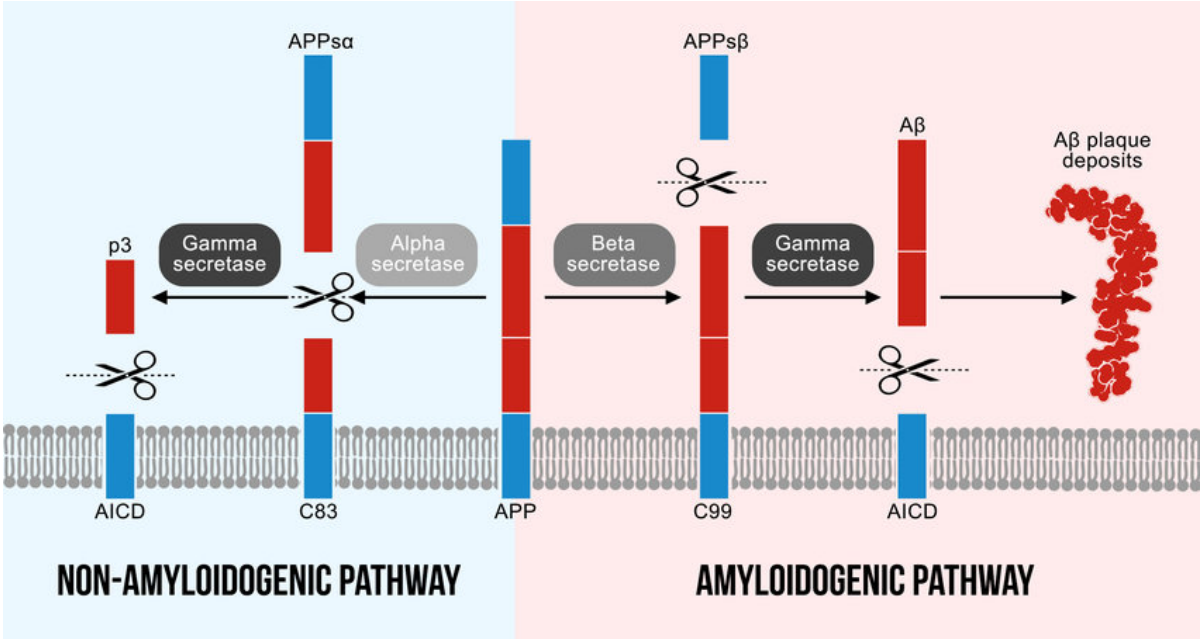

Figure 3. **Non-amyloidogenic and amyloidogenic pathways of APP (adapted from: LaFerla et al., 2007).** In the amyloidogenic pathway, monomers of Aβ40 and Aβ42 peptides are derived from APP and form aggregates of different molecular weights that lead to amyloid plaques, which are the hallmark of AD. APP protein is a substrate for enzymatic cleavage by β secretase (BACE), which releases sAPPB and the C99 fragment within the membrane. Then, the C99 fragment is cleaved by the γ-secretase complex formed by presenilin 1 or 2 and nicastrin. In the non-amyloidogenic pathway, the cleavage by α-secretase occurs within the Aβ region, the C83 peptide is cut by γ-secretase, and the peptide P3 fragment is then produced, which precludes Aβ formation.

Aβ is generated by the sequential proteolytic cleavage of the much larger amyloid precursor protein (APP) by β-secretase and γ-secretase (Figure 3). APP is a ubiquitously expressed type I transmembrane glycoprotein. In vitro and in vivo studies had shown important activities of APP in various neuronal and synaptic processes, which can be executed either as a full-length protein or as one of the processing products (Muller and Zheng, 2012). This protein is subject to two catabolic pathways: the amyloidogenic pathway and the non-amyloidogenic pathway. In contrast, cleavage of APP by γ-secretase generate two types of Aβ peptides known as Aβ40 (cleaved in position 40) and Aβ42 (cleaved in position 42) and these two peptides make up the amyloid deposits. The exact physiological function of Aβ remains unknown. In AD brain, Aβ adopts a highly ordered structure known as cross-β spine, or amyloid (Lührs et al., 2005). The non-amyloiogenic pathway is called a protective pathway because it prevents the formation of Aβ peptides by the early action of the α-secretase (Figure 3). In addition, this pathway allows the production of sAPPα, which have neuroprotective properties (Chasseigneaux and Allinquant, 2012). An imbalance between these two pathways therefore leads to the accumulation of Aβ40 and Aβ42 peptides.

2.2. Neurofibrillary tangles:

Unlike amyloid deposition, there is a correlation between spatiotemporal evolution of NFTs and clinical signs observed in patients with AD (Arriagada et al., 1992; Delacourte et al., 1999; Duyckaerts et al., 1997). Histological work by Heiko Braak and Eva Braak has shared the evolution of AD into six stages (Braak et al., 2011; Braak and Braak, 1991). Stages I and II known as the transentorhinal stages are the earliest stages and are marked by an invasion of NFTs in the locus coeruleus and the trans-entorhinal region. Stages III and IV represent the so-called “limbic” stages of the pathology with progression of NFTs to the hippocampus. Finally, stages V and VI known as «isocortical» are the most severe stages with a general impairment of the isocortex (Figure 4).

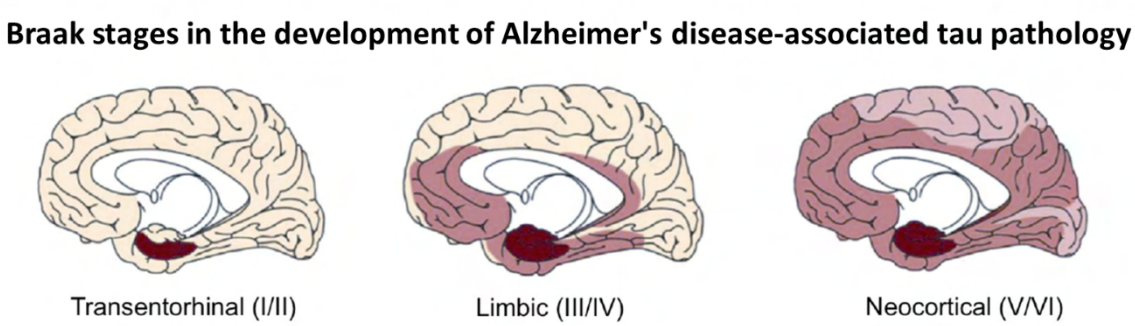

Figure 4. **Schematic display of Braak stages in the development of Alzheimer's disease-associated tau pathology based on post mortem data (adapted from: Braak and Braak, 1991).** Adapted from "Stages of the Pathologic Process in Alzheimer Disease: Age Categories From 1 to 100 Years"

Chapter III: Tau structure and function

Tau for Tubulin Associated Unit was discovered in 1975 as a microtubule polymerization factor (Weingarten et al., 1975). Tau belongs to the family of microtubule-associated protein (MAP). Tau protein plays an essential role in the regulation of microtubular dynamics, axonal transport and neurite growth during neuronal differentiation. In humans, tau is mainly expressed within neurons. It appears as a multi-faceted protein, mainly located in the axonal compartment, but it can also be found at the somato-dendritic compartment, or in the nucleus (Morris et al., 2015; Sergeant et al., 2008b). These cellular localizations allow it to play a role in signal transduction pathways or in the protection of DNA in case of stress.

1. Tau gene and tau isoforms:

Human tau is encoded by the MAPT gene (microtubule associated protein tau), located on chromosome 17q21. The MAPT gene comprises 16 exons. The primary tau transcript contains 16 exons numbered 1 to 14 (Andreadis et al., 1992). Exons 1, 4, 5, 7, 9, 11, 12 and 13 are constitutive and exons 2, 3, 4A, 6, 8 and 10 are alternative. Splicing of these exons had a developmental and tissue-specific regulation (Andreadis, 2005; Goedert et al., 1989). Exons -1 and 14 are never translated (region 5' UTR for "Untranslated Region" and 3' UTR respectively).

In the central nervous system (CNS), exons 4A and 8 are systematically excluded, while in the peripheral nervous system (PNS), exon 4A is included and gives rise to the largest tau isoform commonly known as "Big Tau" (Georgieff et al., 1993). Exon 6 is expressed in a minority level in the tau mRNAs in the cerebellum and leads to the expression of a truncated tau protein in its carboxy-terminal part (Luo et al., 2004; Wei and Andreadis, 2002). The adult human brain contains six tau isoforms, which vary in the number of N-terminal inserts (0N, 1N, or 2N) and C-terminal repeat domains (3R or 4R) due to alternative splicing of exons 2, 3, and 10, resulting in sizes between 48 kDa (0N3R) and 67 kDa (2N4R) of the corresponding proteins (Goedert et al., 1989) (Figure 5). Tau

isoform expression is directly linked to brain development: During neurogenesis, only the shortest Tau isoform 0N3R is expressed, whereas in the adult brain, all six isoforms are present with roughly equal amounts of 3R and 4R isoforms (Goedert et al., 1989; Trabzuni et al., 2012).

Isoforms can be categorized on one hand depending on the number of 29-residue near-amino-terminal inserts, which are encoded by exon 2 and exon 3: isoforms containing 0, 1 or 2 inserts are known as 0N, 1N and 2N, respectively, and on the other hand according to whether they contain three or four carboxy-terminal repeat domains [(3R (three microtubule-binding domains) or 4R (four microtubule-binding domains), respectively; Figure 5, (Sergeant et al., 2008b; Wang and Mandelkow, 2016)].

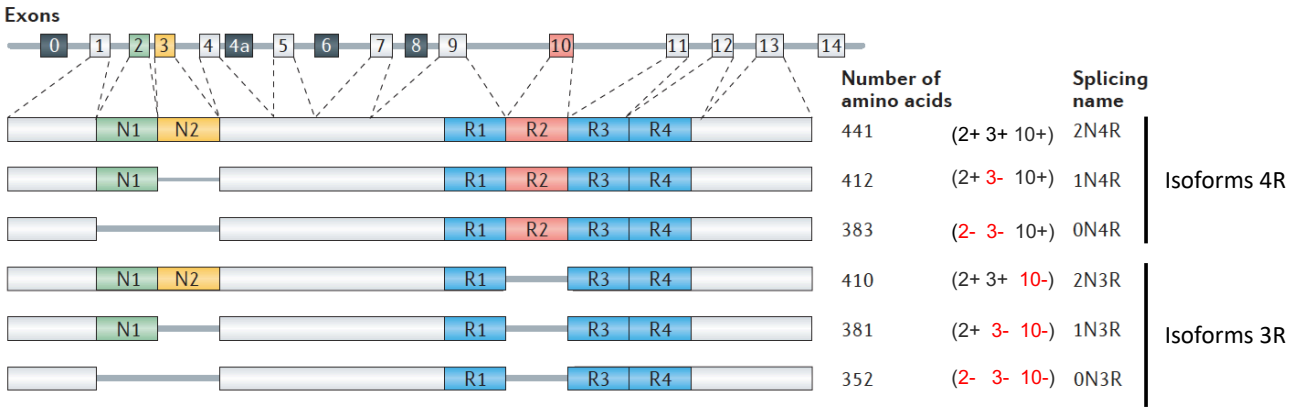

Figure 5. Representation of the MAPT gene, its primary transcription and the six Tau protein isoforms in the adult human brain (Adapted from: Wang & Mandelkow, 2016). The human MAPT gene coding for the Tau protein is locate on chromosome 17 at the 17q21 position and contains 16 exons. Exons 1 and 14 are never translate. Exon 8 is systematically exclude; exon 4A is only expressed in the SNP giving rise to the "Big Tau". Exons 2, 3 and 10 are also subjected to alternative splicing that leads to the generation of 6 protein isoforms in adults. The inclusion or not of exon 10 generates at protein level 3 or 4 repeated patterns (R1, R2, R3 and R4) giving rise to the isoforms of Tau called 3R or 4R. The exclusion of exons 2, 3 and 10 leads to the production of the so-called fetal isoform.

Human tau protein size varies between 352 and 441 amino acids (Figure 5). Tau is a basic protein; however, the ~120 N-terminal residues are predominantly acidic, and the ~40-residue C terminus is roughly neutral. This asymmetry of charges is important for interactions with microtubules and other partners, for internal folding and for aggregation.

The structure of tau can be subdivided into two major domains, on the one hand, an acidic region including the N-ter end and the projection domain allowing interaction with other cytoskeletal elements, mitochondria, plasma membrane and protein partners; and on the other hand, a basic region composed of a proline-rich domain, a microtubule binding domain, consisting of three to four repeated domains (3R or 4R), and the C-terminal end (Sergeant et al., 2008b; Wang and Mandelkow, 2016).

2. Functions of tau protein:

Initially described as a microtubular polymerization factor (Cleveland et al., 1977; Weingarten et al., 1975), tau play a major role in regulating microtubule dynamics within neurons. This function of microtubular dynamics regulator ensures to tau an indirect role in the modulation of axonal transport, which allows ensuring the integrity of the neuronal cell, and in the neuronal differentiation by participating in the neuritic growth. Although, today this function of regulating microtubules' dynamics remains highly studied, new tau functions are emerging in the literature.

2.1. Regulation of microtubule dynamics:

Microtubules are a protein structures composed of heterodimeric tubulin units α and β able to associate longitudinally in a first time thus forming protofilaments. The latter in turn join helically to form the microtubules. These cylindrical structures have a diameter of 25 nm determined by the number of protofilaments (usually 13) and a variable length (Amos and Schlieper, 2005; Conde and Cáceres, 2009). Microtubules are subject to dynamic instability defined by continuous elongation

(also known as polymerization phase) and shortening (depolymerization phase). Microtubules are polarized by the presence of + end on which are added tubulin dimers and a – end where dimers disassemble (Figure 6). Interestingly, microtubules are more stable in neurons compared to other cell types through the presence of MAPs (Seitz-Tutter et al., 1988).

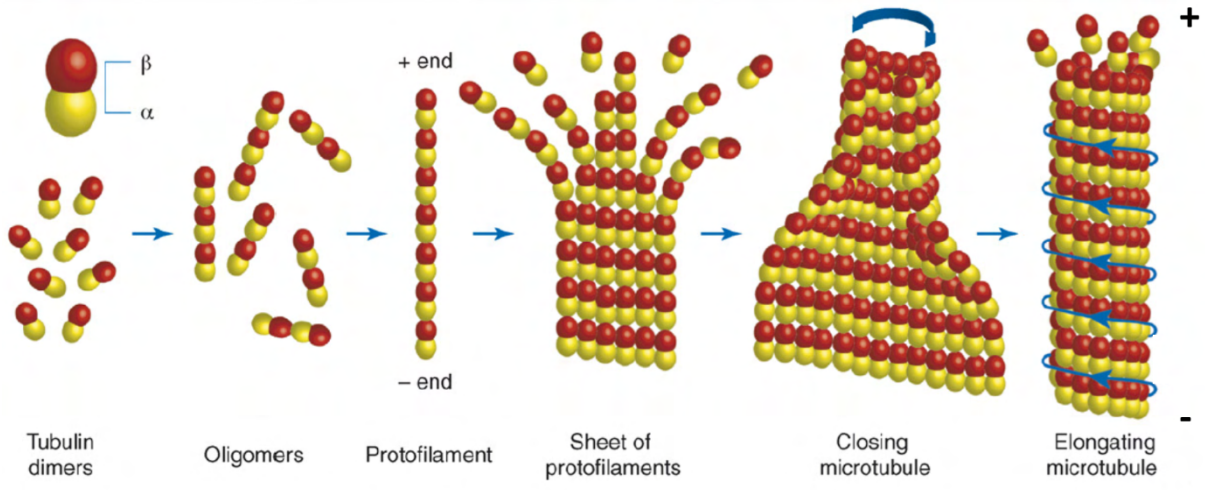

Figure 6. Polymerization of microtubules. (Adapted from: Conde and Cáceres, 2009). Tubulin dimers assemble 'head-to-tail', forming oligomers that elongate into protofilaments. Protofilaments start to interact laterally forming sheets. At a typical number of 13 protofilaments, the tubulin sheet closes into a tube, forming a microtubule.

Tau shares, with the other members of the MAPs family, the property of binding to microtubules. This interaction is possible through the presence of the 3 or 4 replicate motifs composed of 18 amino acids (Lee et al., 1989, 1989) highly conserved and separated by 13 or 14 less conserved amino acids constituting iR1, iR2 and iR3 "inter-repeat". In addition to repeated domains, the proline-rich region P2 was also shown as a key component of Tau's microtubule connection (Goode et al., 1997). Tau structure when bound to microtubules has been the object of numerous investigations. Tau was shown to diffuse along the microtubules, bi-directionally and independently from active transport, in a manner described as kiss-and-hop interactions, the repeated domains structured in β-sheets as well as

the proline-rich P2 domain interact with the glutamic acid-rich regions of the tubulin (Hinrichs et al., 2012; Mukrasch et al., 2007; Sillen et al., 2007).

Several in vitro and in cellulo studies have documented the molecular and cellular consequences of the tau binding to microtubules. The first in vitro research using porcine brain extracts showed that tau was co-purified with tubulin (Cleveland et al., 1977; Weingarten et al., 1975), and that the presence of tau allowed the tubulin to assemble into a larger molecular mass complex. Mechanistic studies showed that tau modulates different aspects of microtubular dynamics. Indeed, tau acts as a factor serving both to increase the microtubules assembly speed and to increase the quantity of polymerized microtubules (Witman et al., 1976). The average elongation length of an isolated polymerized microtubule in the presence of tau is nine times greater than the elongation length of a polymerized microtubule in the absence of tau (Drechsel et al., 1992). This can be explained by the combination of different elements: the increase in elongation and the decrease in shortening.

Functional studies in cell and mouse models had allowed to definitively validate the role of tau in microtubular dynamics (Barbier et al., 2019). In fact, a micro-injection of purified tau protein in fibroblast cultures increases the microtubular density and protects the microtubules from pharmacologically induced depolymerization (Drubin and Kirschner, 1986). In addition, Tau overexpression leads to the formation of microtubular beams (Kanai et al., 1989).

Microtubules are a dynamic structure of the cytoskeleton involved, among further things, in the regulation of axonal transport. They are also involved in the process of formation of axon and neuritis during neuronal differentiation. By regulating microtubular dynamics, tau actively participates in the resulting cellular consequences.

2.2.Neuronal development and neuritic growth:

Neurons are polarized cells with a cellular body (called the soma) and two types of extensions: dendrites that receive information from the efferent neurons and the axon that conducts nerve information to terminal connections that transmit information to adjacent related neurons (Kolarova

et al., 2012) (Figure 7A). The establishment of neuronal polarization is a complex process that constitutes a fundamental step in the development of the nervous system. The formation of the axon is one of the primary mechanisms in this neuronal polarization and its implementation is partly dependent on microtubular dynamics. Hence, many studies have investigated tau's involvement in this process. In a cell line model PC12 (rat pheochromocytoma) differentiated into neuronal cells, a correlation was established between neuritis increase, polymerized microtubule increase and tau expression (Drubin et al., 1985).

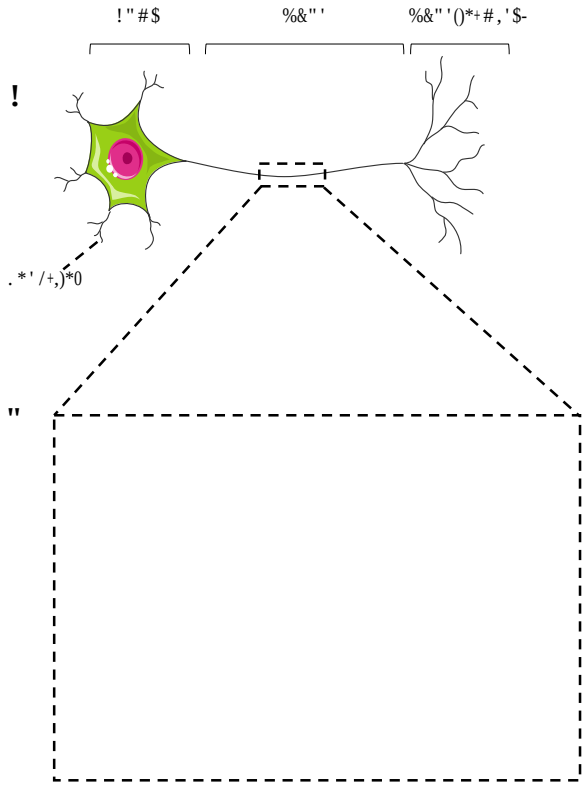

Figure 7. Neuronal polarization and binding of tau protein to the microtubules. (A) Neurons are polarized cells with a somato-dendritic pole, an axon and axonal endings. **(B)** Binding of tau protein to the microtubules is maintained in equilibrium by coordinated actions of kinases and phosphatases. The phosphorylation of tau (pink balls) regulates its activity to bind to microtubules and can affect axonal transport. This interaction modulates the anterograde and retrograde axonal transport of kinesin and dynein motor proteins respectively. (Adapted from: Kolarova et al., 2012).

2.3.Axonal transport:

Axonal transport represents a vital cellular process to maintain the integrity of synaptic and neuronal connections and functions. Axonal microtubules provide bidirectional axonal transport of vesicles, neurotransmitters and mitochondria.

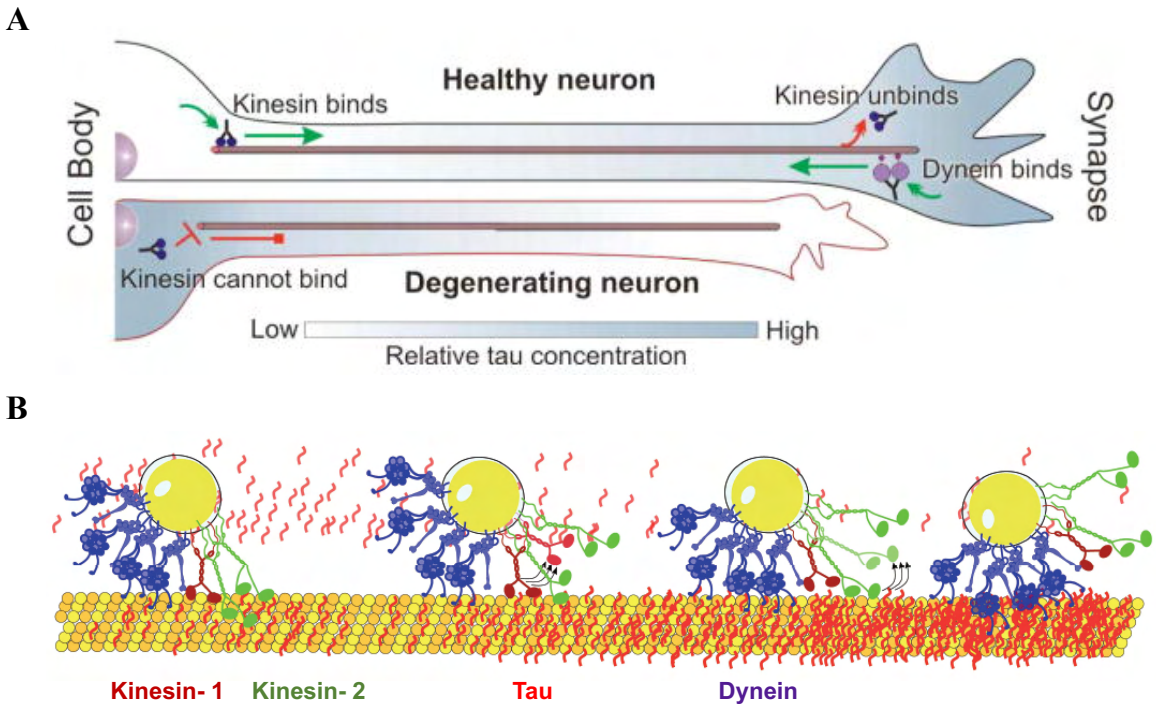

Figure 8. Tau protein inhibits type 1 kinesin, increases the dynein-microtubule bond and promotes the retrograde transport.

(A) In the healthy neuron, the high concentration of tau in the distal axon inhibits the kinesin-microtubule bond and promotes the dynein-microtubule bond. In the degenerating neuron, the concentration gradient is inverted and disrupts the transport of microtubular cargo (Adapted from: Dixit et al., 2008).

(B) Microtubules are shown in yellow/orange and tau proteins in red. The motile protein families of microtubules are represented in dark red for kinesin-1, green for kinesin-2 and blue for dynein. (Adapted from: Chaudhary et al., 2018).

The microtubules will serve as a support for motor MAPs such as dynein and kinesin, which respectively modulate retrograde transport (from synapses to soma) and anterograde (from soma to synapses) (Figure 7B).

In the neuron axon, there is a gradient of increasing tau concentration from the axon cone to the synapse (Figure 8A). This difference in tau location plays a crucial role in neuronal physiology. Indeed, beyond its strict interaction with tubulin, tau also interacts with the motile proteins of microtubules: kinesin and dynein (Chaudhary et al., 2018).

In the axon, the transport of cargo from the proximal region to the distal region and vice versa is elementary for the correct functioning of nerve impulses. Also, it has been shown that tau promotes the bond of dynein to tubulin and conversely prevents the fixation of kinesin (Figure 8B). Accordingly, the presence of tau at the synaptic level is favorable to retrograde transport and its low concentration at the base of the axon is rather favorable to anterograde transport (Chaudhary et al., 2018; Dixit et al., 2008). The correct functioning of the neuron involves microtubular dynamics and strictly regulated intracellular traffic. In some neurodegenerative diseases, synapse is depleted in tau proteins that accumulate in the cell body causing inversion of the concentration gradient and alteration of cargo transport, contributing to neuronal death [Figure 8A, (Dixit et al., 2008)]. This event occurs in part when tau protein adopts an abnormal conformation that prevents its fixation on the tubulin in a group of pathologies called tauopathies.

Other many studies suggest that Tau would be much more than MAP since Tau can be located within the nucleus and at the synaptic level. These new cellular locations of Tau are accompanied by new functions.

2.4.DNA protection:

In addition to its cytosolic localization, tau is also found in the nucleus of neuronal cells (Loomis et al., 1990) and non-neuronal cells (Sjöberg et al., 2006), suggesting that tau could develop other functions within the cell. Indeed, in cellulo studies had shown that tau is present within the nucleolus [a nuclear sub-compartment where ribosomal ribonucleic acids (rRNA) are synthesized], and more particularly implicated in chromatin structure (Sjöberg et al., 2006). These results suggest that tau may play a function in nucleolar organization and/or heterochromatinization of rRNA coding genes. A previous study using atomic force microscopy had reported that neuronal tau binds to the DNA double strands and induces DNA conformational changes (Qu et al., 2004). Both repeated patterns and proline-rich domains would be involved in this interaction (Wei et al., 2008).

A little over a decade ago, a study in a mouse model of primary neuron culture, indicated that tau, in a condition of thermal or oxidizing stress, is able to migrate to the nucleus and bind to DNA. This nuclear relocation of tau would protect the DNA from stress-induced damage (Sultan et al., 2011).

These results were also validated in mouse models since induced heat stress in tau KO mice increases DNA damage compared to wild mice (Violet et al., 2014). This works opened up new research perspectives on the physiological functions of tau within the neuron.

2.5.Signal transduction:

Due to the presence of proline-rich domains, tau is able to interact with some SH3-domain proteins through its PXXP patterns (seven sequences located in proline-rich domains) including proteins of the Src family at the plasma membrane (Lee et al., 1998). Tau can associate with various other proteins in addition to tubulin, including the SH3 domains of Fyn or Src family tyrosine kinases. Among other function, Fyn and Src tyrosine kinases are involved in the phosphorylation of the NMDA (N-methyl-D-aspartate) receptor (Lee et al., 1998; Reynolds et al., 2008). NMDA is a post-synaptic receptor essential for molecular signaling of memory and neuronal synaptic plasticity.

Tau regulates anterograde fast axonal transport through a protein phosphatase 1 (PP1)- glycogen synthase kinase 3β (GSK3β) pathway. Previous studies showed that tau protein had a specific motif in the extreme N-terminal end, termed the Phosphatase Activating Domain (PAD), which is necessary and sufficient to activate the PP1-GSK3β pathway in axons and favorite the fast axonal transport (Kanaan et al., 2013, 2011). Fast axonal transport (FAT) is a cellular process of rapid movement of membrane vesicles and their contents over long distances within a neuron. Previous studies established that material moving in fast axonal transport was associated with membrane-bound organelles. FAT is critical for appropriate maintenance of neuronal connectivity and survival (Black, 2016).

Interestingly, a recent study published by our laboratory identified a novel function of tau protein as a modulator of brain insulin signalling and highlighted a potential mechanistic explanation whereby alteration of insulin signaling would happen in AD through pathological tau loss-of-function (Marciniak et al., 2017).

The former study showed that tau modulates central insulin signaling by positively regulating IRS-1 and blocking the inhibitory effects of the phosphatase PTEN (Phosphatase and TENsin homolog, which is known to inhibit insulin signalling). Accordingly, the interaction between tau and PTEN restrains PTEN's lipid phosphatase activity, favoring pro-cognitive insulin signaling (Marciniak et al., 2017) (Figure 9).

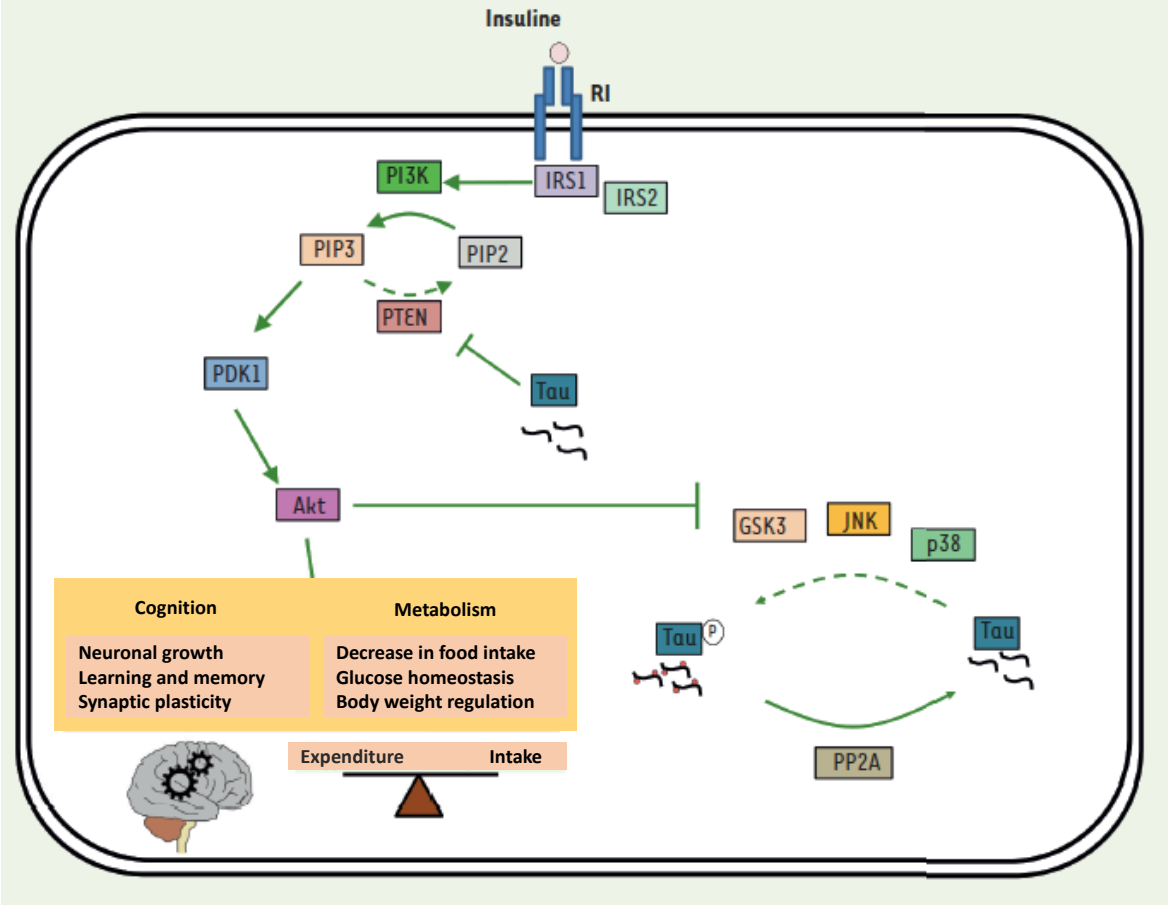

Figure 9. Relationship between Tau and central insulin signaling (Adapted from: Joly-Amado et al.,2018). Under physiological conditions, insulin binds to its receptor and induces phosphorylation and activation of the PDK1 and Akt pathway through PI3K, leading to increased cognition and metabolism regulation. Additionally, insulin inhibits soma tau kinases such as GSK3β and p38 by Akt, thus limiting tau hyperphosphorylation. Monomers of tau protein also contribute to normal insulin signaling by inhibiting the conversion of PIP3 (phosphatidylinositol-3-kinases) back to PIP2 through PTEN.

Abreviations: IR, insulin receptor; IRS-1/2, insulin receptor substrate 1/2; PI3K, phosphatidylinositol-3-kinases; PIP2, phosphatidylinositol 4,5-bisphosphate; PIP3, phosphatidylinositol (3,4,5)-trisphosphate; PTEN, phosphatase and tensin homolog; PDK1, 3-phosphoinositide-dependent protein kinase-1; Akt, protein kinase B; GSK3β, glycogen synthase kinase 3 beta; JNK, c-Jun N-terminal kinases; P38, p38 mitogen-activated protein kinases; PP2A, protein phosphatase 2.

3. **Post-translational modifications of tau protein**:

In human, tau protein is subject to several post-translational modifications including: phosphorylation, acetylation, glycosylation, glycation, deamidation, isomerization, nitration, methylation, ubiquitylation, sumoylation and truncation. The main role of post-translational modifications is to regulate and improve functional diversity usually by changing protein electrostatic characteristics and/or structure. About 35% of the amino acid residues in tau are susceptible to modification peri- or post-translationally. These residues are serine (S), threonine (T), tyrosine (Y), lysine (K), arginine (R), asparagine (N), histidine (H), and cysteine (C).

3.1.Phosphorylation:

Among post-translational modifications of tau protein, phosphorylation was the most studied, on the one hand for its involvement in the physiological regulation of microtubular dynamics, but also, for its alteration in neurodegeneration.

In the mid-1950s, Edwin Krebs and Edmon Fisher found that an enzyme called phosphorylase was activated in the presence of ATP and that this reaction was catalyzed by a kinase. Conversely, the elimination of a phosphate group by a phosphatase on phosphorylase inactivate it (Krebs and Fischer, 1955). This work earned them the Nobel Prize in physiology and medicine in 1972 for the discovery of protein's reversible phosphorylation.

Phosphorylation implicates the reversible addition of a phosphate (PO_4) group to the polar group of serine, threonine or tyrosine amino acid residues (Humphrey et al., 2015). Protein phosphorylation increase hydrophilicity, and modulates some important protein functions including protein-protein interactions, signaling cascades, and protein degradation (Ravid and Hochstrasser, 2008). Additionally, phosphorylation is involved in essential cellular functions such as metabolism and intracellular signaling.

There are 85 potential phosphorylation sites (44 S, 35 T, and five Y) in the longest isoform of tau [(2N4R Tau); (Figure 10)]. The change in tau electrostatic characteristics related to the

phosphorylation may play a crucial role in the regulation of tau function, localization, and interaction with other molecules, including its binding to microtubules, and therefore regulates the stabilization and assembly of microtubules themselves. For example: the phosphorylation at the flanking region of tau in Ser214 and Thr231 can generate the detachment of tau from microtubules by leading to a conformational change of tau from trans to cis isomerization, which reduces the affinity of the protein for microtubules (Lu et al., 1999).

More than 20 kinases can be divided into three groups according to the type of epitope targeted, which can phosphorylate tau protein in vitro and/or in vivo (Table 3):

1) the PDPK group for Proline Directed Protein Kinases which phosphorylate tau on the Ser or Thr residues followed by a Pro residue;

2) the non-PDKP group which includes tau phosphorylating kinases on Ser and Thr residues not followed by a Pro;

3) finally, the last group includes tyrosine kinases.

Tau phosphorylation regulates biological functions of tau and requires a balanced interplay of kinases and phosphatases. Numerous serine/threonine kinases phosphorylate tau, including glycogen synthase kinase 3 (GSK3β), cyclic AMP-dependent protein kinase (PKA), casein kinase 1 (CK1), cyclin dependent kinase 5 (cdk5), p42/p44 MAPKs (ERKs 1/2), protein kinase C (PKC), calmodulin-dependent protein kinase II (CaMKII), the brain-specific kinases 1 and 2, the tau-tubulin kinases 1 and 2, and some microtubule affinity-regulating kinases (MARKs; also known as PAR1 kinases).

Also, tau can be phosphorylated by tyrosine kinases, such as the ABL family members (ARG and ABL1) and the SRC family members (LCK, SYK, and FYN) (Sergeant et al., 2008b). FYN, SYK, and ABL kinases phosphorylate tau at the Y18, Y197, and Y394 residues, which have been associated with tau aggregation and AD pathology (Alquezar et al., 2021). Several protein phosphatases (PP) 1, 2A, 2B, 2C, and 5 can dephosphorylated Tau (Sergeant et al., 2008b). Among these phosphatases, PP2A accounts for around 70 % of all tau dephosphorylation in the human brain (Figure 10). While

physiological phosphorylation regulates the biological functions of tau, abnormal phosphorylation may be an important element in the pathogenesis of tauopathies (Wegmann et al., 2021).

PDPK group	Non- PDPK group	Tyrosine kinases group
Cdk1	CaMKII	Src kinases
Cdk2	CK1	C-abl
Cdk5	CK2	
GSK3α	DYRK	
GSK3β	GSK3α	
LRRK2	GSK3β	
MAPK (Erk1/2)	MARK	
SAPK1γ/JNK	Phosphorylase kinase	
SAPK2α/p38	PKA	
SAPK2β	PKB/AKT	
SAPK3	PKC	
SAPK4	PKN	
	TTK	

Tableau 3. The three classes of kinases involved in Tau phosphorylation in vitro or in vivo.

Cdk : Cyclin dependant kinase, GSK : Glycogen Synthase Kinase, LRRK2 : Leucine-Rich Repeat Kinase 2, MAPK : Mitogen Activated Protein Kinase, SAPK : Stress Activated Protein Kinase, CaMK : Calmodulin dependant protein Kinase, CK1, CK2 : Casein kinase 1 et 2, DYRK : Dual specificity Tyrosine Regulated Kinase, MARK : Microtubule Affinity Regulating Kinase, PKA, PKB, PKC et PKN : Protein Kinase A, B, C and N, TTK : Tau Tubuline Kinase, C-abl : Kinase Abelson.

Hyperphosphorylation of tau can cause synaptic dysfunction by inducing a missorting of tau from axons to the somatodendritic compartment (Hoover et al., 2010; Thies and Mandelkow, 2007; Zempel et al., 2010). Furthermore, tau phosphorylation can alter its degradation through the proteasome or the autophagy and its cleavage by proteases. For example, the phosphorylation of tau at Ser422 inhibits the cleavage of tau by caspase 3 at Asp421 (Guillozet-Bongaarts et al., 2006).

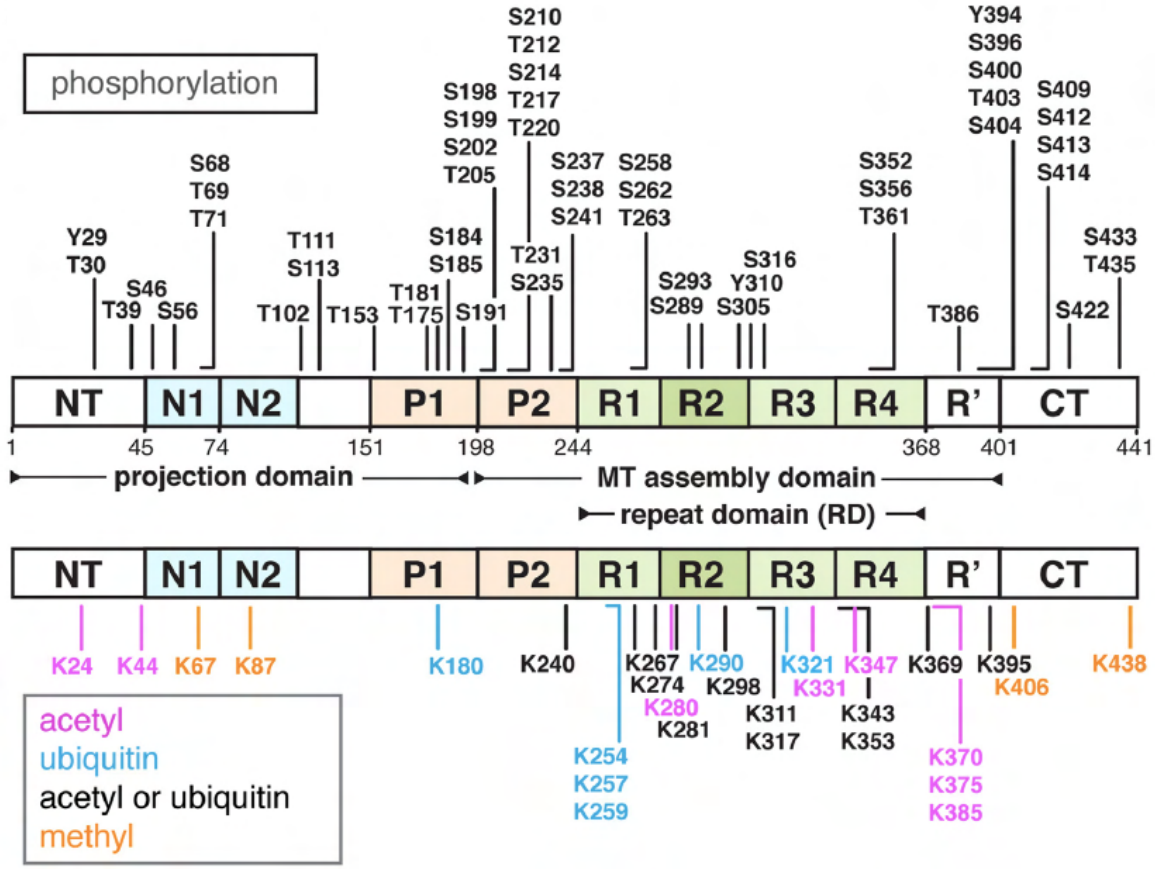

Figure 10. Post-translational modifications (PTMs) occurring in tau isolated from postmortem AD brains (Adapted from: Wegmann et al., 2021). Phosphorylation (residues indicated above the domain structure in gray) is the main PTM of tau and is distributed heterogeneously in the tau sequence, with most abundant p-sites clustering in P1 and P2 of the proline-rich domain (PRD) between residues T181 and S235, and in regions C-terminally of the RD (repeats R1–R4) in between residues S396 and S404 (R0 and CT). The N-terminal projection domain includes the inserts N1 and N2 and is frequently phosphorylated as well. Acetylation (pink) and ubiquitinylation (blue) occur mostly in the MT-assembly domain, and often alternatively at the same residues (black). Methylation (orange) is rare and found only in the projection domain and the C-terminal domain (CT). The position of PTMs other than phosphorylation is indicated below the Tau domain structure.

Tau phosphorylation is usually considered to enhance its aggregation, as both hyperphosphorylation and aggregation of tau are increased in AD (Sergeant et al., 2008a). At last, the phosphorylation of tau may change its association and interaction with its partners. For example, only hyperphosphorylated tau can interact with the kinesin-associated protein JUN N-terminal kinase-interacting protein 1 (JIP1) and therefore impair the formation of the kinesin complex, which mediates axonal transport (Ittner et al., 2009).

3.2.Glycosylation:

3.2.1. O-Linked N-acetylglucosaminylation :

The O-Linked N-acetylglucosaminylation (O-GlcNAc) is a dynamic regulatory post-translational modification discovered in the 1980s, that consists to the addition of a unique monosaccharide, *N*-acetyl-D-glucosamine, to a serine and threonine hydroxyl group by a β-linkage (Torres and Hart, 1984). The dynamism of O-GlcNAc is regulated by two enzymes: β-N-acetylglucosaminyl transferase (OGT) and N-acetyl-β-d-glucosaminidase (OGA). O-GlcNAc has been described to play a role in various cell functions: in nuclear transport (Hanover, 2001; Hanover et al., 1987; Holt et al., 1987); ; in protein degradation, with a reversible inhibition of the proteasome, and the protection of modified protein against proteasomal degradation (Han and Kudlow, 1997; Hatsell et al., 2003). Furthermore, the O-GlcNAc is involved and in the regulation of protein expression, transcription and translation (Comer, 1999). The contribution of O-GlcNAc in protein-protein interactions was described in different biological systems. Indeed, many proteins O-GlcNAc-modified play a key role in organization and assembly of cytoskeleton, like cytokeratins 8, 13, and 18 (Chou et al., 1992; Chou and Omary, 1993), H, L, and M neurofilaments, microtubule-associated proteins MAP1, -2, and -4 (Ding and Vandré, 1996; Dong et al., 1996), and Tau protein (Arnold et al., 1996).

Tau O-GlcNAc was discovered initially with the use of lectins (molecules with a very high affinity for the oses) specific OGlcNAcylated residues on proteins Tau isolated from bovine and human brains (Arnold et al., 1996; Liu et al., 2004). Interestingly, there is a relationship between

phosphorylation and O-GlcNAc for tau protein. Indeed, the pharmacological inhibition of OGA (the enzyme responsible for the release of Glc-NAc residue on Ser and Thr residues) in cell lines leads to a decrease in tau phosphorylation on some epitopes: Ser199, Ser202, Thr205, Thr212, Ser214, Ser262, Ser396, Ser422 (Liu et al., 2004; Yuzwa et al., 2008). Similarly, the use of thiamet-G (specific inhibitor of the OGA) in vivo decreases tau phosphorylation on the following residues: Thr231, Ser396 and Ser422 (Yuzwa et al., 2008). In AD, there is a general decrease in protein O-GlcNAcylation levels, which correlated with an overall decrease in intraneuronal glucose concentration and membrane receptors involved in the internalization of glucose in neuron (Liu et al., 2008). This could partly explain the increased phosphorylation observed in AD and raise a protective role of O-GlcNAc for tau. In addition, previous in-vitro studies had shown that tau O-GlcNacylation on the Ser356 (Yu et al., 2008) and Ser400 (Yuzwa et al., 2012) slow down tau aggregation and inhibition of OGA in mouse models of tauopathies by chronic thiamet-G treatment would decrease the number of neurons with neurofibrillary tangles (Graham et al., 2014; Yuzwa et al., 2012). Taken together, these observations offer interesting perspectives on the role of O-GlcNAc in AD.

3.2.2. N-linked protein glycosylation:

The N-glycosylation process is a co-translational modification consisting of the addition of N-Glycane on the asparagine (Asn) residues of the Asn-X-Ser/Thr sequences and taking place in the endoplasmic reticulum (Breitling and Aebi, 2013). In 1996, it was shown that specific N-glycans lectins were capable of marking paired helical filaments (PHF) extracted from brains of patients with AD (Wang et al., 1996).

3.3.Glycation:

Glycation is a reaction of the proteins non-enzymatic glycosylation. It's frequently observed with aging, which consists in the formation of a bond between the primary amine function of amino acids Lysine or Arginine and the aldehyde function of aldoses such as glucose (Ansari et al., 2011).

It would be noted that Tau protein is particularly rich in Lysines which constitutes a favorable chemical environment to this post-translational modification. In vitro, recombinant tau incubation

with glucose leads to the glycation of twelve sites, seven of which are located in the microtubule binding domains (Nacharaju et al., 1997), which could decrease tau's affinity for microtubules (Ledesma et al., 1994). In situ, the existence of glycated forms of tau protein seems to be limited to a pathological context, since in the human brain only pathological tau proteins extracted from PHFs showed such a modification (Ko et al., 1999; Ledesma et al., 1995). Therefore, these tau glycated proteins could be either a biochemical signature, or participate in the formation of PHFs by accelerating the process of fibrillogenesis or stabilizing them (Kuhla et al., 2007; Ledesma et al., 1995, 1994).

3.4.Acetylation:

The addition of an acetyl group neutralizes the positive charge of lysine residues, thereby producing a molecular impact on protein structure and protein-protein recognition. The acetylation of tau can be mediated by two enzymes, the Cyclic adenosine monophosphate Response Element Binding (CREB)-binding protein or by P300 acetyltransferase at several Lys residues in the flanking region or the repeat domain. There are 44 lysine residues longest isoform of Tau protein (2N4R) and therefore, 10 % of the Tau can potentially be modified by acetylation (Figure 10). Also, tau can be deacetylated at these sites by histone deacetylase 6 (HDAC6) or sirtuin 1 (SIRT1). Particularly, tau has an intrinsic acetyltransferase activity and it can catalyze an auto-acetylation at some Lys sites, including Lys280 (Cohen et al., 2013).

Depending on the sites, the acetylation can impact differently tau. Tau's acetylation could inhibit its degradation (for example, acetylation at Lys163, Lys280, Lys281 or Lys369) or, facilitate its degradation and suppress its phosphorylation and aggregation (for example, acetylation at Lys259, Lys290, Lys321 or Lys353) (Cook et al., 2014; Min et al., 2010). Interestingly, the acetylation at Lys259, Lys290, Lys321 or Lys353 within the KXGS motifs arises in normal tau, and is reduced in brains of individuals with AD (Cook et al., 2014). Also, it was identified in the brain of patient with

AD or other tauopathies an acetylation of tau in Lys280 or Lys174. The acetylation of tau at these two sites appears to delay tau turnover and may be critical for the toxicity induced by tau.

3.5.Ubiquitination:

Similar to acetylation, ubiquitination arises on lysine residues. Tau protein has a high susceptibility to ubiquitination because of its richness in lysine residues. On the 2N4R Tau isoform, 17 lysine residues out of a total of 44 were found ubiquitinated with most of them located in the tau microtubule-binding domain (Morris et al., 2015; Munari et al., 2020). The principal role of Tau ubiquitination seems to be the regulation of tau clearance by the lysosome-autophagy or proteasomal systems.

Chapter IV: Energy and glucose homeostasis

At the end of the 19th century, Claude Bernard and Walter Canon developed the concept of homeostasis. Homeostasis is the ability of any biological system to maintain relative stability of its internal environment, despite environmental fluctuations. This is a dynamic balance that must be controlled to be maintained.

According to this concept, many physiological functions are controlled in mammals: heart rate, blood pressure, respiratory function or glycemia (blood glucose concentration). Energy homeostasis is often represented as an equilibrate balance between energy inputs and expenditures. Intakes are mainly due to diet, while expenditures are mainly due to basal metabolism and physical activity.

The regulation of blood glucose concentration is one of the representations of energetic homeostasis: in a healthy individual plasma glucose concentration are maintained within a narrow range throughout the day, usually averaging between 70 and 100 mg/dl after an overnight fast.

Glucose is the energy molecule most used by the body under physiological conditions due to its immediate availability. The brain mainly uses it as a source of energy in physiological condition. It is therefore vital to maintain circulating rates within an “acceptable” range. In addition to being an energy substrate, glucose acts as an informative molecule of the energetic status of the organism.

The control of blood glucose concentrations is the result of a fine and primordial regulation requiring the intervention of both the central nervous system and pancreas.

1. Role of the central nervous system in the regulation of glucose homeostasis:

The central nervous system (CNS) plays a fundamental role in controlling energy homeostasis. It is an integrator center that coordinates the activity of many peripheral organs according to metabolic conditions (Figure 11). It is continuously informed of the body’s energy needs and reserves by three main types of signals:

- metabolic (glucose, amino acids, fatty acids)

- endocrines (leptin, insulin, ghrelin, …..)

- nervous (the afferent impulses).

The CNS integrates these signals and in turn produces appropriate central and peripheral responses of behavioral type (by regulating food intake), endocrine (by controlling for example insulin secretion) and vegetative [modulating the activity of some organs through the autonomic nervous system (ANS) to direct metabolic flows].

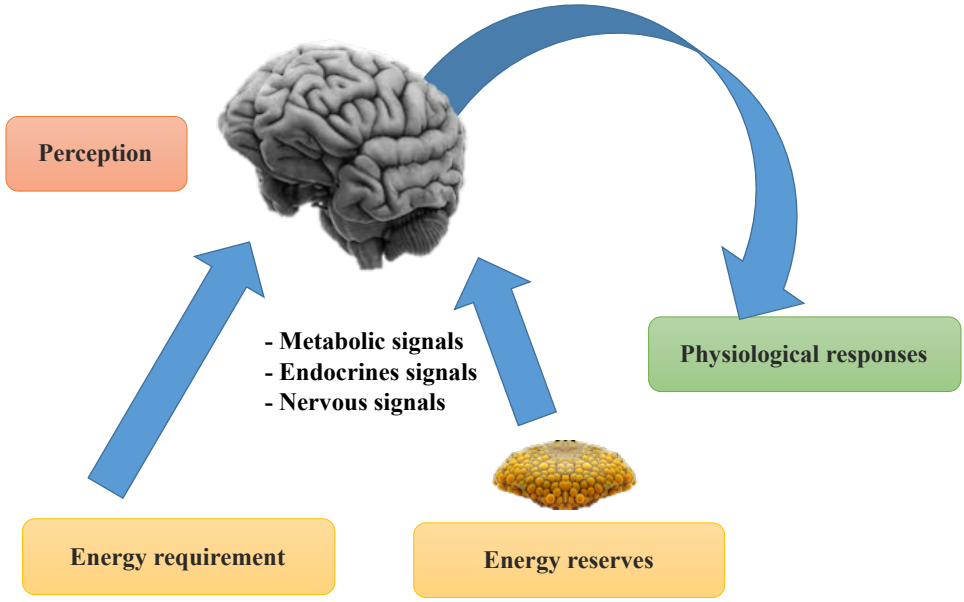

Figure 11. The brain is involved in maintaining glucose homeostasis.
Endocrine, metabolic and nervous signals reach the brain to inform it of the body's requirements and energy reserves (mechanisms of perception). The brain integrates these signals and triggers a set of physiological responses to restore energetic homeostasis.

1.1.Role of the brain stem and hypothalamus:

Among the brain structures involved in controlling glucose homeostasis, the brain stem and hypothalamus play a fundamental role. They are both able to integrate signals from the periphery (Figure 12). In the past, the brain stem was only considered as a relay region between the CNS and

the ANS. Many hypothalamic efferences project to the brainstem that integrates them before modulating the activity of peripheral organs through the ANS (Schneeberger et al., 2014).

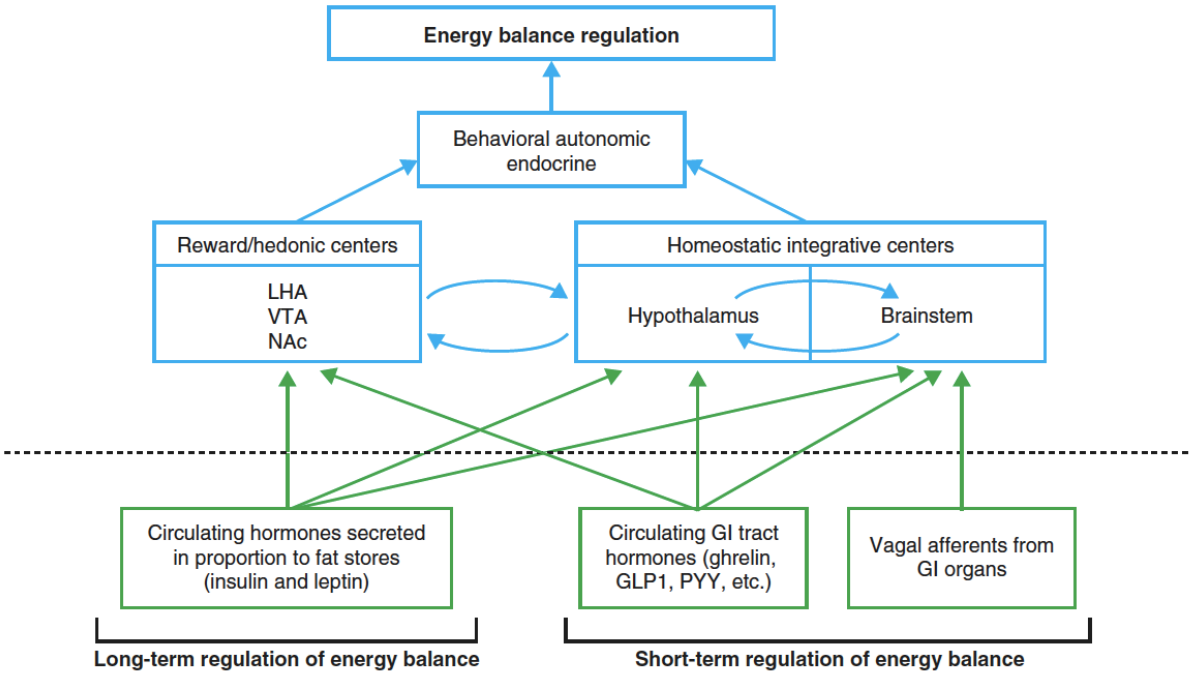

Figure 12. Food intake and energy balance regulation (Adapted from: Schneeberger et al., 2014).

Homeostatic and non-homeostatic neural mechanisms regulated coordinately both food intake and energy balance.Vagus stimuli and circulating hormones inform the CNS about whole-body nutritional and energy status. Insulin and leptin are believed to be implicated in the long-term regulation of energy balance, while gastro-intestinal (GI) hormones and vagal afferents represent a short-term regulatory mechanism. These hormones act in concert to engage specific neuronal circuits in hedonic and homeostatic centers, establishing dynamic and complex interactions between these different brain regions to elaborate coordinated endocrine, autonomic, and behavioral responses to regulate energy balance.

Also, emotional, sensory, and social cues can influence ingestive behaviors through non-homeostatic and higher brain structures.

Abbreviation: LHA, lateral hypothalamic area; VTA, ventral tegmental area; NAc, nucleus accumbens.

It also receives visceral afferences from liver and gastrointestinal tract, and transfers the informations to the hypothalamus. Recent data know that the brain stem is also able to directly detect metabolic and hormonal signals. Indeed, it contains specific neurons modifying their electrical activity in response to changes in blood glucose concentration, which would modulate food intake and ANS activity (Andrew et al., 2007; Dallaporta et al., 1999; Mimee and Ferguson, 2015).

1.1.1. Role of the hypothalamus in the regulation of glucose homeostasis:

Since 1940, pre-clinical studies highlighted the importance of the hypothalamus in the regulation of body weight. Furthermore, science progress in understanding the neurobiology mechanisms involved in the development of obesity had tightly proven that the mediobasal hypothalamus is a fundamental connection in the neuronal hierarchy controlling whole-body energy balance.

The hypothalamus is a brain structure from the Diencephalon, located around the 3rd ventricle (Figures 13 and 14). It is delimited in anterior by optic chiasm, the anterior commissure that connects the two cerebral hemispheres, in posterior by the mammary bodies, and finally in dorsal by the thalamus. The hypothalamus is composed of many small nuclei (forty nuclei) with diverse functions. Among these nuclei, the arcuate nucleus (ARC), the paraventricular nucleus (PVN), the lateral hypothalamic area (LHA), the dorsomedial nucleus (DMN), and the ventromedial nucleus (VMN) are the main structures involved in the nervous control of metabolism and food intake. The mediobasal hypothalamus (MBH) includes the association of VMN and ARC.

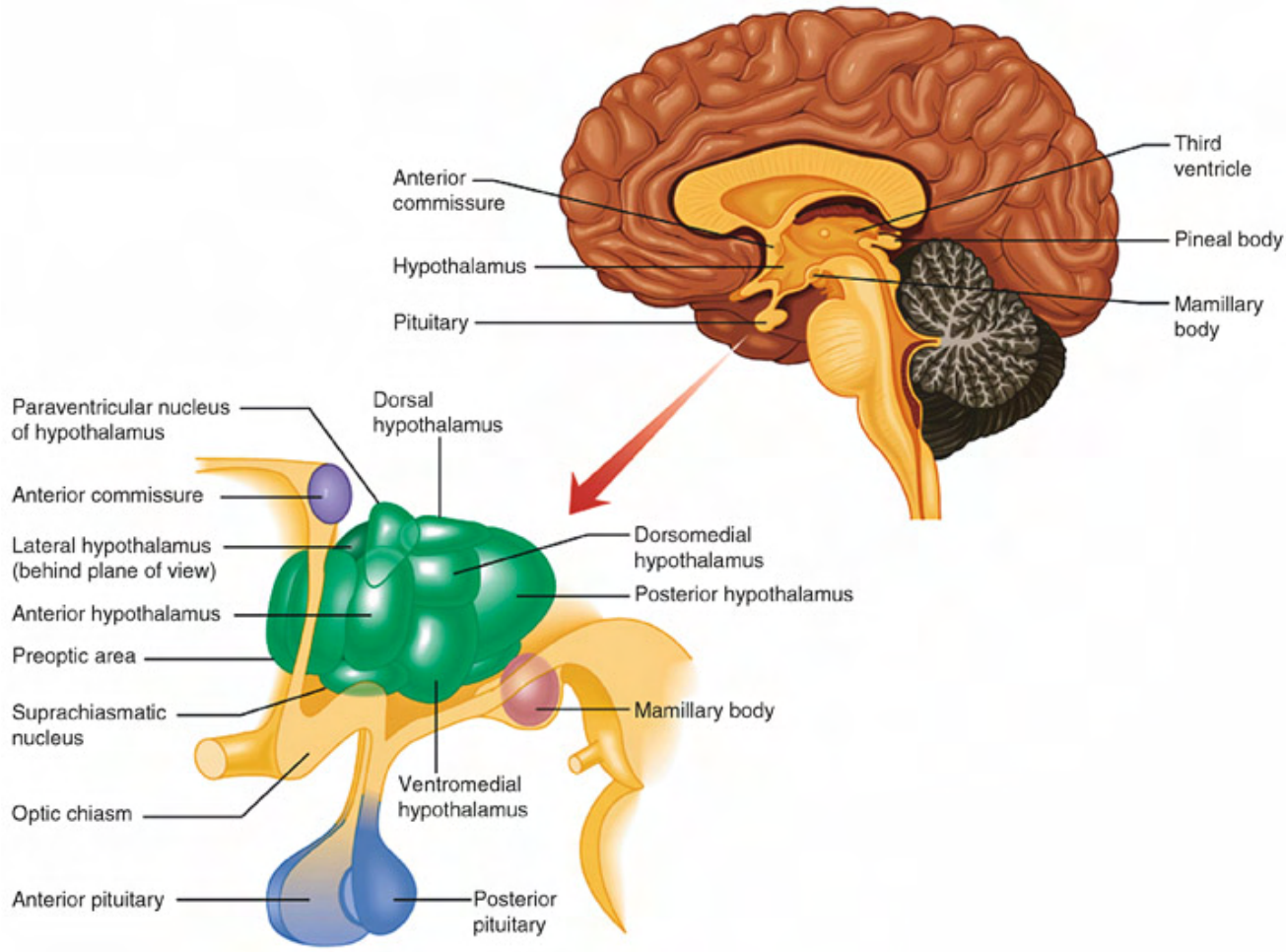

Figure 13. Anatomic localization and schematic representation of the human hypothalamic nuclei.

The human hypothalamus is a small deeply located region placed at the crossroad of neurovegetative, neuroendocrine, limbic, and optic systems.

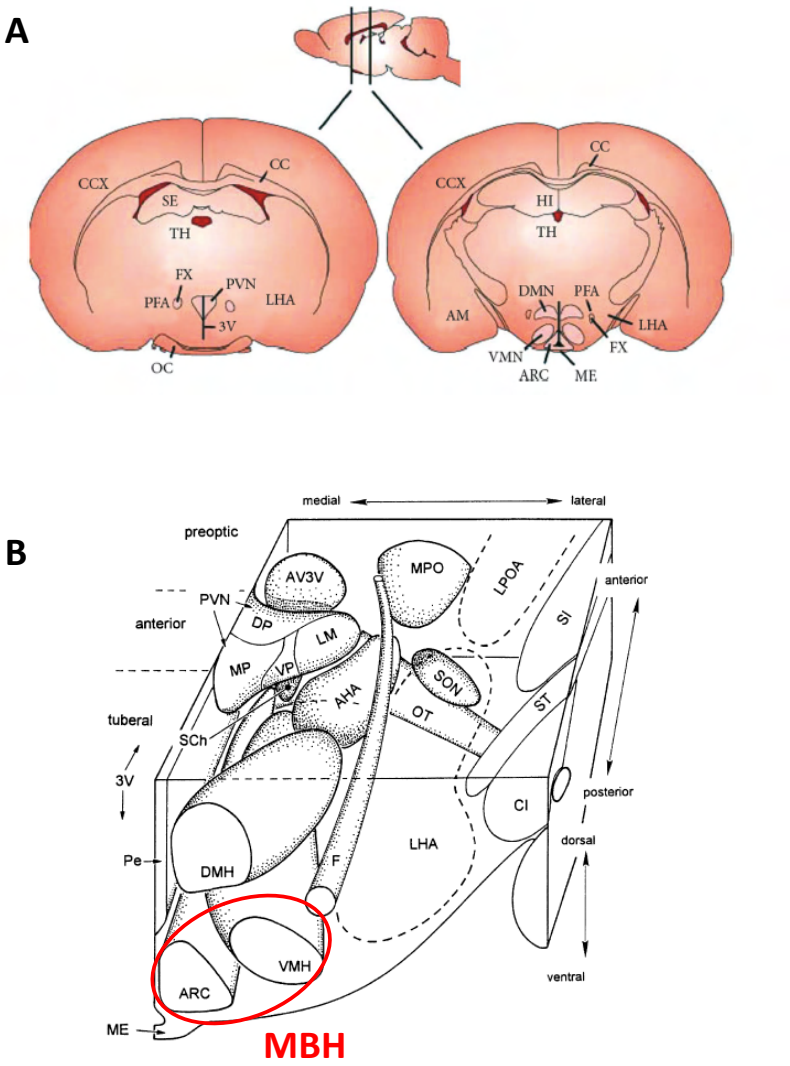

Figure 14. Schematic representation of a rodent brain showing the main hypothalamic regions involved in the regulation of glucose homeostasis.

(A) Two frontal sections showing the main hypothalamic nuclei involved in the regulation of glucose homeostasis.

(B) Three-dimensional view of rodent hypothalamus. View from dorsal and caudal of major hypothalamic nuclei in the right hemisphere of rodent hypothalamus.

Abbreviations: *ARC arcuate nucleus, AM amygdala, CC corpus callosum, CCX cerebral cortex, DMN dorsomedial nucleus, FX fornix, HI hippocampus, LHA lateral hypothalamic area, MDH mediobasal hypothalamus, ME median eminence, OC optic chiasm, PFA perifornical area, PVN paraventricular nucleus, SE septum, 3 V third ventricle, TH thalamus, VMN ventromedial nucleus.*

The involvement of the hypothalamus in the control of energy homeostasis was initially demonstrated, from the 1940, by experiments with induced hypothalamic lesions and electrical stimulation. Bilateral lesion of the MBH induces hyperphagia which leads to the development of obesity. On the other hand, the lesion of LHA causes the opposite effect, a decrease in food intake, while the stimulation of this brain area leads to the development of obesity. These works led scientists to define MBH as the "satiety center" and LHA as the "hunger center" (Elmquist et al., 1999).

In the periventricular region, there are nuclei involved in sensing circulating signals from blood or cerebrospinal fluid (CSF), including ARC, VMN, and PVN. In the middle region, the DMN receives many sensory inputs and forms multiple connections with other regions of the hypothalamus, just like the VMN(Bear et al., 2022).

The hypothalamic nuclei are interconnected with each other. The PVN receives afferents from ARC, VMN, DMN and LHA. VMN projects to ARC, PVN and LHA. The ARC projects to the DMN, PVN and LHA. The DMN receives inputs from ARC, VMN and LHA. LHA neurons project to many intra- and extra-hypothalamic areas, and form an interface between the hypothalamus and the limbic and cortical regions (Bear et al., 2022).

1.1.2. Importance of the mediobasal nucleus of the hypothalamus in glucose homeostasis:

The MBH plays a major role in detecting hypo- and hyperglycemia and initiating appropriate neuroendocrine responses. Several previous studies had attributed an important role to MBH in the detection of hypoglycemia and the initiation of the counter-regulatory responses. Indeed, a chemical lesion of the VMN strongly decreases the secretion of adrenaline, noradrenaline and glucagon in response to hypoglycemia, which allows a rapid return of blood glucose to its basal value (Borg et al., 1994).

Glucopenia induced by infusion of 2-Deoxyglucose (2-DG, a non-metabolizable glucose analogue, which blocks glycolysis and inhibits protein glycosylation) into the VMN results in a rapid rise in blood glucose concentrations and the secretion of glucagon and adrenaline (Borg et al., 1995). In

contrast, glucose infusion into the VMN during hypoglycemia reduces the release of adrenaline, noradrenaline and glucagon by 85% (Borg et al., 1997). These results suggest that MBH plays a role in 2 aspects of the counter-regulatory responses: adreno-medullary activation and glucagon secretion.

Furthermore, MBH is also involved in the detection of hyperglycemia. The injection of glucose specifically into the MBH leads to a decrease in food intake (Carneiro et al., 2012). The intracarotid injection of glucose towards the brain (known to activate certain ARC neurons) triggers insulin secretion through the activation of the vague nerve (Leloup et al., 2009).

Finally, the infusion of glucose into the MBH leads to an increase in the activity of sympathetic nerve fibers innervating the brown adipose tissue and would lead to an increase in thermogenesis (Sakaguchi and Bray, 1987).

To summarize, MBH, by its location and neurons connections, is a privileged area in the control of glucose homeostasis. Within this structure, many recent researchs highlighte the existence of neuronal populations involved in various processes of control of energy homeostasis (control of food intake, energy expenditure and regulation of glucose homeostasis), which constitutes the melanocortin system.

1.1.2.a. Arcuate nucleus:

The arcuate nucleus (ARC) is an important area of the hypothalamus involved in the control of energy homeostasis. It is situated below the ventromedial nucleus (VMN; Figures 13 and 14), on both sides of the third ventricle, and immediately adjacent to the median eminence (ME). This area has a contact with a fenestrated capillary, which represents a semi-permeable blood–brain barrier, and thus it is strategically positioned to sense hormonal and nutrient fluctuations in the bloodstream (Broadwell and Brightman, 1976).

In the ARC, there are two major populations of neurons controlling appetite and energy expenditure:

1) a subset of neurons that co-express orexigenic agouti-related peptide (AgRP) and neuropeptide Y (NPY);

2) a population of neurons that co-express the anorexigenic neuropeptides cocaine- and amphetamine-regulated transcript (CART (CARTPT)) and α-melanocyte-stimulating hormone (α-MSH, a product of proopiomelanocortin (POMC) processing).

These two neuron populations, together with downstream target neurons expressing the melanocortin receptor 4 (MC4R) and MC3R, constitute the central melanocortin system (Figure 15).

A. POMC/CART neurons:

The POMC gene produces two different peptides: melanoconocortin and β-endorphin. Melanocorticotropin can be divided into sub-peptides including corticotropin, α-, β- and γ-melanocyte-stimulating hormone (MSH). In the hypothalamus, α-MSH activates the MC3R and MC4R receptors to decrease food intake (Figure 15). Mice mutated for MC4R and/or MC3R are hyperphagic, and developed obesity and diabetes (Atalayer et al., 2010; Huszar et al., 1997). The natural antagonist of MC4R and MC3R is the AgRP. It blocks the α-MSH signaling pathway (Lu et al., 1994). Also, ICV injections of α-MSH had shown its anorexigenic potency (Edwards et al., 2000). Mice whose POMC gene expression is specifically inhibited in the hypothalamus via Cre-Lox technology (Xu et al., 2005) develop severe obesity. Furthermore, in humans, mutations in the POMC gene were detected and causes significant obesity (Krude et al., 1998). More recently, it has been shown that chronic activation specifically of ARC's POMC neurons (by optogenetics and DREADD) inhibits food intake and decreases body weight of animals (Aponte et al., 2011; Zhan et al., 2013).

B. NPY/AgRP neurons:

Interestingly, IVC injection of AgRP peptides causes prolonged hyperphagia and weight gain in rats (Rossi et al., 2011). In mice, specific ablation of ARC's AgRP neurons in adulthood, by expression of the diphtheria toxin receptor, induces anorexia while their progressive or neonatal

ablation does not induce major abnormalities of energy homeostasis in mice but just a slight weight loss (Luquet et al., 2005). This suggests the establishment of compensatory systems that can correct the absence of one or more orexigenic neuropeptides. Conversely, acute activation of AgRP neurons by optogenetics or DREADD is sufficient to trigger food intake, reduce energy expenditure and increase energy storage in fat tissue (Aponte et al., 2011; Krashes et al., 2011).

Furthermore, AgRP neurons of the ARC co-express NPY, and the injection of NPY into the PVN or 3rd ventricle in rats increases food intake while inhibiting energy expenditure and facilitating energy storage in the fatty tissue (Stanley and Leibowitz, 1984). In fact, NPY acts via its fixation on Y receptors (Lin et al., 2004). A recent study suggests that the effects of NPY on food intake would be relayed by both Y1 and Y5 receptors (Nguyen et al., 2012).

Finally, NPY/AgRP neurons also produce the GABA inhibitor neurotransmitter. The release of GABA following specific activation of AgRP neurons (by DREAAD) is sufficient to rapidly trigger food intake (Krashes et al., 2013). When synaptic release of GABA by NPY/AgRP neurons is stopped, mice energy expenditure is increased, and animals become thin and resistant to obesity (Tong et al., 2008).

C. Interconnections of NPY/AgRP and POMC/CART neurons:

POMC neurons are in contact with NPY/AgRP neurons. NPY/AgRP neurons directly inhibit POMC neurons through GABA(Atasoy et al., 2012; Cowley et al., 2001). In addition, the presence of MC3R on POMC neurons suggests that AgRP neurons can inhibit POMC neurons through this signaling pathway (Bagnol et al., 1999; Sánchez-Lasheras et al., 2010).

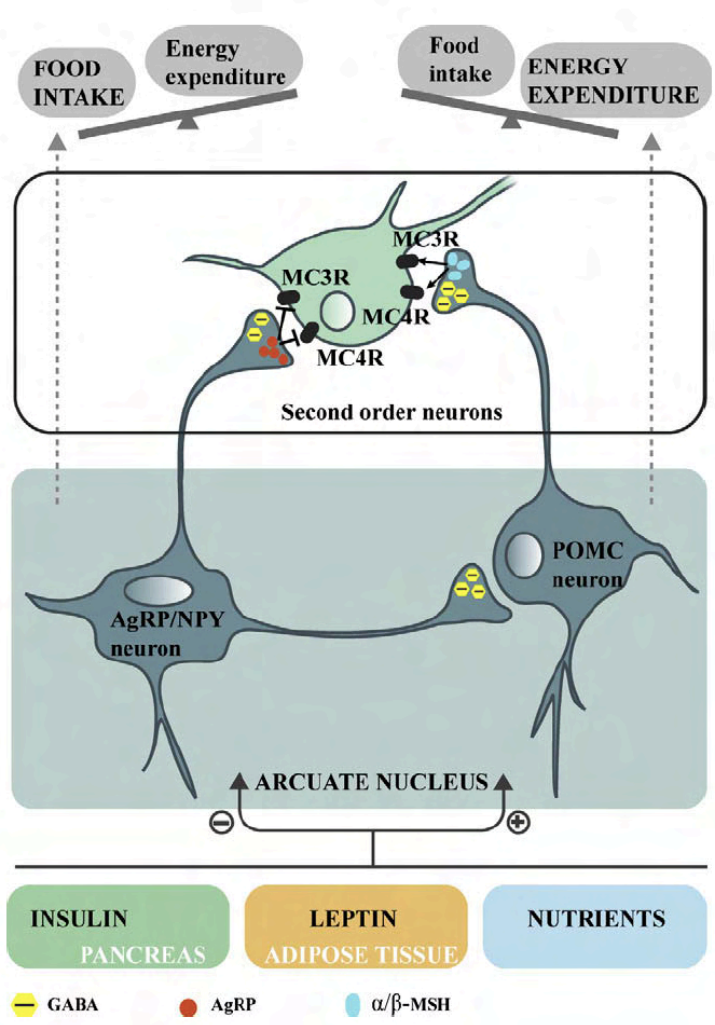

Figure 15. Regulation of energy homeostasis by POMC and AgRP neurons through the melanocortin system (adapted from : Sánchez-Lasheras et al., 2010).

POMC and AgRP localize in the ARC, close to the blood brain barrier, where they have access to various humoral signals. Both neuron populations exert potent effects on energy balance mediated by their characteristic neuropeptides, which allow the modulation of second order neurons. α- and β-MSH act on the MC3R and MC4R to ultimately reduce food intake and increase energy expenditure. AgRP acts as a MC3R and MC4R antagonist and therefore promotes the opposite responses. GABAergic inhibition has been described from both POMC and AgRP neurons to effector neurons as well as from AgRP neurons to POMC neurons.

Abbreviations; GABA: gamma-aminobutyric acid, AgRP: agouti-related peptide, a/b-MSH: alpha and beta melanocyte-stimulating hormone.

1.1.2.b. Ventromedial nucleus:

Ventromedial nucleus (VMN) receives projection from the AgRP and POMC neurons of the ARC. In turn, VMN neurons project into hypothalamic and extrahypothalamic areas such as the brainstem (Figure 16) (Cheung et al., 2013). Many genes are expressed in the VMN. The steroidogenic factor 1 (Sf1) is one of theme, which is directly implicated in the development of the VMN (Davis et al., 2004; Parker, 2002). As demonstrated by the metabolic phenotypes of conditional KO mice, SF1 expressing neurons play significant roles in the control of energy balance (Bingham et al., 2008; Zhang et al., 2008). Additionally, the brain-derived neurotrophic factor (BDNF) is another abundantly expressed protein in the VMN. The lack of BDNF or its receptor leads to hyperphagia and obesity in humans and mice (Lyons et al., 1999; Yeo et al., 2004). Interestingly, previous pre-clinic studies reported that the central or peripheral administration of BDNF resulted in the loss of body weight and reduction in food intake through MC4R signaling (Xu et al., 2003). The VMN also plays a key role in the regulation of thermogenesis (Kim et al., 2011; López et al., 2010; Martínez de Morentin et al., 2012; Whittle et al., 2012).

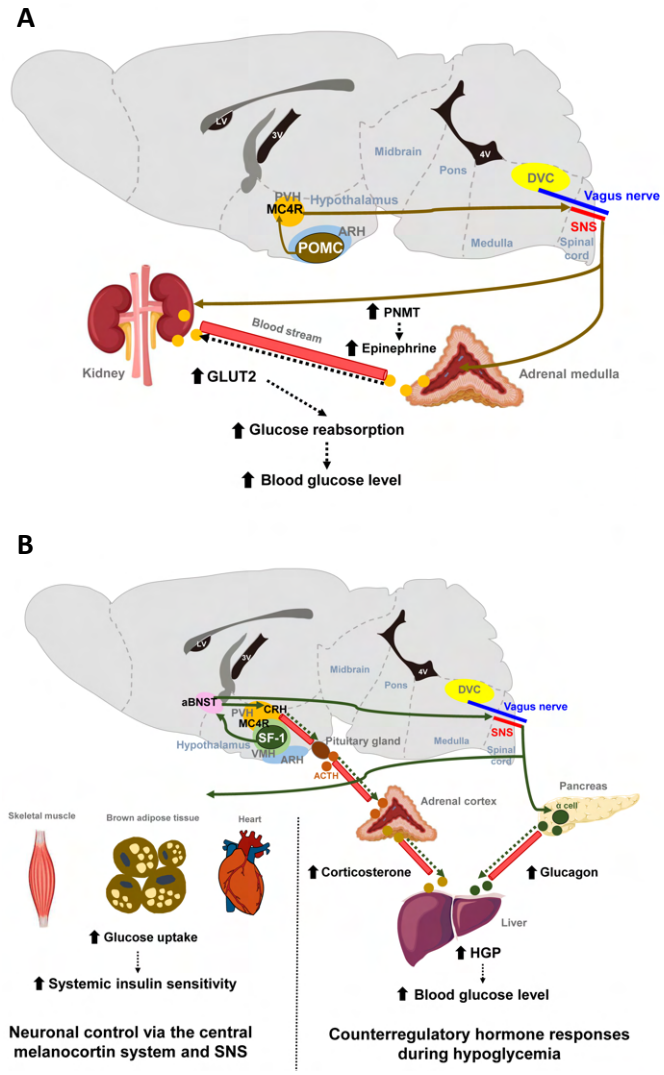

Figure 16. Representative neurons and their neural circuits that regulate various aspects of glucose metabolism (adapted from: Choi and Kim, 2022).

During hypoglycemia: (**A**) proopiomelanocortin-expressing (POMC) neurons in the arcuate nucleus (ARH or ACR) of the hypothalamus promote renal glucose reabsorption by increasing glucose transporter 2 (GLUT2) expression in the kidney via paraventricular hypothalamus (PVH) melanocortin receptor-4 (MC4R) neurons and the sympathetic nervous system (SNS). This regulation occurs directly to the kidney and also indirectly through increased circulating epinephrine by increased phenylethanolamine N-methyltransferase (PNMT) expression in the adrenal medulla. (**B**) steroidogenic factor-1 expressing (SF-1) neurons in the ventromedial hypothalamus (VMH) promote HGP through the secretion of counterregulatory hormones (e.g., glucagon and corticosterone), while they improve insulin sensitivity by increasing glucose uptake in skeletal muscle via the central melanocortin system−SNS.

ACTH, adrenocorticotropic hormone; DVC, dorsal vagal complex; LV, lateral ventricle; 4V, fourth ventricle.

1.1.3. Role of brainstem in the regulation of glucose homeostasis:

Interestingly, the brainstem through the dorsal vagal complex (DVC) play a crucial role for sensing glucose fluctuations and regulating glycemic levels and food intake (Grill and Hayes, 2012; Ritter et al., 2011). The DVC includes the dorsal motor nucleus of the vagus (DMV), the nucleus tractus solitarius (NTS), and the area postrema (AP). Meal-related signals from the gastrointestinal tract are relayed to the NTS and the AP through the sensory vagus nerve (Schwartz, 2000). Similarly to the hypothalamic neurons, NTS neurons produce appetite-regulating peptides such as POMC, NPY, and glucagon-like peptide 1 (GLP-1) (Georgescu et al., 2020; Mercer et al., 1998). The POMC neurons located at the NTS are involved in the short-term regulation of feeding, nonetheless the destruction of these neurons neither alters glucose metabolism nor body weight (Zhan et al., 2013). MC4R is also expressed in the brainstem neurons. Conversely, the deletion of MC4R genes in both sympathetic and parasympathetic neurons impaired glucose homeostasis (Berglund et al., 2014), whereas the re-expression of MC4R gene modestly reduced body weight gain without altering food intake and was sufficient to attenuate hyperglycemia and hepatic glucose production (Rossi et al., 2011). These findings indicate the involvement of brainstem MC4R signaling in the central regulation of glucose metabolism. Additionally, GABAergic neurons located at the NTS sense hypoglycemia and then support recover from hypoglycemia via DMV projections and the parasympathetic stimulation of hepatic glucagon secretion (Xu et al., 2021). Contrariwise, the NTS receives energy-intake signals from gut, which it then transfers them to the hypothalamus through to the DMV (short-loop), or to the parabrachial nucleus (PBN) (long-loop) in order to generate satiety (Wu et al., 2009).

1.2.Contribution of central insulin signaling to systemic glucose metabolism:

Interestingly, insulin receptor (IR) and its downstream signaling molecules, insulin receptor substrate 1 and 2 (IRS1/IRS2), are expressed in brain regions including the hypothalamus (Kleinridders et al., 2014). Moreover, it was reported that neuron-specific IR knockout (NIRKO) mice exhibited mild obesity and insulin resistance. Several previous studies suggested that central insulin signaling improves peripheral glucose metabolism. For example, insulin-induced suppression of hepatic glucose production was reported to be attenuated when the brain IR and its downstream signaling were inhibited (Obici et al., 2002). Moreover, insulin infusion into the cerebroventricle was shown to suppress hepatic glucose production and this effect was transmitted to the liver through hepatic vagal innervation and the α7-nicotinic acetylcholine receptor (Kimura et al., 2016). Consequently, hepatic glucose production is suppressed by insulin through the CNS and via vagus nerve-mediated mechanisms. AgRP neurons of the ARC mediate this central effect of insulin on hepatic glucose production, given that the restoration of IR in AgRP neurons from a generalized IR null mice rescues the ability of insulin to suppress hepatic glucose production (Könner et al., 2007).

Interestingly, Soto et al., in a recent study reported that the hippocampal deletion of IR/IGF1R in male mice was associated with the development of impaired glucose tolerance due to a systemic insulin resistance and a decrease in insulin secretion (Soto et al., 2019). Furthermore, a recent publication from our laboratory suggested that tau deletion promotes brain insulin resistance, and tau KO mice exhibited hippocampal insulin resistance with impaired glucose homeostasis (Marciniak et al., 2017).

2. Glucose-sensing mechanisms and the control of glucose homeostasis:

2.1.Glucose-sensing mechanisms in the hypothalamus:

The central nervous system is structurally and functionally heterogeneous. It is composed by 2 major cell types, neuronal cells and glial cells. In the central nervous system glucose by itself acts as an important afferent signal to the brain.

The brain is isolated and protected from blood circulation by the blood–brain barrier (BBB). The endothelial cells forming the cerebral vessels and capillaries are linked together by tight junctions ensuring selective permeability. Since glucose is a water-soluble molecule, it does not enter freely into brain cells. Its passage from the blood compartment to the nervous parenchyma is ensured by specific proteins, glucose transporters (GLUTs). Furthermore, GLUTs allow glucose to enter the different CNS cell populations. There are 14 GLUTs proteins discovered in human (Holman, 2020).

Glucose transport to the brain is constantly performed by the GLUT1 transporter. It is expressed by the endothelial cells of the BBB and the glial cells, including the tanycytes of the median eminence and the hypothalamic astrocytes (Chari et al., 2011; Peruzzo et al., 2000; Pooja Naik, 2014). At the level of the BBB, GLUT1 is expressed on the luminal and apical surface of the endothelial cells allowing diffusion according to the concentration gradient of glucose (Figure 17).

GLUT2 is distinguished from other isoforms by its low affinity for glucose. It carries glucose in proportion to its circulating concentration and is not saturated when blood glucose increases. It is also found in some MBH neurons and tanycytes (Kang et al., 2004; Orellana et al., 2012).

GLUT3 is the main carrier of neuronal glucose. With a Km around 1 to 3 mM, GLUT3 is saturated at most cerebral glucose levels allowing a relatively constant supply of glucose to neurons under physiological conditions (Simpson et al., 2008).

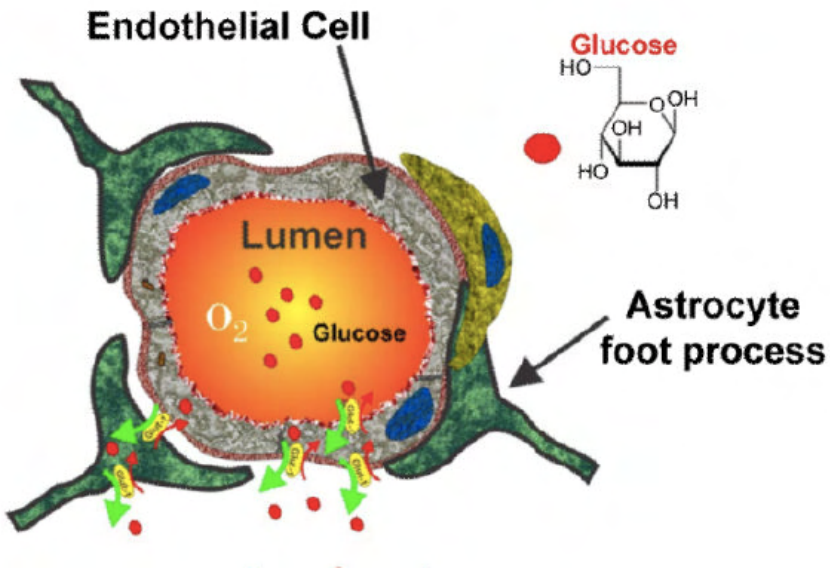

Figure 17. Glucose transport across the blood–brain barrier (BBB) (adapted from Pooja Naik, 2014).

Glut1 transporters is located on microvascular endothelial cells and astrocytes transport glucose across the BBB, while Glut-3 transports glucose is in neurons.

Glucose-sensing mechanisms in the hypothalamus involves neuronal and non-neuronal sensing mechanisms. Silver and Erecinska were the first to measure the variations of extracellular glucose levels in the brain by varying peripheral blood glucose concentrations. They show in the anaesthetized rat that a basal blood glucose of 7.6 mM corresponded to a brain concentration of only 2.4 mM. Also, they reported that extracellular glucose levels in the central nervous system increased in hyperglycemia and decreased in hypoglycemia, paralleling to the changes in blood glucose concentrations (Silver and Erecinska, 1994).

2.1.1. Neuronal glucose-sensing:

Glucose-sensing neurons can be categorized as glucose-excitatory (GE) and glucose-inhibitory (GI) neurons (Figure 18). GE neurons are found in many hypothalamic regions including the ARC, VMN, anterior hypothalamus, paraventricular nucleus, and the lateral hypothalamus (Routh et al., 2014). GE neurons are activated when the extracellular glucose level rises and inhibited otherwise.

While the ARC is adjacent to the median eminence (ME), ARC neurons are the initial neurons to sense the changes in blood glucose. Previous studies in rodents have indicated that POMC neurons are GE, and about 40% of AgRP/NPY neurons are GI (Choi and Kim, 2022). GE neurons were also discovered in the VMH and the PVH, which are critically implicated in satiety generation (Dunn-Meynell et al., 1998). Conversely, GI neurons are distributed in the LH, which is known as a hunger center (Oomura et al., 1969; Routh et al., 2014).

The molecular basis of glucose-sensing in GE neurons is comparable to the glucose-sensing mechanism in pancreatic β-cells [(Fig. 2A, left panel; (Ashford et al., 1990)]. In GE neurons, glucose penetrates the neurons through GLUT2, 3, and 4. Upon uptake, glucose is converted to glucose-6-phosphate by glucokinase (GK) and then undergoes glycolysis and mitochondrial oxidation, resulting in adenosine triphosphate (ATP) production. An increased cellular ATP/adenosine diphosphate (ADP) ratio leads to the closure of ATP-dependent potassium channel (KATP), depolarization of membrane potential, Ca2+ influx through voltage-dependent calcium channel (VDCC), finally the release of neurotransmitter (Marty et al., 2007).

By contrast to GE neurons, GI neurons are activated when the extracellular glucose level decreases, however, a little is known about the underlying mechanism. Similarly, to GE neurons, GI neurons express the same GLUTs and GK (Routh et al., 2014). Close to GE neuron, glucose penetrates glucose-inhibitory (GI) neuron via GLUT2/3/4 and increases the intracellular ATP/adenosine monophosphate (AMP) ratio. Nevertheless, this leads to the inhibition of GI neurons activity possibly through stimulation of the Na+/K+-ATPase activity or opening of Cl− channels

through suppression of adenosine monophosphate kinase (AMPK) and nitric oxide (NO) production [(Fig. 2A, right panel; (Choi and Kim, 2022; Oomura et al., 1974)].

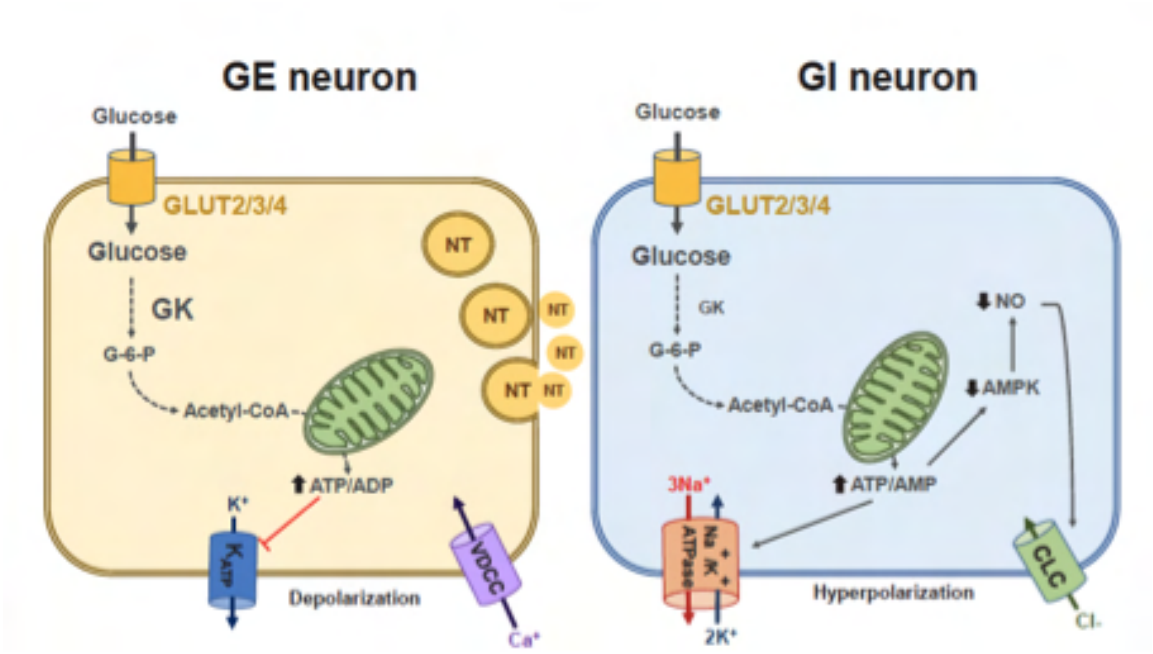

Figure 18. Molecular mechanisms of glucose-sensing in hypothalamic neurons (adapted from Choi and Kim, 2022).

Glucose-sensing mechanisms in hypothalamic neurons. In glucose-excitatory (GE) neurons, glucose penetrates the neuron via glucose transporter (GLUT) 2/3/4 and increases the intracellular adenosine triphosphate (ATP)/adenosine diphosphate (ADP) ratio, resulting in the closure of ATP-dependent potassium channel (KATP), depolarization of membrane potential, Ca2+ influx through voltage-dependent calcium channel (VDCC), finally releasing neurotransmitter (left panel). Close to GE neuron, glucose penetrates glucose-inhibitory (GI) neuron via GLUT2/3/4 and increases the intracellular ATP/adenosine monophosphate (AMP) ratio. However, this leads to the inhibition of GI neurons activity possibly through stimulation of the Na+/K+-ATPase activity or opening of Cl− channels through suppression of adenosine monophosphate kinase (AMPK) and nitric oxide (NO) production (right panel).

2.1.2. Non-neuronal glucose-sensing:

Recent studies indicate an involvement of non-neuronal cells like tanycytes in brain glucose-sensing. Tanycytes are specialized ependymal cells surrounding the third cerebroventricle and have 4 subtypes: α1, α2, β1, and β2 (Prevot et al., 2021). Tanycytes are a polarized cells, as their long processes project and contact the neurons in the VMH (α1) and ARC (α2 and β1), or the fenestrated blood vessels in the ME (β2), and their cell body faces the cerebroventricular side [Figure 19; (Prevot et al., 2021)]. They also express the glucose-sensing molecules GLUT2, GK, and KATP channels and may sense glucose in the cerebrospinal fluid (CSF) which is derived from the blood across the blood–CSF barrier (Freire-Regatillo et al., 2017).

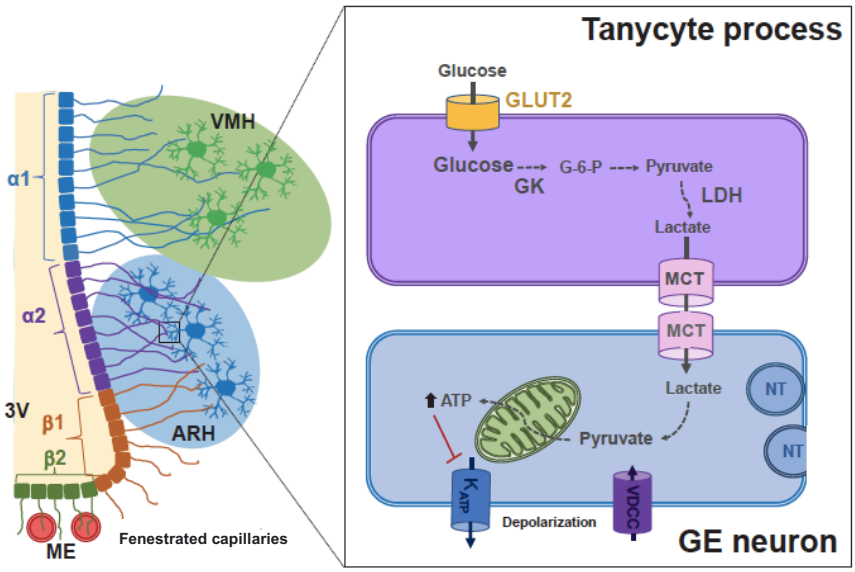

Figure 19. Glucose-sensing mechanisms mediated by hypothalamic tanycytes. (adapted from : Choi and Kim, 2022).

Glucose penetrates hypothalamic tanycytes through GLUT2 and transforms to lactate via glucokinase (GK) and lactate dehydrogenase (LDH). Tanycyte-produced lactate is released via monocarboxylate transporter (MCT) 1/4 and taken by adjacent neurons via MCT2. In the GE neuron, lactate converts to pyruvate, that produces ATP, and depolarizes neuron action potential via inhibition of K^{ATP} channels.

ARC arcuate nucleus, VMH Ventromedial hypothalamus.

As described in Figure 19, tanycytes may play a role in glucose uptake from the CSF through GLUT2 and then release lactate via monocarboxylate transporter, that produces ATP, and depolarizes neuron action potential via inhibition of K^{ATP} channels (Lhomme et al., 2021). In vitro study showed that the selective destruction of tanycytes via the intracerebroventricular injection of alloxan inhibited the counterregulatory responses to hypoglycemia without damaging ARC neurons (Sanders et al., 2004).

2.3.Peripheral Glucose-sensing mechanisms implicated in glucose homeostasis:

2.3.1. Glucose-sensing mechanisms in pancreatic islets:

The pancreas is composed of both an exocrine component (responsible for the release of digestive enzymes into the gastrointestinal lumen), and a smaller endocrine component composed of the islets that are responsible for the regulated release of a variety of hormones into the circulation. The mature pancreatic islet consists of several types of endocrine cells (Figure 20). The most important are the insulin-secreting β-cells (which make up 75% of cells in the mouse, and 50% in human islets), the glucagon-releasing α-cells (15–20% in mice, and 35–40% in human). Moreover, pancreatic islets are extensively innervated by cholinergic, and adrenergic nerve branches (Rorsman and Ashcroft, 2018). In pancreatic islets both α and β cells are Glucose-sensing cells.

A. Glucose sensing by pancreatic β-cells:

The β-cells are the principal component of the pancreatic islets in all species. The major stimulator for insulin secretion in pancreatic β-cells is glucose, with other nutritional and neuronal signals modulating the response. As represented in Figure 21, insulin biogenesis is initiates with the synthesis of preproinsulin in rough endoplastic reticulum and conversion of preproinsulin to proinsulin. After, proinsulin will be packaged in the Trans-Golgi Network and sorted into immature secretory granules, a process termed sorting for entry. These immature granules become acidic through ATP-dependent

proton pump and proinsulin undergoes proteolytic cleavage resulting the formation of insulin and C-peptide. During the granule maturation process, insulin is crystallized with zinc and calcium in the form of dense-core granules and unwanted cargo and membrane proteins undergo selective retrograde trafficking to either the constitutive trafficking pathway for secretion or to degradative pathways (Hou et al., 2009).

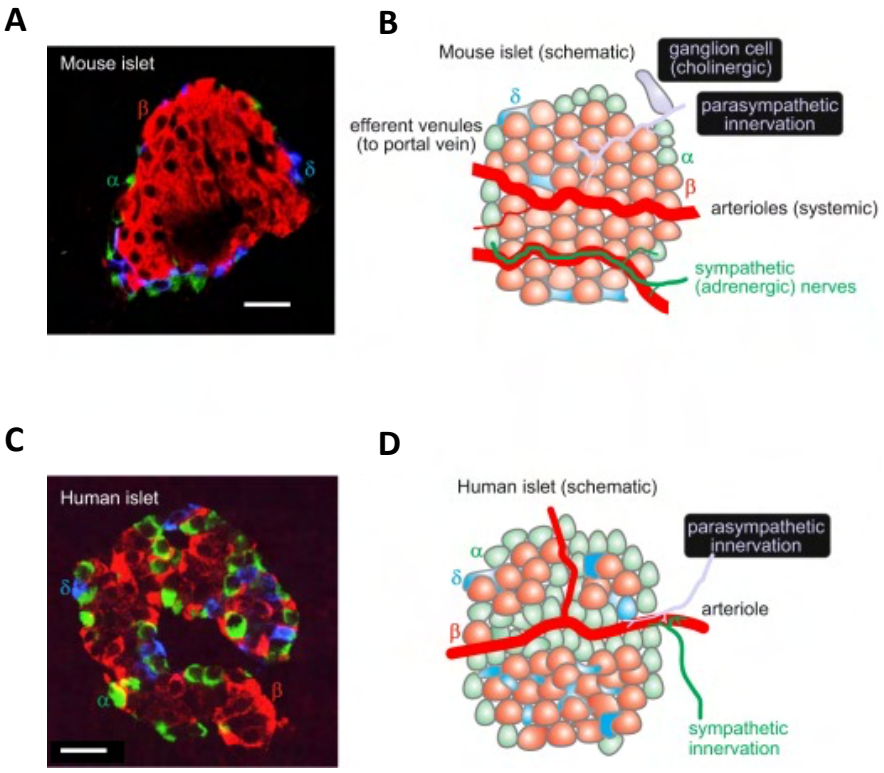

Figure 20. Schematic representation of mouse and human pancreatic islets. (adapted from Rorsman and Ashcroft, 2018).

A and C: immunohistochemistry of mouse (A) and human (C) pancreatic islets (red, insulin; green, glucagon; blue, somatostatin). Scale bars: 20 μm

B and D: schematic of mouse (B) and human (D) islets highlighting differences in blood supply, innervation, and islet cell distribution. The α- (green), β- (red), and δ-cells (blue) are indicated.

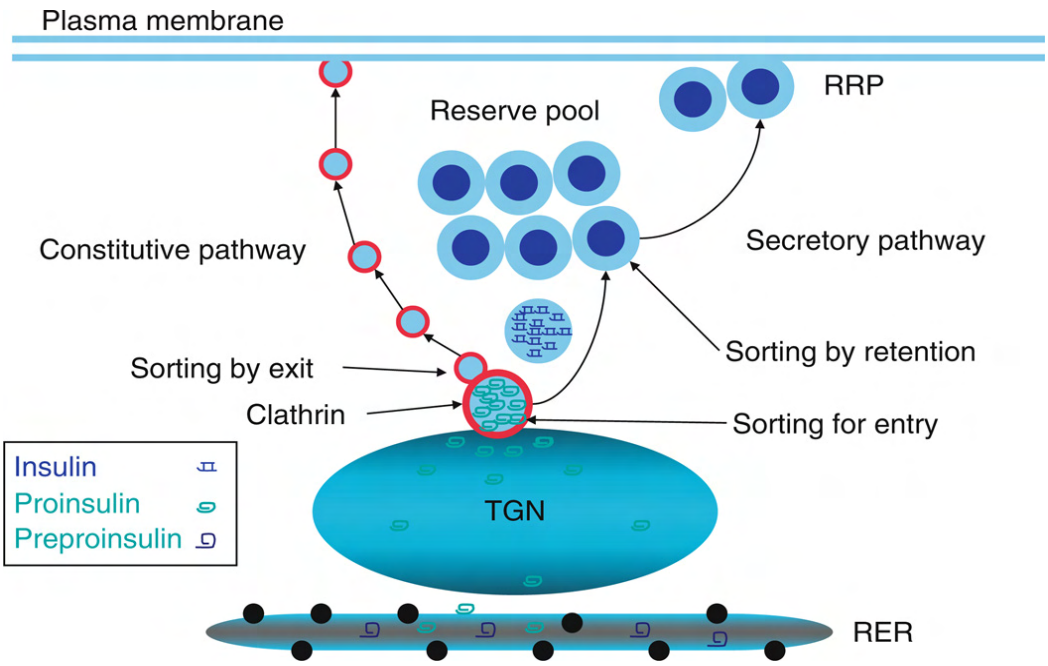

Figure 21. Schematic representation of Insulin biogenesis (adapted from Hou et al., 2009).

Preproinsulin is synthesized in rough endoplasmic reticulum (RER) and is converted to proinsulin. Proinsulin is later transported to Trans-Golgi Network (TGN) and packed into immature granule via sorting for entry. In the TGN cargo molecules destined for constitutive (unregulated secretion) are packaged into small transport vesicles that either directly traffic to and fuse with the plasma membrane or alternatively enters the constitutively recycling endosome system and thereby traffic to the plasma membrane. In parallel, proinsulin is converted to insulin and condensation/crystallization (sorting by retention) happens.

During the secretory granule maturation, proinsulin converts to insulin by excision of the C-peptide through proteolysis by endoproteases or roprotein convertase (PC1/3 and PC2), followed by trimming C-terminal by carboxypeptidase E. The conversion of (Zn2+)2(Ca2+)(Proinsulin)6 to (Zn2+)2(Ca2+)(Insulin)6 significantly decreases the solubility of the hexamer leading to crystallization within the lumen of the granule and formation of the dense-core granule. The newly

formed mature dense-core insulin granules colonize two different intracellular pools, the readily releasable pools (RRP) and the reserved pool. These two distinct pools are thought to be responsible for the biphasic nature of insulin release in which the RRP granules are associated with the plasma membrane and undergo an acute calcium-dependent release accounting for first phase insulin secretion. In contrast, second phase insulin secretion requires the trafficking of the reserved granule pool to the plasma membrane (Hou et al., 2009).

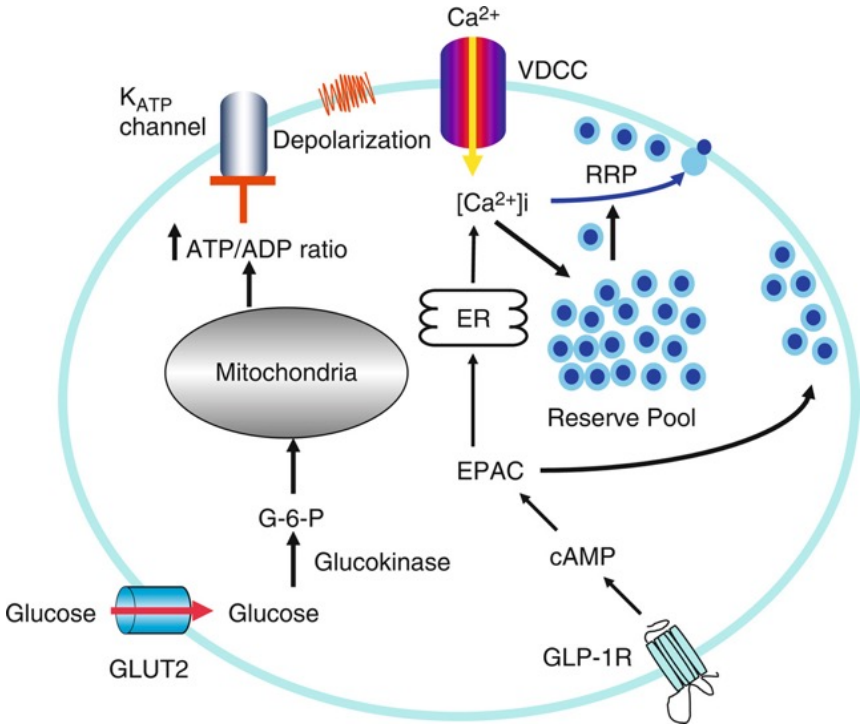

Figure 22. Schematic representation of insulin secretion granules by β cells (adapted from Hou et al., 2009).

Glucose, the major stimulant, through glycolysis and mitochondrial ATP energy production increases the ATP/ADP ratio that leads to the closure of the ATP-sensitive K+ (KATP) channels. The subsequent cellular depolarization activates voltage dependent calcium channels resulting in extracellular Ca2+ influx and fusion of insulin granules with the plasma membrane. The incretin hormone GLP-1 acts on its receptor at β cell plasma membrane to activate adenylyl cyclase and increase intracellular cAMP levels. In turn, cAMP binds and activates protein kinase A and Exchange Protein Directly Activated by cAMP (EPAC). EPAC then functions to increase intracellular calcium level from intracellular calcium stores in the endoplasmic reticulum and to increase the number of readily releasable pool of insulin granules at the plasma membrane. The combination of these two processes results in a potentiation of insulin secretion.

In response to increased blood glucose level, glucose enters in β cells via the glucose transporter GLUT2 [(Figure 22); (Thorens, 2015)]. Once in the β cell, glucose is phosphorylated to glucose-6-phosphate (G6P) by a glucokinase (GK). Therefore, phosphorylated glucose follows the glycolysis pathway and then the Krebs cycle in the mitochondria. This leads to an increase in the cytosolic ATP/ADP ratio and closure of the K^{ATP} potassium channels. Consequently, the membrane depolarizes and leads to the opening of calcium channels voltages dependent. Increased intracellular calcium concentration triggers the exocytosis of insulin granules. Each β cell contains 5,000 to ≥10,000 insulin secretory granules, and acute glucose stimulation causes exocytosis of only 1–2% of this pool (Thurmond and Gaisano, 2020). This is the principal mechanism of insulin release. Additionally, β cells are also influenced by the SNA that innervates it. The parasympathetic SN triggers insulin secretion through acetylcholine, which acts on the muscarinic type 3 receptor. Conversely, the sympathetic SN inhibits insulin secretion via noradrenaline, which binds to the β2 adrenergic receptor (Thorens, 2011).

B. Glucose sensing by pancreatic α-cells:

Glucagon is a hormone secreted by pancreatic α-cells, and it contributes to the maintenance of normal blood glucose concentration by inducing hepatic glucose production in response to declining blood glucose (Figure 23). Also, glucagon is released from pancreatic α-cells in response to other stimuli like amino acids, adrenaline (epinephrine), and some neurotransmitters (Gromada et al., 2007).

The direct sensing of decreased in glucose concentrations by the α cell appears to be of little importance, alone, in glucagon secretion. Indeed, a lesion of VMN in rats decreased by about 80% the secretion of glucagon in response to severe hypoglycemia [(Figure 24); (Borg et al., 1994)].

However, it is evident that glucose is also able to control glucagon release in denervated preparations, such as isolated islets (Vieira et al., 2007; Zhang et al., 2013).

Non-neuronal control of glucagon secretion may be indirect and mediated by glucose-regulated release of paracrine factors from β and δ cells that influence α cell function. Therefore, insulin, Zn^{2+} and the neurotransmitters serotonin, γ-aminobutyric acid and its metabolite γ-hydroxybutyrate from β cells were reported to suppress glucagon secretion (Almaça et al., 2016; Ishihara et al., 2003; Li et al., 2013; Östenson, 1979; Wendt et al., 2004).

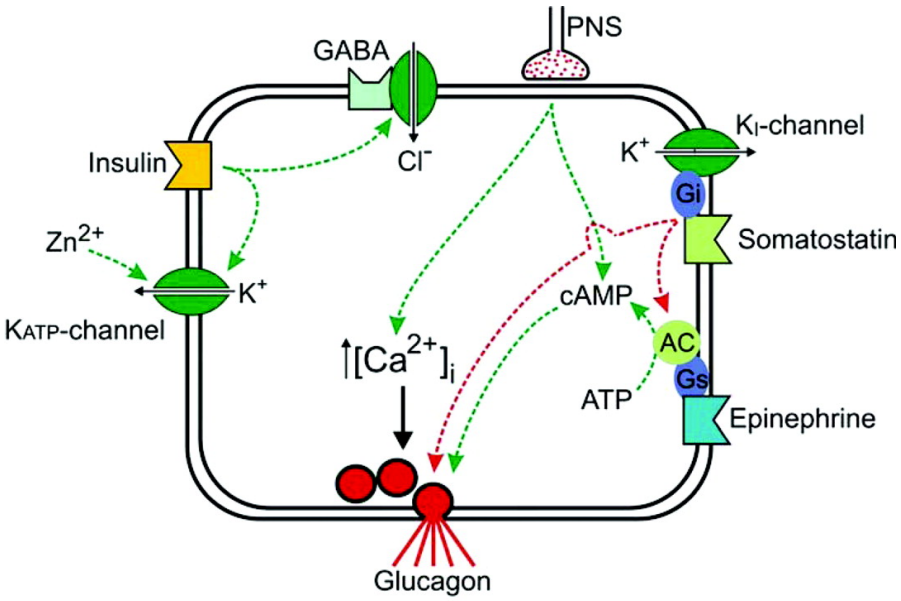

Figure 23. Schematic representation of the main physiological regulators of α-cell function and glucagon secretion. (adapted from Gromada et al., 2007).

Schematic representation summarizing site of action and intracellular signaling mechanisms for main physiological modulators of α-cell stimulus-secretion coupling. Green dotted lines depict activation, whereas red dotted lines represent inhibition of ion channel activity or intracellular signaling pathways.
Abbreviations: AC, Adenylate cyclase; Gs, stimulatory G protein; Gi, inhibitory G protein; PNS, parasympathetic nervous system.

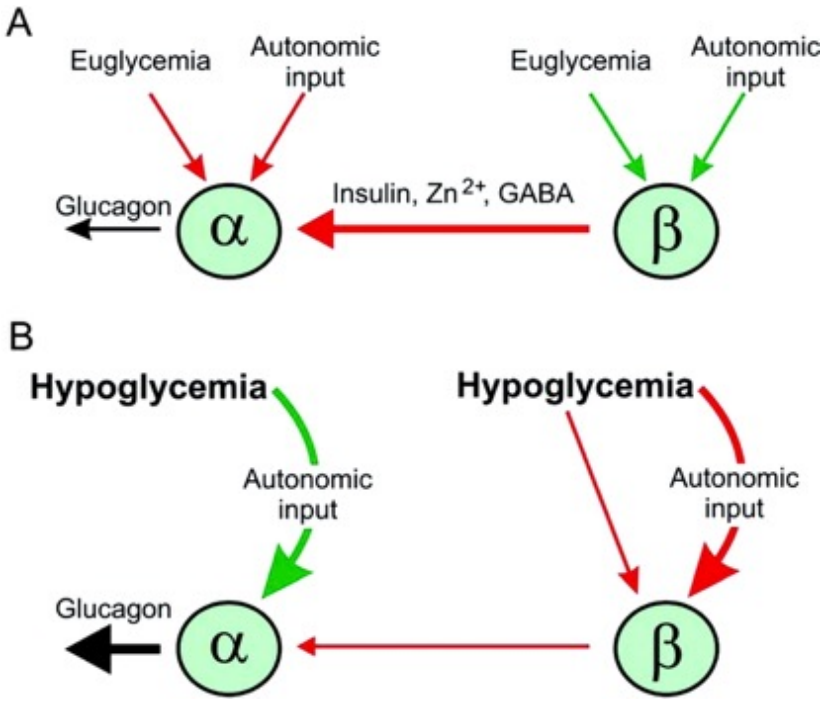

Figure 24. Schematic representation of the mechanisms involved in the regulation of glucagon release in response to hypoglycemia (adapted from Gromada et al., 2007).

(A)Throughout euglycemia, glucagon secretion could be suppressed (thin arrow) as a result of: 1) the lack of autonomic stimulation, including adrenergic stimulation of the α-cell; and 2) a marked paracrine inhibition by factors released from β-cells (and δ-cells, not indicated in figure) within the islet. Green arrows indicate stimulatory pathways, whereas red arrows symbolize inhibitory pathways.

(B) During hypoglycemia, glucagon secretion is increased (thick arrow). This may arise from a marked reduction of the paracrine inhibitory effects (including α2-adrenergic receptor activation in β-cells) as well as a stimulatory action of the autonomic nervous system (involving β-adrenergic receptor activation in α-cells) secondary to its activation by central hypoglycemia.

Additionally, in the periphery, important glucose sensors have been identified in the carotid bodies, and portal-mesenteric vein

2.3.2. Glucose sensing by the hepatic portal vein:

After a meal, nutrients are absorbed through the intestine, collected and transported by mesenteric capillaries to the hepatic portal vein before reaching the liver and blood circulation. A system of plasma glucose-sensing in the portal vein plays a key role in glucose homoeostasis. Connected to the lateral hypothalamus nucleus through the fibers of the vagus nerve, the system allows the body to adapt its response to any variation of portal glycaemia (Burcelin et al., 2000a; Delaere et al., 2010). Also, hepatic portal vein is implicated in the detection hypoglycemia (Saberi et al., 2008). Previous Animal studies have recurrently showed that blocking portal glucose sensing through portal glucose infusion (Donovan et al., 1994) or denervating the portal vein (Fujita et al., 2007) markedly suppresses the sympathoadrenal response to hypoglycemia. Although the cellular and molecular mechanisms involved in glucose detection are not clearly identified, GLUT2 appears to play an essential role (Burcelin et al., 2000b). More recently, it was suggested that the Sodium Glucose Cotransporter 3 (SGLT3) would also be involved (Delaere et al., 2013).

2.3.3. Glucose sensing by carotid body glomus cells:

The carotid body is a chemoreceptor structure in which glomus cells sense changes in blood O_2, CO_2, pH levels, and also was reported to detect hypoglycemia in both non-primate mammals and humans [(Figure 25A); (Gao et al., 2014; Nurse and Piskuric, 2013)]. Carotid body glomus cells are connected to the nerve fibers of the vague nerve, they play an important role in the activation of the glucose counterregulatory responses to hypoglycemia. Indeed, their removal in dogs altered the release of glucagon and cortisol in response to insulin-induced hypoglycemia (Koyama et al., 2000). Additionally, it was reported that the effects of physiological hypoglycemia in the carotid body are mediated through a direct action of low glucose on chemoreceptors for type I glomus cells (Figure

25B). This action leads to a depolarizing receptor potential and release of the fast acting excitatory neurotransmitters ATP and acetylcholine, which stimulate afferent sensory nerve endings and increased impulse activity in the CSN (Zhang et al., 2007).

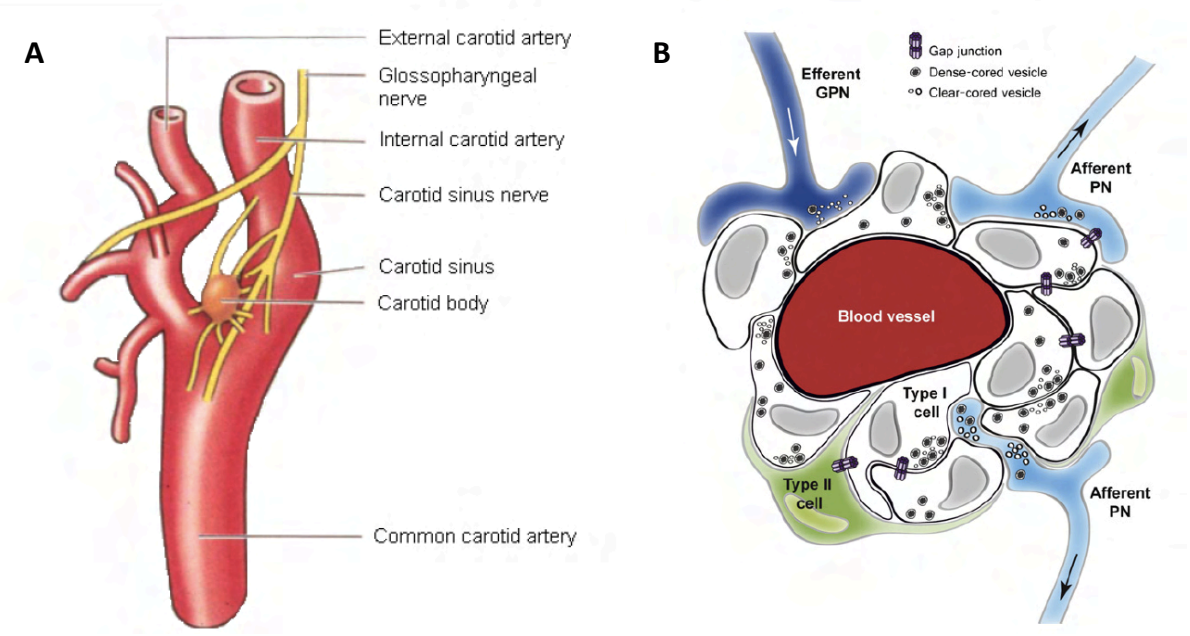

Figure 25. Anatomical localization, organization and innervation of the carotid body (adapted from: Nurse and Piskuric, 2013).

(A) Anatomy of the right carotid artery with carotid body. **(B)** Schematic representation showing the innervation of chemoreceptor (type I) cell clusters by afferent fibers from petrosal neurons (PNs) and efferent fibers from the glossopharyngeal nerve (GPN). The mammalian carotid body consists of clusters of parenchymal chemoreceptor type I (glomus) cells interdigitated by glia-like type II cells.

3. Peripheral Hormones involved in brain regulation of glucose metabolism:

Interestingly, serval peripheral hormones like leptin, glucagon-like peptide 1 (GLP-1), and glucagon can modulate peripheral glucose metabolism via a central action.

Leptin is an adipocyte-derived hormone, and serum levels are positively correlated with the amount of body fat (Considine et al., 1996). In addition to the regulation of body weight, leptin regulates also glucose metabolism by acting on the brain (Figure 26).

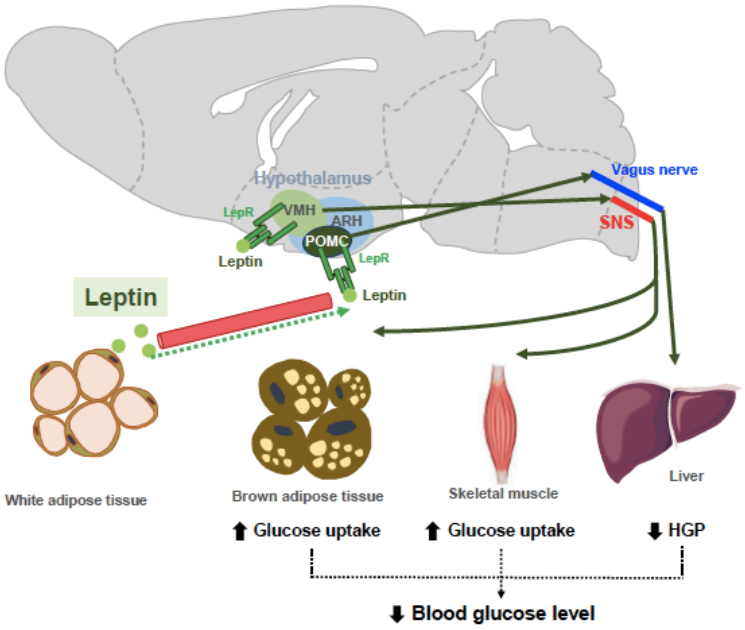

Figure 26. Leptin signaling modulates peripheral glucose metabolism through central actions (adapted from: Choi and Kim, 2022).

Leptin signaling in both proopiomelanocortin-expressing neuron (POMC) of the arcuate nucleus (ARH or ARC) and on the ventromedial hypothalamus (VMH) neurons leads to decreased hepatic glucose production (HGP) and increased insulin-independent glucose uptake in the skeletal muscle and brown adipose tissue (BAT). The two last actions are mediated through the sympathetic nervous system (SNS).

Abreviations : LepR, leptin receptor.

Previous studies showed that intracerebroventricular Leptin Infusion improves hyperglycemia in mice or rats with insulin-deficient diabetes (da Silva et al., 2017; Li et al., 2011). The glucose-lowering effect of leptin is due to reduced HGP and increased insulin-independent glucose uptake into the brain and skeletal muscle, and BAT (Figure 26). POMC neurons of the ARC seem to mediate the modulation of peripheral glucose metabolism by leptin. Furthermore, it was reported a normalization of blood glucose levels in leptin receptor-null mice after the reconstitution of leptin receptors specifically in POMC neurons of the ARC. These observed effects were independent of food intake and body weights (Coppari et al., 2005). Additionally, experiments in rodents showed that the suppression of HGP during the hyperinsulinemic-euglycemic clamp was impossible in mice with double knockout of insulin and leptin receptors in POMC neurons (Hill et al., 2010).

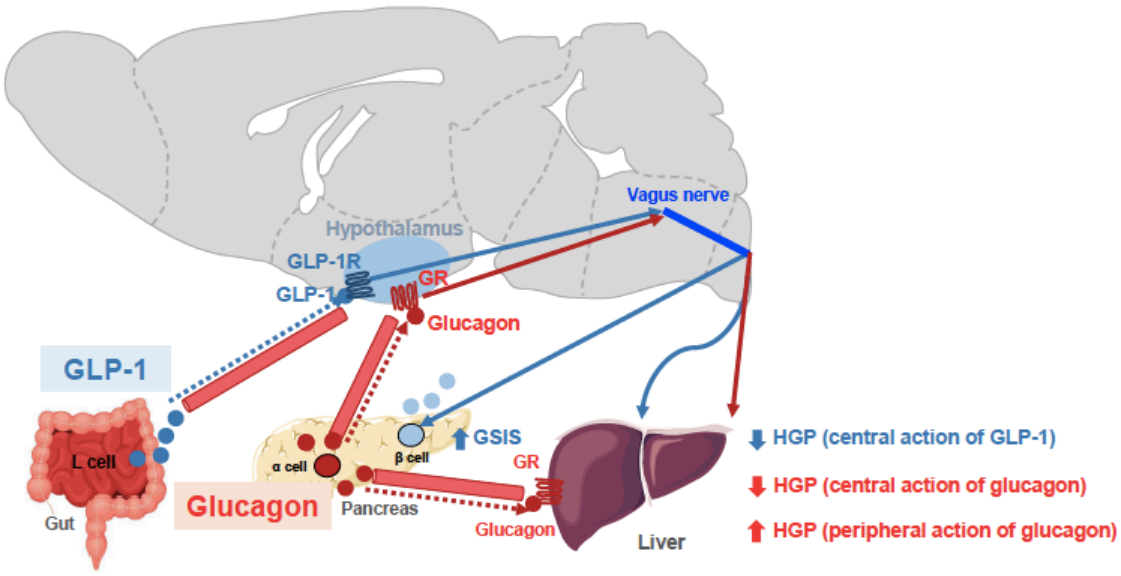

Figure 27. Glucagon-like peptide 1 (GLP-1), and glucagon signaling modulates peripheral glucose metabolism via central actions (adapted from Choi and Kim, 2022).

GLP-1 increases glucose-stimulated insulin secretion (GSIS) and inhibits hepatic glucose production (HGP) via GLP-1 receptor signaling in the ARC.

Glucagon enhances HGP through a direct action on hepatocytes whereas it acts on the ARC of the hypothalamus to inhibit HGP.

Abreviations: GLP-1R, GLP-1 receptor; GR, glucagon receptor; LepR.

Glucagon-like peptide 1 (GLP-1) is a 30-amino acid peptide hormone produced in the intestinal epithelial endocrine L-cells. In addition to its direct effects on pancreatic islets, GLP-1 increases glucose-stimulated insulin secretion (GSIS), and inhibits HGP via GLP-1 receptor signaling in the ARC of the hypothalamus [(Figure 27); (Sandoval et al., 2008)].

Glucagon, is peptide hormone secreted by pancreatic α-cells. Peripheral action of glucagon on the hepatocytes induced increasing HGP. In contrast, the activation of hypothalamic glucagon receptor signaling inhibits HGP via a K^{ATP} channel-dependent mechanism (Mighiu et al., 2013).

Aims of the PhD project

Aims of the PhD project

Tau is a microtubule-associated protein that plays a role in neuronal trafficking. Its dysfunctions (hyperphosphorylation, aggregation) have been involved in Alzheimer's Disease pathophysiology. While cognitive deficits remain the cardinal manifestation of AD, development of tau pathology may therefore be likely involved in the underappreciated metabolic and non-cognitive abnormalities, such as glucose homeostasis impairments. Interestingly, previous observational studies suggested that AD favors the emergence of glucose homeostasis alteration, and impaired glucose homeostasis was also suggested to increase AD risk and a pathological loss of tau function. Furthermore, a recent study from the laboratory showed that constitutive tau knock-out (tau KO) mice exhibited impaired glucose homeostasis, characterized by hyperinsulinemia and impaired glucose tolerance, with increased body weight gain and food intake. Conversely, neuronal overexpression of a human mutated tau protein was associated with improved glucose tolerance. Nonetheless, the links between tau loss of function and glucose homeostasis remain unclear.

In this context, the first aim of my PhD was to evaluate the metabolic phenotype of an original knock-in (KI) mice model expressing a human tau protein bearing a mutation, under the control of the murine tau promoter. This mouse model allowed us to evaluate the impact of expressing dysfunctional tau proteins at a physiological level, in the same tissues than native tau protein, without any bias of overexpression.

As reported previously, both energy and glucose homeostasis are the results of a fine and primordial regulation requiring the intervention of both the central nervous system and pancreas. Additionally, tau is largely considered as a neuronal protein but is also expressed by other tissues, particularly pancreatic ß-cells. But again, its peripheral functions have been overlooked. Accordingly, two mutually non-exclusive mechanisms could explain the metabolic alterations related to tau loss of

function observed in tau KO mice: tau impacts peripheral glucose homeostasis by a central-based regulation possibly involving the hypothalamus; or, in non-mutually manner, tau regulates ß-cell function in the pancreas.

In line with this hypothesis, the second main goal of my project was therefore to understand the basis of glucose homeostasis regulation by tau by investigating central (hypothalamus) and peripheral (pancreatic) mechanisms. To achieve this objective, an innovative transgenic tau floxed mice combined with different models/virus expressing CRE recombinase, was characterized and used. Our data revealed a hypomorphic status of homozygous tau flox mice in the absence of CRE. We thus used heterozygous tau flox animals that were combined with CRE approaches to knock-down tau from the mediobasal hypothalamus (cKO-Tau^{hyp}) or pancreatic ß-cells (cKO-Tau$^{\beta}$ animals). In these models, complete metabolic phenotyping was carried out under chow diet and HFD.

Materials and methods

Materials and methods

1. Human Samples:

Human tissues were obtained in accordance with French bylaws (Good Practice Concerning the Conservation, Transformation, and Transportation of Human Tissue to be Used Therapeutically, published on 29 December 1998). Permission to use human tissues was obtained from the French Agency for Biomedical Research (Agence de la Biomedecine, Saint-Denis la Plaine, France, protocol no. PFS16-002) and the Lille Neurobank (DC-2008-642). To monitor tau isoforms in human islets, we used 3 mRNA samples obtained from TEBU-Bio (France). As control of tau isoform expression in the brain, we used mRNA extracted from the cortical area of one 29-year-old male individual who had donated his body to science. To evaluate tau expression in human islets by immunohistochemistry, we used pancreatic sections from a 77-year-old male obtained from Biochain1 (T2234188, Hayward, CA).

2. Experimental Animals and Diet:

Tau knock-in mice (tau KI; C57BL6/J background) were generated by knock-in targeted inserting way, into the murine locus Mapt gene, of a cDNA encoding human 1N4R isoform mutated at P301L and tagged with a V5 epitope (GKPIPNPLLGLDST; this epitope tracks transgene expression) in exon 1 after initiation codon of protein translation (ATG).

A Stop codon is present at the end of the human transgene as well as a poly(A) tail (Genoway, France; Figure 29A). Human tau expression in this KI model was assessed by Western blot.

To obtain animals of interest, we crossed heterozygous tau KI male mice with heterozygous females tau KI animals to generate the homozygous tau KI mice and their littermate WT controls used for experiments. It is noteworthy that the body weight at weaning was similar in tau KI mice as compared to WT littermate (not shown). Animals were maintained in standard animal cages under

conventional laboratory conditions (12-h/12-h light/dark cycle, 22_C), with ad libitum access to food and water. Tau KI mice and WT littermates were fed with CHOW diet (SAFE D04; for composition see: https://safe-lab.com/safe-wAssets/ docs/product-data-sheets/diets/safe_d04ds.pdf) or High-Fat Diet (HFD; 58% kCal from fat; Research Diets D12331; for composition see: https://researchdiets.com/formulas/d12331) from 2 months of age. Body weights were measured weekly.

At the completion of the experiment (i.e., following 12w of diet), mice were about 5-month-old. Comparison of the metabolic phenotype of the KI mice with littermate WT was performed under chow diet in a first experiment; the effect of the HFD diet was evaluated in a second experiment. The HFD used is similar to what we published previously (Leboucher et al., 2019). This HFD was subjected to an initial evaluation of metabolic properties in WT littermate mice of the KI strain to ensure the ability to promote glucose intolerance.

Tau floxed mouse model (C57Bl6J) generated by flanking the murine Tau exon 3, harboring the ATG initiation codon, with loxP sites (Genoway, France). This has been combined with the FLEx monitoring strategy allowing that CRE recombinase turns-off murine Tau expression while the expression of an eGFP reporter is concomitantly turned-on. The use of these tau floxed mice was the basis of different strategies of a conditional deletion of tau protein in the mediobasal hypothalamus (cKO-Tau^{hyp} model), and pancreatic β cells (cKO-Tau$^{\beta}$ model). Also, these animals were maintained in standard animal cages under conventional laboratory conditions (12-h/12-h light/dark cycle, 22_C), with ad libitum access to food and water. Different strategies are developed in the results chapiter.

The animals were maintained in compliance with European standards for the care and use of laboratory animals and experimental protocols approved by the local Animal Ethical Committee (agreement APAFIS# 12787-2015101320441671 v9 from CEEA75, Lille, France).

3. Tamoxifen administration:

Tamoxifen (TM, T5648; Sigma-Aldrich, St. Louis, MO) was dissolved in 90% (v/v) filtered corn oil (C8267; Sigma-Aldrich, St. Louis, MO), and 10% (v/v) ethanol to make a solution of 40 mg/ml. 8-week-old C57Bl/6J mice were administered 1 mg of Tamoxifen (100 µL volume) or vehicle corn oil per 20g of mice weight by intraperitoneally injections once every 24 hours for a total of 5 consecutive day.

4. Lentivirus shRNA tau Knockdown Vector:

The lentivirus shRNA tau knockdown vector system used in this project was a homemade viral vector. It is a highly efficient method for stably knocking down expression of tau. Once the viral genome is reverse transcribed and permanently integrated into the host cell genome, the shRNA tau is expressed from the H1 promoter, leading to degradation of target tau mRNA. The permanent nature of knockdown by lentivirus has several major advantages over transient knockdown by synthetic siRNA. The efficacy and non-toxicity of the lentivirus shRNA tau was tested initially in-vitro in a primary neuronal cell culture. Equal numbers of 16 week-old mice from the same litter were injected with either lentivirus shRNA tau and a control virus. The viral transduction can be followed through the Green fluorescent protein expression.

5. Adeno-associated Viral vectors:

AAV-CMV-eGFP-WPRE 7, 8, 9 and 10 serotypes were ordered from Vector Builder. Green fluorescent protein (GFP) expression was driven by CMV promoter. To select the best viral vector able to transduce the endocrine cells of pancreatic adult mice. Equal numbers of 8 week-old mice from the same litter were injected with the AAV-CMV-eGFP-WPRE 7, or 8, or 9, or 10 serotypes. The latter vectors were administered systemically by unilateral retro-orbital venous sinus injection (100µl per side of 5×10^{11} viral genome particles/ml). Mice were anesthetized with isoflurane prior to retro-orbital venous sinus injection.

AAV2/5-synapsin-CRE-Tomato virus or the AAV2/5-synapsin-Tomato (control) were also ordered from Vector Builder. The both vectors were under a synapsin promoter which confers a highly neuron-specific transduction. The viral transduction can be followed through the Tomato protein expression.

6. In vivo intra-parenchymal administration of virus vectors:

For stereotaxic injection, animals were anesthetized by injection of a mix of ketamine (80 mg/kg) and xylazine (20 mg/kg) administered intraperitoneally. Experiments began 8 weeks after AAV or lentivirus injection. Equal numbers of 12 week-old mice from the same litter were injected with AAV2/5-synapsin-CRE-Tomato virus or the AAV2/5-synapsin-Tomato (control). AAV were injected unilaterally for setups and bilaterally for experiments (10^8 viral genome particles/ml) using a 33G needle and a stereotaxic frame with blunt ear bars.

Equal numbers of 16 week-old mice from the same litter were injected with a lentivirus shRNA tau or the lentivirus shRNA tau control lentivirus. Both lentiviruses were injected unilaterally for setups and bilaterally for experiments (250ng/ml) into the hypothalamus and the hippocampus, associated with a stereotaxic frame with blunt ear bars.

Coordinates (from bregma) according to Mouse Brain Atlas (by Paxinos and Franklin) were as follows:

- The coordinates for targeting the mediobasal hypothalamus were A (rostrocaudal), -1.64; L (mediolateral), ±0.5; V (dorsoventral), -5.8; with 0.25 µl injected at each depth.
- The coordinates for targeting the Hippocampus: were A (rostrocaudal), -2.5; L (mediolateral), ± 1; V (dorsoventral), -1.8; with 2 µl injected at each depth.

Injections were performed using a Hamilton syringe (Seringue 7002 for the hypothalamus, and Seringue 7000 for the hippocampus) driven by a syringe pump at a flow rate of 0.1 µl/min, or 0.25 µl/min, for the hypothalamus or the hippocampus, respectively. Following the injection, the needle was left in place for 2 min prior to being slowly retracted to avoid vector leakage from the injection tract. After surgery, the skin was sutured, and animals were kept under constant monitoring with ad

libitum access to food and water. The needle remained in place at each injection site for 1 additional min before the cannula was moved/removed slowly. The skin was sutured, and the animal was placed on a heating pad until it began to recover from the surgery, before being returned to its cages.

7. Metabolic Cages:

Spontaneous feeding, locomotor activity (total beam breaks/hour), respiratory exchange ratio, and O2 consumption were monitored continuously for 24 h using metabolic cages (Phenomaster, TSE Systems, Germany). Food intake was measured by the integration of weighing sensors fixed at the top of the cage from which the food containers were suspended into the home cage. Locomotor activity was assessed using a metal frame placed around the cage. Evenly spaced infrared light beams are emitted along the x axis. Beam interruptions caused by movements of the animals are sensed and registered at high resolution. The sensors for detection of movement operate efficiently under both light and dark phases, allowing continuous recording. Metabolic rates were (Respiratory exchange ratio, O2 consumption) measured by indirect calorimetry. Mice were housed individually and acclimated to the home cage for 72 h prior to experimental measurements.

8. Biochemical plasma parameters:

Blood was collected at the tail vein after 6 h of morning fasting. Within 30 min of the collection of blood samples, blood was centrifuged at 1,500 g for 15 min at 4°C. Plasma was separated, transferred to 1.5 ml Eppendorf tubes, and stored at -80°C until analysis. Plasma concentrations of insulin were measured using the mouse insulin ELISA kit (Mercodia AB, 10-1247-01; no cross-reactivity with proinsulin) following the manufacturer's instructions. Plasma concentrations of adiponectin were measured using a mouse

Adiponectin ELISA kit (Invitrogen, KMP0041) following the manufacturer's instructions.

9. Metabolic tolerance tests:

Intraperitoneal glucose tolerance tests (IPGTT) were assessed following 6 h of morning fasting. D (+) glucose (1 g/ kg body mass; Sigma-Aldrich) was injected intraperitoneally. Blood glucose was then measured at 0, 15, 30, 60, 90, and 120min following injection.

For the pyruvate tolerance test (PTT), mice were fasted overnight and given an intraperitoneal injection of sodium pyruvate (2.0 g/kg) dissolved in sterile saline. Blood glucose was then measured at 0, 15, 30, 60, 90, and 120min following injection.

For the insulin tolerance tests (ITT) were assessed following 6 h of morning fasting. Human insulin solution (0.75 IU insulin/kg body mass; Sigma-Aldrich) was injected intraperitoneally. Blood glucose was then measured at 0, 15, 30, 60, 90, and 120min following injection.

For fasting-refeeding experiments, mice were fasted overnight (16 h of fast) and re-fed. Blood glucose was measured at 16 h (overnight) of fasting and during the 1st, 2nd, and 4th h after re-feeding. Blood glucose was measured at the tail vein after 6 h of morning fasting, an overnight fasting, and in fed or refeeding conditions using One Touch Verio Flex glucometer (LifeScan).

10. Tissue Fixation, Immunohistochemistry and Imaging:

Animals were sacrificed by cervical dislocation. Following dissection, pancreases were laid flat in cassettes, fixed for 4 h in 4% paraformaldehyde, dehydrated, and embedded in paraffin. Longitudinal serial sections (5 mm) were processed for immunofluorescent (IF) analysis. Tissue sections from human adult normal pancreas were obtained from Biochain (T2234188, Hayward, CA).

Immunohistochemistry of the human pancreas was performed on 5 mm sections embedded in paraffin. The sections were de-paraffinized in three changes of toluene (5 min each) and re-hydrated in decreasing serial solutions of ethanol (100%, 95%, and 70%) and PBS. Sections were submitted to heat-induced antigen retrieval in citrate-buffer (10 mM citrate acid, 0.05% Tween 20 in distilled water), using microwave: two cycles for 5 and 10 min at power level 520 W and 160 W, respectively, followed by a 2 min break, cooled to room temperature for 20 min. Pancreatic tissue samples were

incubated with blocking solution (5% goat serum and 1% BSA in PBS) for 1h at RT, and washed once with PBS, then incubated with the primary anti-tau antibodies (laboratory-made mouse monoclonal IgG1 tau C-ter 9F6 raised against amino-acids (aas) 427–441, homemade mouse monoclonal IgG2b tau 9H12 raised against aas 162–175, for human sections a homemade mouse polyclonal IgG tau C-ter 993S5 raised against aas 394–408; see Figure 28) diluted at 1:200 in antibody buffer (PBS, 1% BSA) overnight at +4_C. After washing in PBS, slides were incubated with the detecting secondary antibodies conjugated to Alexa Fluor 568 (IgG H + L, Highly Cross-Adsorbed Goat anti-Mouse, Invitrogen, A-1103, Darmstadt, Germany) diluted at 1:200 in antibody buffer for 1h at RT. For detecting human tau in tau KI mice sections, a homemade rabbit monoclonal tau N-ter (hTauE1, raised against aas 12–21; Supplementary Figure 2) was used, diluted at 1:200 in antibody buffer (PBS, 1% BSA) 48 h at + 4_C. Amplified immunohistochemistry processes were used. After washing in PBS, slides were incubated with Goat Anti-Rabbit IgG biotinylated secondary antibody (BA-1000-1.5), washed, and incubated with fluorophore-coupled streptavidin (Alexa FluorTM 647 Conjugate, S32357) diluted at 1:600 in PBS. For detection of glucagon and insulin, slides were incubated with either a recombinant monoclonal Rabbit anti-glucagon antibody (Abcam, ab92517) diluted at 1:500 or a Polyclonal Guinea Pig Anti-insulin antibody ready-to-use (Agilent, IR00261-2) overnight at +4_C, followed by the secondary antibodies conjugated to Alexa Fluor 488 [for glucagon: IgG H + L, Highly Cross-Adsorbed Goat anti-Rabbit, Invitrogen, A32731, Darmstadt, Germany; for insulin: IgG H + L, Highly Cross- Adsorbed Goat anti-Guinea Pig, A-11073, Darmstadt, Germany] diluted at1:200 in antibody buffer (PBS, 1% BSA) for 1 h at RT. Nuclear counterstaining was performed using DAPI (Invitrogen).

Sections were quenched for autofluorescence using the Vector TrueVIEW Autofluorescence Quenching Kit (Vector Laboratories, Burlingame, CA, USA). Slides were mounted using Dako Fluorescence Mounting Medium (Agilent Technologies, California, USA). Immunofluorescence-stained slides were imaged using a Zeiss Spinning disk confocal microscopy with a 40X oil-immersion lens (NA 1.3 with an optical resolution of 176 nm). Images were processed with ZEN

software (Carl Zeiss, version 14.0.0.201, Germany). Colocalizations between islet signals given using tau antibodies vs. insulin or glucagon were determined through Pearson's overlap coefficient using Image J (Adler and Parmryd, 2010).

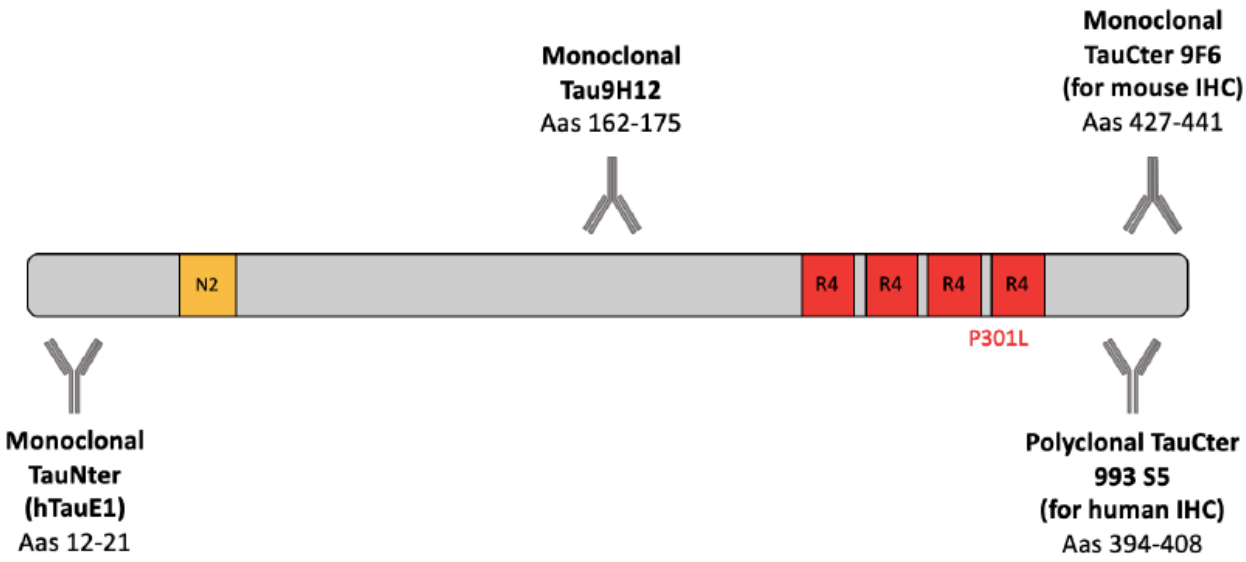

Figure 28. Home-made antibodies used for tau immunohistochemistry and Western blots with respective epitopes. Tau 9H12, tauCter 9F6/993 S5 and tauNter htauE1 targeting epitopes are represented. Epitopes are shown with their associated sites corresponding to the longest isoform of tau protein.

11. Immunohistochemistry and Image Analysis of free-floating brain sections:

Animals used for immunohistochemical studies, were deeply anaesthetized with pentobarbital sodium (50 mg/kg, intraperitoneally), then transcardially perfused with cold NaCl (0.9%) and with 4% paraformaldehyde in PBS (pH 7.4). Brains were removed, post-fixed for 24 h in 4% paraformaldehyde and cryoprotected in 30% sucrose before being frozen at −40°C in isopentane (methyl-butane) and stored at −80°C. Brains were cut into six series of 35-µm thick coronal sections using a Leica cryostat, and were stored in sodium phosphate buffer-azide (0.2%) at 4°C.

First of all, coronal brain sections were washed with sodium phosphate buffer and permeabilized with 0.3% Triton X-100/sodium phosphate buffer. Sections where blocked for 1 hour with the incubation solution (5% normal goat serum, 1 mg/mL bovine serum albumin in sodium phosphate buffer -0.3% Triton, pH 7.4), flowed also, by the incubation with Avidin/Biotin Blocking Solution (Vector, SP-2001) for 30 minutes.

For double immunostaining, samples were simultaneously incubated with an Anti-Tau 9H12 antibody and another antibody as listed in table 4 for 48 hours at 4°C.

Primary antibodies were then rinsed out before incubation with a secondary Goat Anti-Mouse IgG2b heavy chain biotinylated antibody (ab97248), diluted 1:200 in sodium phosphate buffer, and one of the following fluorophore-coupled secondary antibodies: Alexa Fluor 488 Goat anti-Rabbit IgG [(H + L), Invitrogen, dilution 1/500], Alexa Fluor 568 Goat anti-Mouse IgG (H + L) [(H + L), Invitrogen, dilution 1/500], Alexa Fluor 568 Donkey anti-Sheep IgG (H+L) Cross-Adsorbed (A-21099 ; Invitrogen, dilution 1/500 in sodium phosphate buffer); diluted 1:600 in PBS 1× for 2 hours in PBS-0.3% Triton at room temperature].

After washing in sodium phosphate buffer, the sections were then incubated with streptavidin Alexa Fluo 647 conjugate (1/600; Thermo Fisher Scientific) for 1 hour. After, sections were washed, and counterstained with diaminopyrolylindole 4,6-diamino, 2-pyrolylindole (Invitrogen) or NeuroTrace™ 435/455 Blue Fluorescent Nissl Stain (Invitrogen, N-21479). Finally, the sections were quenched for autofluorescence using Autofluorescence Eliminator Reagent (Sigma-Aldrich) following the manufacturer's instructions and then mounted using Dako Fluorescence Mounting Medium (Agilent Technologies). Immunofluorescence-stained slides were imaged using a Zeiss Spinning disk confocal microscope. Images were processed with ZEN software (Carl Zeiss, version 14.0.0.201, Germany). Quantitative colocalization analysis with Pearson coefficients was performed using Imaris Software.

Name	Epitope	Type	Origin	Provider	Dilution
Anti-Tau 9H12	Tau aas 162–175	Monoclonal	Rabbit	Home made	1/200
Anti-POMC	POMC	Polyclonal	Rabbit	Phoenix	1/1000
Anti-GnRH	GnRH	Polyclonal	Sheep	Home made	1/10000
Anti-AgRP	AgRP	Polyclonal	Rabbit	Phoenix	1/1000
Anti-Vimentin	Vimentin	Polyclonal	Chicken	BioLegend	1/1000
Anti-GFAP	GFAP	Polyclonal	Rabbit	Dako	1/1000

Table 4. Antibodies used in immunohistochemistry for free-floating brain sections.
Abreviations: AgRP: Agouti-Related Peptide, GFAP: Glial fibrillary acidic protein, POMC: Pro-opiomelanocortin.

12. Identification of 3R and 4R Tau Isoforms:

Following mRNA extraction, one microliter of the RT-product was used as the template for subsequent PCR amplification. All PCR primers used in this study are reported in (Table 5). Regarding mouse tau exon 10 splicing, we performed a nested PCR with TMF1/TMR1 primers to ensure the specificity of the PCR products obtained and a second PCR using TMF1/TRR2 primers. As internal controls, we used mouse or human cortex samples. The TMF1/TRR2 PCR products obtained were resolved in an 1.75% agarose gel in TAE buffer (40mMTris, 20 mM acetic acid, 2 mM EDTA, pH 8.5).

Primer used	Annealing T°C Cycles	Primer sequence	PCR products	Products length (bp)
Mouse tau exon 10 alternative splicing				
TMF1 TMR1	59°C 35 cycles	CTG AAG CAC CAG CCA GGA GG CGA TGC TGC CCG TGG AGG AGA		
TMF1 TRR2	59°C 35 cycles	CTG AAG CAC CAG CCA GGA GG GTC TGT CTT GGC TTT GGC ATT CTC	4R (10+) 3R (10-)	600 500
Human tau exon 10 alternative splicing				
Forward Reverse	60°C 30 cycles	CAT GCC AGA CCT GAA TGT CAA G TCA CAA ACC CTG CTT GGC CA	4R (10+) 3R (10-)	244 151

Table 5. PCR primers used in the PCR of 3R and 4R Tau Isoforms.

Abreviations: bp base pair.

13. Morphometric Analysis of Pancreatic Islets:

Longitudinal pancreatic sections were cut at a 5 mm thickness, collected at 250 mm intervals, and plated on glass slides. This resulted in the collection of sections of 10 depths per pancreas.

The sections were then proceeded as previously described (Rabhi et al., 2016). Sections were incubated with anti-glucagon and anti-insulin antibodies, followed by the secondary antibodies conjugated to Alexa Fluor 568 [IgG (H + L) Highly Cross- Adsorbed Goat anti-Rabbit, A-11008, Darmstadt, Germany], and Alexa Fluor 488 [IgG (H + L) Highly Cross-Adsorbed Goat anti-Guinea Pig, A-11073, Darmstadt, Germany], respectively.

All images were acquired on a ZEISS Axio Scan.Z1 slide scanner (Carl Zeiss Microscopy GmbH, Germany) at _20 magnification (resolution of 0.5 mm/pixel) and uploaded into a Spectrum digital slide interface. Images of whole pancreatic sections acquired were analyzed by a macro-based automated approach. First, pancreatic islets were detected by an automated approach using ImageJ

software (Scion Software) based on immunofluorescence signal of insulin and glucagon. Then, to appreciate the relative mass of β and α cells in each detected pancreatic islet, the surface area of both insulin and glucagon positive cells was determined using the following equations:

β-cell surface area:

$[(\sum_{i=0}^{n} i = \%\text{ of insulin signal })/(\sum_{i=0}^{n} i\ \%\text{ of insulin and glucagon signals}) \times 100]$

α-cells surface area:

$[(\sum_{i=0}^{n} i = \%\text{ of glucagon signal })/(\sum_{i=0}^{n} i\ \%\text{ of insulin and glucagon signals}) \times 100]$

14. Quantification of the AAV transduction rate in pancreatic islets from adult mice:

The quantification was performed in 18 pancreas sections per animal (two animals/group; sections 250 μm apart). The percentage of transduced islets was calculated by dividing the number of GFP+ islets by total islets of the pancreas section. Islets were deemed positive when at least one cell produced GFP.

15. Cell Culture, siRNA Knock-Down, and Glucose-Stimulated Insulin Secretion (GSIS) :

The mouse pancreatic b-cell line Min6 (AddexBio) was cultured in DMEM (Gibco) with 15% fetal bovine serum, 100 mg/ml penicillin-streptomycin, and 55 mM b-mercaptoethanol (Sigma, M6250). Cells were transfected with non-targeting siRNA mouse negative controls (siCont, D-001810-0X) and siTau (L-061561-01-0005, SMARTpool, Dharmacon) using Dharmafect1 (T-2001-03, GE Dharmacon) and GSIS experiments were performed 48 h later.

For GSIS, following a 1 h preincubation in Krebs-HEPESbicarbonate buffer (KHB; 140 mM NaCl, 3.6 mM KCl, 0.5 mM NaH2PO4, 0.2 mM MgSO4, 1.5 mM CaCl2, 10 mM HEPES, 25 mM NaHCO3) with 2.8 mM glucose, GSIS was assessed by static incubation of siCont and siTau transfected Min6 cells in KHB with 2.8 mM or 20 mM glucose for 1 h at 37_C. Mature insulin secreted into the media and total mature insulin content were quantified through insulin ELISA (Mercodia AB; no crossreactivity with proinsulin) following the manufacturer's instructions.

16. Western Blot Analysis:

Cortical brain and liver tissues, sampled at mouse sacrifice, were homogenized in a buffer Tris Base 10 mM; Sucrose 10%; pH = 7.4 with protease inhibitors (1 tablet for 10 ml solution—Sigmar Complete Mini EDTA Free). Protein amounts were evaluated using the BCA assay (PierceTM BCA ProteinAssay Kit). Protein lysates were then diluted with LDS (Lithium Dodecyl Sulfate) 2_ supplemented with reducing agents (NuPAGEr), and then separated on 18-well 4–12% acrylamide gel (Criterion XT, Biorad). Twenty micrograms of total proteins for cortex as the hippocampus and 40 mg for liver were loaded per well. Proteins were transferred onto nitrocellulose membranes, which were saturated with 5% nonfat dry milk or Bovine Serum Albumin in Tris 15 mmol/L, pH 8; NaCl 140 mmol/L and 0.05% Tween then incubated with primary (listed below) and secondary antibodies (PI-1000-1 Goat Anti-Rabbit IgG Antibody (H + L), Peroxidase, Vector laboratories). Signals were visualized using chemiluminescence HRP substrate ECL kit (Amersham ECL Detection Reagents) and Amersham ImageQuant 800 imaging system (Cytiva). Results were normalized to GAPDH used as loading control, and quantifications were performed using ImageJ software. Anti-tau antibodies used for Western blot were Cter 9F6 and human tau-specific antibody Nter hTauE1 (Figure 28).

An antibody raised against V5 tag (GKPIPNPLLGLDST) that was inserted on human transgene (catalog no. AB3792 Anti-V5 Epitope Tag (Rabbit polyclonal; Millipore) has been used to specifically label the human transgene. Phospho-Akt(S473) and Akt(pan) antibodies (Cell signaling) were used on liver tissue. Loading control anti-GAPDH antibody (catalog no. G9545- 200UL, Sigmar).

17. mRNA Extraction and Quantitative Real-Time RT-PCR:

Total RNAs from human (N = 3) and mouse (WT, N = 3) isolated pancreatic islets, as well mouse cortex were extracted from tissues using the RNeasy Lipid Tissue Kit (Qiagen, Courtaboeuf, France) following the manufacturer's instructions. Samples were quantified with a NanoDrop ND-1000. Five-

hundred nanograms of total RNA were reverse-transcribed using the High-Capacity cDNA reverse transcription kit (Applied Biosystem, Saint-Aubin, France). Quantitative real-time RT-PCR analysis was performed on an Applied BiosystemsTM StepOnePlusTM Real-Time PCR Systems using TaqManTM Gene Expression Master Mix (Life Technologies Corp., Grand Island, NY). The thermal cycler conditions were as follows: 95_C for 10 min, then 40 cycles at 95_C for 15 s and 60_C for 1 min. Predesigned TaqmanTM gene expression assays (Life Technologies Corp., Grand Island, NY) were used for mouse Mapt (Mm00521988_m1). Peptidylprolyl isomerase A (PPIA, Mm02342430_g1) expression was assessed as a reference housekeeping gene for normalization. Amplifications were carried out in duplicates and the relative expression of target genes was determined by the ΔΔCt method.

18. Statistics:

Results are expressed as mean ± SEM. Statistics were performed using either Student's t-test as well as One or Two-way analysis of variance (ANOVA), followed by a post hoc Tukey's test. We used Kruskall-Wallis when data failed a Kolmogorov-Smirnov or a Shapiro-Wilk normality test. Statistics were performed using Graphpad Prism Software. P values <0.05 were considered significant.

Results

Results

As described above, in my thesis project, I had performed firstly a metabolic evaluation, focusing on glucose homeostasis, of an original tau KI mouse. In this mice model, the loss of tau function was associated with impaired glucose homeostasis and increased body weight gain in male but not in females' mice under HFD.

Secondly, in order to explore finely whether impaired glucose homeostasis related to tau loss of function had a peripheral and or a central origin, I used different approach to induce a downregulation or a knockdown of tau protein in neurons of the mediobasal hypothalamus or pancreatic β-cells.

Part I: Characterization and metabolic phenotyping of tau KI mouse model

1. Generation and validation of tau KI mouse model:

In our original tau KI mice, a human tau 1N4R isoform mutated at P301L has been inserted at the locus of the mouse Mapt gene. MAPT human transgene is composed of 10 exonic regions with P301L mutation on exon 10. Additionally, a V5 epitope tag was inserted after exon 2. STOP codon was inserted followed by exogenous poly(A) Tail. Insertion of the targeting vector was mediated by cre-loxP recombination (Figure 29A). A floxed neomycin resistance (Neor) cassette used for positive selection was removed from the targeted allele by FRT (FRT sites shown as black rectangles) recombination sites.

Interestingly, this transgene is under the control of the Mapt mouse endogenous promoter, and is expressed physiologically instead of the mouse tau protein.

In tau KI mouse model, human tau expression was validated by western-blot analysis (Figure 29B). Noteworthy, similarly to other KI strains reported (Hashimoto et al., 2019; Saito et al., 2019), the present model does not exhibit tau aggregation at the age studied (2–5 months of

age; data not shown). This allowed us to evaluate the impact of an expression of soluble mutated (dysfunctional) tau proteins in absence of overexpression.

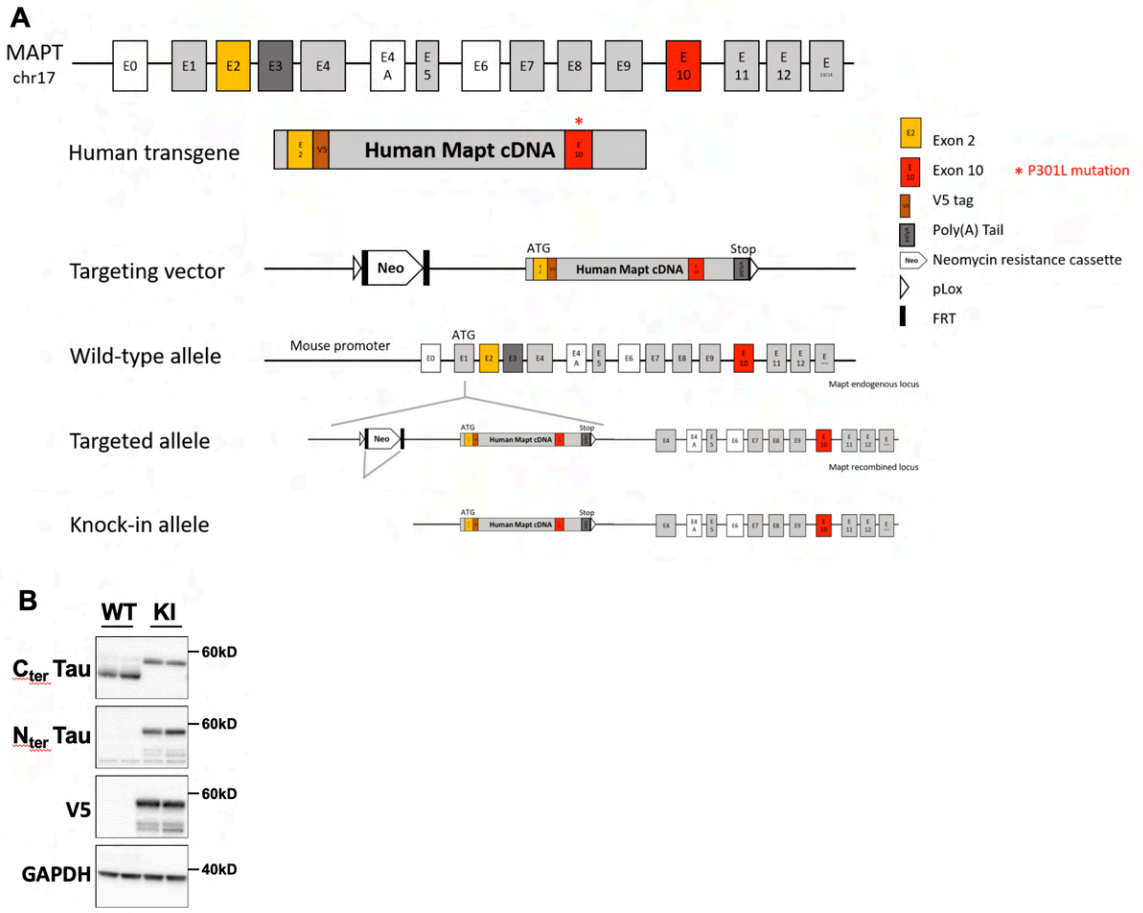

Figure 29. Generation and tau expression in the tau knock-in mouse model.

(A) Generation strategy of tau knock-in (KI) mice. MAPT human transgene is composed of 10 exonic regions with P301L mutation on exon 10. A V5 epitope tag is inserted after exon 2. STOP codon is inserted followed by exogenous poly(A) Tail. The transgene is under the control of the Mapt mouse endogenous promoter. Insertion of the targeting vector was mediated by cre-loxP recombination (pLox sites shown as empty arrows). A floxed neomycin resistance (Neor) cassette used for positive selection was removed from the targeted allele by FRT (FRT sites shown as black rectangles) recombination sites. Positions and sizes of exons and introns are not to scale. **(B)** Representative expression of tau and V5 in the cortex and hippocampus of tau KI mice and WT littermates (two showed mice out of eight/genotype).

2. Metabolic phenotyping of tau KI mouse model:

2.1. Metabolic phenotyping of tau KI mice under Chow diet:

In a first attempt, we investigated the metabolic phenotype of male animals under a chow diet. Among all parameters measured i.e., food intake, ambulatory activity, respiratory exchange ratio (RER), and energy expenditure—indirectly represented by oxygen consumption VO2-using metabolic cages (Figure 30A–D), as well as fed and fasted glycemia, plasma insulin, body weight gain over a 3-month period (from 2 to 5 months of age), glucose tolerance or rectal temperature, no significant change could be observed (Figures 31). Hence, under chow diet, tau KI mice did not exhibit altered basal energy homeostasis or glucose metabolism.

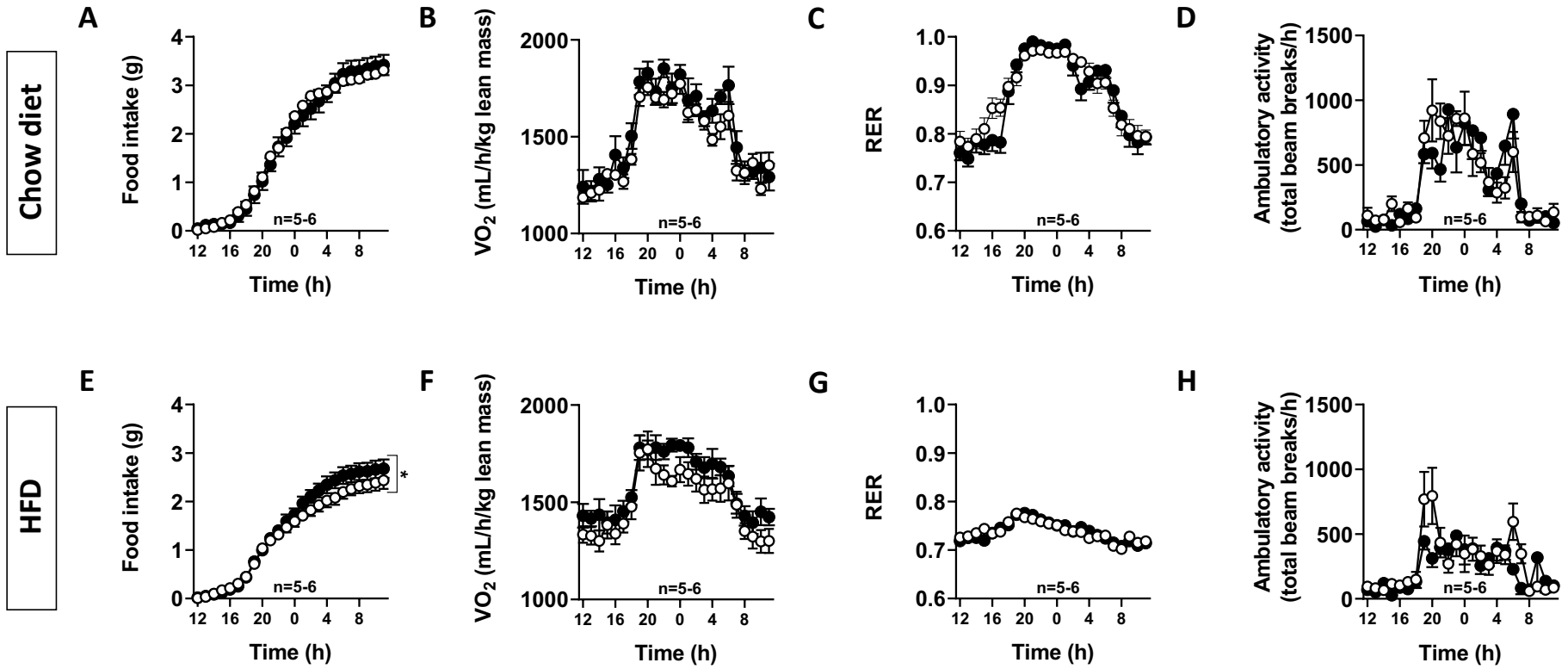

Figure 30. Metabolic cage evaluation of tau KI male mice under Chow and High Fat diets (HFD).

For mice under Chow diet: **(A)** 24 h-cumulative food intake (g). **(B)** 24 h spontaneous locomotor activity (total beam breaks/h). **(C)** 24 h-respiratory exchange ratio (RER = VCO2/VO2). **(D)** 24 h-O2 consumption.

For mice under HFD: **(E)** 24 h-cumulative food intake (g) (Two-Way ANOVA; F (23,207) = 2.401, *p < 0.05 vs. WT). **(F)** 24 h spontaneous locomotor activity (total beam breaks/h). **(G)** 24 h-respiratory exchange ratio (RER = VCO2/VO2). **(H)** 24 h-O2 consumption.

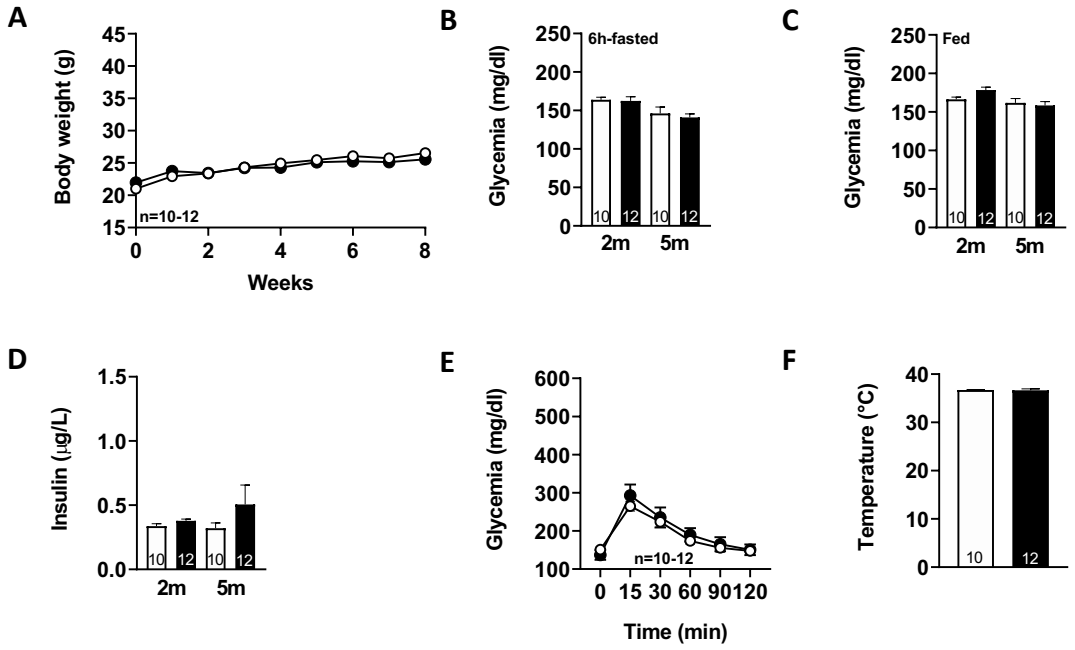

Figure 31. Metabolic phenotyping of tau KI male mice under chow diet.

(A) Body weight gain of WT and tau KI mice from 2 to 5 months of age (NS). **(B)** Glycemia after 6 hours of fasting at 2 to 5 months of age (NS). **(C)** Glycemia in fed condition (9.a.m) at 2 to 5 months of age (NS). **(D)** Insulinemia after 6 hours of fasting at 2 to 5 months of age (NS). **(E)** Intraperitoneal glucose tolerance test (IPGTT) at 5 months of age (NS). **(F)** Rectal temperature at 2 to 5 months of age (NS). Results are expressed as mean ± SEM. WT mice are indicated as white circles/bars, tau KI mice as black circles/bars.

2.2. Metabolic phenotyping of tau KI mice under High-Fat Diet:

In order to uncover a possible metabolic disorder related to the expression of the mutated human tau protein, we challenged tau KI male mice and their littermate controls with HFD for a period of 12 weeks, to promote the development of metabolic changes, approaching features of human metabolic syndrome or type 2 diabetes (Winzell and Ahren, 2004). Interestingly, male and female mice were studied in order to explore if the mice sex can impact the metabolic phenotype in tau KI mouse model. HFD was given from 2 months of age, a time-point at which animals do not display any metabolic change in chow diet condition (Figure 31). The time-line for metabolic investigations is given in Figure 32.

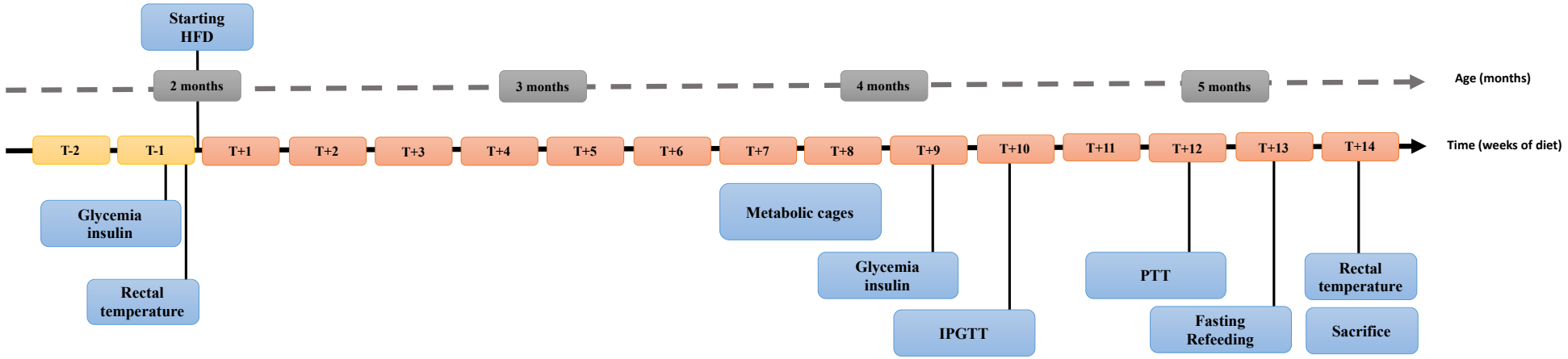

Figure 32. Time-line of metabolism investigations in tau KI and littermate WT animals under high-fat diet.

Baseline glycemia and plasma insulin measurement were performed after 6 hours of fasting and collected at the age of 7 weeks. Feeding with high-fat diet was started at 2 months old. Following metabolic cage measurements (6-7 weeks after HFD onset), metabolic exploration was performed from 8 to 12 weeks following HFD onset. Glycemia and plasma insulin measurements after 6 hours of fasting were determined 9 weeks after HFD onset. Intraperitoneal glucose tolerance tests (IPGTT) after 6 hours of fasting was performed at the 10th week of HFD. Pyruvate tolerance test (PTT) after an overnight fasting was performed at the 121th week of HFD. Glycemia measurement after overnight fasting and during the first 4 hours of refeeding was performed at the 13th week of HFD (20 weeks old). At the 14th week of HFD rectal temperature was measured and animals sacrificed.

First, we observed that the body weight gain was significantly, even moderately, increased in tau KI as compared to littermate WT male mice (Figure 33A, reaching, at the completion of the experiment, i.e., after 12 weeks of HFD at 5 months of age, 39.0 ± 3.1% above the initial body weight (2 months of age) vs. 28.9 ± 3.3% in WT mice ($p < 0.05$, Student's t-test). In accordance with such enhanced body weight gain, we found, using metabolic cages, that tau KI male mice exhibited an increased food intake (Figure 30E) without modification of locomotor activity (Figure 30H) nor energy expenditure (Figure 30F). The respiratory exchange ratio (RER) remained unaltered suggesting that under HFD, tau KI mice do not exhibit major energy metabolism nor change of energy substrate oxidation at the tissue level (Figure 30G).

Interestingly, further investigations were indicative of glucose homeostasis disorders in tau KI as compared to littermate WT male mice under HFD. While 6-h-fasting or fed glycemia remained unaltered by HFD (Figures 33B and 33 C), insulinemia (Figure 33D), as well as overnight fasting glycemia (Figure 33E) were found significantly enhanced in tau KI animals. Further, tau KI male mice fed under HFD also exhibited impaired glucose tolerance as assessed using the IPGTT (glucose tolerance) test (Figure 33H).

Impaired glucose homeostasis was plainly not accompanied by peripheral insulin resistance since levels of liver pAkt, a downstream target of the insulin signaling pathway, remained similar between WT and tau KI animals (Figure 34A). In line, levels of plasma adiponectin, an adipose tissue secreted endogenous insulin sensitizer whose reduction is associated with insulin resistance, were not decreased. Contrariwise, the mean of plasma adiponectin levels was significantly higher in tau KI male mice compared to WT under HFD (Figure 34B). Unfortunately, following the appearance of the COVID-19 pandemic, the insulin tolerance test could not be performed.

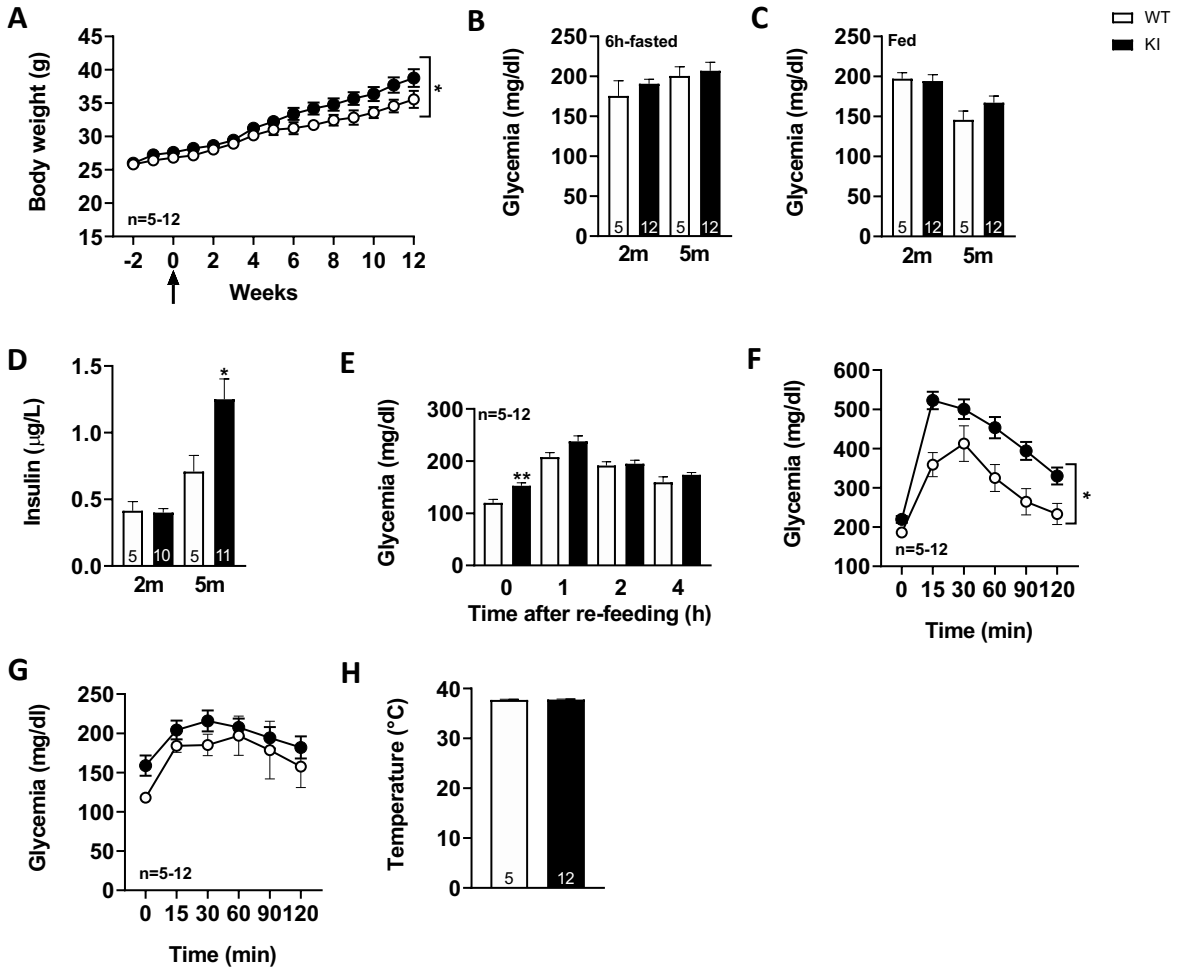

Figure 33. Metabolic phenotyping of tau KI male mice under High Fat diet (HFD; given from 2 to 5 months of age).

(A) Body weight gain of WT and tau KI mice under HFD from 2 to 5 months of age (Two-Way ANOVA; $F(14,210) = 1.807$, $^*p < 0.05$ vs. WT). **(B)** Glycemia after 6 h of fasting before (2 m) and at the completion of HFD (5 m; NS, One-Way ANOVA). **(C)** Glycemia in fed condition (9 a.m) before (2 m) and at the completion of HFD (5 m; NS, One-Way ANOVA). **(D)** Insulinemia after 6 h of fasting before (2 m) and at the completion of HFD (5 m; One-Way ANOVA followed by Tukey's post-hoc test; $F(3,27) = 13.34$ $p < 0.0001$; $^*p < 0.05$ vs. WT). **(E)** Glycemic variations during the 1st, 2nd and 4th h following re-feeding after 16 h of fasting at the completion of the HFD, i.e., 5 months of age (One-Way ANOVA followed by Tukey's post-hoc test; $F(7,60) = 19.83$ $p < 0.0001$; $^*p < 0.05$ vs. WT $^*p < 0.05$ vs. WT for glycemia after 16 h). **(F)** Intraperitoneal glucose tolerance test (IPGTT) at completion of the HFD, i.e., 5 months of age ($^*p < 0.05$, Two-Way ANOVA). **(G)** Pyruvate tolerance test (PTT) at completion of the HFD, i.e., 5 months of age (NS,Two-Way ANOVA). **(H)** Rectal temperature before (2 months) and at the completion (5 months) of HFD (NS). Results are expressed as mean ± SEM. WT mice are indicated as white circles/bars, tau KI mice as black circles/bars.

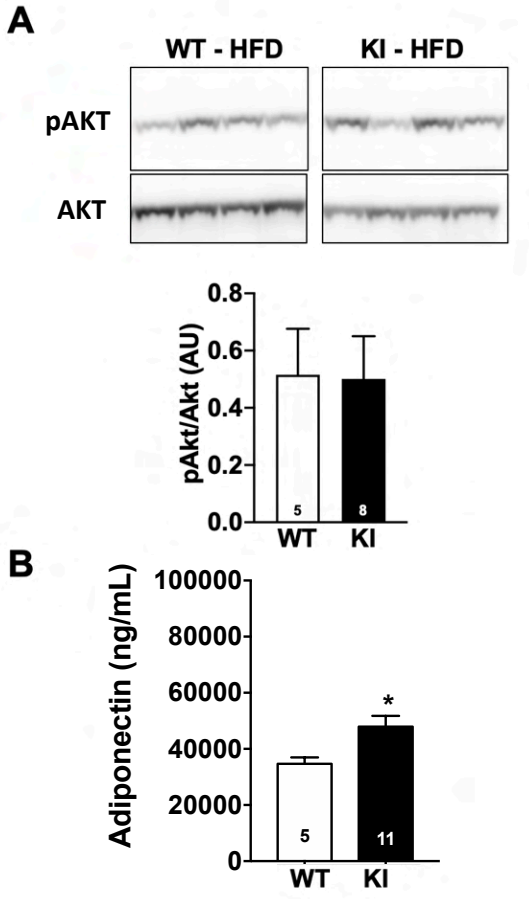

Figure 34. pAkt and Akt protein expression in the liver and Adiponectin dosage in the plasma of WT and KI mice under HFD.

(A) pAkt and Akt protein expression in the liver of WT and KI mice under HFD (NS Student's t-test). Western blots are representative.

(B) Adiponectin dosage in the plasma of WT and KI mice under, *p < 0.05, Student's t-test.

WT and KI are indicated as open bars and black, respectively. Mice were 5 months old.

Finally, to assess the possibility that hepatic glucose homeostasis could also be impaired in tau KI mice, animals were also challenged with pyruvate, a gluconeogenic precursor (Clementi et al., 2011). Pyruvate tolerance remained unaltered in tau KI mice as compared to their control littermates (Figure 33G) suggesting that liver glucose production was not associated with the glucose metabolic disturbances observed. Body temperature remained similar between genotypes (Figure 33H), possibly excluding rough thermogenesis alterations.

Importantly, we could uncover a sexual dimorphism in the glucose homeostasis impairments of tau KI mice since neither fasting glycemia, glucose tolerance nor body weight gain were affected in females KI mice under HFD as compared to their control littermates (Figures 35A–H).

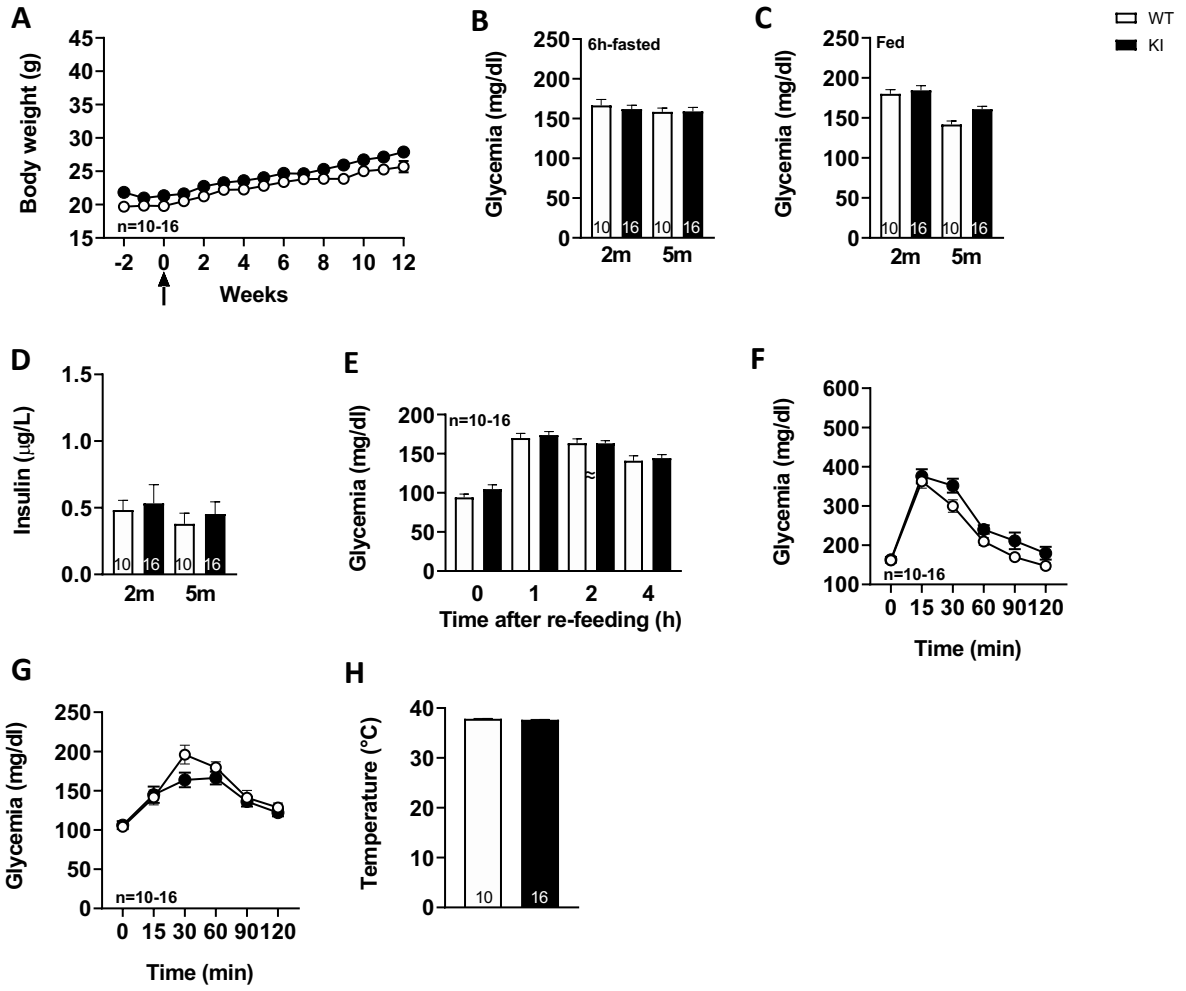

Figure 35. Metabolic phenotyping of tau KI female mice under High Fat diet (HFD; given from 2 to 5 months of age).

(A) Body weight gain of WT and tau KI mice under HFD from 2 to 5 months of age (NS). **(B)** Glycemia after 6 h of fasting before (2 m) and at the completion of HFD (5 m; NS). **(C)** Glycemia in fed condition 9 a.m. before (2 m) and at the completion of HFD (5 m; NS). **(D)** Insulinemia after 6 h of fasting before (2 m) and at the completion of HFD (5 m; NS). **(E)** Glycemic variations during the 1st, 2nd and 4th h following re-feeding after 16 h of fasting at the completion of the HFD, i.e., 5 months of age (NS). (**F**) Intraperitoneal glucose tolerance test (IPGTT) at the completion of the HFD, i.e., 5 months of age (NS). **(G)** Pyruvate tolerance test (PTT) at the completion of the HFD, i.e., 5 months of age (NS). **(H)** Rectal temperature before (2 months) and at the completion (5 months) of HFD (NS). Results are expressed as mean ± SEM. WT mice are indicated as white circles/bars, tau KI mice as black circles/bars.

Altogether, the present data suggested that, when challenged with HFD, tau KI male mice exhibit significant impaired glucose homeostasis, increased body wight gain and food intake. This could be related to the impact of tau loss of function in the pancreas and/or in the central nervous system (particularly the hypothalamus).

However, these metabolic phenotyping data do not allow us to know the origin of impaired glucose homeostasis observed in tau KI male mice.

Different approaches were used in order to explore the impact of tau loss of function separately in pancreatic islets, and in the hypothalamus.

Part II: Different approaches to explore the metabolic consequences of tau loss of function in pancreatic islets

1. Exploring the impact of tau loss of function in tau KI male mice pancreatic islets:

Firstly, since tau KI animals have impaired glucose tolerance upon HFD, we next investigated whether insulin-producing β-cell mass could be altered. Indeed, increased β-cell mass may be indicative of an adaptive mechanism to impaired insulin secretion and therefore altered glucose homeostasis (Weir and Bonner-Weir, 2004). We thus evaluated the relative mass of α and β-cells in pancreatic islets of WT and tau KI mice under HFD. Interestingly, enhanced insulinemia and glucose intolerance of tau KI mice under HFD were associated with an increased fraction of β-cells in the islets of tau KI mice as compared to WT littermates while glucagon-producing α-cells remained unaffected (Figure 36).

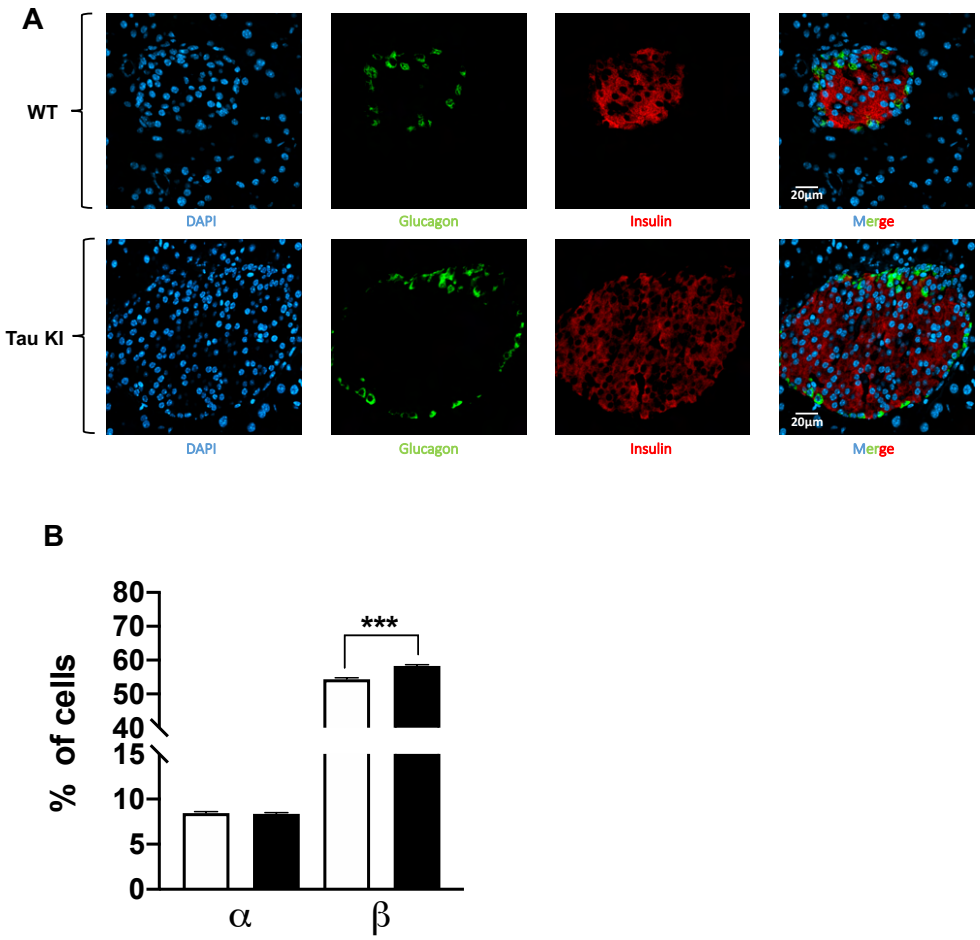

Figure 36. Analysis for both α and β cell fraction.

(A) Representative double immunofluorescence staining for insulin (red) and glucagon (green) in pancreas sections from adult WT and tau KI mice. DAPI nuclear counterstaining was used (blue). Magnification for pancreatic sections = x40, scale bars = 20 mm. **(B)** Automated analysis of a and b cell fraction in pancreatic sections from tau KI and WT male mice under HFD (N = 1521–1883 islets from three mice/group; Kruskal Wallis test, $p < 0.001$; **p = 0.0096 using Dunn's multiple comparisons test). Results are expressed as mean ± SEM. WT mice are indicated as white bars, tau KI mice as black bars.

The increase of β-cell mass can be explained by the increase of both the number of pancreatic islets and the area of β-cells in KI mice. These data suggest that impaired glucose tolerance might relate to defective insulin secretion in response to glucose, more than a direct effect on beta cell mass.

2. Tau is expressed by insulin-producing cells of mouse and human islets: Changes in insulin levels, impaired glucose homeostasis, and changes in β-cell mass observed in KI male mice point

towards a potential link between tau and function of pancreatic β-cells. It is noteworthy that while tau is particularly enriched in the brain, Mapt mRNA expression in pancreatic mouse islets represents 10% of its level in the hippocampus (Figure 37A).

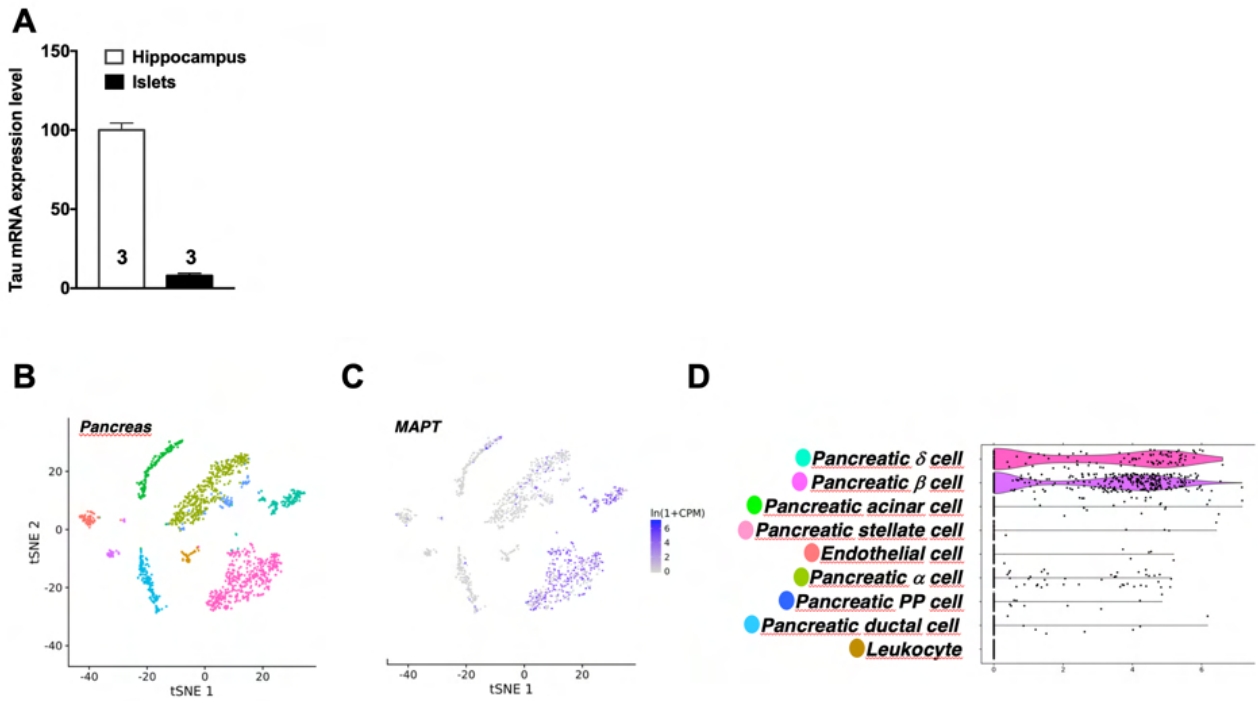

Figure 37. Tau mRNA expression in mouse pancreas.

(A) Tau mRNA expression in pancreatic islets and hippocampus of adult wild type mice (5 months). Tau mRNA expression in endocrine pancreatic islets represents 10 % of its expression in the hippocampus. Results are expressed as mean ± SEM. **(B)** t-Distributed Stochastic Neighbor Embedding (t-SNE) visualization of all mouse pancreatic cells collected by fluorescence-activated cell sorting (FACS). **(C)** Single-cell transcriptomic data of Mapt gene from adult mouse pancreatic tissue. **(D)** Differential expression of Mapt gene between different mouse pancreatic islets cells. For images B, C, and D data were extracted from the Tabula Moris single-cell RNA-sequencing database.

This is in line with public single-cell RNA sequencing data reporting tau mRNA enrichment in pancreatic β-cells (but also δ cells), of pancreatic islets vs. α-cells [(Figures 37B–D; (Segerstolpe et al., 2016). It is noteworthy that mouse islets expressed tau 4R isoforms (Figure 38A) while human

islets equally expressed both 3R and 4R tau isoforms (Figure 38B), in agreement with brain expressions.

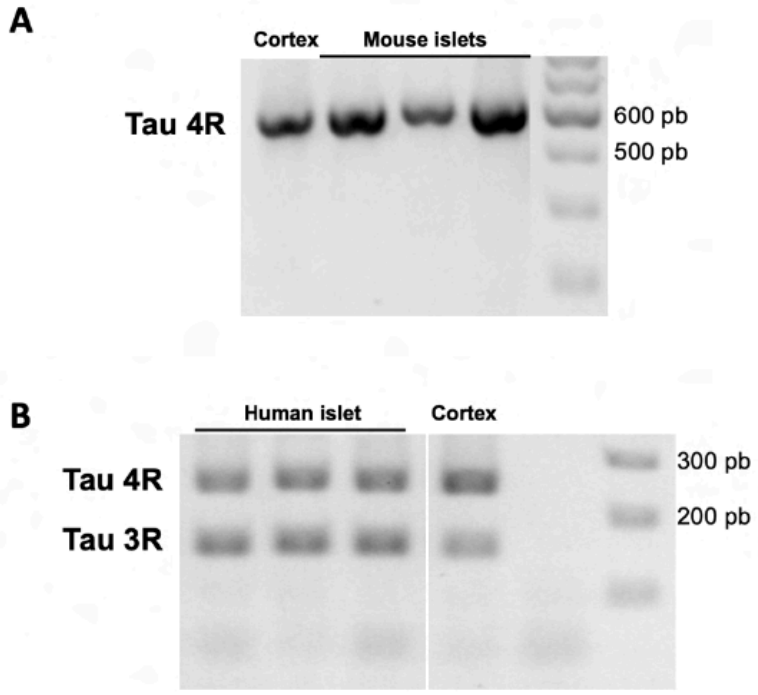

Figure 38. PCR analysis of mouse and human tau exon 10 splicing in mouse and human pancreatic islets. (A) Mouse analysis in pancreatic islets vs. cerebral cortex. Mice were 5 months old. **(B)** Human analysis in pancreatic islets vs. cerebral cortex.

Importantly, at the protein level, we investigated the expression of tau in the islets of WT and tau KI mice using various antibodies raised against the C-terminal (9F6) and the N-terminal (hTauE1) parts of tau (Figures 39 and 41) as well as an antibody raised against the 162–175 amino-acids of tau (9H12; Figure 40). We also evaluated the expression of tau in human islets (993S5 antibody; Figure 42). In line with previous studies (Maj et al., 2016a; Martinez-Valbuena et al., 2019b; Miklossy et al., 2010a; Wijesekara et al., 2018a), pancreatic islets from both WT and KI mice (9F6 and 9H12 antibodies; Figures 39 and 40), as well as humans (Figure 42), expressed tau protein.

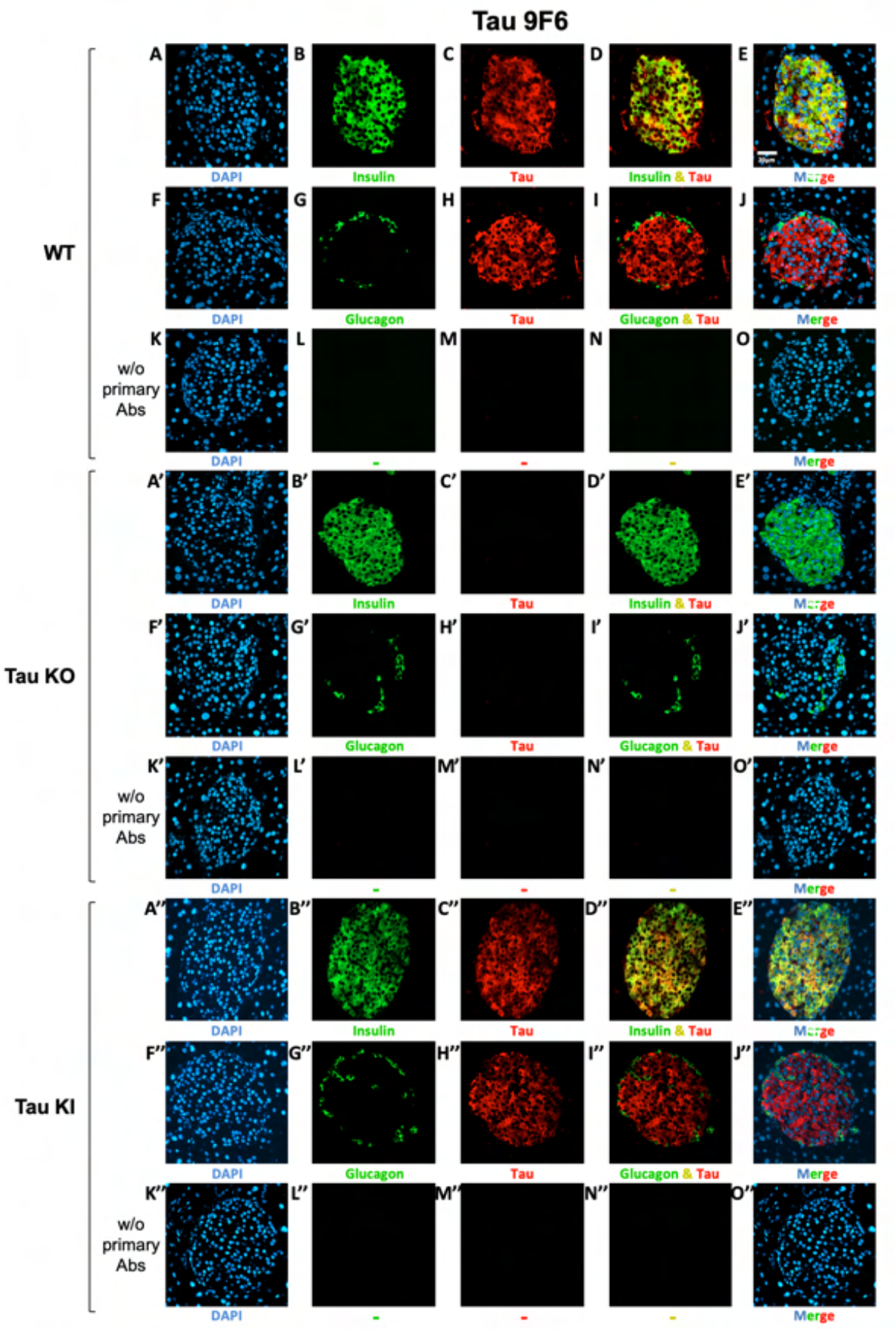
Tau 9F6
WT
Tau KO
Tau KI
w/o primary Abs
A
B
C
D
E
F
G
H
I
J
K
L
M
N
O
A'
B'
C'
D'
E'
F'
G'
H'
I'
J'
K'
L'
M'
N'
O'
A''
B''
C''
D''
E''
F''
G''
H''
I''
J''
K''
L''
M''
N''
O''
DAPI
Insulin
Tau
Insulin & Tau
Merge
Glucagon
Glucagon & Tau
-

Figure 39. Tau expression (tau 9F6 antibody) in mouse islets from WT, tau KO and tau KI mice and colocalization with insulin and glucagon. Tau WT mice. **(A-E)** Double immunofluorescence staining for insulin (green) and tau (red) in pancreatic islets from adult WT mice. Blue: DAPI nuclear counterstaining. **(F-J)** Double immunofluorescence staining for glucagon (green) and tau (red) in pancreatic islets from adult WT mice. Blue: DAPI nuclear counterstaining. **(K-O)** Absence of staining without primary antibodies. Only secondary antibodies and DAPI nuclear counterstaining (blue) were used. Tau KO mice **(A'-E')** Double immunofluorescence staining for insulin (green) and tau (red) in pancreatic islets from adult tau KO mice. Blue: DAPI nuclear counterstaining. **(F'-J')** Double immunofluorescence staining for glucagon (green) and tau (red) in pancreatic islet from adult tau KO mice. Blue: DAPI nuclear counterstaining. **(K'-O')** Absence of staining without primary antibodies. Only secondary antibodies and DAPI nuclear counterstaining (blue) were used.

Tau KI mice **(A''-E'')** Double immunofluorescence staining for insulin (green) and tau (red) in pancreatic islets from adult KI mice. Blue: DAPI nuclear counterstaining. **(F''-J'')** Double immunofluorescence staining for glucagon (green) and tau (red) in pancreatic islet from adult tau KI mice. Blue: DAPI nuclear counterstaining. **(K''-O'')** Absence of staining without primary antibodies. Only secondary antibodies and DAPI nuclear counterstaining (blue) were used. Mice were 5 months old. Scale: 20µm.

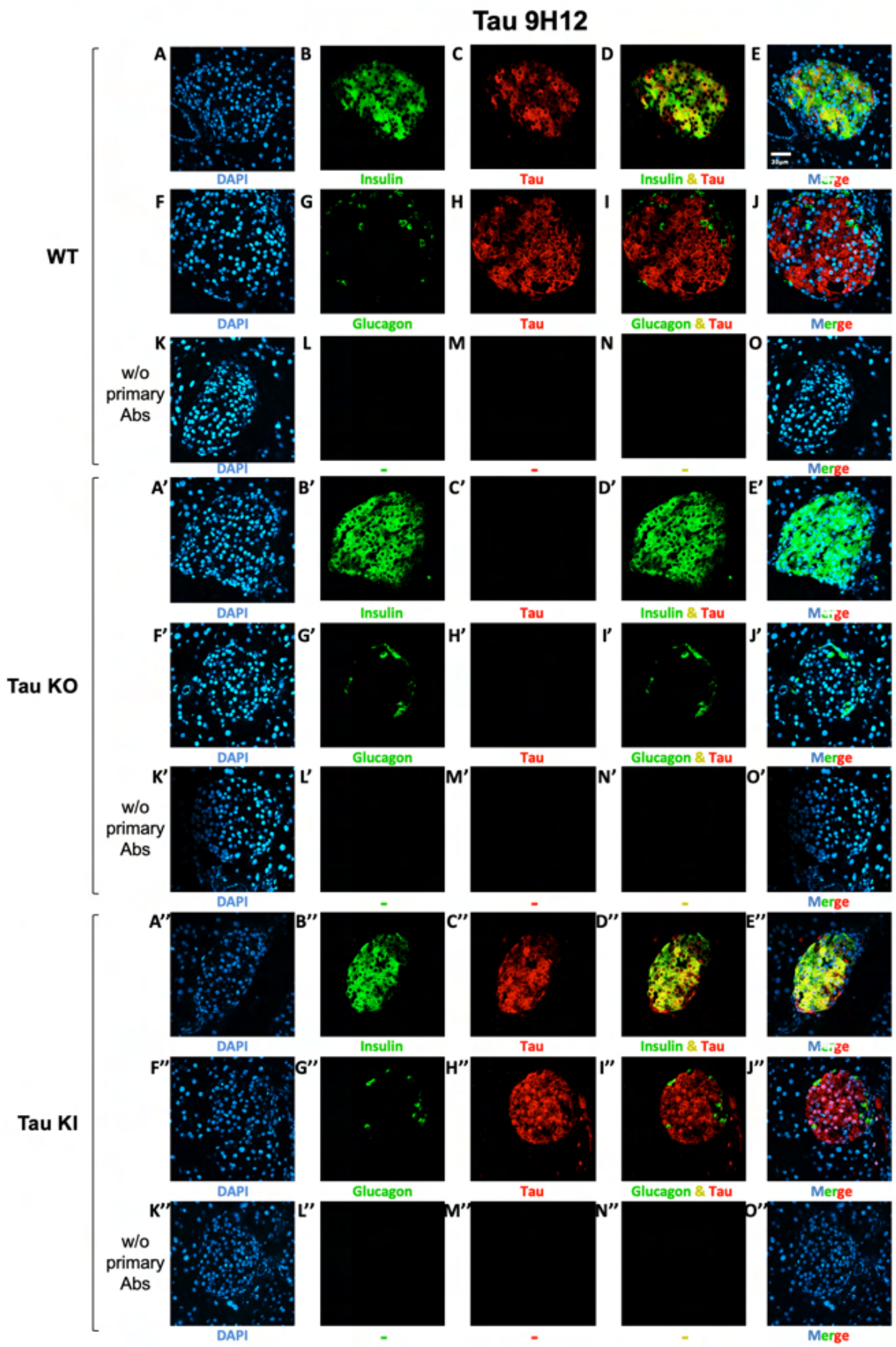
Tau 9H12
WT
Tau KO
Tau KI
w/o primary Abs
A
B
C
D
E
F
G
H
I
J
K
L
M
N
O
A'
B'
C'
D'
E'
F'
G'
H'
I'
J'
K'
L'
M'
N'
O'
A''
B''
C''
D''
E''
F''
G''
H''
I''
J''
K''
L''
M''
N''
O''
DAPI
Insulin
Tau
Insulin & Tau
Merge
Glucagon
Glucagon & Tau
-

Figure 40. Tau expression (tau 9H12 antibody) in mouse islets from WT, tau KO and tau KI mice and colocalization with insulin and glucagon. Tau WT mice. **(A-E)** Double immunofluorescence staining for insulin (green) and tau (red) in pancreatic islets from adult WT mice. Blue: DAPI nuclear counterstaining. **(F-J)** Double immunofluorescence staining for glucagon (green) and tau (red) in pancreatic islets from adult WT mice. Blue: DAPI nuclear counterstaining. **(K-O)** Absence of staining without primary antibodies. Only secondary antibodies and DAPI nuclear counterstaining (blue) were used. Tau KO mice **(A'-E')** Double immunofluorescence staining for insulin (green) and tau (red) in pancreatic islets from adult tau KO mice. Blue: DAPI nuclear counterstaining. **(F'-J')** Double immunofluorescence staining for glucagon (green) and tau (red) in pancreatic islet from adult tau KO mice. Blue: DAPI nuclear counterstaining. **(K'-O')** Absence of staining without primary antibodies. Only secondary antibodies and DAPI nuclear counterstaining (blue) were used.
Tau KI mice **(A''-E'')** Double immunofluorescence staining for insulin (green) and tau (red) in pancreatic islets from adult KI mice. Blue: DAPI nuclear counterstaining. **(F''-J'')** Double immunofluorescence staining for glucagon (green) and tau (red) in pancreatic islet from adult tau KI mice. Blue: DAPI nuclear counterstaining. **(K''-O'')** Absence of staining without primary antibodies. Only secondary antibodies and DAPI nuclear counterstaining (blue) were used. Mice were 5 months old. Scale: 20µm.

As expected, pancreatic islets from tau KI but not WT mice expressed human tau (hTauE1 antibody; Figure 41). The specificity of the signal in mouse samples was attested by the lack of signal found in the pancreatic islets from tau KO mice (Figures 39, 40 and 41). The absence of signal was always observed when primary antibodies were omitted (Figures 39, 40 and 41).

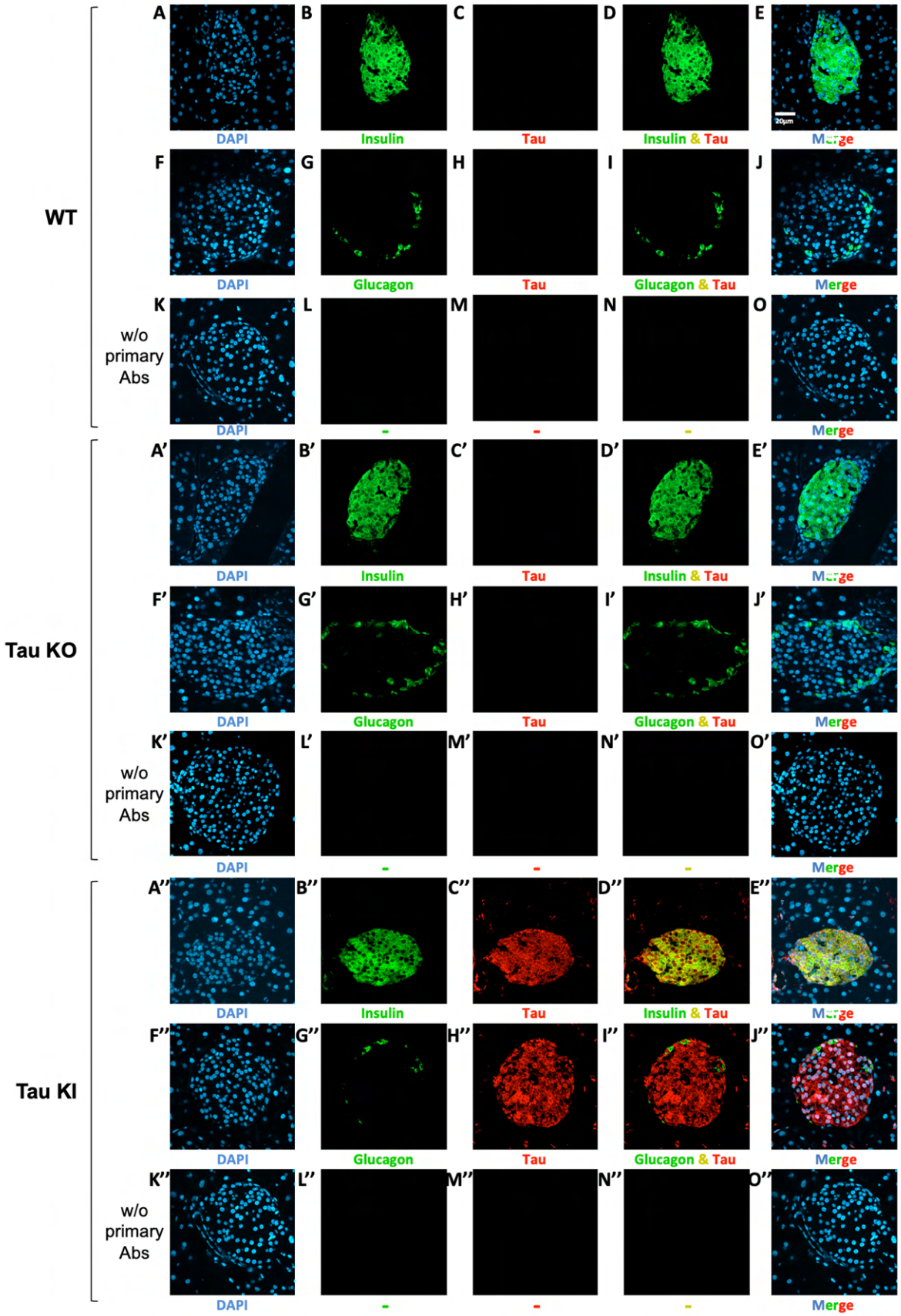
Tau hTauE1
WT
Tau KO
Tau KI
w/o primary Abs
A
B
C
D
E
F
G
H
I
J
K
L
M
N
O
A'
B'
C'
D'
E'
F'
G'
H'
I'
J'
K'
L'
M'
N'
O'
A''
B''
C''
D''
E''
F''
G''
H''
I''
J''
K''
L''
M''
N''
O''
DAPI
Insulin
Tau
Insulin & Tau
Merge
Glucagon
Glucagon & Tau
-

Figure 41. Tau expression (tau hTauE1 antibody) in mouse islets from WT, tau KO and tau KI mice and colocalization with insulin and glucagon. Tau WT mice. **(A-E)** Double immunofluorescence staining for insulin (green) and tau (red) in pancreatic islets from adult WT mice. Blue: DAPI nuclear counterstaining. **(F-J)** Double immunofluorescence staining for glucagon (green) and tau (red) in pancreatic islets from adult WT mice. Blue: DAPI nuclear counterstaining. **(K-O)** Absence of staining without primary antibodies. Only secondary antibodies and DAPI nuclear counterstaining (blue) were used. Tau KO mice **(A'-E')** Double immunofluorescence staining for insulin (green) and tau (red) in pancreatic islets from adult tau KO mice. Blue: DAPI nuclear counterstaining. **(F'-J')** Double immunofluorescence staining for glucagon (green) and tau (red) in pancreatic islet from adult tau KO mice. Blue: DAPI nuclear counterstaining. **(K'-O')** Absence of staining without primary antibodies. Only secondary antibodies and DAPI nuclear counterstaining (blue) were used.

Tau KI mice **(A''-E'')** Double immunofluorescence staining for insulin (green) and tau (red) in pancreatic islets from adult KI mice. Blue: DAPI nuclear counterstaining. **(F''-J'')** Double immunofluorescence staining for glucagon (green) and tau (red) in pancreatic islet from adult tau KI mice. Blue: DAPI nuclear counterstaining. **(K''-O'')** Absence of staining without primary antibodies. Only secondary antibodies and DAPI nuclear counterstaining (blue) were used. Mice were 5 months old. Scale: 20µm.

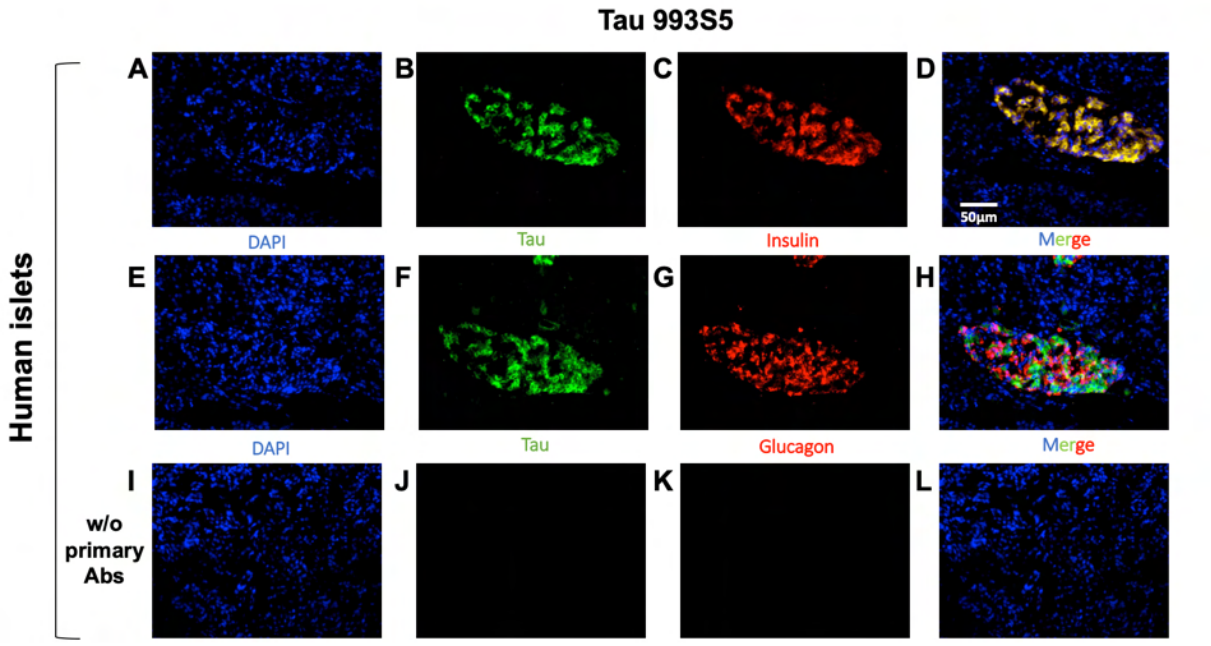

Figure 42. Tau expression (tau 993S5 antibody) in human pancreatic islets and colocalization with insulin and glucagon.

(A–D) Double immunofluorescence staining for tau (green) and insulin (red). Blue: DAPI nuclear counterstaining. **(E–H)** Double immunofluorescence staining for tau (green) and glucagon (red). Blue: DAPI nuclear counterstaining. Scale: 50 mm. **(I-L)** Absence of staining without primary antibodies. Only secondary antibodies and DAPI nuclear counterstaining (blue) were used.

Importantly, in both mouse and human pancreatic islets, tau protein was clearly expressed by β-cells, expressing insulin (Figures 39, 40, 41 and 42) but not by α-cells, expressing glucagon.

To corroborate these observations, we performed an overlapping quantification using the Pearson's overlap coefficient as an index. The latter was determined using ImageJ Software on confocal Z-stacks. In WT mice (9F6 antibody), the Pearson coefficient for insulin/tau was found to be 0.74 ± 0.01 (n = 5) while values for glucagon/tau were extremely low 0.0005 ± 0.0006 (n = 5). In KI mice (hTauE1 antibody), the Pearson coefficient for insulin/tau was found to be 0.81 ± 0.02 (n =

5) while values for glucagon/tau were extremely low 0.02 ± 0.0004 (n = 5). In human islet (993S5 antibody), values were found to be 0.90 ± 0.06 (n = 3) for insulin/tau colocalization, while 0.18 ± 0.05 for glucagon/tau. Together, these data strongly support that in pancreatic islets, tau protein is largely enriched in β-cells.

In addition to testing different antibodies targeting diverse sites of human or mice tau protein, we also tested other antibodies raised different physiological and pathological phosphorylated sites of tau. In animals under chow diet, we observed in pancreatic islets of both tau KI and WT, a signal from phosphorylated tau at serine 199, as well as at serine 404 (Figures 43 and 44). However, no signal was observed in pancreatic islets of both tau KI and WT animals with antibodies that raised phosphorylated tau at serine 396 or phosphorylated tau at both serine 202 and threonine 205.

The specificity of the signal in mouse samples was attested by the lack of signal found in the pancreatic islets from tau KO mice (Figures 43 and 44).

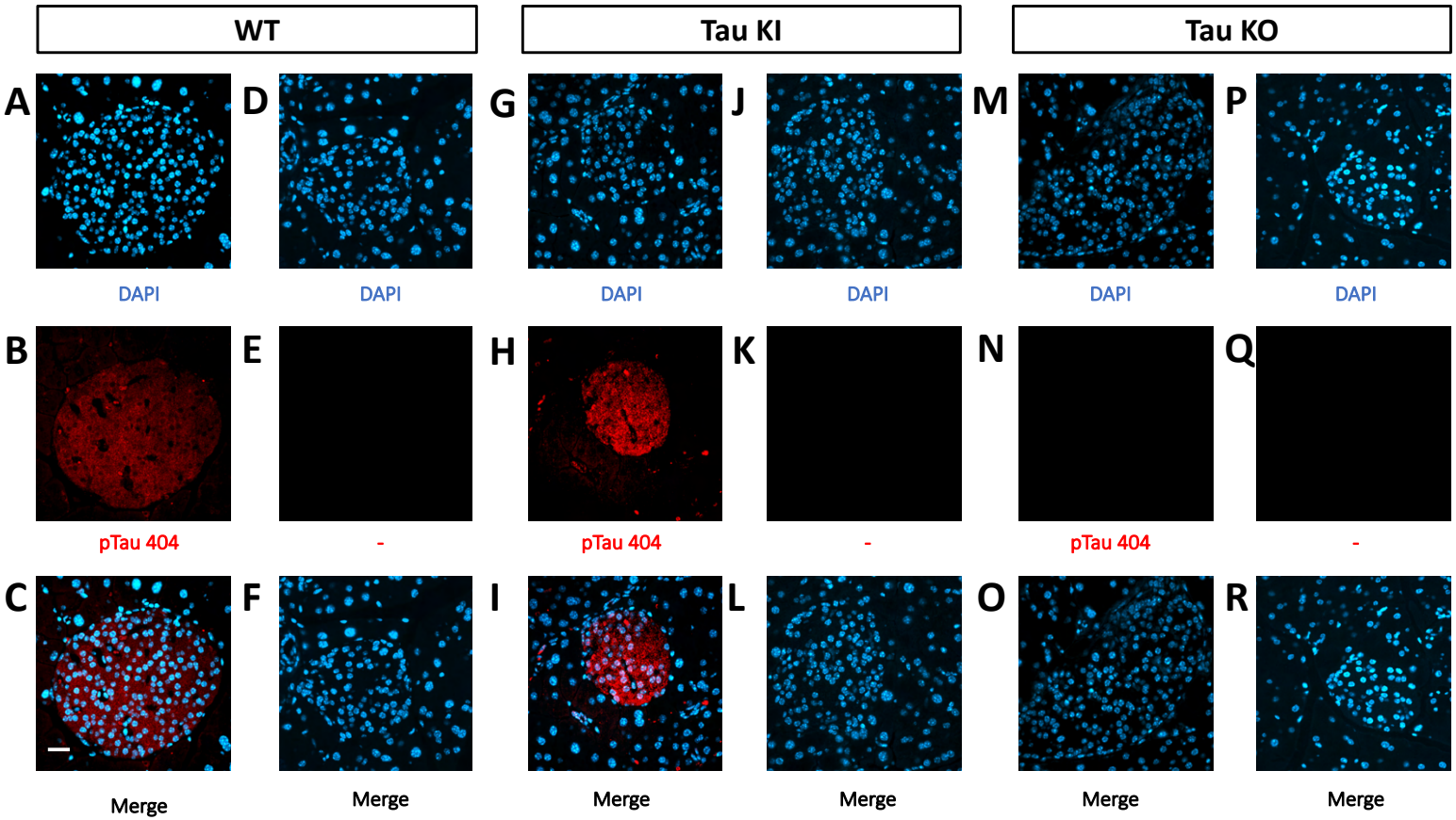

Figure 43. Phosphorylated tau expression (pTau 404 antibody) in mouse islets from WT, tau KO and tau KI mice.
Tau WT mice: (A-C) Immunofluorescence staining for pTau 404 (red) in pancreatic islets from adult WT mice. Blue: DAPI nuclear counterstaining. **(D-F)** Absence of staining without primary antibodies. Only secondary antibodies and DAPI nuclear counterstaining (blue) were used.
Tau KI mice: (G-I) Immunofluorescence staining for pTau 404 (red) in pancreatic islets from adult tau KI mice. Blue: DAPI nuclear counterstaining. **(J-L)** Absence of staining without primary antibodies. Only secondary antibodies and DAPI nuclear counterstaining (blue) were used.
Tau KO mice: (M-O) Immunofluorescence staining for pTau 404 (red) in pancreatic islets from adult tau KO mice. Blue: DAPI nuclear counterstaining. **(P-R)** Absence of staining without primary antibodies. Only secondary antibodies and DAPI nuclear counterstaining (blue) were used.
Mice were 5 months old. Scale: 20µm.

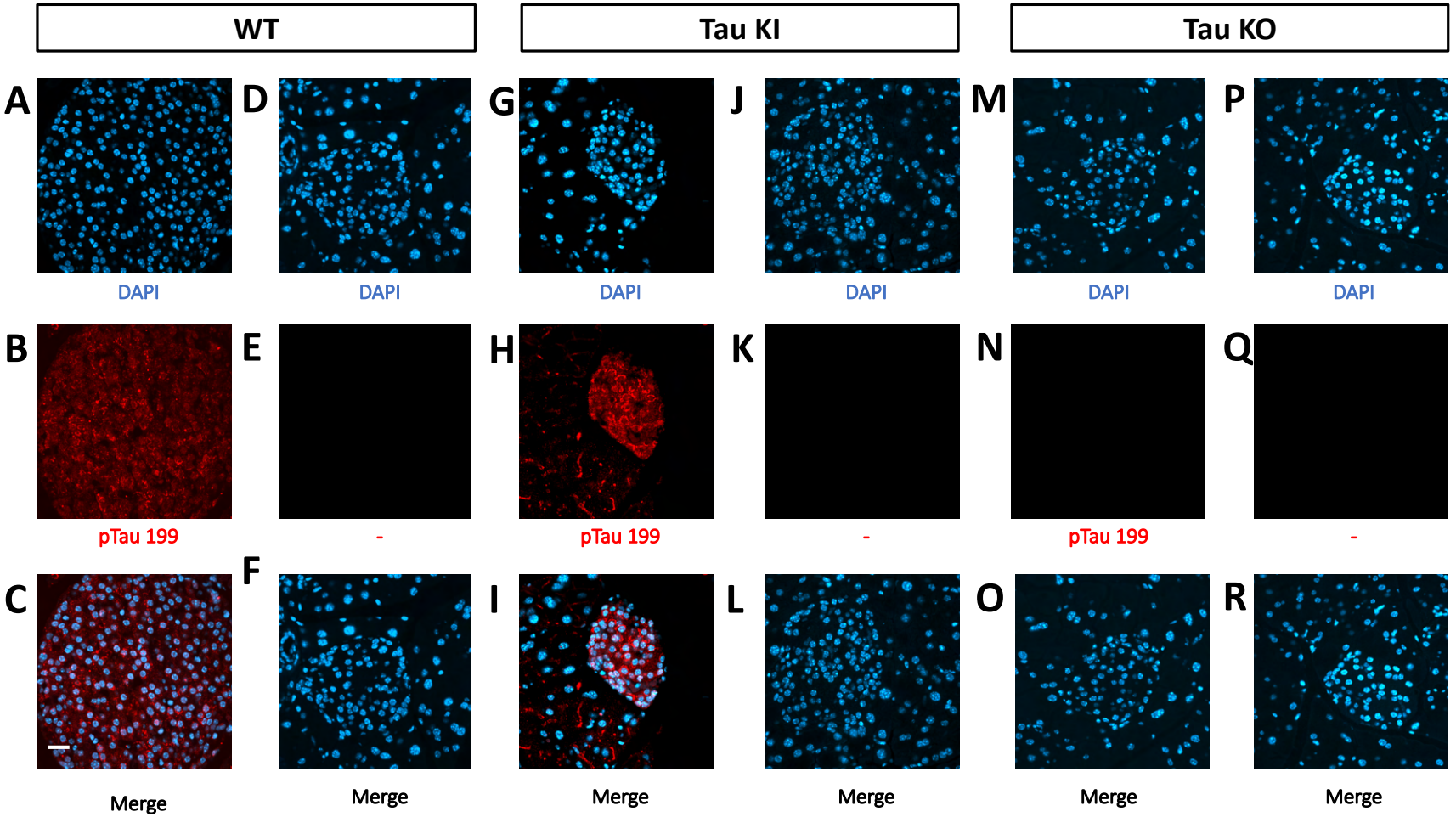

Figure 44. Phosphorylated tau expression (pTau 199 antibody) in mouse islets from WT, tau KO and tau KI mice.
Tau WT mice: (A-C) Immunofluorescence staining for pTau 199 (red) in pancreatic islets from adult WT mice. Blue: DAPI nuclear counterstaining. **(D-F)** Absence of staining without primary antibodies. Only secondary antibodies and DAPI nuclear counterstaining (blue) were used.
Tau KI mice: (G-I) Immunofluorescence staining for pTau 199 (red) in pancreatic islets from adult tau KI mice. Blue: DAPI nuclear counterstaining. **(J-L)** Absence of staining without primary antibodies. Only secondary antibodies and DAPI nuclear counterstaining (blue) were used.
Tau KO mice: (M-O) Immunofluorescence staining for pTau 199 (red) in pancreatic islets from adult tau KO mice. Blue: DAPI nuclear counterstaining. **(P-R)** Absence of staining without primary antibodies. Only secondary antibodies and DAPI nuclear counterstaining (blue) were used.
Mice were 5 months old. Scale: 20µm.

3. Evaluation of glucose-stimulated insulin secretion in isolated islets from tau KI, WT and KO mice:

To fully appreciate the functional impact of tau loss-of-function on tau KI mice to β-cell function, in collaboration with Dr. Jean-Sébastien Annicotte team, we evaluated glucose stimulated insulin secretion (GSIS) in low and high glucose conditions from pancreatic islets isolated from WT, tau KI mice, and tau KO male mice, taken as a control. Although the level of insulin expressed by islets was not significantly different in KO and KI mice vs. WT (Figure 45A), constitutive tau deletion or expression of the mutated form in KI significantly impaired insulin secretion upon high (16.7 mM) glucose stimulation (Figure 45B).

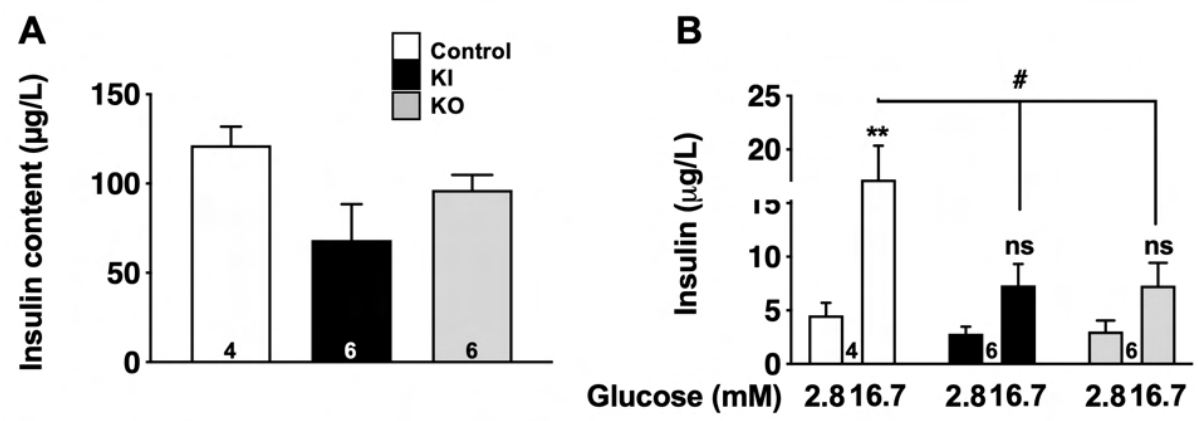

Figure 45. Glucose-stimulated insulin secretion (GSIS) on islets isolated from tau knock-in and knock-out mice. (A) Insulin content (mg/L) from isolated islets (N = 4–6 mice/group; NS using Kruskal Wallis test). **(B)** Insulin secretion from control, tau KI and tau KO islets stimulated with low (2.8 mM) and high (16.7 mM). glucose for 1 h (N = 4–6 mice/group; Two-Way ANOVA; $F(5,26) = 7.544$ $p < 0.001$; Tukey's post hoc test $^{**}p < 0.01$, $\#p < 0.05$ vs. 2.8 mM). WT, tau KI, and tau KO are indicated as open bars, black bars and gray bars, respectively. Mice were 5 months old. ns, non significant.

In addition, using the mouse pancreatic β-cell line Min6, we could also observe that tau knock-down by shRNA significantly impaired GSIS (Figure 46). Taken together, these results support that loss of tau function (knockdown, KO, or KI) impairs insulin secretion in response to glucose without affecting insulin content, suggestive of a direct effect of tau loss-of-function on insulin secretion rather than insulin biogenesis.

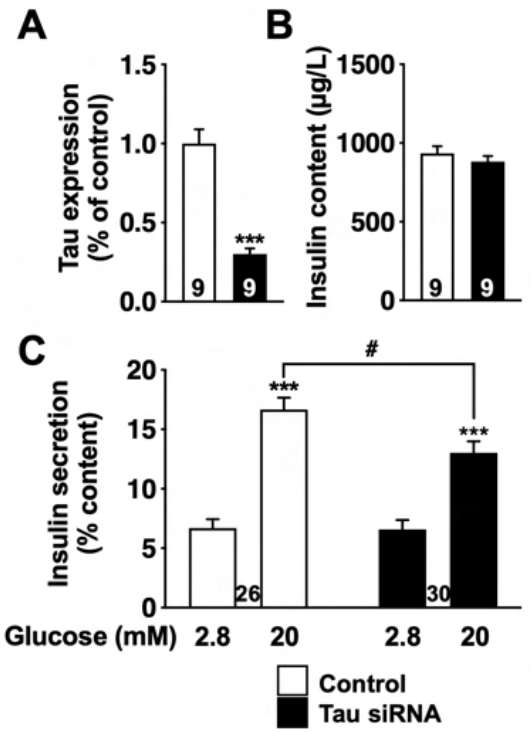

Figure 46. Effect of tau knock-down on insulin secretion at glucose stimulated insulin secretion (GSIS) in β pancreatic mouse line Min6. (A) Tau mRNA expression level in control and tau siRNA conditions (***p< .0001, Student's t-test). **(B)** Min6 cells insulin content at GSIS (NS, Student's t-test). **(C)** Effect of tau knock-down on insulin release by Min6 cells in low and high glucose conditions at GSIS (***p< .0001, # p< .05, Two-Way ANOVA test and Tukey's post-hoc test).

To sum up, immunofluorescences data showed that tau is co-localized with insulin in pancreatic β-cells, and in vitro experiments revealed the involvement of tau protein in insulin secretion. Furthermore, to study in vivo the impact of tau loss of function specifically in pancreatic β-cells different approach were adopted:

4. Exploration of the in vivo impact of tau los of function in pancreatic β-cells:

For exploring the in vivo impact of tau los of function in pancreatic β-cells, we chose first a selective tau knockdown in mice pancreatic β-cells strategy. This approach was made possible by the use of an original mouse model developed by the laboratory.

4.1. Approach using tau floxed mouse model and tau conditional deletion strategy in pancreatic β-cells:

Interestingly, the laboratory had developed an original tau floxed mouse model (C57Bl6J) generated by flanking the murine tau exon 3, harboring the ATG initiation codon, with loxP sites. This was combined with the FLEx monitoring strategy allowing that CRE recombinase turns-off murine tau expression while the expression of an eGFP reporter is concomitantly turned-on (Figure 47, (Schnütgen et al., 2003)).

It is noteworthy that in our model, expression of the eGFP following CRE recombination only takes place in cells in which the promoter of tau is effectively active i.e. in cells physiologically expressing tau transcript.

The aim of the strategy using these tau floxed mice was to delete tau from pancreatic β-cells and obtained cKO-Tau$^{\beta}$ model. To generate β-cell specific tau KO mice (cKO-Tau$^{\beta}$ animals), tau flox mice were crossed with inducible Insulin Promoter (Ins1)-Cre/ERT (MIP-CREERT animals, Jax N° 024709), harboring a transgene encompassing the mouse Insulin 1 Promoter (MIP) driving the expression of the tamoxifen-inducible Cre recombinase [(CREERT), Figure 48]. The MIP-CreERT mouse line is the most efficient and specific model compared to other β-cell specific Cre lines (Wicksteed et al., 2010).

In MIP-CerERT mice, Cre-ERT proteins are sequestered in the cytoplasm of β-cells through association with the HSP90 chaperone. Upon addition of tamoxifen, tamoxifen-bound Cre-ERT, then the last will dissociate from HSP90, and translocates into the nucleus, which carries out site-specific recombination between flanking loxP sites (Reinert et al., 2012).

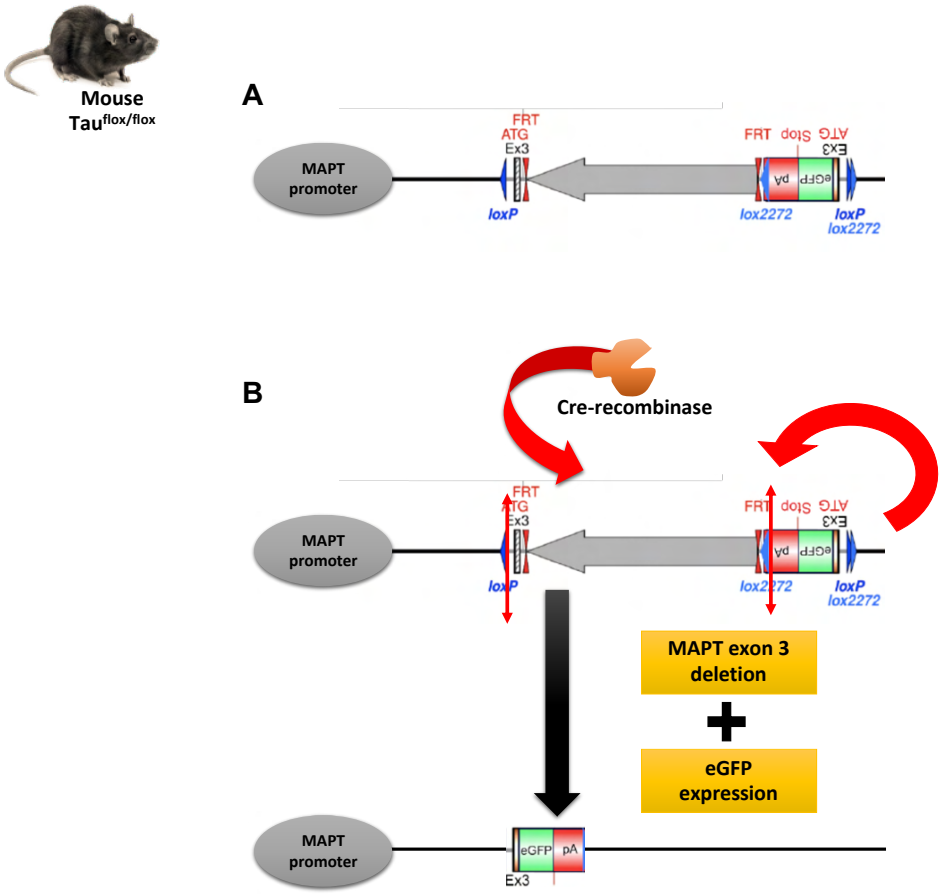

Figure 47. Tau floxed mouse model and overall tau conditional deletion strategy.

Tau floxed ($Tau^{Flox/Flox}$) mouse model (C57Bl6J) was generated by: **(A)** flanking the murine tau exon 3, harboring the ATG initiation codon, with loxP sites. **(B)** It has been combined with the FLEx monitoring strategy allowing that CRE recombinase turns-off murine tau expression while the expression of an eGFP reporter is concomitantly turned-on.

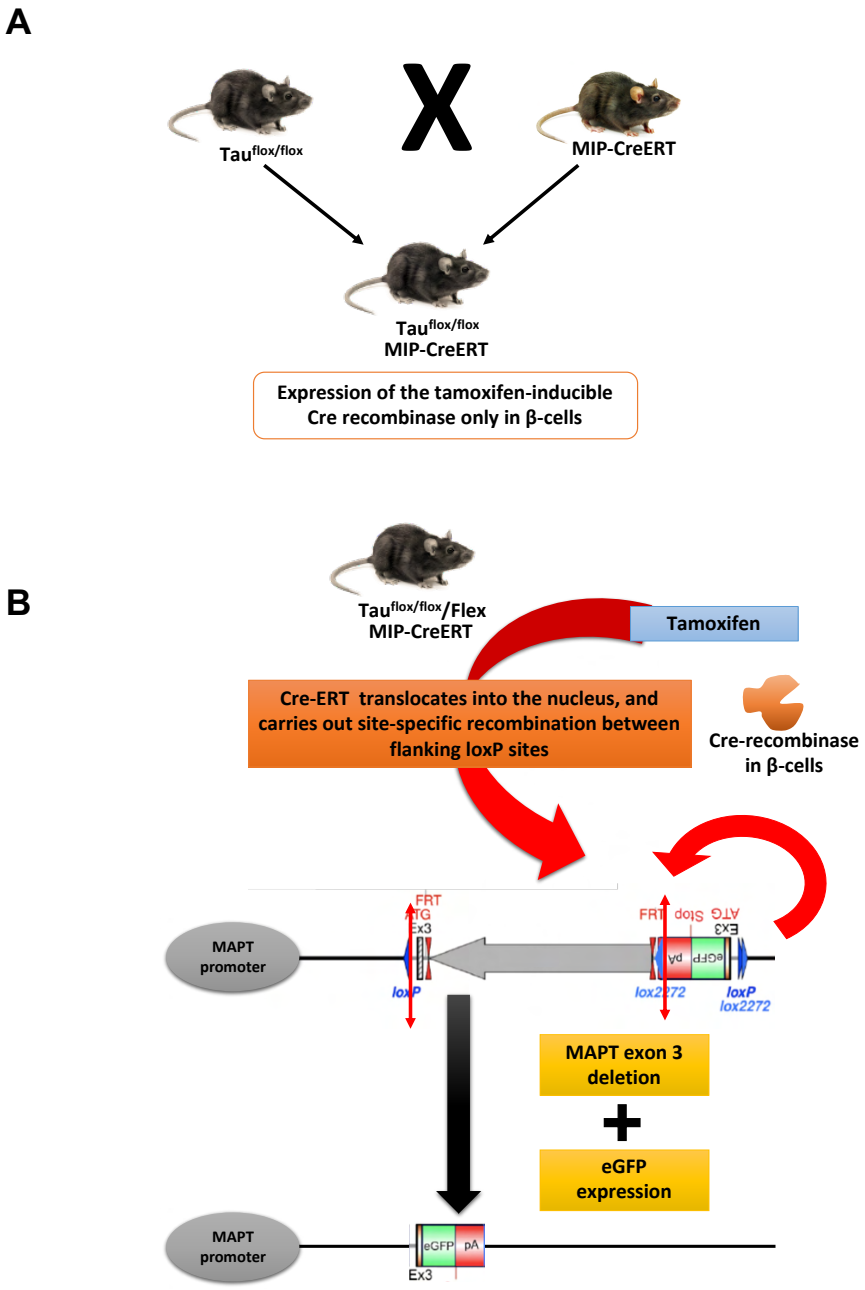

Figure 48. Generation of β-cell specific tau KO mice (cKO-Tau$^{\beta}$).

(A) MIP-CerERT animals express a tamoxifen-inducible Cre recombinase (cre/ERT) driven by the mouse insulin I promoter (Ins1). Tau$^{flox/flox}$ mice were crossed with MIP-CerERT animals in order to generate Tau$^{flox/flox}$//MIP-CreERT animals.

(B) In Tau$^{flox/flox}$//MIP-CreERT offspring inducible Cre recombinase activity is present specifically in the pancreatic β-cells. CreERT protein is restricted to the cytoplasm, and it can only gain access to the nuclear compartment after exposure to tamoxifen. The combination of the FLEx monitoring strategy allowed that when CRE recombinase turns-off murine tau expression, the expression of an eGFP reporter is concomitantly turned-on in the pancreatic β-cells.

Before starting animals' generation and the conditional deletion strategy, we did firstly the characterization of tau flox mouse model in order to validate it.

4.2. Evaluation of tau expression in pancreatic islets from tau floxed mice:

The first step of tau flox mouse model validation was the study of tau expression in pancreatic islets. Males and females $tau^{Flox/+}$ (heterozygotes) animals were crossed in order to obtain: $tau^{Flox/Flox}$ (homozygotes), $tau^{Flox/+}$ (heterozygotes) and their littermate (WT). Also, tau KO mice were used as additional negative control (absence of tau expression).

Tau protein expression in pancreatic islets was studied using immunochemistry approach. As observed in Figure 49, the immunofluorescence signal of tau protein (red) was reduced in both $tau^{Flox/+}$ and $tau^{Flox/Flox}$ mice compared to WT mice (-60% and -80% compared to WT, respectively).

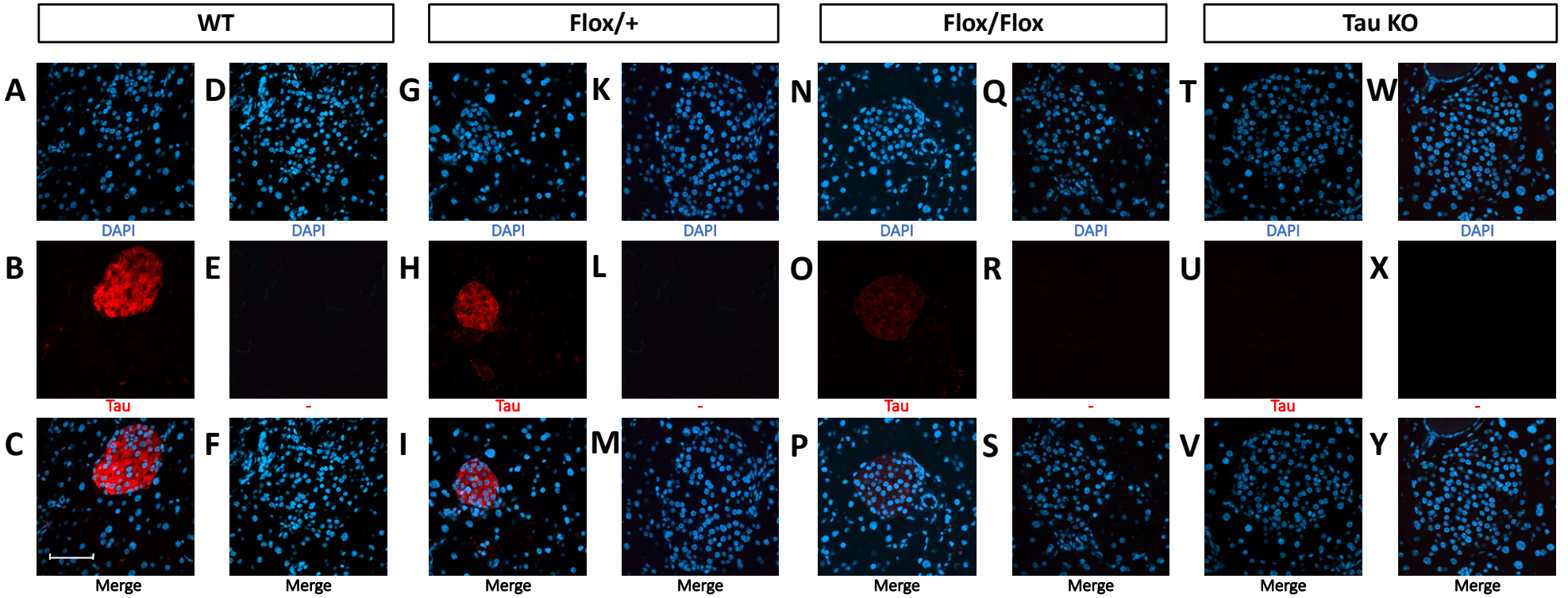

Figure 49. Tau expression (tau 9F6 antibody) in mouse islets from WT, tau KO, tau$^{Flox/Flox}$ and tau$^{Flox/+}$ mice.

Tau WT mice: **(A-C)** Immunofluorescence staining for tau (red) in mouse islets from adult WT mice. Blue: DAPI nuclear counterstaining. **(D-F)** Absence of staining without primary antibodies. Only secondary antibodies and DAPI nuclear counterstaining (blue) were used.

Tau$^{Flox/+}$ mice: **(G-I)** Immunofluorescence staining for tau (red) in mouse islets from adult Tau$^{Flox/+}$ mice. Blue: DAPI nuclear counterstaining. **(K-M)** Absence of staining without primary antibodies. Only secondary antibodies and DAPI nuclear counterstaining (blue) were used.

Tau$^{Flox/Flox}$ mice: (N-P) Immunofluorescence staining for tau (red) in mouse islets from adult Tau$^{Flox/Flox}$ mice. Blue: DAPI nuclear counterstaining. (Q-S) Absence of staining without primary antibodies. Only secondary antibodies and DAPI nuclear counterstaining (blue) were used.

Tau KO mice: (T-V) Immunofluorescence staining for tau (red) in mouse islets from adult tau KO mice. Blue: DAPI nuclear counterstaining. (W-Y) Absence of staining without primary antibodies. Only secondary antibodies and DAPI nuclear counterstaining (blue) were used.

Scale: 20µm.

4.3. Initial metabolic phenotyping of tau flox mice under Chow diet:

Unexpectedly, tau$^{Flox/Flox}$ mice presented impaired glucose homeostasis with a significant elevated glycemia in fed condition and glucose intolerance 15 minutes after glucose injection at IPGTT, compared to WT or tau$^{Flox/+}$ mice (Figure 50 C and D). Glycemia after 6h of fating were not different between the three groups. Tau$^{Flox/+}$ chowed a nearly similar profile to that of WT mice (Figure 50).

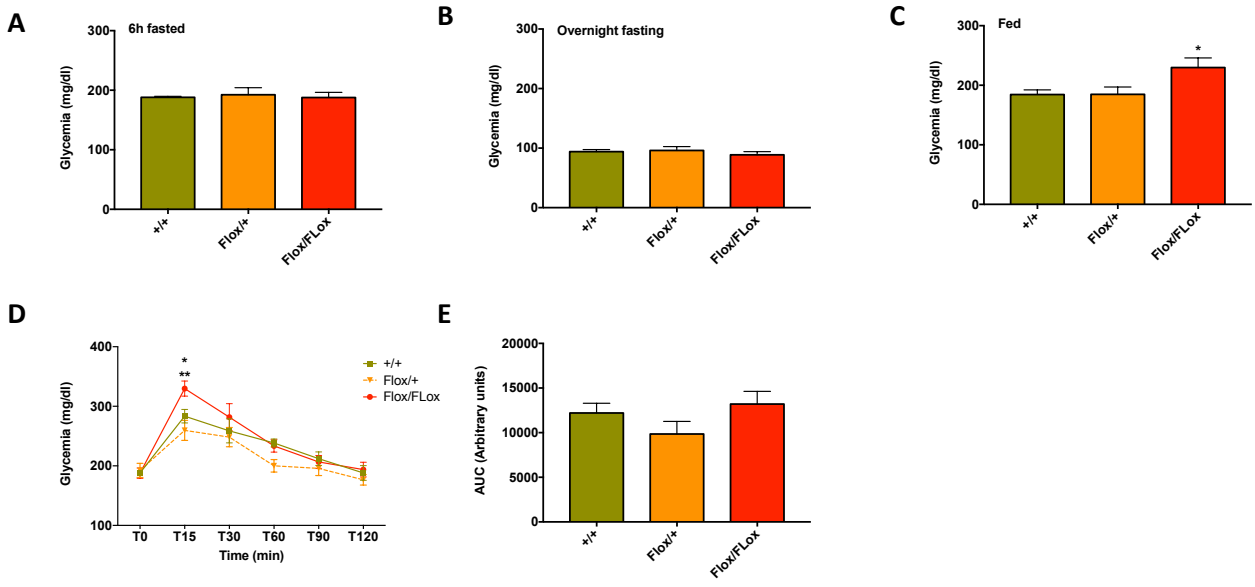

Figure 50. Metabolic phenotyping of tau flox mice under chow diet.

A) Glycemia after 6 h of fasting (NS). **(B)** Glycemia after an overnight fasting (NS). **(C)** Glycemia in fed condition 8 a.m (* tau$^{Flox/+}$ vs. tau$^{Flox/FLox}$; $p<0.05$). **(D)** Intraperitoneal glucose tolerance test (IPGTT), (* +/+ vs. tau$^{Flox/FLox}$ at T 15 minutes; $p<0.05$, ** tau$^{Flox/+}$ vs. tau$^{Flox/FLox}$ at T 15 minutes ; $p<0.0001$). **(E)** Area under the curve (AUC) for IPGTT (NS).
Results are expressed as mean ± SEM. +/+ mice are indicated as green squares, tau$^{Flox/FLox}$ mice red circles, and tau$^{Flox/+}$ orange triangles.

Accordingly, these data revealed a hypomorphic status of homozygous tau flox mice in the absence of CRE. Also, they developed impaired glucose homeostasis similarly to tau KI and tau KO. Conversely, $tau^{Flox/+}$ had a close metabolic phenotype to WT mice, we thus used heterozygous tau flox animals that were combined with CRE approaches to knock-down tau from pancreatic ß-cells (cKO-Tau^{β} animals).

4.4. Generation of β-cell specific Tau KO mice:

To generate β-cell specific Tau KO mice (cKO-Tau^{β} animals), $Tau^{flox/+}$ mice were crossed with inducible Insulin Promoter (Ins1)-Cre/ERT (MIP-CREERT animals, Jax N° 024709), harboring a transgene encompassing the mouse Insulin 1 Promoter (MIP) driving the expression of the tamoxifen-inducible Cre recombinase (CreERT). The MIP-CreERT mouse line is the most efficient and specific model compared to other β-cell specific Cre lines (Wicksteed et al., 2010). Figure 51 demonstrate the efficient recombination in mice injected intraperitoneally with three doses of 2-mg tamoxifen over a period of 5 days.

The crossing of $Tau^{flox/+}$ mice with MIP-CreERT mice resulted in two genotypes: $Tau^{flox/+//MIP\text{-}CRE/+}$, $Tau^{flox/+//+/+}$ (Figure 52).

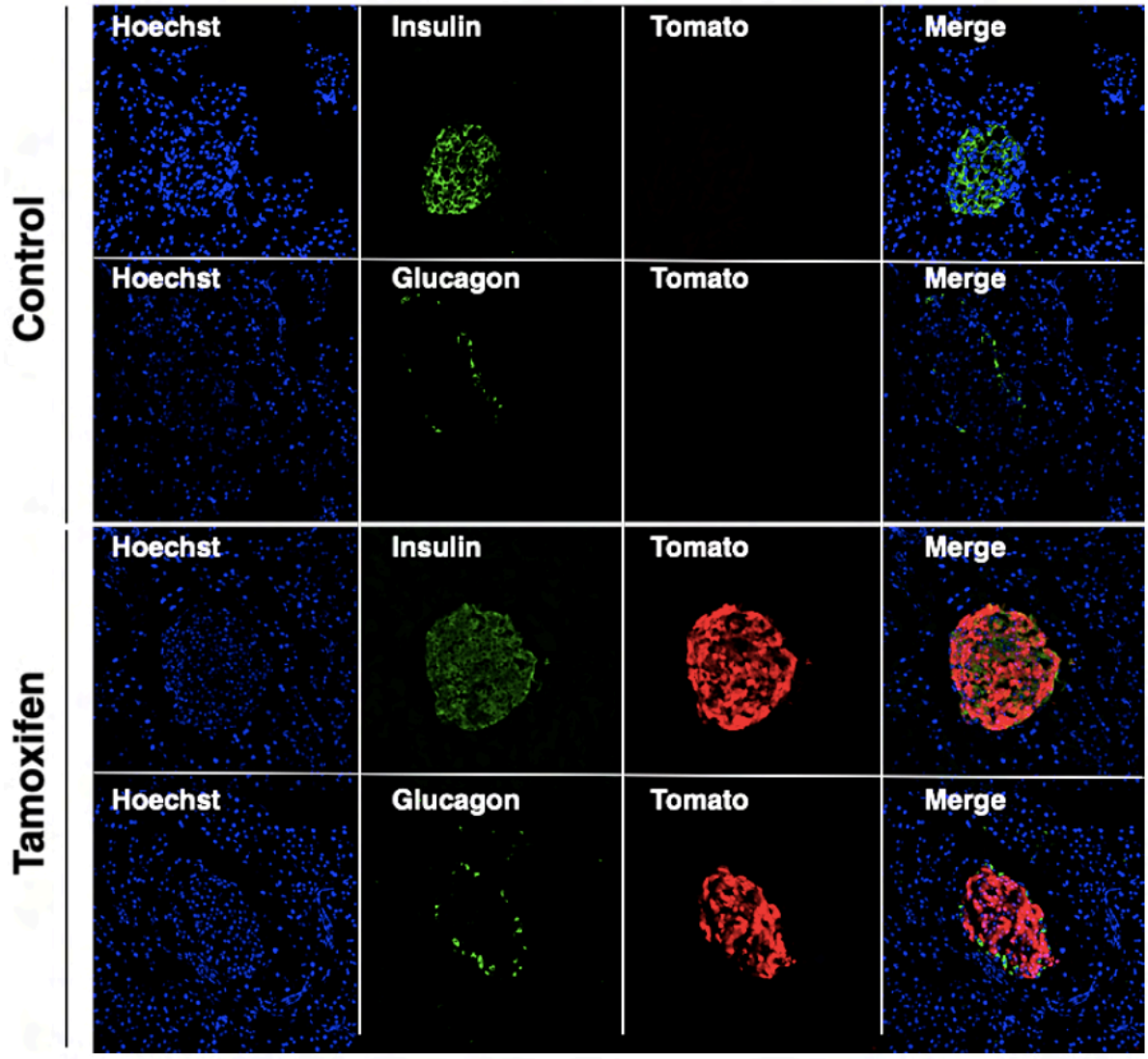

Figure 51. Effective recombination in beta pancreatic cells using the MIP-CreERT transgenic line.

Tamoxifen-inducible MIP-CreERT mice were crossed with the reporter tdTomato line where Tomato protein is expressed in cell undergoing CRE recombination when CRE expression is induced by tamoxifen injection (5 days).

As compared to control (upper panels), Tamoxifen-treated animals (lower panels) exhibit effective recombination in beta pancreatic cells, signed by Tomato expression in insulin but not glucagon-positive cells.

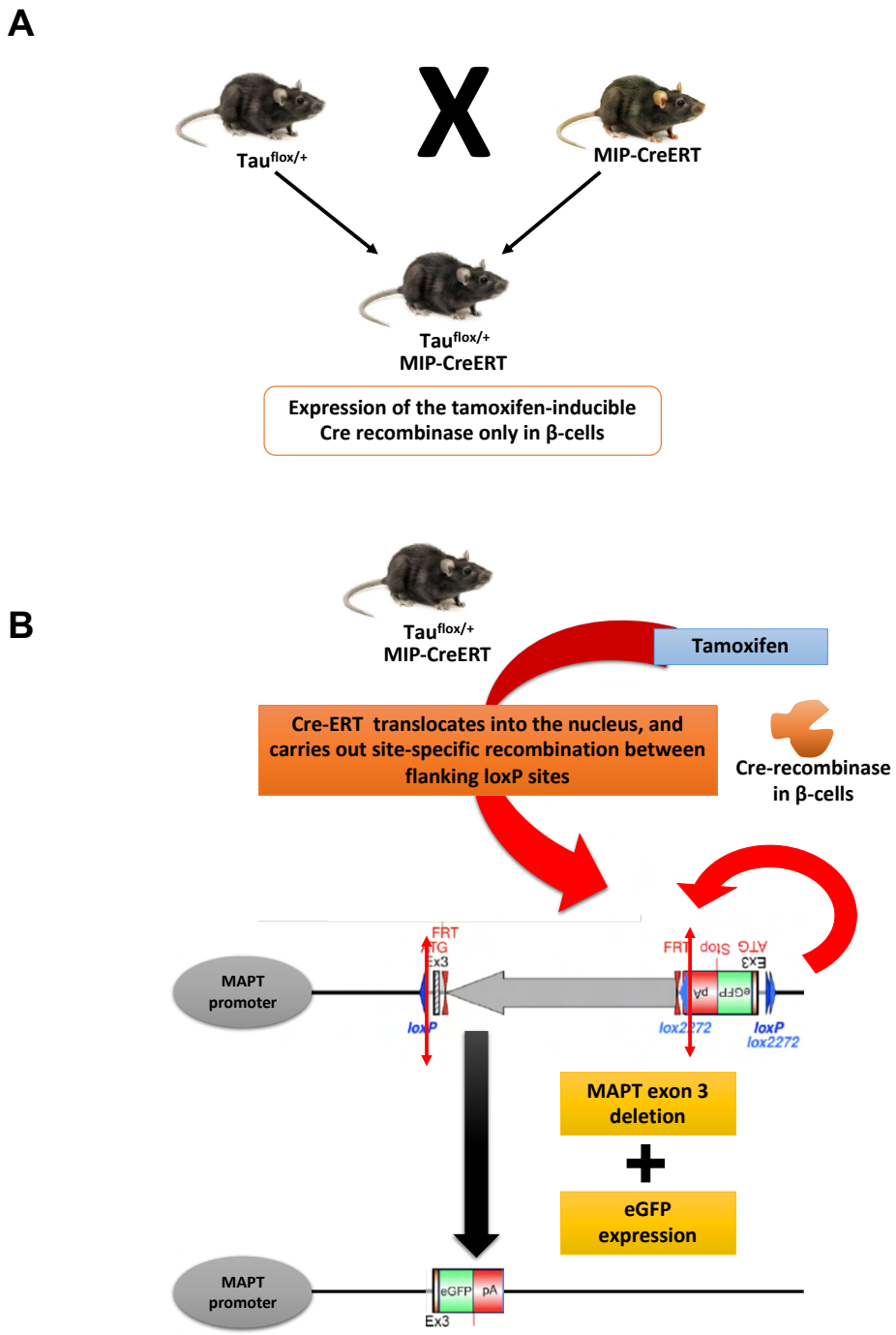

Figure 52. Generation of β-cell specific Tau KO mice using Tau$^{flox/+}$ MIP-CreERT mice.

(A) MIP-CREERT animals express a tamoxifen-inducible Cre recombinase (cre/ERT) driven by the mouse Ins1, insulin I, promoter. Tau$^{flox/+}$ mice were crossed with MIP-CREERT animals. **(B)**. In tau$^{flox/+}$ MIP-CreERT offspring inducible Cre recombinase activity is present specifically in the pancreatic β-cells. Cre/ERT is restricted to the cytoplasm, the Cre/ERT protein can only gain access to the nuclear compartment after exposure to tamoxifen. The combination of the FLEx monitoring strategy allowed that when CRE recombinase turns-off murine tau expression, the expression of an eGFP reporter is concomitantly turned-on in the pancreatic β-cells.

4.5. Metabolic evaluation of β-cell specific Tau KO mice:

As described above, $tau^{flox/+}$ animals were used for the evaluation of the metabolic impact of evaluation of β-cell specific Tau KO mice. Two months after tamoxifen or control solution injections, animals had a first metabolic evaluation under Chow diet. In the same way of the metabolic phenotyping of tau KI mice, animals were challenged with HFD for a period of 16 weeks. HFD was given from 6 months to 10 months of age. The time-line for metabolic investigations is given in Figure 53.

Unexpectedly, under both chow diet and HFD, no significant metabolic alterations or glucose homeostasis modifications were observed between different animals' groups (Figure 54).

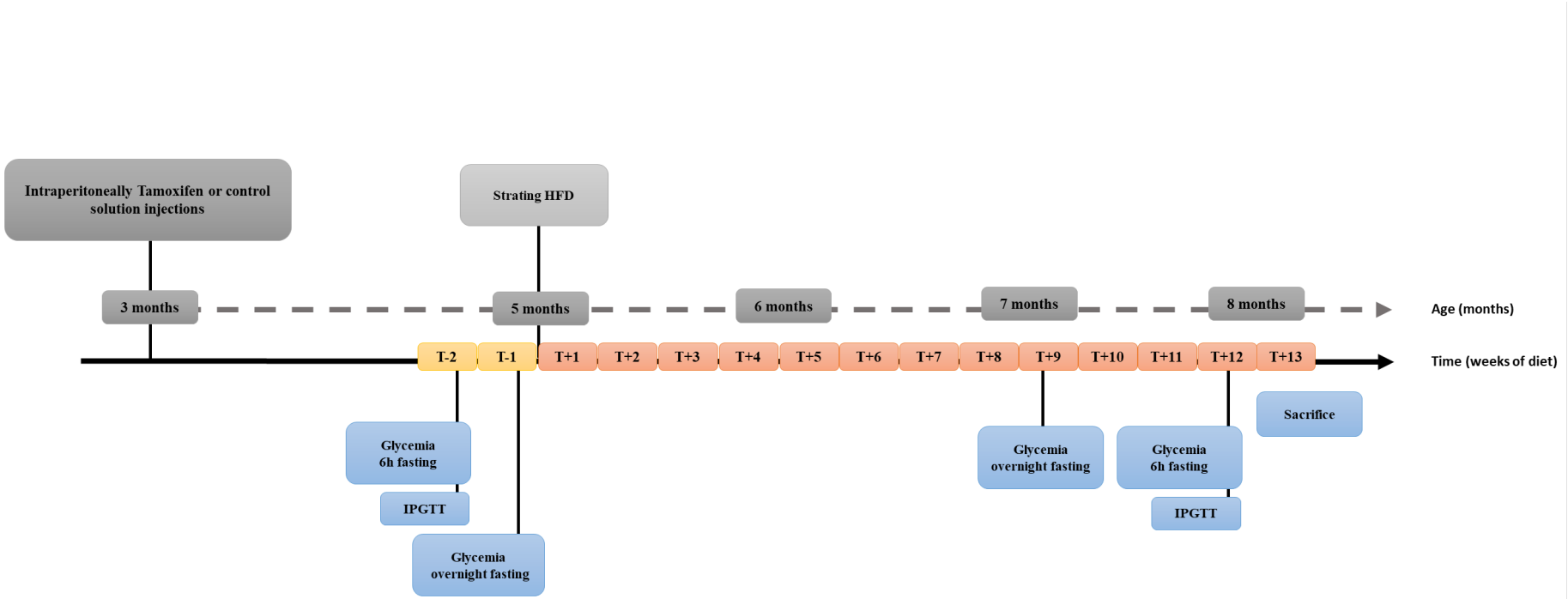

Figure 53. Time-line of metabolism investigations under Chow diet and high-fat diet in Tau$^{flox/+}$ MIP-CreERT mice and their controls injected by Tamoxifen or a control solution.

At 3 months old, a tamoxifen or control solution were intraperitoneally injected in Tau$^{flox/+//MIP\text{-}CRE/+}$, Tau$^{flox/+//+/+}$ animals. At baseline, six to seven weeks after virus injection, a first metabolic evaluation [glycemia after 6 hours of fasting, and after an overnight fasting, and also, intraperitoneal glucose tolerance test (IPGTT)] was performed. Feeding with high-fat diet was started at 8 weeks after a tamoxifen or control solution injections (5 months old). Glycemia after an overnight fasting was performed at 9 weeks after starting HFD (7 months old). Glycemia measurements after 6 hours of fasting and IPGTT were determined 12 weeks after HFD onset. Animals were sacrificed at the end of 13th week of HFD.

Seven Tau$^{Flox/+//+/+}$ mice were injected with Tamoxifen, seven Tau$^{Flox/+//+/+}$ mice were injected with a control solution, and seven Tau$^{Flox/+//MIP\text{-}CRE/+}$ mice were injected with Tamoxifen, and six Tau$^{Flox/+//MIP\text{-}CRE/+}$ mice were injected with a control solution.

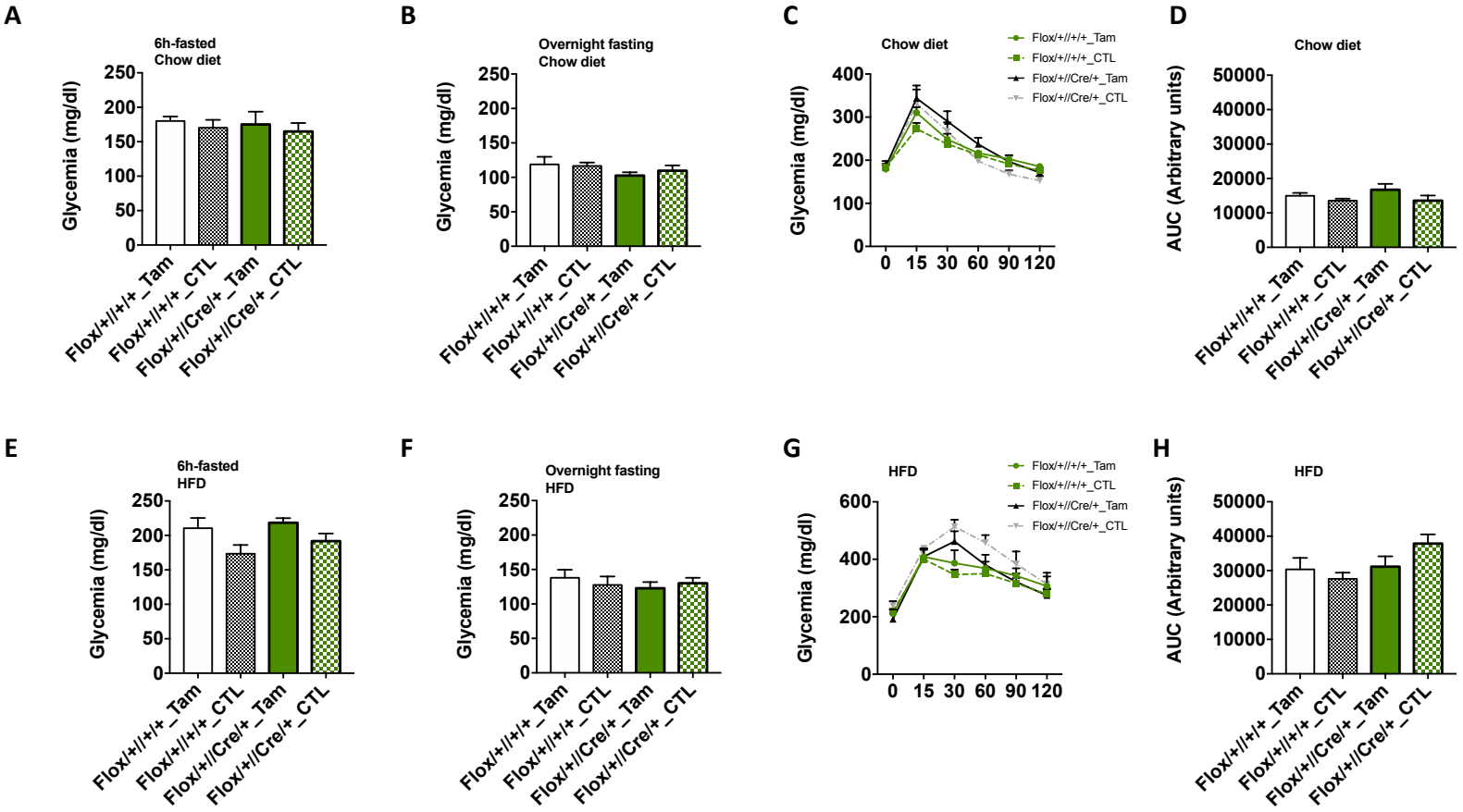

Figure 54. Metabolic evaluation of β-cell specific Tau KO male mice under chow diet and high fat diet (HFD).

(A) Glycemia after 6 h of fasting under chow diet (NS). **(B)** Glycemia after an overnight fasting under chow diet (NS). **(C)** Intraperitoneal glucose tolerance test (IPGTT) under chow diet (NS) **(D)** Area under the curve (AUC) for IPGTT under chow diet (NS). **(E)** Glycemia after 6 h of fasting under HFD (NS). **(F)** Glycemia after an overnight fasting under HFD(NS). **(G)** Intraperitoneal glucose tolerance test (IPGTT) under HFD (NS) **(H)** Area under the curve (AUC) for IPGTT under HFD (NS). Results are expressed as mean ± SEM. $Tau^{Flox/+//+/+}$ (N=7) mice injected with Tamoxifen are indicated as green circles, $Tau^{Flox/+//+/+}$ (N=7) mice injected with control solution as green squares, and $Tau^{Flox/+//MIP\text{-}CRE/+}$ (N=7) injected with Tamoxifen as black triangles, and $Tau^{Flox/+//MIP\text{-}CRE/+}$ (N=6) injected with control solution as grey triangles.

4.6. Alternative approach to evaluate in vivo the impact of tau loss of function in pancreatic β-cells:

The first step of this approach was to select the viral vector able to target mice pancreatic β-cells in vivo. In this experiment, we evaluated the ability of different adeno-associated viral vectors (AAV) to transduce the pancreas in vivo. To this end, C57BL/6J mice were injected by AAV serotypes 7, 8, 9 and 10 in retro-orbital venous sinus and scarified 2 months later. At sacrifice, pancreas and brains were dissected and were fixed for immunohistochemistry.

As observed in figure 55, the better transduction of pancreatic islets was observed with AAV serotypes 7 and 10. Furthermore, when we analyzed several pancreatic sections representatives of the whole pancreas from animals injected with AAV serotypes 7 or 10, we observed that AAV serotypes 10 transduced more pancreatic islets and especially β-cells, compared to AAV serotypes 7 (Figure 56).

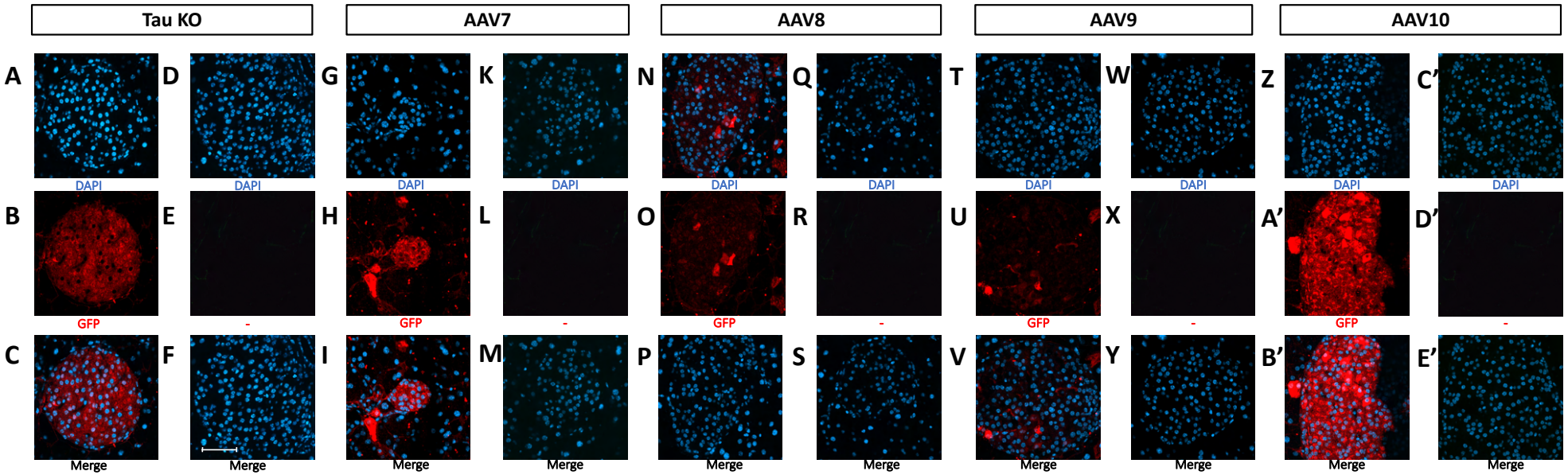

Figure 55. Green Fluorescent Protein (GFP) expression in mouse islets from WT mice transduced by adeno-associated viral vectors (AAV) of serotypes 7, 8, 9 and 10.

Tau KO mice: (A-C) Immunofluorescence staining for GFP (red) in mouse islets from adult tau KO mice. Blue: DAPI nuclear counterstaining. (D-F) Absence of staining without primary antibodies. Only secondary antibodies and DAPI nuclear counterstaining (blue) were used.

AAV7: (G-I) Immunofluorescence staining for GFP (red) in mouse islets from adult WT mice injected by AAV7. Blue: DAPI nuclear counterstaining. (K-M) Absence of staining without primary antibodies. Only secondary antibodies and DAPI nuclear counterstaining (blue) were used.

AAV8: (N-P) Immunofluorescence staining for GFP (red) in mouse islets from adult WT mice injected by AAV8. Blue: DAPI nuclear counterstaining. (Q-S) Absence of staining without primary antibodies. Only secondary antibodies and DAPI nuclear counterstaining (blue) were used.

AAV9: (N-P) Immunofluorescence staining for GFP (red) in mouse islets from adult WT mice injected by AAV9. Blue: DAPI nuclear counterstaining. (W-Y) Absence of staining without primary antibodies. Only secondary antibodies and DAPI nuclear counterstaining (blue) were used.

AAV10: (Z-B') Immunofluorescence staining for GFP (red) in mouse islets from adult WT mice injected by AAV10. Blue: DAPI nuclear counterstaining. (C'-E') Absence of staining without primary antibodies. Only secondary antibodies and DAPI nuclear counterstaining (blue) were used. Scale: 20µm.

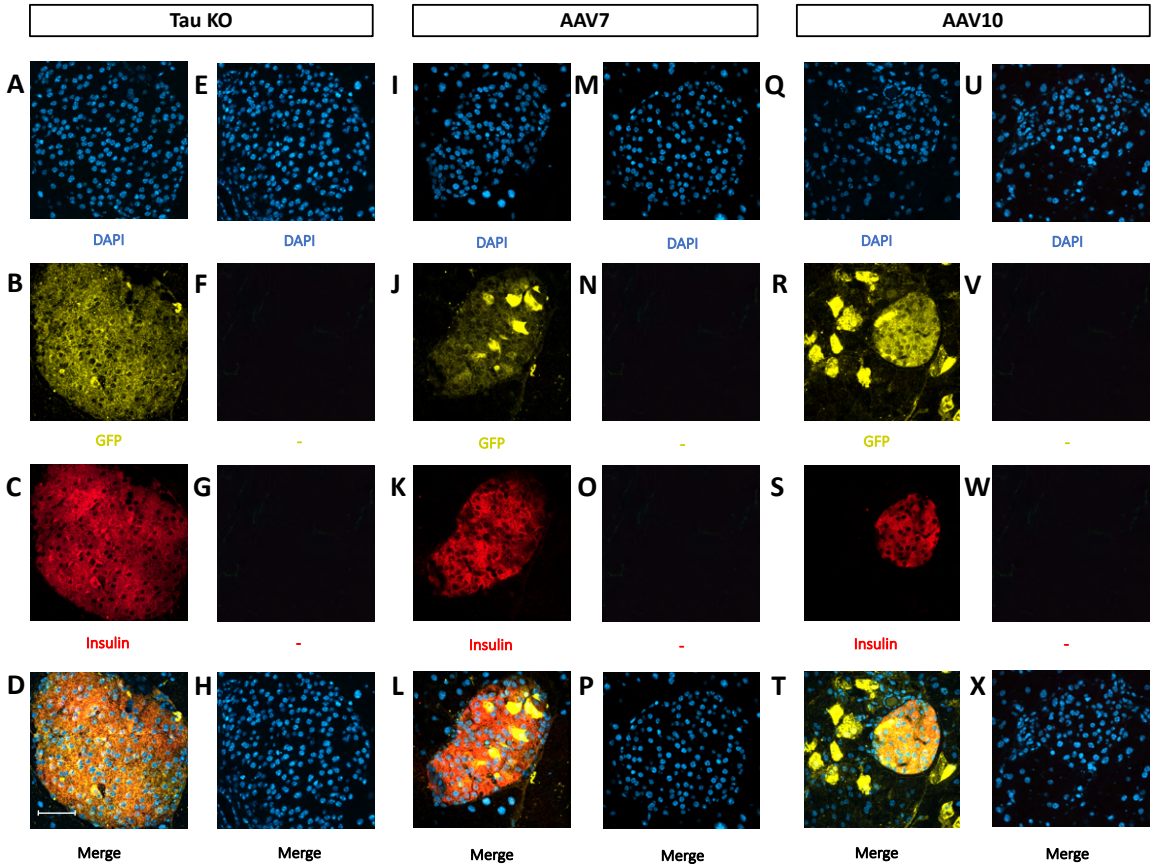

Figure 56. Green Fluorescent Protein (GFP) and insulin expression in mouse islets from WT mice transduced by adeno-associated viral vectors (AAV) of serotypes 7, and 10.

Tau KO mice: (A-D) Double immunofluorescence staining for GFP (yellow, B) and insulin (red, C) in mouse islets from adult tau KO mice. Blue: DAPI nuclear counterstaining. (E-H) Absence of staining without primary antibodies. Only secondary antibodies and DAPI nuclear counterstaining (blue) were used.

AAV7: (I-L) Double immunofluorescence staining for GFP (yellow, J) and insulin (red, K) in mouse islets from adult WT mice injected by AAV7. Blue: DAPI nuclear counterstaining. (M-P) Absence of staining without primary antibodies. Only secondary antibodies and DAPI nuclear counterstaining (blue) were used.

AAV10: (Q-T) Double immunofluorescence staining for GFP (yellow, R) and insulin (red, S) in mouse islets from adult WT mice injected by AAV10. Blue: DAPI nuclear counterstaining. (U-X) Absence of staining without primary antibodies. Only secondary antibodies and DAPI nuclear counterstaining (blue) were used.

Scale: 20µm.

Part III: Approach of tau knockdown in the medio basal hypothalamus

1. Generation and validation of tau flox mice model:

1.1. Evaluation of tau expression in the brain of tau flox mouse model:

At the beginning, tau protein expression was evaluated both in the hippocampus and the hypothalamus. However, mRNA tau expression was studied only in the hippocampus.

First, males $tau^{flox/+}$ (heterozygotes) animals were crossed in order to obtain: $tau^{flox/flox}$ (homozygotes), $tau^{flox/+}$ and their littermate (WT). Also, tau KO mice were used as a proper negative control (absence of tau expression).

Tau protein expression in the hippocampus were studied using immunohistochemistry, western blot and Elisa. However, only immunohistochemistry was used to evaluate tau protein expression in the hypothalamus.

Similarly to the results of tau expression in the pancreas from $tau^{flox/flox}$ mice, and as observed in Figures 57 and 58, the immunofluorescence signal of tau protein (red) was reduced in both hypothalamus and hippocampus of $tau^{flox/+}$ mice. Contrariwise, the immunofluorescence signal of tau protein was not detected in both hypothalamus and hippocampus of $tau^{flox/flox}$ mice. The former results were close to those obtained in the hypothalamus and hippocampus from tau KO mice. Furthermore, the evaluation of tau expression by Elisa and WB showed a reduced expression of tau protein in the hippocampus of both $tau^{flox/+}$ and $tau^{flox/flox}$ mice (-40% and -80%, respectively; Figures 59B and 59C). Close results were observed for the expression of tau mRNA in the hippocampus of both $tau^{flox/+}$ and $tau^{flox/flox}$ compared to WT mice (Figure 59D).

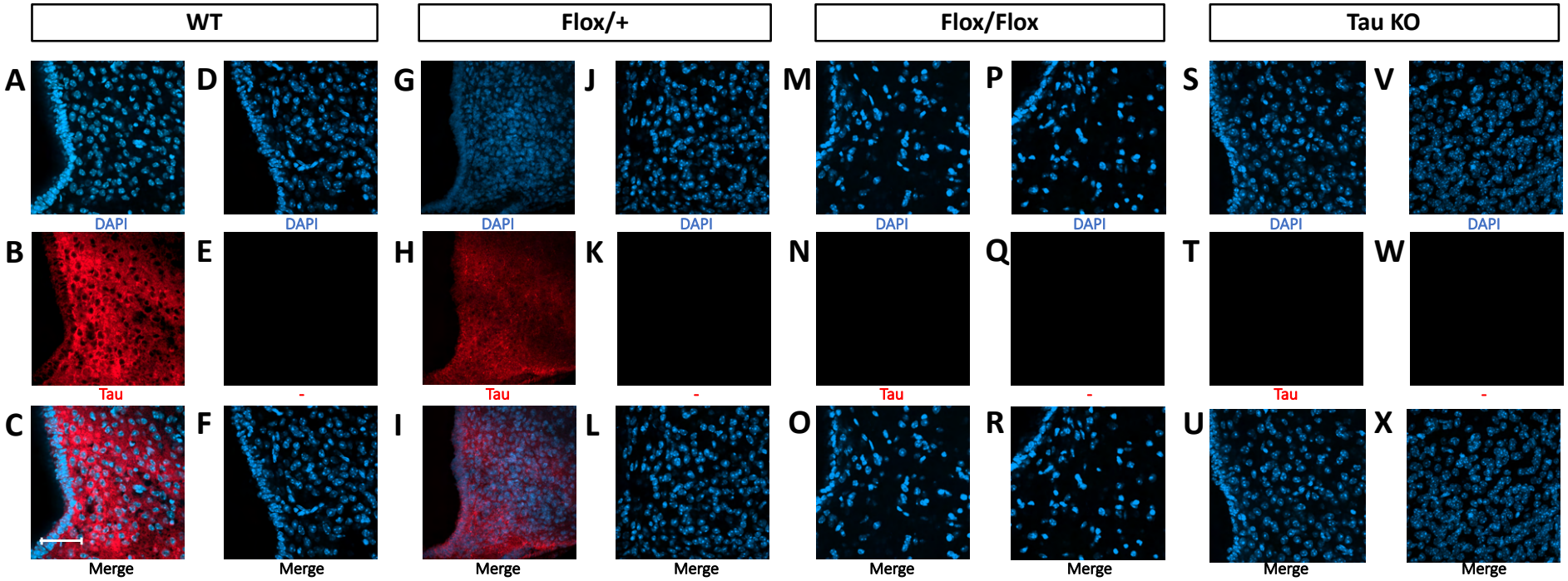

Figure 57. Tau expression (tau 9H12 antibody) in the mediobasal hypothalamus from WT, tau KO, tau$^{Flox/Flox}$ and tau$^{Flox/+}$ mice.

Tau WT mice: (A-C) Immunofluorescence staining for tau (red) in the mediobasal hypothalamus from adult WT mice. Blue: DAPI nuclear counterstaining. (D-F) Absence of staining without primary antibodies. Only secondary antibodies and DAPI nuclear counterstaining (blue) were used.

Tau$^{Flox/+}$ mice: (G-I) Immunofluorescence staining for tau (red) in the the mediobasal hypothalamus from adult Tau$^{Flox/+}$ mice. Blue: DAPI nuclear counterstaining. (K-M) Absence of staining without primary antibodies. Only secondary antibodies and DAPI nuclear counterstaining (blue) were used.

Tau$^{Flox/Flox}$ mice: (N-P) Immunofluorescence staining for tau (red) in the mediobasal hypothalamus from adult Tau$^{Flox/Flox}$ mice. Blue: DAPI nuclear counterstaining. (Q-S) Absence of staining without primary antibodies. Only secondary antibodies and DAPI nuclear counterstaining (blue) were used.

Tau KO mice: (T-V) Immunofluorescence staining for tau (red) in the mediobasal hypothalamus from adult tau KO mice. Blue: DAPI nuclear counterstaining. (W-Y) Absence of staining without primary antibodies. Only secondary antibodies and DAPI nuclear counterstaining (blue) were used.

Scale: 20µm.

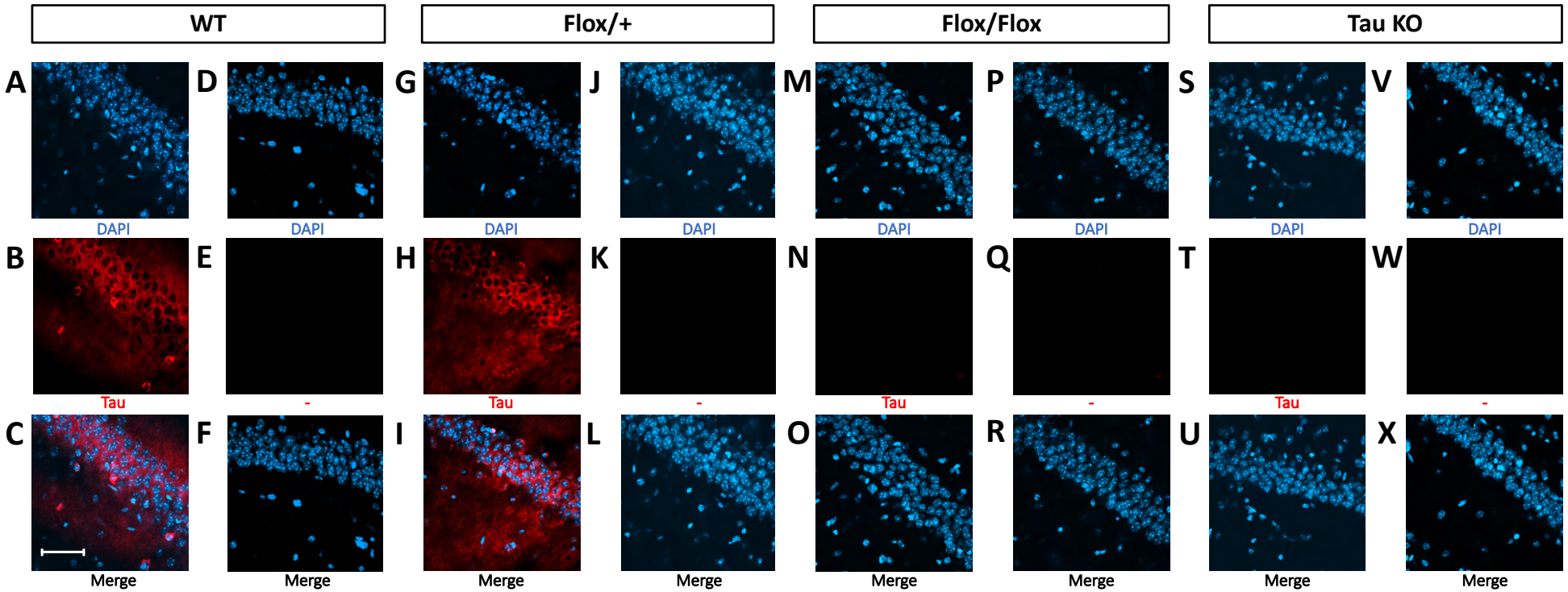

Figure 58. Tau expression (tau 9H12 antibody) in mouse hippocampus from WT, tau KO, tau$^{Flox/Flox}$ and tau$^{Flox/+}$ mice.

Tau WT mice: (A-C) Immunofluorescence staining for tau (red) in the CA1 of the hippocampus from adult WT mice. Blue: DAPI nuclear counterstaining. (D-F) Absence of staining without primary antibodies. Only secondary antibodies and DAPI nuclear counterstaining (blue) were used.

Tau$^{Flox/+}$ mice: (G-I) Immunofluorescence staining for tau (red) in the CA1 of the hippocampus from adult Tau$^{Flox/+}$ mice. Blue: DAPI nuclear counterstaining. (K-M) Absence of staining without primary antibodies. Only secondary antibodies and DAPI nuclear counterstaining (blue) were used.

Tau$^{Flox/Flox}$ mice: (N-P) Immunofluorescence staining for tau (red) in the CA1 of the hippocampus from adult Tau$^{Flox/Flox}$ mice. Blue: DAPI nuclear counterstaining. (Q-S) Absence of staining without primary antibodies. Only secondary antibodies and DAPI nuclear counterstaining (blue) were used.

Tau KO mice: (T-V) Immunofluorescence staining for tau (red) in the CA1 of the hippocampus from adult tau KO mice. Blue: DAPI nuclear counterstaining. (W-Y) Absence of staining without primary antibodies. Only secondary antibodies and DAPI nuclear counterstaining (blue) were used.

Scale: 20µm.

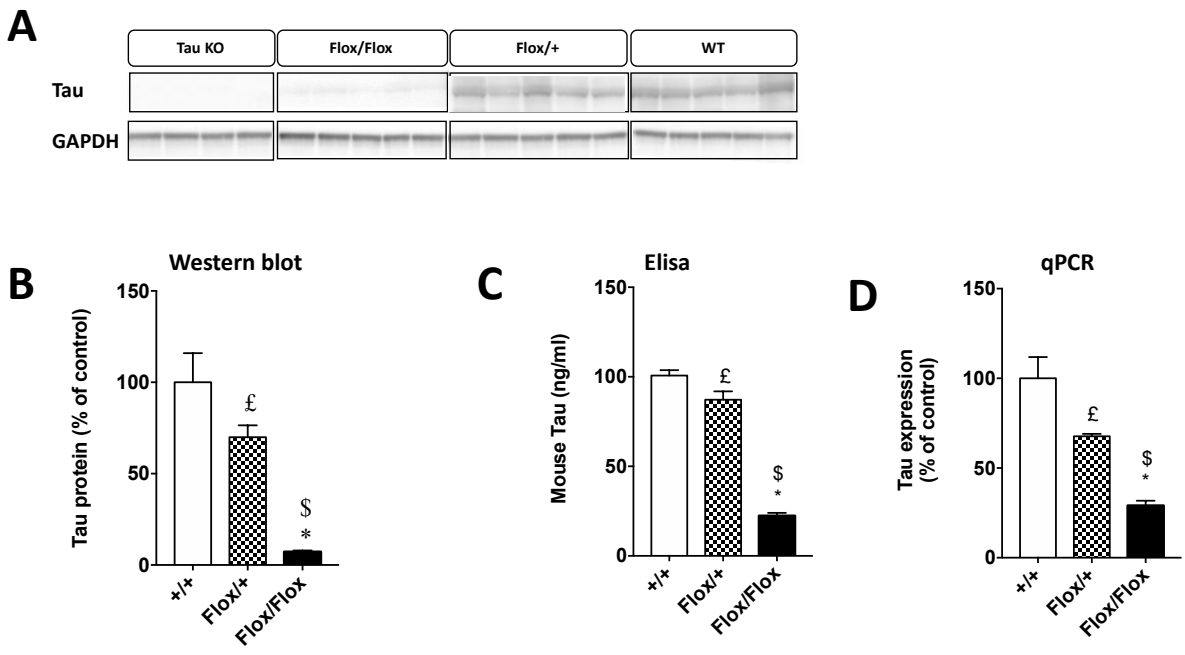

Figure 59. Evaluation of tau expression in mouse hippocampus from WT, tau KO, tau$^{Flox/Flox}$ and tau$^{Flox/+}$ mice.

(A and B) Tau protein expression by western blot in the hippocampus of adult tau$^{Flox/Flox}$, and tau$^{Flox/+}$ compared to wild type mice (+/+). Tau expression in the hippocampus of adult tau$^{Flox/Flox}$, and tau$^{Flox/+}$ was reduced -40% and -80%, respectively (One-Way ANOVA followed by Tukey's post-hoc test; **£** $p < 0.05$ tau$^{Flox/+}$ vs. WT; **$** $p < 0.0001$ tau$^{Flox/Flox}$ vs. WT; ***** $p < 0.0001$ tau$^{Flox/Flox}$ vs. tau$^{Flox/+}$), compared to +/+.

(C) Tau protein expression by Elisa in hippocampus lysates of adult tau$^{Flox/Flox}$, and tau$^{Flox/+}$ compared to wild type mice (+/+).). Tau expression in the hippocampus of adult tau$^{Flox/Flox}$, and tau$^{Flox/+}$ was reduced -30% and -80%, respectively (One-Way ANOVA followed by Tukey's post-hoc test; **£** $p < 0.05$ tau$^{Flox/+}$ vs. WT; **$** $p < 0.0001$ tau$^{Flox/Flox}$ vs. WT; ***** $p < 0.0001$ tau$^{Flox/Flox}$ vs. tau$^{Flox/+}$), compared to +/+.

(D) Tau mRNA expression in the hippocampus of adult tau$^{Flox/Flox}$, and tau$^{Flox/+}$ compared to wild type mice (+/+).). mRNA tau expression in the hippocampus of adult tau$^{Flox/Flox}$, and tau$^{Flox/+}$ was reduced -40% and -70%, respectively (One-Way ANOVA followed by Tukey's post-hoc test; **£** $p < 0.05$ tau$^{Flox/+}$ vs. WT; **$** $p < 0.0001$ tau$^{Flox/Flox}$ vs. WT; ***** $p < 0.001$ tau$^{Flox/Flox}$ vs. tau$^{Flox/+}$), compared to +/+.

Taken to gather, results of the metabolic phenotyping (described in page 143) and the evaluation of tau expression in both hippocampus and hypothalamus, revealed a hypomorphic status of homozygous tau flox mice in the absence of CRE, which favors the development metabolic disorders close to those observed in tau KO mice. Contrariwise, $tau^{flox/+}$ had a close metabolic phenotype to WT mice, we thus used heterozygous tau flox animals that were combined with CRE approaches to knock-down tau from the mediobasal hypothalamus (cKO-Tau^{hypo} animals).

1.2. Validation of the stereotaxic coordinates to target the mediobasal hypothalamus and the evaluation of the tau knock-down efficacy:

$Tau^{flox/flox}$ mice were used in the initial characterization of the tau flox mouse model and the validation of the mediobasal hypothalamus coordinate and to evaluate the effective reduction of tau expression by the developed CRE-lox approach.

Different coordinates to target the mediobasal hypothalamus were tested. We used unilateral stereotaxic injection to deliver AAV2/5-synapsin-CRE-Tomato virus in the mediobasal hypothalamus of $tau^{flox/flox}$ mice. Figure 60 represent the good coordinates chosen. The expression of Tomato (red) signs the selective transduction of neurons by the AAV-CRE, and the expression of GFP (green) signs the recombination of tau gene in tau expressing cells.

The hippocampus, a brain structure in which tau protein is widely expressed was chosen for the evaluation of tau knock-down efficacy. Accordingly, we used a unilateral stereotaxic injection to deliver AAV2/5-synapsin-CRE-Tomato virus or the AAV2/5-synapsin-Tomato (control) in the hippocampus (CA2) of $tau^{flox/flox}$ mice. First, the virus transduction in the hippocampus was verified by immunofluorescence as observed in Figures 61A-C. Secondly, a RNAscop approach was used to evaluate the tau knock-down efficacy by measuring tau mRNA expression level in $tau^{flox/flox}$ mice injected by AAV2/5-synapsin-CRE-Tomato virus, and compared to animals injected by the control

virus (AAV2/5-synapsin-Tomato). As observed in the Figure 61D-G, RNA-Scope analysis chowed the effective reduction of tau mRNA expression (-60%) by the CRE-lox approach.

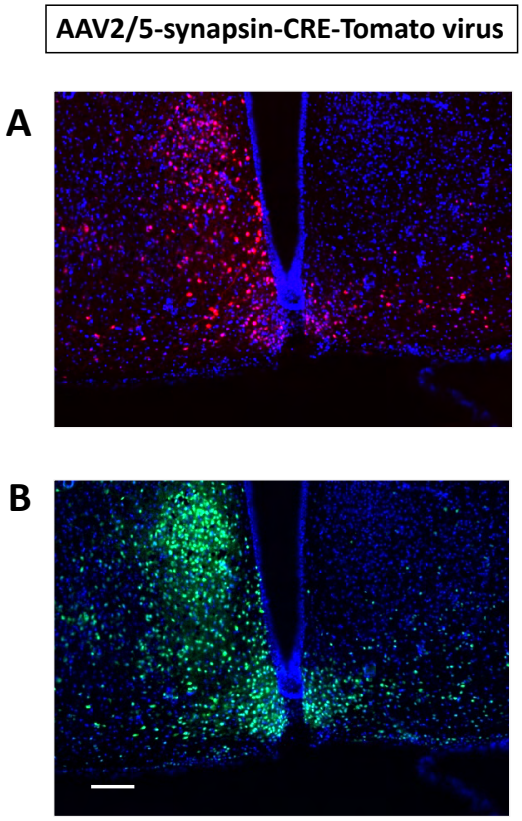

Figure 60. Evaluation of GFP and Tomato expression in the hypothalamus from tau$^{flox/flox}$ mice injected with AAV2/5-synapsin-CRE-Tomato.

(A) Expression of Tomato (red) signs the selective transduction of mediobasal hypothalamus neurons by the AAV2/5-synapsin-CRE-Tomato.

(B) Expression of GFP (green) signs the recombination of tau gene in tau expressing cells.

Scale: 50µm.

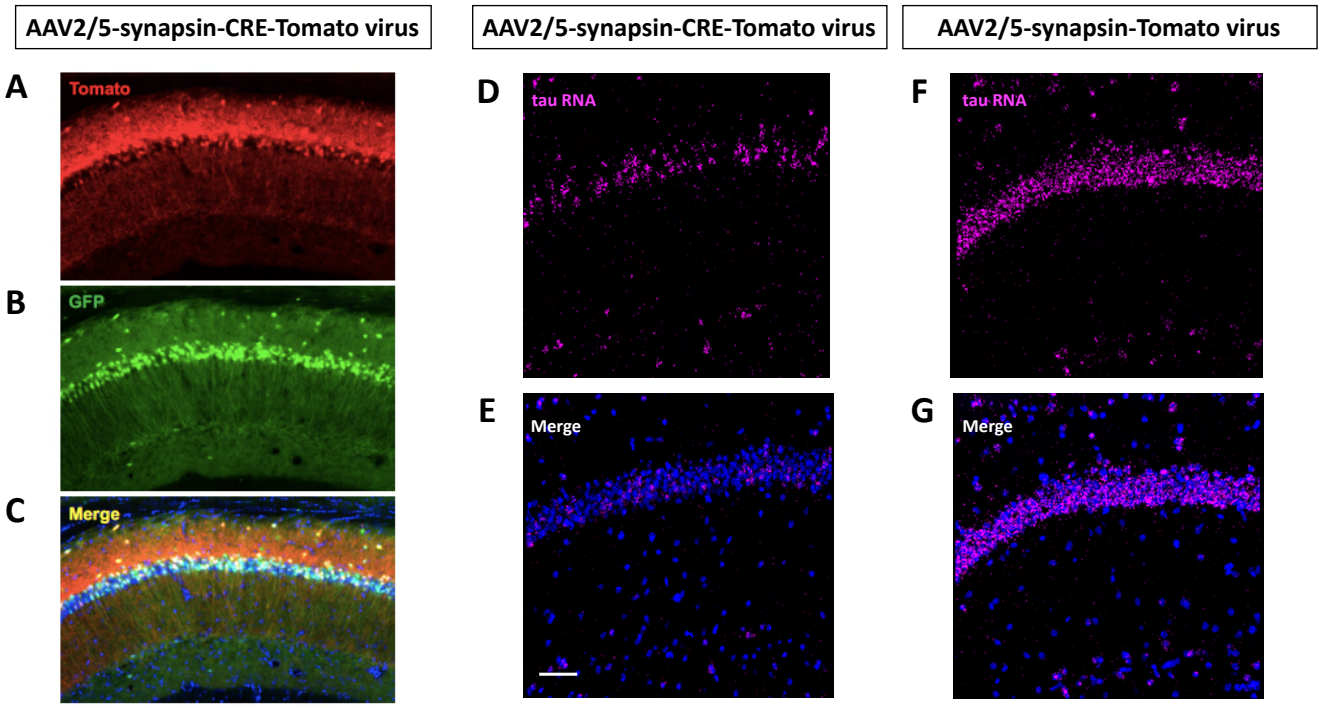

Figure 61. Tau recombination in the hippocampus of Tau$^{flox/flox}$ mice.

(A-C) AAV2/5-synapsin-CRE-Tomato virus has been injected in the hippocampus of Tau$^{flox/flox}$ mice. **(A)** Expression of Tomato (red) signs the selective transduction of neurons by the AAV-CRE. **(A)** Expression of GFP (green) signs the recombination of Tau gene in Tau-expressing cells.

(D-G) RNA-Scope analysis of tau mRNA expression in an AAV2/5-synapsin-CRE-Tomato virus **(D-E)** and the control virus **(F-G)** showing the effective reduction of tau expression by the developed CRE-lox approach.

Scale: 50µm.

2. Characterization of cellular population expressing tau protein in the mediobasal hypothalamus and the median eminence:

Interestingly, beside hippocampus, AD exhibit accumulation of hyperphosphorylated and misconformed tau in hypothalamic neurons (Ishii and Iadecola, 2015; Schultz et al., 1999) and Tanycytes (Sauvé et al., unpublished data). In line with these observation in pathological condition, using immunohistochemistry approach, we decided to study and characterize neural populations of the mediobasal hypothalamus that express tau protein. Also, with the same approach, we evaluated the physiological expression of tau in Tanycytes. The characterization of cellular population expressing tau protein in the mediobasal hypothalamus and the median eminence was carried out using tau 9H12 antibody.

As observed in the Figures 62 and 63, tau protein is expressed in POMC neurons of the arcuate nucleus, as well as in their axonal extensions in the ventromedial nucleus of the mediobasal hypothalamus. Colocalization of both signals was observed in POMC neurons of the arcuate nucleus and their axonal extensions in the ventromedial nucleus. This colocalization was evaluated using a Pearson correlation coefficient, and it was 0.47 and, 0.38 respectively.

Also, tau protein is expressed in AgRP neurons of the arcuate nucleus (Figure 64). The colocalization of both signals was estimated at 0.40 by Pearson correlation coefficient.

Also, tau is expressed in β2-Tanycytes in the median eminence (Figure 65). The colocalization of both signals was estimated at 0.28 by Pearson correlation coefficient.

Interestingly, tau protein is expressed in the axonal extensions of GnRH neurons in the arcuate nucleus, and also in the median eminence (Figure 66). The colocalization of both signals in the median eminence was estimated at 0.25 by a Pearson correlation coefficient.

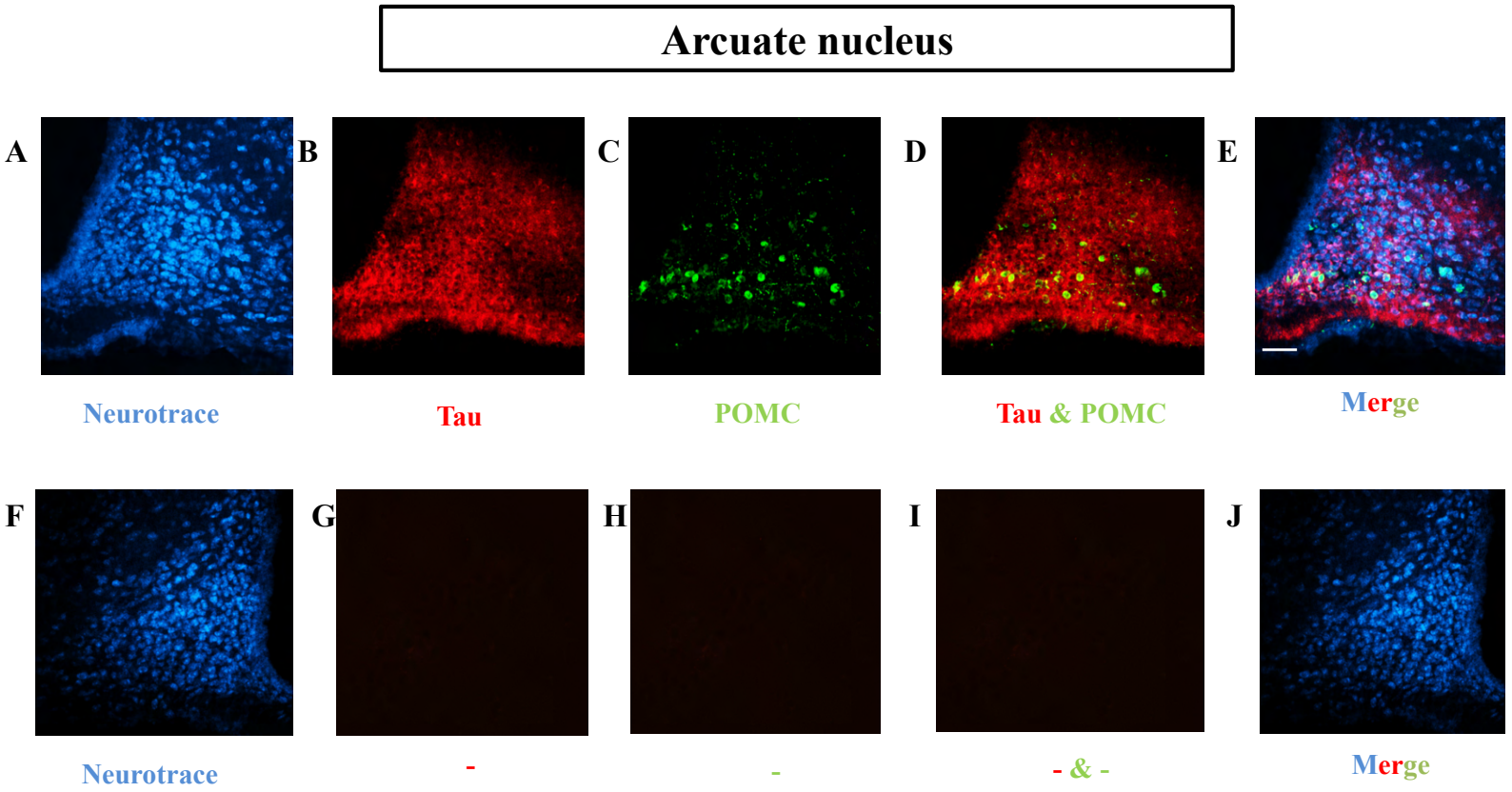

Figure 62. Tau (tau 9H12 antibody), and POMC expression in the arcuate nucleus of the mediobasal hypothalamus from WT mice.

(A-E) Immunofluorescence staining for tau (red) and POMC (green) in the arcuate nucleus of the mediobasal hypothalamus from adult WT mice. Blue: Neurotrace Nissl stain. **(F-J)** Absence of staining without primary antibodies. Only secondary antibodies and Neurotrace Nissl stain (blue) were used.

Scale: 50µm.

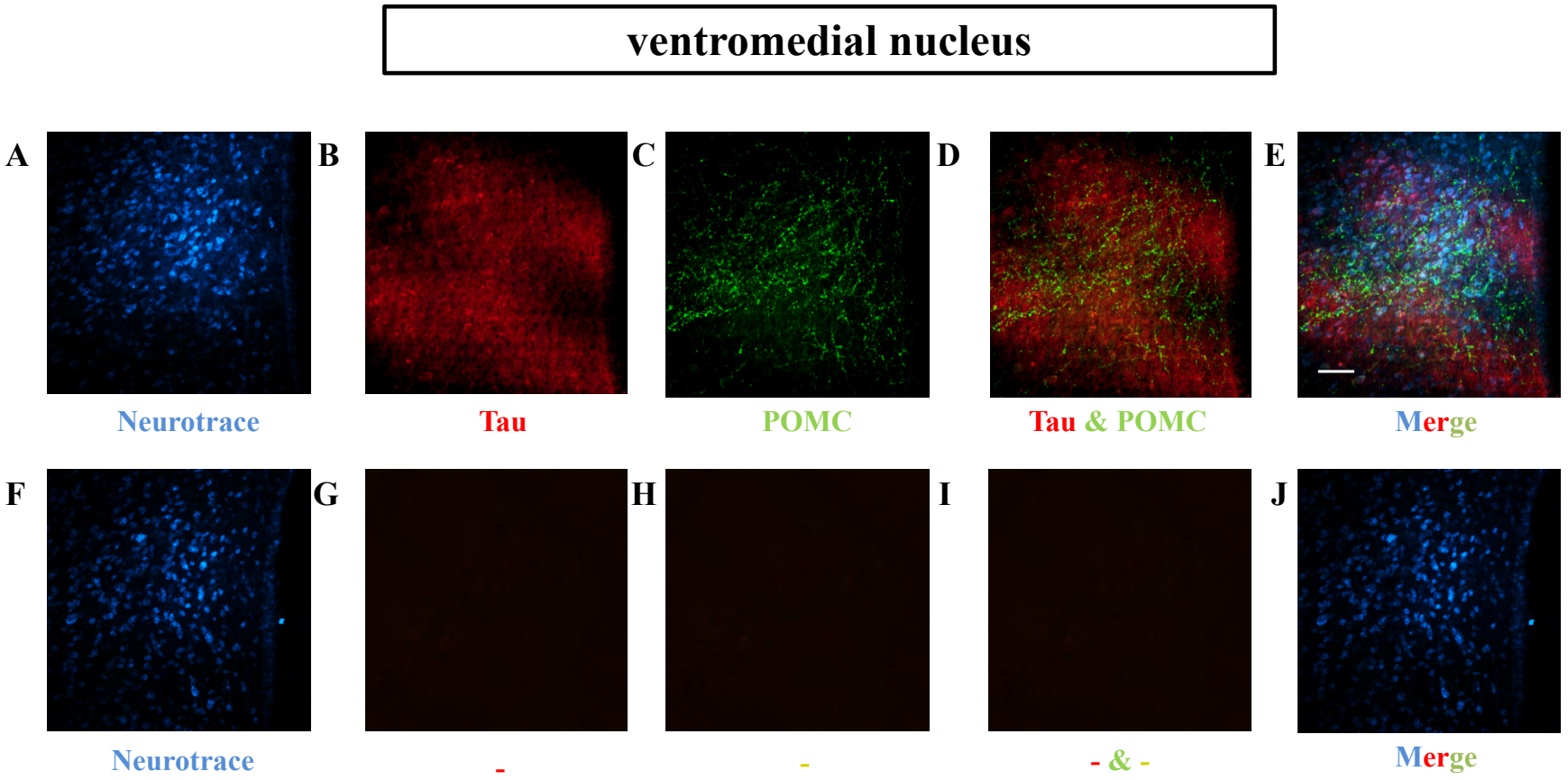

Figure 63. Tau (tau 9H12 antibody), and POMC expression in the ventromedial nucleus of the mediobasal hypothalamus from WT mice.

(A-E) Immunofluorescence staining for tau (red) and POMC (green) in the ventromedial nucleus of the mediobasal hypothalamus from adult WT mice. Blue: Neurotrace Nissl stain. **(F-J)** Absence of staining without primary antibodies. Only secondary antibodies and Neurotrace Nissl stain (blue) were used. Scale: 50µm.

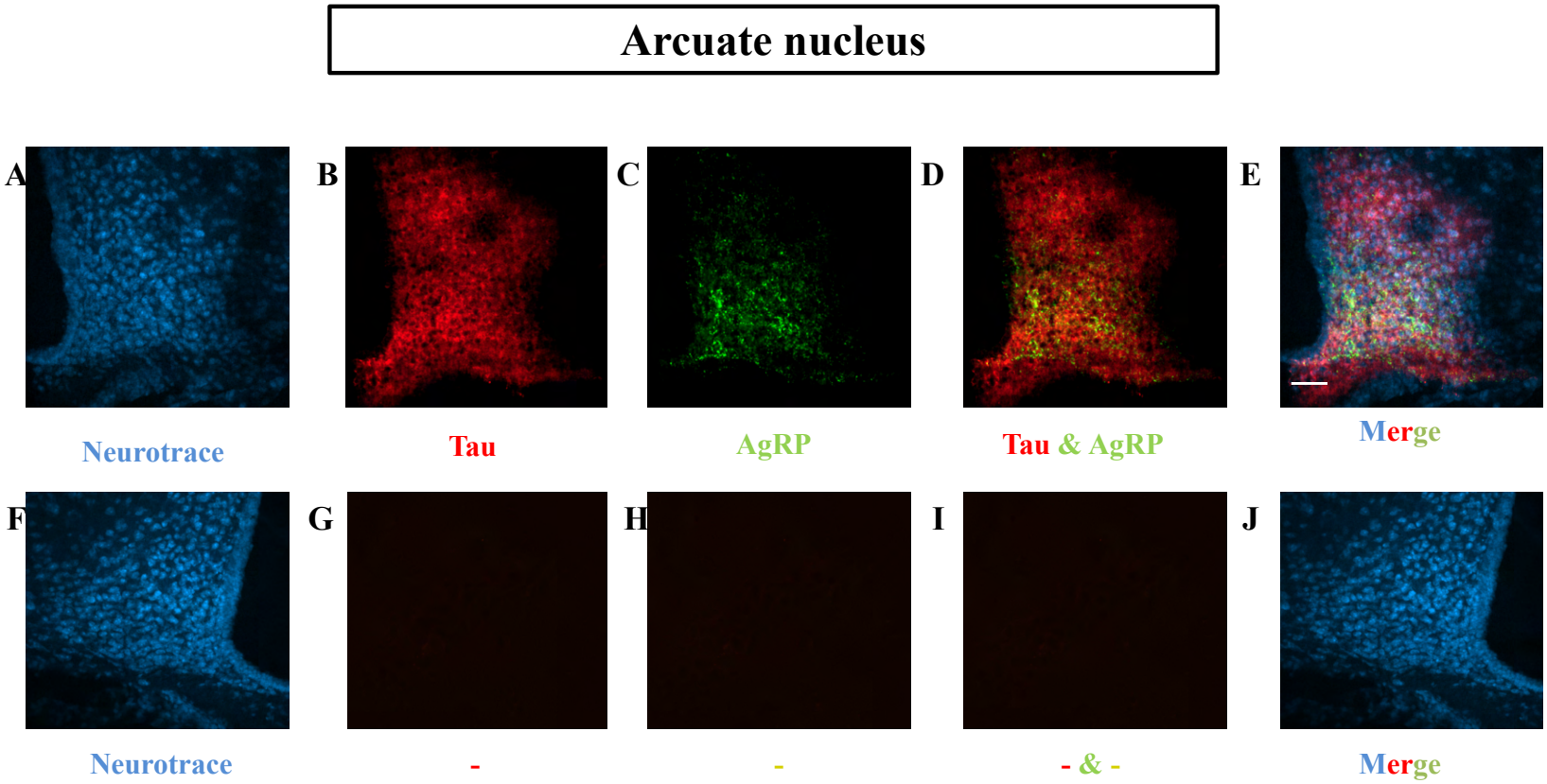

Figure 64. Tau (tau 9H12 antibody), and AgRP expression in the arcuate nucleus of the mediobasal hypothalamus from WT mice. (A-E) Immunofluorescence staining for tau (red) and AgRP (green) in the arcuate nucleus of the mediobasal hypothalamus from adult WT mice. Blue: Neurotrace Nissl stain. **(F-J)** Absence of staining without primary antibodies. Only secondary antibodies and Neurotrace Nissl stain (blue) were used.

Scale: 50µm.

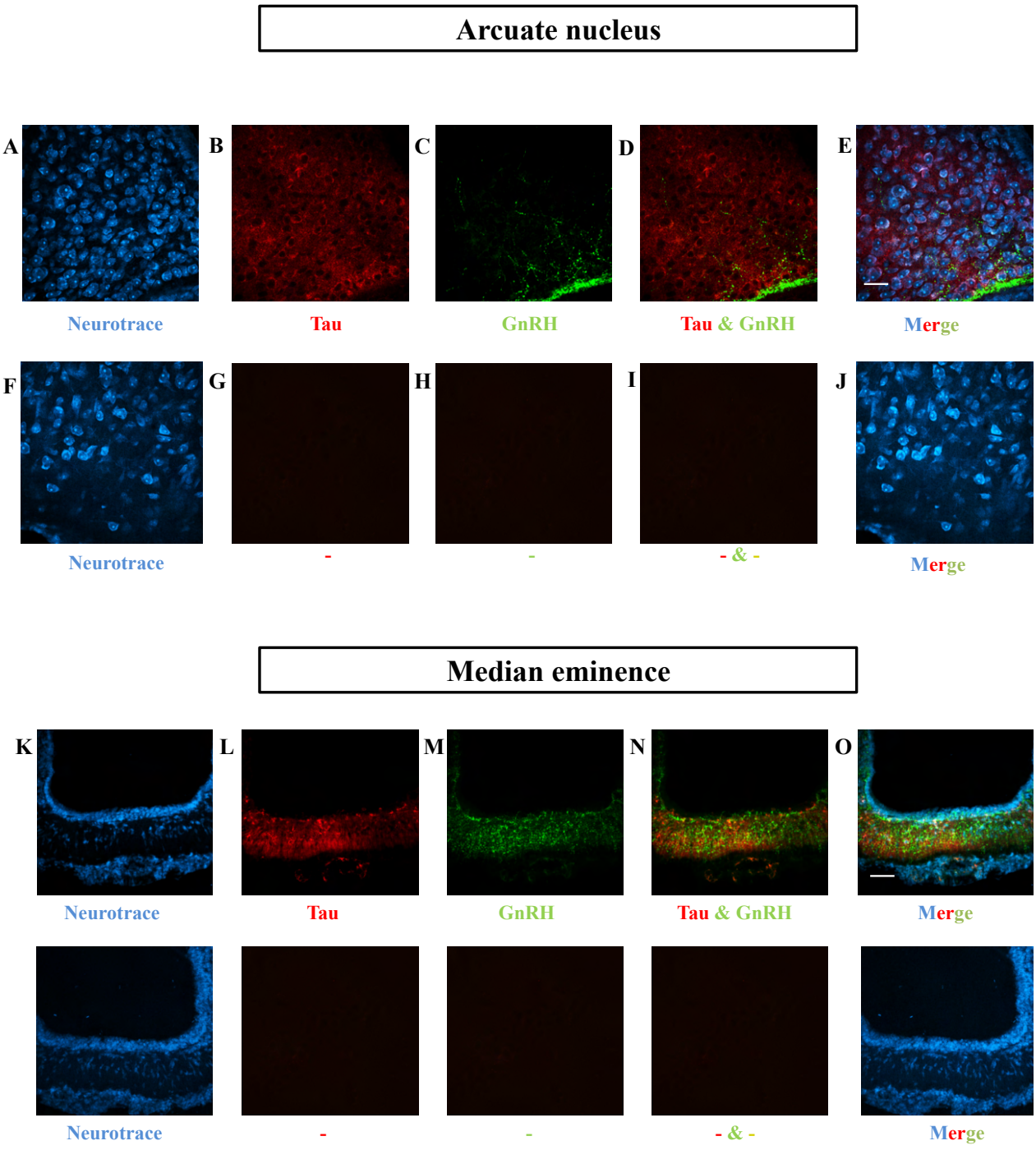

Figure 65. Tau (tau 9H12 antibody), and GnRH expression in the arcuate nucleus of hypothalamus and the median eminence from WT mice.

(A-E) Immunofluorescence staining for tau (red) and GnRH (green) in the arcuate nucleus of the mediobasal hypothalamus from adult WT mice. Blue: Neurotrace Nissl stain. **(F-J)** Absence of staining without primary antibodies. Only secondary antibodies and Neurotrace Nissl stain (blue) were used.

(K-O) Immunofluorescence staining for tau (red) and POMC (green) in the median eminence from adult WT mice. Blue: Neurotrace Nissl stain. **(Q-U)** Absence of staining without primary antibodies. Only secondary antibodies and Neurotrace Nissl stain (blue) were used.

Scale: 50µm.

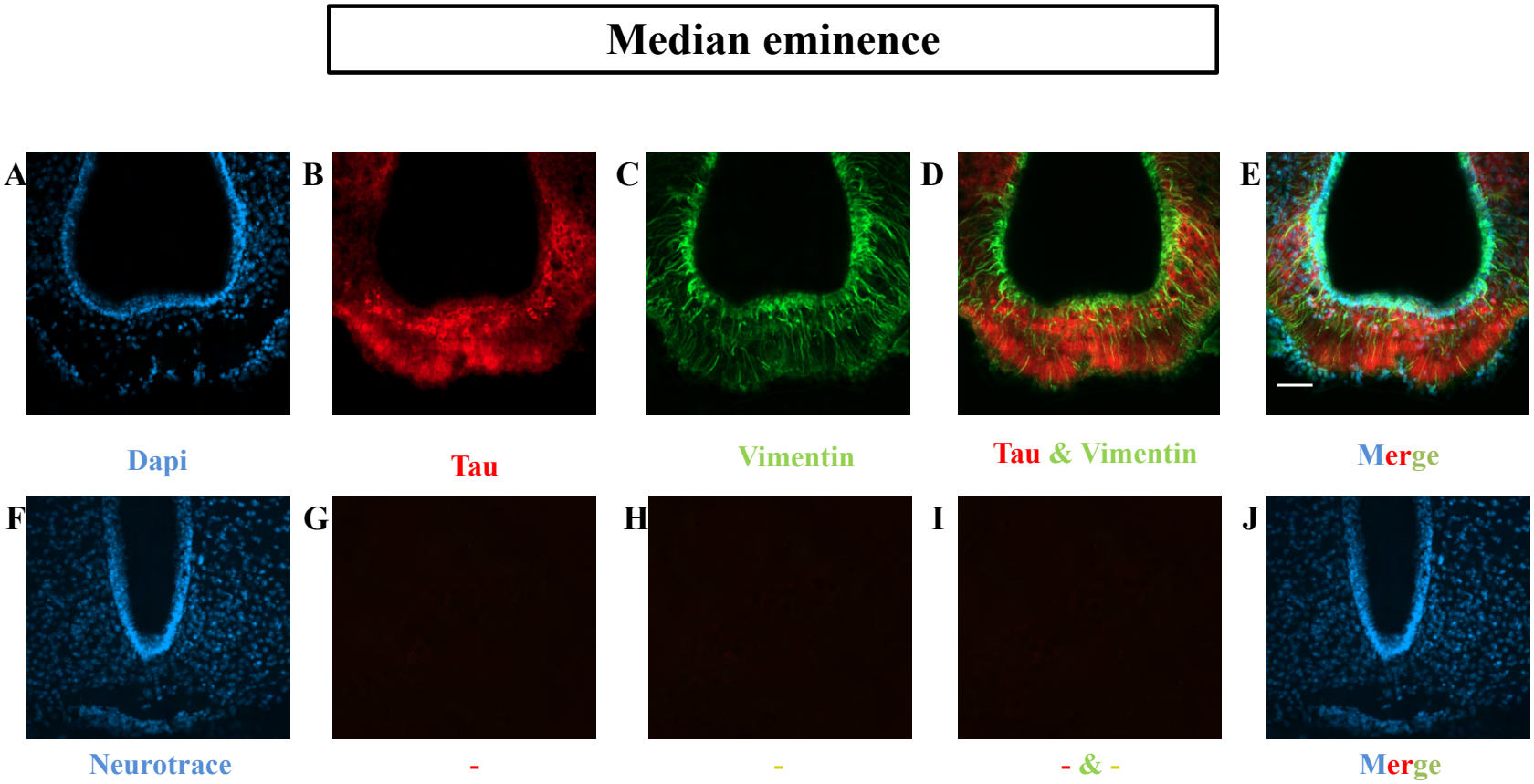

Figure 66. Tau (tau 9H12 antibody), and Vimentin expression in the median eminence from WT mice.

(A-E) Immunofluorescence staining for tau (red) and Vimentin (green) in the median eminence from adult WT mice. Blue: Neurotrace Nissl stain. **(F-J)** Absence of staining without primary antibodies. Only secondary antibodies and Neurotrace Nissl stain (blue) were used. Scale: 50µm.

3. Metabolic phenotyping of cKO-Tau^{hyp} model:

As described above, tau$^{flox/+}$ animals were used for the evaluation of the metabolic impact of tau deletion in the mediobasal hypothalamus. We used bilateral stereotaxic injections to deliver AAV2/5-synapsin-CRE-Tomato virus or the AAV2/5-synapsin-Tomato (control) in the mediobasal hypothalamus of tau$^{flox/+}$ male mice. At stereotaxic injections animals had 2 months old. This approach allowed us to get cKO-Tau^{hyp} mice (animals with tau knock-down in the mediobasal hypothalamus). Two months after stereotaxic injections, animals had a first metabolic evaluation under Chow diet. In order to uncover a possible metabolic disorder related to the tau knock-down in the mediobasal hypothalamus, 2 months after injection we challenged cKO-Tau^{hyp} mice and their mice controls (injected by AAV2/5-synapsin-Tomato) with HFD for a period of 16 weeks. HFD was given from 5 months to 9 months of age. However, an initial metabolic evaluation was carried under Chow diet before starting HFD.

The time-line for metabolic investigations is given in Figure 67.

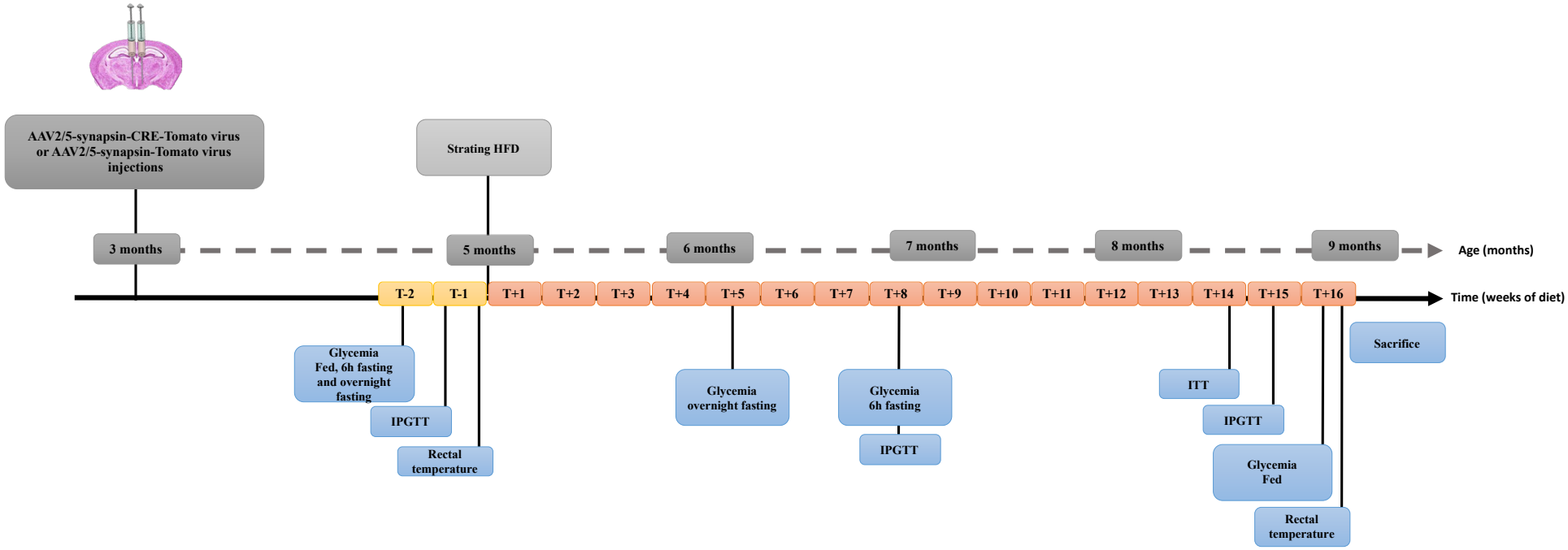

Figure 67. Time-line of metabolism investigations under high-fat diet in tau$^{flox/+}$ animals injected by an AAV2/5-synapsin-CRE-Tomato virus or the AAV2/5-synapsin-Tomato (control) in the mediobasal hypothalamus.

At 3 months old, a bilateral stereotaxic injection in the mediobasal hypothalamus of tau$^{flox/+}$ male mice of AAV2/5-synapsin-CRE-Tomato virus or the AAV2/5-synapsin-Tomato (control) were performed.

At baseline six weeks after virus injection, a first metabolic evaluation (glycemia after 6 hours of fasting, after an overnight fasting and in fed condition, insulin after 6 hours of fasting, intraperitoneal glucose tolerance test (IPGTT), and rectal temperature measurement) was performed. Feeding with high-fat diet was started at 8 weeks after virus injections (5 months old). Glycemia after an overnight fasting was performed at 5 weeks after starting HFD (6 months old). Glycemia, plasma insulin measurements after 6 hours of fasting and IPGTT were determined 8 weeks after HFD onset. Insulin tolerance tests (ITT) was performed at the 14th week of HFD. A second IPGTT was performed at the 15th week of HFD. Glycemia measurement in fed conditions was performed at the 16th week of HFD (9 months old). At the end of 16th week of HFD rectal temperature was measured and animals sacrificed.

Interestingly, two months after bilateral stereotaxic injections and under chow diet condition, cKO-Tau^{hyp} mice exhibited impaired glucose homeostasis. While overnight-fasting or fed glycemia, 6h-fasting insulinemia remained unaltered 2 moths after stereotaxic injections, 6-h-fasting glycemia as well as glycemia 30 minutes after glucose injection at IPGTT were found significantly enhanced in cKO-Tau^{hyp} mice compared to control animals (Figure 68).

Under HFD body weight gain was not different between cKO-Tau^{hyp} mice and their controls Figure 68A). Additionally, 6-h-fasting, overnight-fasting or fed glycemia, 6h-fasting insulinemia were unaltered by HFD (Figure 68). However, glucose homeostasis disturbances were observed at IPGTT. Interestingly, IPGTT realized at the age of 7 months (7 weeks under HFD) showed a significant increased glycemia values 30 and 60 minutes after glucose injection (Figure 68J). After 13 weeks of HFD, IPGTT showed a significant increased glycemia 60 minutes after glucose injection in cKO-Tau^{hyp} mice (Figure 68M). Impaired glucose homeostasis was apparently not accompanied by a significant peripheral insulin resistance, since under HFD the evolution of glycemia at ITT were not significantly different between cKO-Tau^{hyp} mice and their controls, except 2 hours after insulin injection (Figure 68P).

Interestingly, on the IPGTT realized under chow diet insulinemia was significantly higher at 30 minutes after glucose injection in control animals. However, no significant modifications were observed in cKO-Tau^{hyp} mice. Conversely, under HFD no significant modifications were observed for insulinemia at both IPGTT realized after 7 or 13 weeks of HFD (Figure 68K and 68N). Body temperature remained similar between cKO-Tau^{hyp} mice and their controls under both chow diet et HFD.

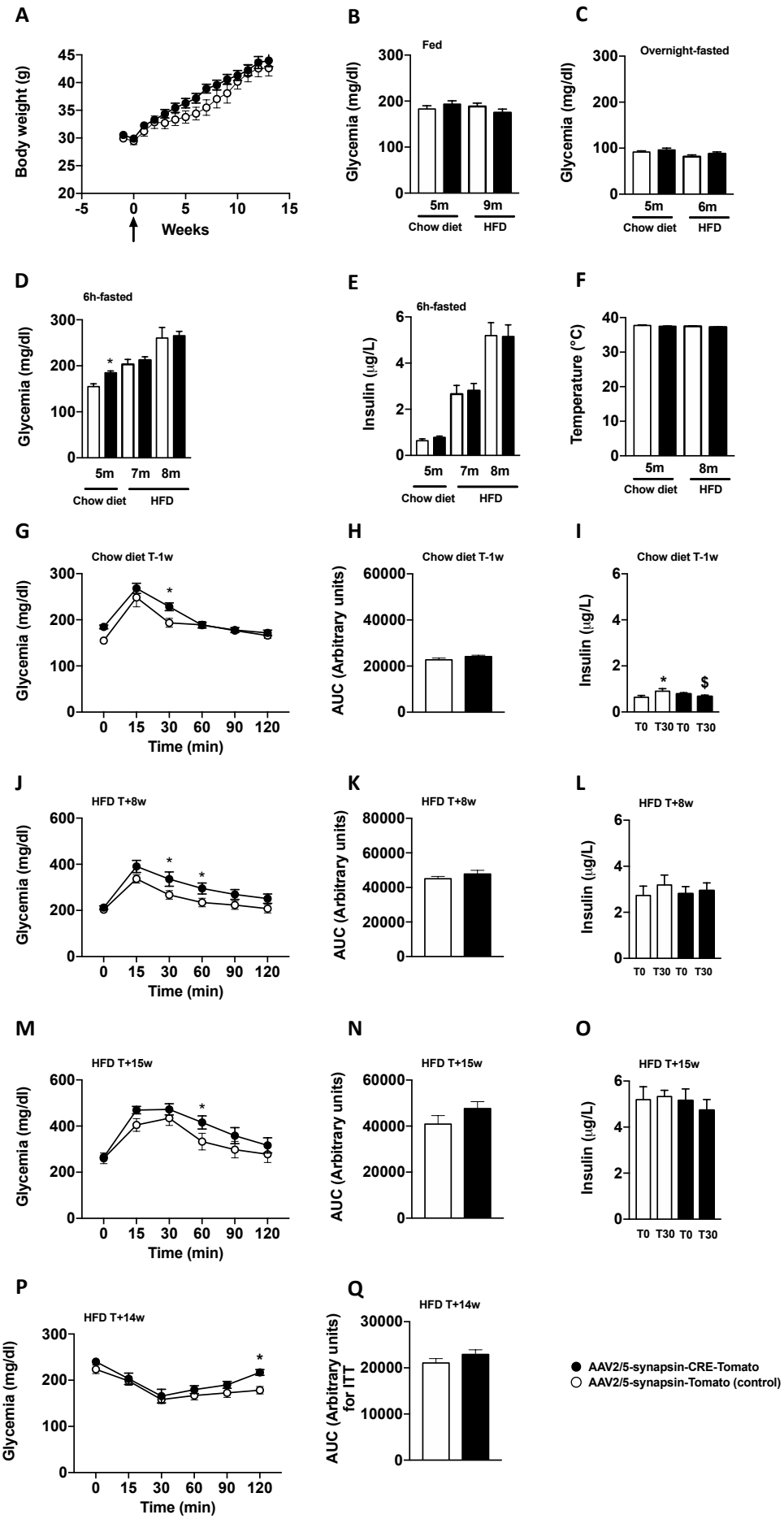
A
Body weight (g)
Weeks
B
Fed
Glycemia (mg/dl)
5m
9m
Chow diet
HFD
C
Overnight-fasted
Glycemia (mg/dl)
5m
6m
Chow diet
HFD
D
6h-fasted
Glycemia (mg/dl)
5m
7m
8m
Chow diet
HFD
E
6h-fasted
Insulin (µg/L)
5m
7m
8m
Chow diet
HFD
F
Temperature (°C)
5m
8m
Chow diet
HFD
G
Chow diet T-1w
Glycemia (mg/dl)
Time (min)
H
Chow diet T-1w
AUC (Arbitrary units)
I
Chow diet T-1w
Insulin (µg/L)
T0 T30 T0 T30
J
HFD T+8w
Glycemia (mg/dl)
Time (min)
K
HFD T+8w
AUC (Arbitrary units)
L
HFD T+8w
Insulin (µg/L)
T0 T30 T0 T30
M
HFD T+15w
Glycemia (mg/dl)
Time (min)
N
HFD T+15w
AUC (Arbitrary units)
O
HFD T+15w
Insulin (µg/L)
T0 T30 T0 T30
P
HFD T+14w
Glycemia (mg/dl)
Time (min)
Q
HFD T+14w
AUC (Arbitrary units) for ITT
AAV2/5-synapsin-CRE-Tomato
AAV2/5-synapsin-Tomato (control)

Figure 68. Metabolic phenotyping of cKO-Tau^{hyp} (injected by AAV2/5-synapsin-CRE-Tomato virus) mice and their controls (injected by AAV2/5-synapsin-Tomato) under (HFD; given from 5 to 9 months of age).

(A) Body weight gain of cKO-Tau^{hyp} and control mice under HFD from 5 to 9 months of age (NS, Two-Way ANOVA).

(B) Glycemia in fed condition (9 a.m) before (5 m) and at the completion of HFD (9 m; * $p<0.0001$, Student's t-test).

(C) Glycemia after an overnight fasting before (5 m) and at the middle of HFD (6 m; NS, One-Way ANOVA).

(D) Glycemia after 6 h of fasting before (2 m), at the middle and the completion of HFD (7 m and 8 m, respectively, NS between cKO-Tau^{hyp} mice and their controls at each time, One-Way ANOVA).

(E) Insulinemia after 6 h of fasting before (2 m), at the middle and the completion of HFD (7 m and 8 m, respectively, NS between cKO-Tau^{hyp} mice and their controls at each time, One-Way ANOVA followed by Tukey's post-hoc test).

(F) Rectal temperature before (5 m) and at the completion (9 m) of HFD (NS, One-Way ANOVA).

(G) Intraperitoneal glucose tolerance test (IPGTT) before HFD onset at 5 months of age (cKO-Tau^{hyp} mice vs. controls at T 30 minutes *$p < 0.05$, Two-Way ANOVA followed by Sidak's post-hoc test).

(H) Area under the curve for IPGTT before HFD onset at 5 months of age (NS, Student's t-test).

(I) Insulinemia at IPGTT before (T0) and 30 minutes (T30) after glucose injection previously to HFD onset (*$p < 0.05$: for control mice at T0 vs. T30 minutes, **$** $p < 0.05$: for cKO-Tau^{hyp} mice vs. controls at T30 minutes, One-Way ANOVA).

(J) IPGTT at the 8th week of HFD (7m, cKO-Tau^{hyp} vs. controls at T 30 and at 60 minutes *$p < 0.05$, respectively, Two-Way ANOVA).

(K) Area under the curve for IPGTT at the 8th week of HFD (7m, NS, Student's t-test).

(L) Insulinemia at IPGTT before and 30 minutes after glucose injection at the 8th week of HFD (NS, One-Way ANOVA followed by Tukey's post-hoc test).

(M) IPGTT at the 15th week of HFD (7m, cKO-Tau^{hyp} vs. controls at 60 minutes *$p < 0.05$, respectively, Two-Way ANOVA).

(N) Area under the curve for IPGTT at the 15th week of HFD (8m, NS, Student's t-test).

(O) Insulinemia at IPGTT before and 30 minutes after glucose injection at the 15th week of HFD (8m, NS, One-Way ANOVA followed by Tukey's post-hoc test).

(P) Insulin tolerance test (ITT) at the 14th week of HFD (NS, Two-Way ANOVA).

(Q) Area under the curve for ITT at the 14th week of HFD (NS, One-Way ANOVA).

Results are expressed as mean ± SEM. Control mice are indicated as white circles/bars, cKO-Tau^{hyp} mice as black circles/bars.

4. Evaluation of the second approach to down-regulate tau protein in the hypothalamus using a lentivirus vector combined with an shRNA tau:

Since the expression of tau protein in tau flox mice was reduced, we adopted a second approach for targeting the mediobasal hypothalamus in order to anticipate a possible failure of the experiments using $tau^{flox/+}$ animals.

For this approach a lentivirus vector combined with a shRNA tau was used to down-regulate tau protein expression in C57BL6J mice. A lentivirus vector without shRNA tau was used as a control vector. In both viral vectors, neuronal transduction was followed by the expression of eGFP. Since the hippocampus is a brain structure in which tau protein is widely expressed, the former was chosen for the evaluation of tau knock-down efficacy.

4.1. Evaluation of the efficacy of tau knock-down strategy:

For the evaluation of tau knock-down effectiveness with lentivirus shRNA tau vector, we used unilateral stereotaxic injection to deliver a lentivirus tau shRNA or lentivirus control vector in the hippocampus of C57BL6J mice (n=12/ group). Later, animals were scarified 2, 3, and 4 months after injections.

As described in the figure 69, lentivirus shRNA tau vector allowed a clear reduction of tau protein expression in the hippocampus once the second month post-stereotaxic injection. The efficacy of tau knock-down was not associated with neuronal death or inflammatory reaction (Figures 69 and 70). The intensity of both Neurotrace (preferentially marks Nissl substance which is present in high amounts in neuronal cells), and Glial fibrillary acidic protein (**GFAP**), which is a specific marker of astrocytes, were not modified in the injected site, compared to the contralateral region of the hippocampus in animals injected with a lentivirus shRNA tau or in animals injected with the virus control (Figures 70).

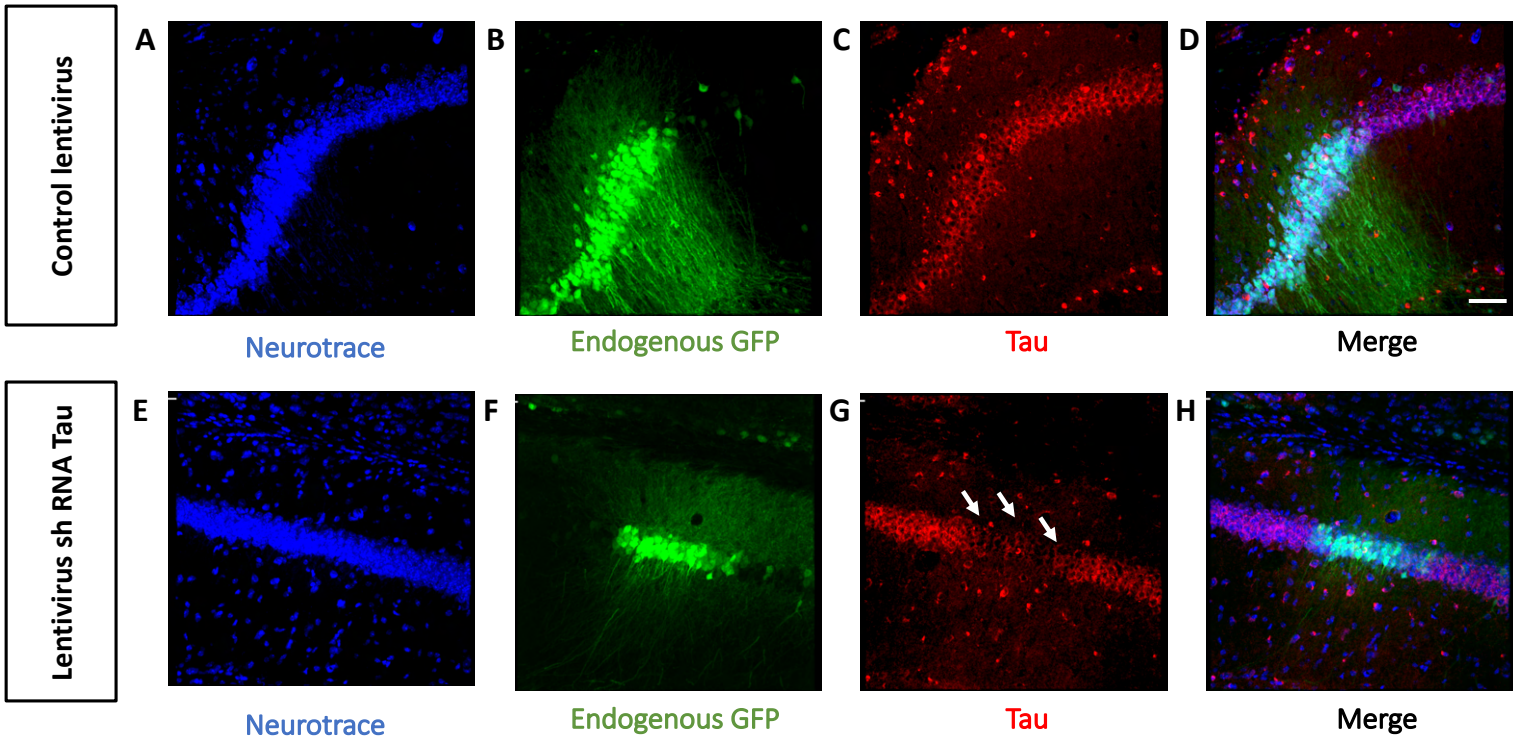

Figure 69. Lentivirus shRNA tau vector mediates efficient down-regulation of tau protein in mouse hippocampus without induction of neuronal death.

Tau expression in mouse hippocampus from animals injected with a shRNA tau and the control lentivirus.

Control lentivirus: **(A-D)** Immunofluorescence staining at the injected site for endogenous GFP (green), and tau protein (red, tau 9H12 antibody) in the CA1 of the hippocampus. Blue: Neurotrace stains label the Nissl substance which is present in high amounts in neuronal cells.

Lentivirus shRNA tau: **(E-H)** Immunofluorescence staining at the injected site for endogenous GFP (green), and tau protein (red, tau 9H12 antibody) in the CA1 of the hippocampus. Blue: Neurotrace stains label the Nissl substance which is present in high amounts in neuronal cells. White arrows show the reduction of tau expression in transfected hippocampus site by lentivirus shRNA tau.

Scale: 50µm.

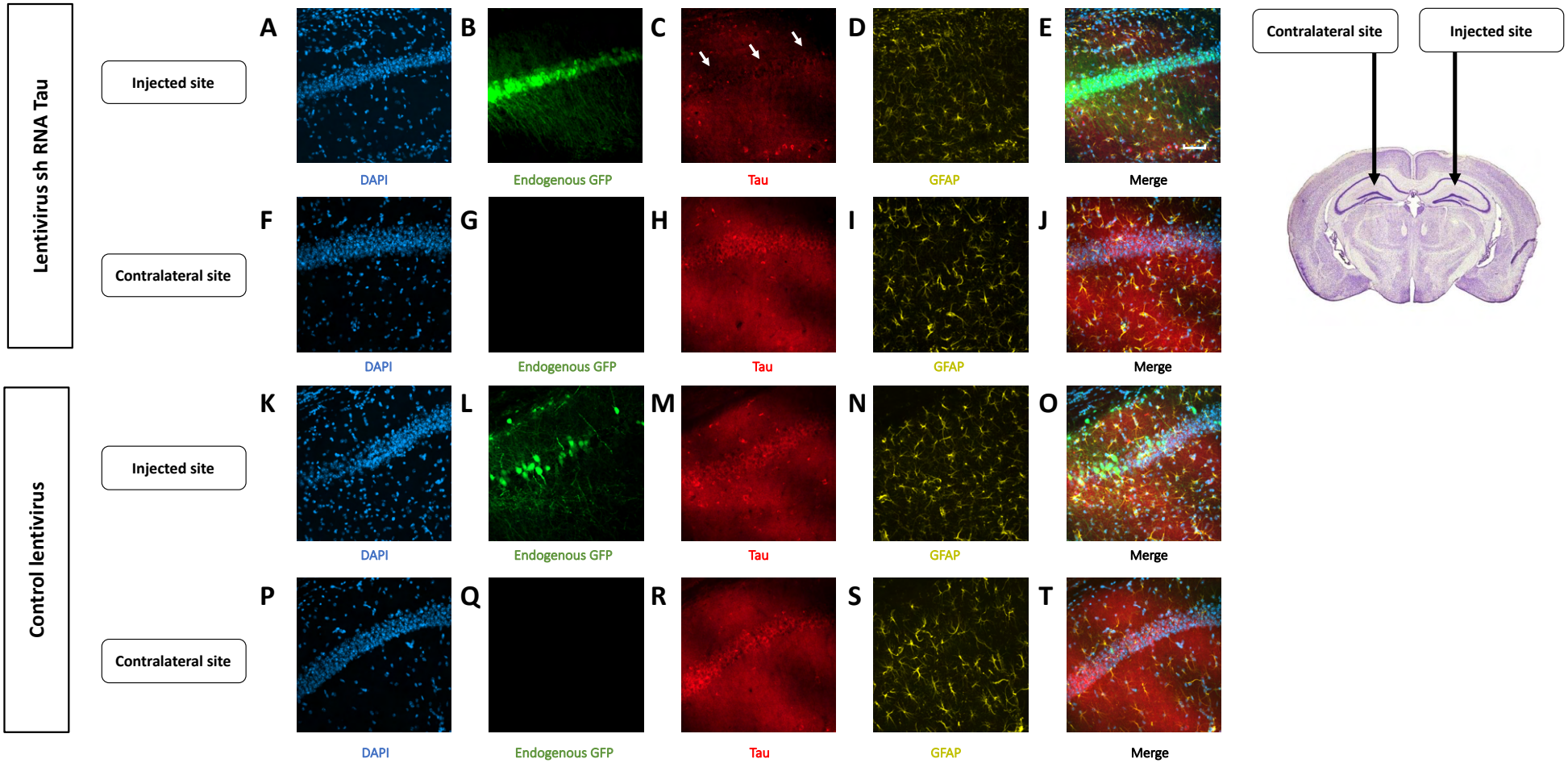
Lentivirus sh RNA Tau
Injected site
Contralateral site
Control lentivirus
Injected site
Contralateral site
A
B
C
D
E
F
G
H
I
J
K
L
M
N
O
P
Q
R
S
T
DAPI
Endogenous GFP
Tau
GFAP
Merge
Contralateral site
Injected site

Figure 70. Lentivirus shRNA tau vector mediates efficient down-regulation of tau protein in mouse hippocampus without induction of neuroinflammation.

Mice injected with Lentivirus shRNA tau: (A-E) Immunofluorescence staining at the injected site for endogenous GFP (green), tau protein (red, tau 9H12 antibody), and the Glial Fibrillary Acidic Protein (GFAP, yellow) in the CA1 of the hippocampus. Blue: DAPI nuclear counterstaining. White arrows show the reduction of tau expression in transfected hippocampus site by lentivirus shRNA tau.

Mice injected with Lentivirus shRNA tau: (F-J) Immunofluorescence staining at the contralateral site for endogenous GFP (green), tau protein (red, tau 9H12 antibody), and the Glial Fibrillary Acidic Protein (GFAP, yellow) in the CA1 of the hippocampus. Blue: DAPI nuclear counterstaining.

Mice injected with the control lentivirus: (K-O) Immunofluorescence staining at the injected site for endogenous GFP (green), tau protein (red, tau 9H12 antibody), and the Glial Fibrillary Acidic Protein (GFAP, yellow) in the CA1 of the hippocampus. Blue: DAPI nuclear counterstaining.

Mice injected with the control lentivirus: (P-T) Immunofluorescence staining at the contralateral site for endogenous GFP (green), tau protein (red, tau 9H12 antibody), and the Glial Fibrillary Acidic Protein (GFAP, yellow) in the CA1 of the hippocampus. Blue: DAPI nuclear counterstaining.

Scale: 50μm.

4.2. Metabolic phenotyping of animals with mediobasal hypothalamic tau knock-down by lentivirus tau shRNA:

Firstly, we used bilateral stereotaxic injections to deliver lentivirus shRNA tau or the virus control (lentivirus without shRNA tau) in the mediobasal hypothalamus of a C57BL6J mice. At stereotaxic injections animals had 4 months old. Two months after stereotaxic injections, animals had a first metabolic evaluation under Chow diet. In the same way for the metabolic phenotyping of tau KI or cKO-Tau^{hyp} mice, animals were challenged with HFD for a period of 16 weeks. HFD was given from 6 months to 10 months of age. The time-line for metabolic investigations is given in Figure 71.

Under chow diet condition, metabolic evaluation two months after bilateral stereotaxic injections showed no clear signs of impaired glucose homeostasis (Figure 72), except a significant elevation of overnight-fasting glycemia (Figure 72C).

Under HFD body weight gain was not different between mice injected by the lentivirus shRNA tau or the control virus (Figure 72A). Furthermore, 6-h-fasting, overnight-fasting or fed glycemia, 6h-fasting insulinemia were unaltered by HFD (Figures 72B-E).

Conversely, glucose homeostasis disturbances were observed at IPGTT. Interestingly, IPGTT achieved at the age of 7 months (8 weeks of HFD) showed a significant increased glycemia values 30 minutes after glucose injection (Figure 72J) in mice. As observed in Figure 72M, no significant glycemic modifications were observed on the IPGTT achieved at the age of 9 months (15 weeks under HFD). Also, no significant difference of insulinemia were observed before glucose injection and 30 minutes after, on both IPGTT achieved at 8 and 15 weeks of HFD (Figures 72L and 72O). Also, glycemia at ITT were not significantly different between mice injected by lentivirus tau shRNA and animals injected by control virus (Figure 72P).

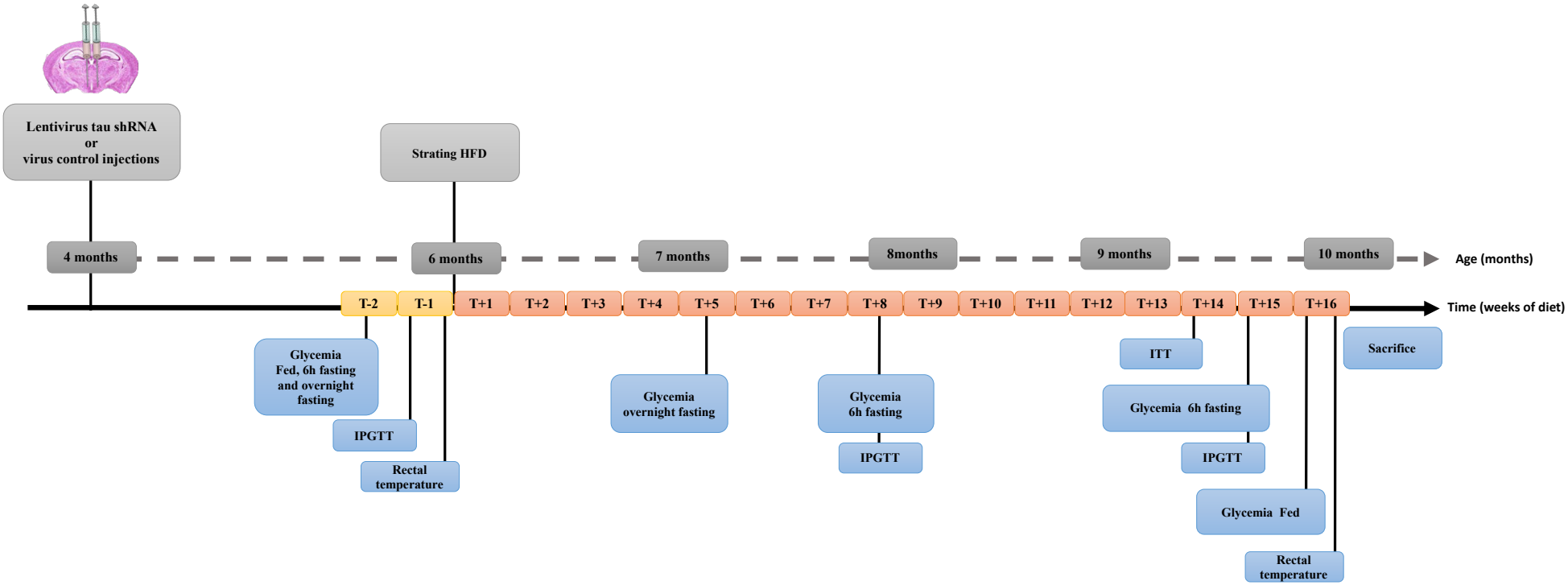

Figure 71. Time-line of metabolism investigations under high-fat diet in C57BL6J animals injected by a Lentivirus shRNA tau or the control lentivirus in the mediobasal hypothalamus.

At 4 months old, a bilateral stereotaxic injection in the mediobasal hypothalamus of C57BL6J male mice of a Lentivirus shRNA tau or the Control Lentivirus were performed. At baseline, six weeks after virus injection, a first metabolic evaluation (glycemia after 6 hours of fasting, after an overnight fasting and in fed condition, insulin after 6 hours of fasting, intraperitoneal glucose tolerance test (IPGTT), and rectal temperature measurement) was performed. Feeding with high-fat diet was started at 8 weeks after virus injections (6 months old). Glycemia after an overnight fasting was performed at 5 weeks after starting HFD (7 months old). Glycemia, plasma insulin measurements after 6 hours of fasting and IPGTT were determined 8 weeks after HFD onset. Insulin tolerance tests (ITT) was performed at the 14th week of HFD. A second IPGTT was performed at the 15th week of HFD. Glycemia measurement in fed conditions was performed at the 16th week of HFD (9 months old). At the end of 16th week of HFD rectal temperature was measured and animals sacrificed.

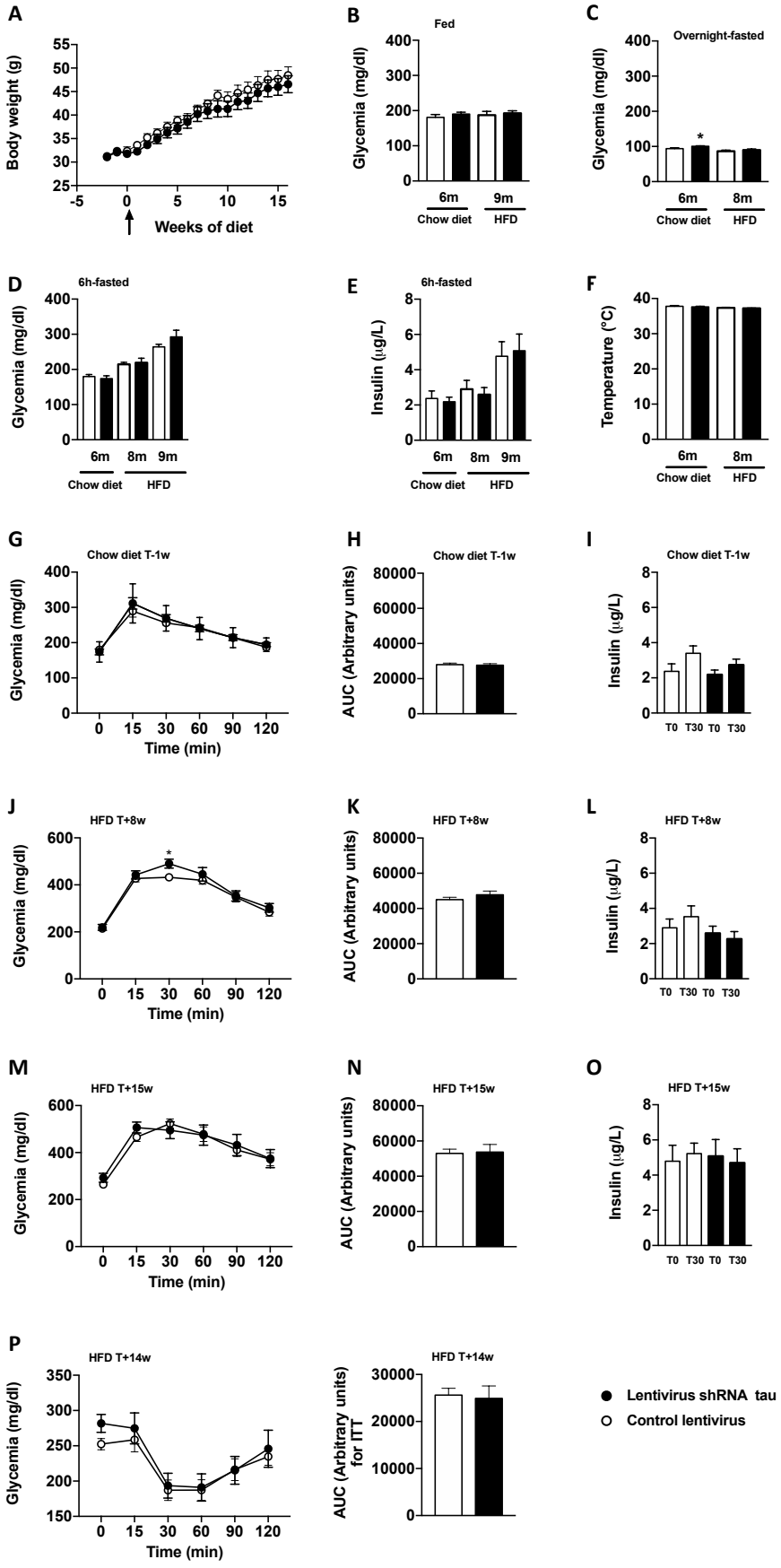
A
Body weight (g)
Weeks of diet
B
Fed
Glycemia (mg/dl)
6m
9m
Chow diet
HFD
C
Overnight-fasted
Glycemia (mg/dl)
6m
8m
Chow diet
HFD
D
6h-fasted
Glycemia (mg/dl)
6m
8m
9m
Chow diet
HFD
E
6h-fasted
Insulin (µg/L)
6m
8m
9m
Chow diet
HFD
F
Temperature (°C)
6m
8m
Chow diet
HFD
G
Chow diet T-1w
Glycemia (mg/dl)
Time (min)
H
Chow diet T-1w
AUC (Arbitrary units)
I
Chow diet T-1w
Insulin (µg/L)
T0 T30 T0 T30
J
HFD T+8w
Glycemia (mg/dl)
Time (min)
K
HFD T+8w
AUC (Arbitrary units)
L
HFD T+8w
Insulin (µg/L)
T0 T30 T0 T30
M
HFD T+15w
Glycemia (mg/dl)
Time (min)
N
HFD T+15w
AUC (Arbitrary units)
O
HFD T+15w
Insulin (µg/L)
T0 T30 T0 T30
P
HFD T+14w
Glycemia (mg/dl)
Time (min)
HFD T+14w
AUC (Arbitrary units) for ITT
Lentivirus shRNA tau
Control lentivirus

Figure 72. Metabolic phenotyping C57BL6J animals injected by a Lentivirus shRNA tau or the control lentivirus in the mediobasal hypothalamus under high-fat diet (HFD; given from 6 to 10 months of age).

(A) Body weight gain of animals injected by a Lentivirus shRNA tau or the control lentivirus mice under HFD from 6 to 10 months of age (NS, Two-Way ANOVA).

(B) Glycemia in fed condition (9 a.m) before (6 months) and at the completion of HFD (10 months; NS, One-Way ANOVA).

(C) Glycemia after an overnight fasting before (6 months) and at the middle of HFD (7 months; *p< 0.05 for mice injected by a Lentivirus shRNA tau and their controls before HFD onset, One-Way ANOVA).

(D) Glycemia after 6 h of fasting before (6 months), at the middle and the completion of HFD (8 and 9 months, respectively, NS between mice injected by a Lentivirus shRNA tau and their controls at each time, One-Way ANOVA).

(E) Insulinemia after 6 h of fasting before (6 months), at the middle and the completion of HFD (8 and 9 months, respectively, NS between mice injected by a Lentivirus shRNA tau and their controls at each time, One-Way ANOVA).

(F) Rectal temperature before (6 months) and at the completion (10 months) of HFD (NS, One-Way ANOVA).

(G) Intraperitoneal glucose tolerance test (IPGTT) before HFD onset at 6 months of age (NS, Two-Way ANOVA followed by Sidak's post-hoc test).

(H) Area under the curve for IPGTT before HFD onset at 5 months of age (NS, Student's t-test).

(I) Insulinemia at IPGTT before (T0) and 30 minutes (T30) after glucose injection previously to HFD onset (NS, One-Way ANOVA followed by Sidak's post-hoc test).

(J) IPGTT at the 8^{th} week of HFD (8 months, *p < 0.05 : mice injected by a Lentivirus shRNA tau and their controls at 60 minutes, Two-Way ANOVA followed by Sidak's post-hoc test).

(K) Area under the curve for IPGTT at the 8^{th} week of HFD (8 months, NS, Student's t-test).

(L) Insulinemia at IPGTT before and 30 minutes after glucose injection at the 8^{th} week of HFD (NS, One-Way ANOVA followed by Tukey's post-hoc test).

(M) IPGTT at the 15^{th} week of HFD (9 months, NS, Two-Way ANOVA followed by Sidak's post-hoc test).

(N) Area under the curve for IPGTT at the 15^{th} week of HFD (9 months, NS, Student's t-test).

(O) Insulinemia at IPGTT before and 30 minutes after glucose injection at the 15^{th} week of HFD (9 months, NS, One-Way ANOVA followed by Tukey's post-hoc test).

(P) Insulin tolerance test (ITT) at the 14^{th} week of HFD (9 months, NS, Two-Way ANOVA).

(Q) Area under the curve for ITT at the 14^{th} week of HFD (9 months, NS, One-Way ANOVA).

Results are expressed as mean ± SEM. mice injected by a Control Lentivirus are indicated as white circles/bars, mice injected by a Lentivirus shRNA tau as black circles/bars.

Discussion

Discussion

Previous studies suggested that AD lesions favor the emergence of glucose homeostasis alterations. However, the origin of impaired glucose homeostasis in AD but also Frontotemporal lobar degeneration (FTLD) patients remains unclear (Bucht et al., 1983; Calsolaro and Edison, 2016; Craft et al., 1998, 1992; Fujisawa et al., 1991; Janson et al., 2004; Matsuzaki et al., 2010a; Tortelli et al., 2017). Previous works, from our laboratory and others, using germline tau KO mice, supported that constitutive loss of tau function may lead to glucose homeostasis alterations, increased food intake, and body weight gain observed in adult tau KO mice (Marciniak et al., 2017; Wijesekara et al., 2018a, 2021). However, these data are not sufficient to determine whether these changes solely relate to tau deletion, which is pathophysiologically irrelevant, or to the loss of some tau functions.

In the first part of my PhD thesis, to address more specifically this question, the principal microtubule-binding property of tau can be reduced by the insertion of mutations in the microtubules domains such as those described in FTLD with tau mutations (Pottier et al., 2016). Therefore, to further address the link between tau and glucose homeostasis, we, therefore, used a novel knock-in tau mouse model expressing a mutated human tau protein, under the endogenous Mapt mouse gene promoter, allowing expression of a mutated human tau protein at a physiological level and thereby avoiding the biases of mouse models based on tau-overexpression (Leboucher et al., 2019) or constitutive deletion (Marciniak et al., 2017; Wijesekara et al., 2018a). This mouse model was chosen to determine to which extent a loss of tau microtubule-binding activity due to P301L mutation (Delobel et al., 2002) was prone to recapitulate metabolic impairments observed in tau KO animals. The metabolic phenotyping was performed at an age when the model does not exhibit any tau aggregation allowing us to evaluate the real impact of the expression of a dysfunctional tau protein.

1. Metabolic phenotyping of tau KI mouse model under Chow diet and HFD:

Interestingly, metabolic phenotyping data of a tau KI mouse model demonstrate that expressing a mutated form of tau favors the development, in males, of glucose homeostasis impairments under metabolic stress (HFD), as exemplified by the significant increase in insulinemia as well as impaired glucose tolerance. Also, glucose homeostasis alterations were associated with both increased body weight gain and food intake only in tau KI male mice. The metabolic phenotype observed in tau KI mice under HFD mirrored what our laboratory and others previously observed in constitutive tau KO animals (Marciniak et al., 2017; Wijesekara et al., 2018a, 2021) , likely suggesting that disorders observed in tau KI and tau KO mice are likely attributed to an impaired tau function such as the loss of microtubule-binding activity. This view is in agreement with the reversion of tau KO phenotype observed following re-expression of human tau as recently reported (Wijesekara et al., 2018a, 2021). Nonetheless, glucose homeostasis defects have been observed in another tau KI model, where mutated tau sequence is inserted in the permissive HPRT site and expressed at the physiological level in the presence of murine tau (Hull et al., 2020). Impairment glucose homeostasis in this tau KI model was associated with the development of important peripheral insulin resistance at the age of 8 months, without any modifications of body wight gain or food intake (Hull et al., 2020). The former results suggest that metabolic dysregulations are not solely ascribed to tau loss-of-function and that mechanistic insights on the precise role of tau in the control of glucose homeostasis require additional molecular studies.

Although, in the base our unpublished data, tau RNA is expressed in both mouse skeletal muscle and fat tissue. Also, its expression was previously shown in rat skeletal muscle (Gu et al., 1996). Data from Protein Atlas site reported that tau protein is expressed in human insulin-sensitive tissues, skeletal muscle and fat tissue (Figure 73).

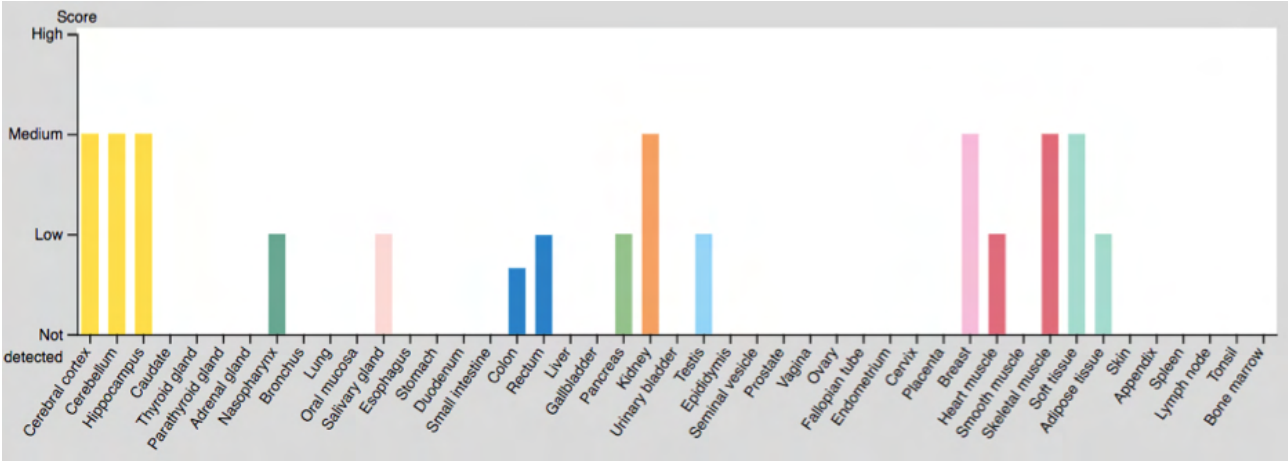

Figure 73. Tau protein expression in different human tissues.

Adapted from : https://www.proteinatlas.org/ENSG00000186868-MAPT/tissue

Interestingly, it was shown that overexpression of tau protein, despite being localized to microtubules in 3T3-L1 adipocytes, delays the initial appearance of GLUT4 at the cell membrane following insulin stimulation (Emoto et al., 2001). Some previous studies suggested that an intact microtubule system is important for the translocation of the insulin-sensitive glucose transporter isoform 4 (GLUT4), after insulin stimulation, from an intracellular compartment to the cell surface, which accomplish the stimulation of GLUT4 exocytosis [(Figure 74); (Emoto et al., 2001; Liu et al., 2013; Olson et al., 2001)]. In the basal conditions, GLUT4 is predominantly localized in the intracellular membrane compartments, including the trans-Golgi network, the early endosomes, and other membranous elements in the cytoplasm. Upon insulin stimulation, vesicles containing GLUT4 translocated rapidly from these compartments to the plasma membrane (Huang et al., 2001). After insulin is withdrawn, GLUT4 will be internalized in newly formed vesicles and returned to its intracellular localization via the microtubule-based motor protein dynein (Huang et al., 2001).

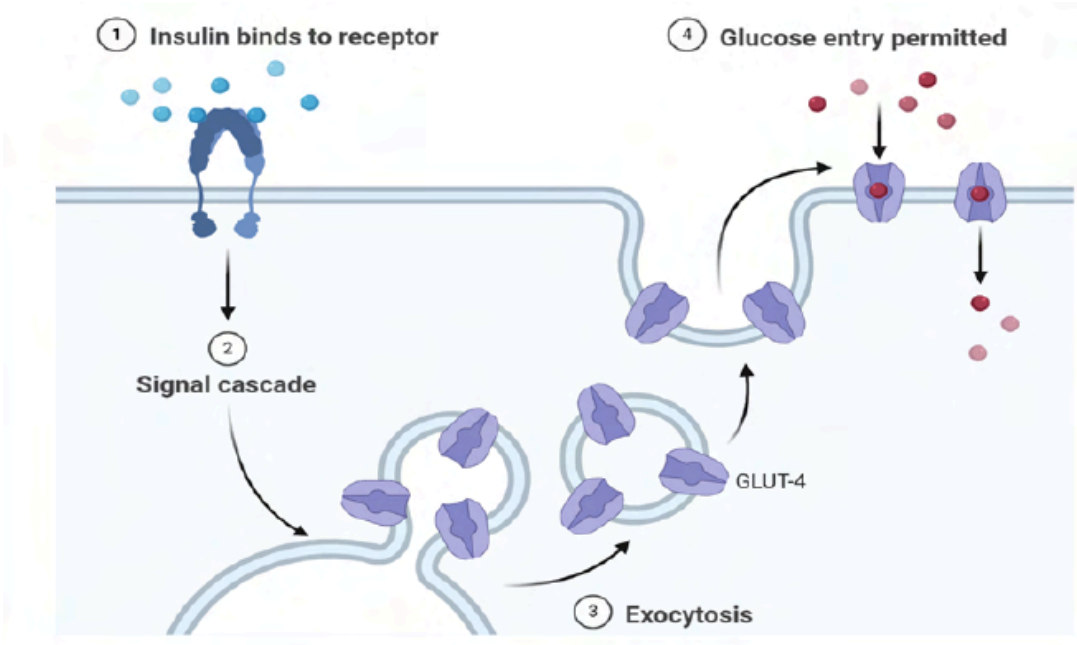

Figure 73. Activation of the glucose transporter GLUT4 by insulin.
The glucose transporter GLUT4 facilitates insulin-stimulated glucose uptake into muscle and adipose tissue.

Furthermore, it was reported in a recent publication that tau deletion or loss-of-function promotes peripheral insulin resistance as seen by the inhibition of insulin signaling proteins and the reduction of glucose uptake into primary hepatocytes isolated from tau KO and P301L mice, respectively (Al-Lahham et al., 2021). Also, in the same study, sub-toxic exposure of wild-type primary hepatocytes to tau aggregates resulted in inhibition of insulin signaling and glucose uptake (Al-Lahham et al., 2021).

Our metabolic phenotyping data support that glucose metabolism impairments seen in male tau KI mice clearly involve pancreatic islets dysfunction rather than peripheral insulin resistance. To evaluate insulin resistance, we analyzed two key molecular parameters that are impaired during insulin resistance, phosphorylated serine/threonine kinase protein kinase B (pAkt) and circulating adiponectin. Indeed, insulin signaling in the liver or adipose tissue induces the phosphorylation of

Akt and its subsequent activation (Silva Rosa et al., 2020). In several models of insulin resistance, it was shown that reduced glucose uptake is due to defects in insulin signaling (Huang et al., 2018; Ng et al., 2010) and is associated with impaired Akt phosphorylation, leading to the development of insulin resistance in obesity and type 2 diabetes (Choi and Kim, 2010). Adiponectin is an adipose tissue-secreted endogenous insulin sensitizer, which plays a key role as a modulator of peroxisome proliferator-activated receptor γ action. Low levels of adiponectin, as observed in Adiponectin knockout mice or in patients affected by type 2 diabetes, have been associated with insulin resistance in diabetes (Ziemke and Mantzoros, 2010). In our tau KI mouse model, pAkt levels were not significantly different between KI and WT mice fed with HFD, and circulating plasma adiponectin concentrations were significantly increased in tau KI mice compared to control animals fed with HFD, suggesting that insulin sensitivity was not impaired in tau KI mice.

Based on these data, tau loss of function is associated with impaired glucose homeostasis, which fits with the initial metabolic phenotype observed in tau KO mice. However, two mutually non-exclusive mechanisms could explain the metabolic alterations observed in both tau KO and tau KI mice: tau impacts peripheral glucose homeostasis by a central-based regulation possibly involving the hypothalamus; or, in non-mutually manner, tau regulates ß-cell function in the pancreas.

In the second part of my PhD thesis, to explore more specifically the origin of glucose homeostasis impairment, different approaches were used.

2. Impact of tau los of function in pancreatic β cells:

First, using immunohistochemistry we provide clear evidence of the large enrichment of tau in insulin-producing β cells in WT, tau KI mice as well as the human pancreas. Furthermore, we observed, in tau KI mice, a significant increase of β-cell mass similar to what was previously reported during hyperglycemia and/or insulin resistance (Weir and Bonner-Weir, 2004). This adaptation might relate to the impaired insulin secretion. In fact, we observed in ex vivo experiments on isolated

pancreatic islets; itself linked to a loss-of-function of mutated tau, these observations being replicated in isolated islets from tau KO mice as well as from tau knock-down in Min6 pancreatic cell line. Although it was already known that pancreas and islets of Langerhans expressed tau mRNA (Maj et al., 2016b; Vanier et al., 1998). Interestingly, our data are the first reporting that isoforms expressed are a mix of 3R/4R or 4R only, in human and mouse islets respectively, in agreement with the brain profile. Previous studies suggested the presence of tau protein into human pancreatic β cells (Martinez-Valbuena et al., 2021; Miklossy et al., 2010b). Our study is also the first to report the colocalization of tau with insulin but not glucagon in human islets. Other studies suggested that, in rat or mouse islets, tau colocalizes with insulin (Maj et al., 2016b; Wijesekara et al., 2021).

Extending these primary findings, our data unambiguously show, using several tau antibodies and proper controls (tau KO tissue combined with confocal microscopy) that, in the mouse, tau is selectively expressed by insulin but not glucagon-positive cells. Such demonstration was also important given a recent article suggesting that tau might not be expressed by pancreatic islets (Zhou et al., 2020).

In vitro GSIS from isolated pancreatic islets from tau KO mice, consistent with previous observations (Wijesekara et al., 2018a, 2021), or tau KI mice, showed an impaired insulin secretion upon high glucose conditions. Altered GSIS was however not associated with a defective insulin production. Hence, the mechanism that controls insulin secretion in response to glucose is impaired in tau KI mice, probably contributing to hyperglycemia observed in these mice. In the context of glucose dyshomeostasis, such as during type 2 diabetes development, it is not fully inconsistent to observe both defective insulin secretion and increased fasting hyperglycemia and insulinemia (DeFronzo et al., 2015). Increased fasting plasma insulin levels, observed in tau KI mice, can be caused by a compensatory mechanism induced by hyperglycemia that leads to an increase of β-cell mass (Weir and Bonner-Weir, 2004). In addition, reduced insulin clearance is observed during HFD feeding and can contribute to maintaining elevated fasting insulinemia (Strömblad and Björntorp,

1986). Interestingly, studies in humans (Bonora et al., 1983), and animals (Kim et al., 2007) have shown that reduced insulin clearance can cooperate with elevated insulin secretion to regulate glucose homeostasis.

How tau regulates the ability to secrete insulin in response to high glucose remains unclear. Notably, microtubules play a major role in the intracellular trafficking of vesicles in endocrine cells like pancreatic β cells (Fourriere et al., 2020; Müller et al., 2021). The microtubule of pancreatic islet β-cells regulates GSIS. A previous study reported that the microtubule-mediated movement of insulin vesicles away from the plasma membrane limits insulin secretion, high glucose–induced remodeling of microtubule network facilitates robust GSIS, and this remodeling involves disassembly of old microtubules and nucleation of new microtubules (Mourad et al., 2011; Zhu et al., 2015).

A recent study demonstrated that high levels of glucose induce rapid microtubule disassembly mediated by tau hyperphosphorylation through glucose-responsive kinases, leading to tau dissociation from microtubules and favoring insulin secretion (Ho et al., 2020). In the same study also, tau knockdown in mouse islet β-cells facilitates microtubule turnover, causing increased basal insulin secretion, depleting insulin vesicles from the cytoplasm, and impairing GSIS. Results of the former study suggests that tau suppresses peripheral microtubules turning-over to restrict insulin over-secretion in basal conditions and preserve the insulin reserve pool, which can be released following glucose stimulation (Ho et al., 2020). Hence, in β cells, tau plays an important role in glucose-mediated insulin secretion.

Considering the presence of hyperphosphorylated and misconformed tau in the pancreatic islets of patients with type 2 diabetes and patients with AD (Martinez-Valbuena et al., 2021; Miklossy et al., 2010b). Whether this contributes to diabetes pathogenesis or is a consequence of diabetes itself remains to be understood. Interestingly, during diabetes, PI3 kinase pathway is classically down-regulated and consequently, GSK3 activity may be up-regulated, which could drive phosphorylation of tau in diabetes (Hooper et al., 2008). Indeed, in vitro inhibition of P13K in pancreatic beta cell-

derived rodent cell line, RIN-5F, was associated to the increase of tau phosphorylation (Maj et al., 2016b).

Furthermore, it is likely that glucose homeostasis impairments seen in AD, at least in part, related to tau loss of microtubule-binding activity. Nonetheless, it is probable that glucose metabolism impairments of AD patients likely arise from a synergistic impact of both pancreatic tau pathology and amyloidosis. Indeed, Aβ has been shown to deposit in the pancreas of both humans and APP mouse models (Miklossy et al., 2010b; Vandal et al., 2014; Wijesekara et al., 2017).

Since that tau is more than a microtubule-associated protein (Sotiropoulos et al., 2017), and plays a role in chromatin organization and RNA metabolism (Galas et al., 2019), it is also possible that the impaired tau function also alters ß-cell function by other mechanisms.

Despite the use MIP-CreERT mouse line, which is the most efficient and specific model compared to other β-cell specific Cre lines, unfortunately, in our project this approach to study in vivo the impact of a specific tau deletion in pancreatic β-cells was failed. In the last mouse model, under the action of Tamoxifen, the recombination should occur only in β-cells. However, it was reported that delivery of tamoxifen itself (to induce recombination) can alter glucose homeostasis and impair β-cell proliferation (Carboneau et al., 2016). Additionally, recent studies suggested that DNA hypermethylation of the Ins1-Cre and Ins1-CreER knock-in alleles in some colonies can lead to very poor rates of recombination and it may be necessary to validate Cre efficiency regularly (Mosleh et al., 2020). In our project, the Cre efficiency was validate initially in our MIP-CreERT animals. Furthermore, in parallel of the first $tau^{flox/+}$//MIP-CreERT animals' batch which served to the metabolic phenotyping, another batch of $tau^{flox/+}$//MIP-CreERT animals were generated and injected by Tamoxifen. Animals of the last batch were scarified, and their islets isolated one month after the injection of Tamoxifen. Regrettably, following a technical problem related to the RNA extraction kit, the RNA from isolated islets were destroyed, and consequently, we lost the possibility to evaluate the Cre efficiency in $tau^{flox/+}$//MIP-CreERT animals by qPCR.

Accordingly, it is crucial to find a new way to avoid caveats of developmental deletion of LoxP flanked genes, tamoxifen toxicity, and unplanned recombination before tamoxifen administration. In this end, we tried to study the possibility of using an adeno-associated virus vector in order to target β-cells and thus induce a tau deletion. Adeno associated virus (AAV) is non-pathogenic and a simple systemic delivery of AAV can infect tissues of interest, including the pancreas. Also, AAV infection does not cause any easily detected or common symptoms (Kotin et al., 1990; Mingozzi and High, 2007).

First, we screened many AAV serotypes to find the appropriate serotypes, which can transduce pancreatic endocrine cells in adult mouse. Among, different AAV serotypes tested, we find that the serotype 10, administered by intravenous injection, had a highest affinity for the endocrine pancreatic β-cells. Conversely, a previous study reported that eighth serotype (AAV8) had the highest affinity for the pancreas when delivered by intraperitoneal or intravenous injection (Jiang et al., 2006).

The second step will be the generation of an AAV10 coupled with both an shRNA tau and a Cre-loxP system, which will be activated only by under the action of the a Cre-recombinase. Later, the AAV10-shRNA tau will be administered by intravenous injection in Mip-CreERT mice. In the later animals, the activation of shRNA tau will occur by the injection of tamoxifen, which will activate the Cre-recombinase only in pancreatic endocrine β-cells. The setups of this approaches will take several times.

Furthermore, to explore more specifically the impact of tau loss of function the mediobasal hypothalamus on glucose homeostasis, different approaches for the conditional deletion or downregulation of tau protein in neurons of the mediobasal hypothalamus were adopted.

3. Impact of tau loss of function in neurons of the mediobasal hypothalamus:

One of these approaches was the downregulation of tau protein in neurons of the mediobasal hypothalamus by intraparenchymal injection of a lentivirus driven a shRNA tau.

Despite initial setups demonstrating the effectiveness of tau downregulation by the shRNA tau, in our study, a few significant glucose homeostasis disorders under both Chow diet and HFD were observed in animals injected by a lentivirus shRNA tau compared to controls. In fact, under chow diet and compared to control animals, only glycemia after an overnight fasting was significantly increased in mice injected by lentivirus shRNA tau. Furthermore, glycemia 30 minutes after glucose injection at IPGTT was significantly elevated in mice injected by lentivirus shRNA tau, and the later was associated with no increased insulin secretion compared to insulin kinetic in control animals. Unexpectedly, under HFD glucose homeostasis profile was similar in both mice injected by lentivirus shRNA tau and control animals. These results could be related the few diffusion of lentivirus vectors compared to AAV vectors. A previous study had reported that AAV vector are more efficient to transduce rat hypothalamus than a lentiviral vector (de Backer et al., 2010).

Interestingly, tau flox/+ animals injected by AAV2/5-synapsin-CRE-Tomato virus compared to controls developed glucose homeostasis disorders under both chow diet and HFD. These results confirm the hypothesis that tau loss of function in the hypothalamus, related to the conditional deletion of tau in neurons of the mediobasal hypothalamus, favors the development of glucose dyshomeostasis. Also, our finding highlights the importance of tau physiological function in the central regulation of glucose homeostasis. As reported previously by our laboratory, tau play a key role neuronal insulin signaling, and the constitutive deletion of tau in tau KO mice was associated with a development of central insulin resistance (Marciniak et al., 2017). In addition to impaired glucose homeostasis, tau KO mice exhibited increased body weight gain and food intake. The same metabolic phenotype was observed in tau KI mice.

Increased food intake and body weight gain may be related to the loss of tau function in POMC neurons of the arcuate nucleus. Interestingly, this hypothesis can be supported by the co-localization of tau protein in POMC and AgRP neurons of the arcuate nucleus. Additionally, mice with a neuron-specific deletion of the insulin receptor (NIRKO mice) developed obesity, increased food intake, and impaired glucose homeostasis (Brüning et al., 2000), and thereby a close metabolic disorders as observed in both tau KI and tau KO mice.

In NIRKO, obesity was associated to high leptin levels, which demonstrating that central leptin actions require intact insulin signaling in the CNS. Furthermore, previous works reported that insulin acts in POMC and AgRP neurons of the arcuate nucleus, and the central administration of insulin induced hyperpolarization of both POMC and AgRP neurons (Hill et al., 2010; Könner et al., 2007; Williams et al., 2010). Unlike leptin, the selective ablation of insulin receptor (IR) in AgRP or POMC neurons had no effect on body weight or food intake (Könner et al., 2007). However, these animals developed glucose intolerance. Taken together, these results demonstrate that AgRP and POMC neurons mediate insulin effects on glucose homeostasis, and leptin actions in the hypothalamus require intact brain insulin signaling.

Also, impaired glucose homeostasis related to tau loss of function in the axonal extensions of GnRH neurons at the arcuate nucleus cannot be excluded. We reported her the co-localization of tau protein in the axonal extensions of GnRH neurons. Furthermore, Brüning et al., demonstrated previously for the first time that normal insulin signaling within the central nervous system is essential for the correct activation of the gonadotrope axis in rodents, and interestingly, the selective deletion of the insulin receptor from GnRH neurons leads to a reduction in LH concentrations by 60%–90% and low testosterone concentrations (Brüning et al., 2000). Also, another group observed that increasing circulating insulin levels, by performing hyperinsulinemic clamp studies in male mice, was associated with a significant rise in LH secretion (Burcelin et al., 2003). Male hypogonadism causes obesity, and also exacerbates HFD-induced metabolic alterations in male mice (Aoki et al., 2016; Dubois et al., 2016). Additionally, animals with hypogonadism displayed strongly increased

circulating levels of adiponectin (Combs et al., 2003; Yanase et al., 2008). Usually, the reduction in adiponectin serum concentrations occurs through weight gain. Despite the higher proportion of body fat associated with hypogonadism, serum adiponectin concentrations are higher in hypogonadal male versus eugonadal men. Similarly, both proportion of body fat and adiponectin concentrations are elevated in male androgen receptor knockout (ARKO) mice or in castrated mice versus wild-types or non-castrated mice (Combs et al., 2003; Yanase et al., 2008). Contrariwise, testosterone administration reduced visceral and total-body fat mass in both hypogonadal and eugonadal men (Bhasin et al., 2005, 2001).

As seen previously, in tau KI male mice, circulating adiponectin levels were significantly increased compared to control animals. These data, suggest the possibility of the installation of a hypogonadism in tau KI male mice. Furthermore, given the role of the mediobasal hypothalamus in the regulation of the hypothalamic–pituitary–gonadal axis (Seoane et al., 2018), and the metabolic phenotype observed in tau KO mice or mice injected by AAV2/5-synapsin-CRE-Tomato virus, the installation of a hypogonadism is possible in these animals compared to their controls. Therefore, to draw a definitive conclusion, it is necessary to dose plasma LH and testosterone from tau KI, tau KO male mice, and also animals injected by AAV2/5-synapsin-CRE-Tomato virus vectors in the mediobasal hypothalamus.

Strikingly, a recent study showed that the metabolic control by central insulin signaling is not limited to the hypothalamus, and the hippocampal deletion of IR/IGF1R in male mice was associated with the development of impaired glucose tolerance due to a systemic insulin resistance and a decrease in insulin secretion (Soto et al., 2019). Since tau play a role in central insulin signaling and particularly, tau KO mice exhibited hippocampal insulin resistance (Marciniak et al., 2017), it is important to evaluate the metabolic impact of a specific tau loss of function in the hippocampus by a conditional deletion or a down regulation strategies. This approach could help to uncover the hippocampal mechanisms implicated tau in the regulation of glucose hemostasis. To draw a definitive

conclusion, it's important to target the downregulation of the hippocampal tau protein by the intraparenchymal injection of an AAV combined with an shRNA tau.

4. Sexual dimorphism in the ability of tau to regulate glucose homeostasis:

Interestingly, an important observation of the metabolic phenotype evaluation of tau KI mice is the sexual dimorphism in the ability of tau to regulate glucose homeostasis, with male tau KI mice being significantly more impacted than female littermates. Until then, previous works investigating the metabolic outcomes of tau deletion were only performed in males (Marciniak et al., 2017; Wijesekara et al., 2021, 2018b). Sex is known to impact the response to metabolic stress and β-cell engagement. Like in humans, where women are less likely than men to develop type 2 diabetes (Kautzky-Willer et al., 2016), female mice are more resistant to HFD than males (Oliveira et al., 2015) and manifest improved glucose tolerance, with greater insulin sensitivity in liver, muscles and adipose tissue (Goren et al., 2004). Conversely, male rodents exhibit a greater propensity for β cell failure (Gannon, 2010). Increased estrogen receptor signaling, differences in islet DNA methylation status, expression differences of antioxidant genes and of islet-enriched genes transcription factors have all been suggested as causes for these differences allowing females to tolerate HFD better than males (Liu and Mauvais-Jarvis, 2010; Osipovich et al., 2020). In accordance, another important point that has not been addressed in GSIS experiments is the potential sexual-dimorphism of insulin secretion by isolated islets in response to glucose. Therefore, the sex-related differences we uncovered in tau KI mice could be likely due to the action of sex hormones but also estrus cycle issues that will need to be further investigated. These data also highlight that tau is dispensable into the mechanisms underlying the protective influence of female hormones in mice.

Additionally, the incidence of AD is higher in women than in men, and particularly AD appears in menopaused women. Also, after menopause, women exhibit a higher prevalence of the metabolic disorders (Gurka et al., 2016). However, we observed in tau KI mice a sexual dimorphism of tau loss of function in inducing glucose homeostasis disorders. This observation should not exclude the

screening of glucose homeostasis disorders in AD women. Probably, female tau KI mice were protected by estrogens. To draw a definitive conclusion concerning the impact of sexual dimorphism of tau loss of function on glucose homeostasis, it is necessary to do again the same experiments in females by comparing a group of ovariectomized adult females versus control mice. Ovariectomized females will developpe a hypogonadism, which will mime the menopause stat observed in women with a sporadic AD.

Conclusion and perspectives

In summary, despite some limitations of different approaches used, my project thesis highlights that tau loss of function favors the development of glucose homeostasis impairments and also pancreatic ß-cell dysfunction, supporting not only a role of central tau pathology in the development of metabolic disturbances in AD patients but also providing new insights on the physiological role of tau in the control of peripheral metabolism by acting in pancreatic ß-cell and the hypothalamus.

Regardless of whether pancreatic β cells or brain area are primarily involved in glucose metabolism impairments seen in AD and FTLD patients, considering that diabetes and impaired glucose tolerance are important risk factors for both (Golimstok et al., 2014; Livingston et al., 2017; Reitz et al., 2011), and that both exacerbate learning and memory defects and underlying pathology in different models reproducing the amyloid and tau lesions (Takeda et al., 2010; Wijesekara et al., 2021; Leboucher et al., 2013), glucose metabolism deficits promoted by both tau and amyloid lesions would then be part of a detrimental circle that would ultimately favor cognitive decline. Accordingly, our results are of great importance for clinical practice, such a mutual relationship between glucose homeostasis disturbance and AD, with probably common pathophysiological mechanisms, requires a change in public health policies by focusing more on primary prevention of common risk factors for diabetes and AD. General public awareness is needed about the risk of developing these two diseases, and the importance of correcting modifiable risk factors, such as healthier eating, weight loss, and increased physical activity. Furthermore, it is essential to perform a metabolic exploration including at least a glycated hemoglobin, fasted glycemia and insulinemia to investigate glucose homeostasis disorders, and pharmacologically managing it's, at an early pathological stage of AD or FTLD patients would be then of clinical interest in cross-consultations between neurology and endocrinology departments.

References

A

Adler, J., Parmryd, I., 2010. Quantifying colocalization by correlation: The Pearson correlation coefficient is superior to the Mander's overlap coefficient. Cytometry A 77A, 733–742. https://doi.org/10.1002/cyto.a.20896

Al-Lahham, R., Mukherjee, A., Soto, C., 2021. Tau deletion or loss of function promotes peripheral insulin resistance. Alzheimers Dement. 17. https://doi.org/10.1002/alz.055059

Almaça, J., Molina, J., Menegaz, D., Pronin, A.N., Tamayo, A., Slepak, V., Berggren, P.-O., Caicedo, A., 2016. Human Beta Cells Produce and Release Serotonin to Inhibit Glucagon Secretion from Alpha Cells. Cell Rep. 17, 3281–3291. https://doi.org/10.1016/j.celrep.2016.11.072

Alquezar, C., Arya, S., Kao, A.W., 2021. Tau Post-translational Modifications: Dynamic Transformers of Tau Function, Degradation, and Aggregation. Front. Neurol. 11, 595532. https://doi.org/10.3389/fneur.2020.595532

Amos, L.A., Schlieper, D., 2005. Microtubules and Maps, in: Advances in Protein Chemistry. Elsevier, pp. 257–298. https://doi.org/10.1016/S0065-3233(04)71007-4

Andreadis, A., 2005. Tau gene alternative splicing: expression patterns, regulation and modulation of function in normal brain and neurodegenerative diseases. Biochim. Biophys. Acta BBA - Mol. Basis Dis. 1739, 91–103. https://doi.org/10.1016/j.bbadis.2004.08.010

Andreadis, A., Brown, W.M., Kosik, K.S., 1992. Structure and novel exons of the human .tau. gene. Biochemistry 31, 10626–10633. https://doi.org/10.1021/bi00158a027

Andrew, S.F., Dinh, T.T., Ritter, S., 2007. Localized glucoprivation of hindbrain sites elicits corticosterone and glucagon secretion. Am. J. Physiol.-Regul. Integr. Comp. Physiol. 292, R1792–R1798. https://doi.org/10.1152/ajpregu.00777.2006

Ansari, N.A., Moinuddin, Ali, R., 2011. Glycated Lysine Residues: A Marker for Non-Enzymatic Protein Glycation in Age-Related Diseases. Dis. Markers 30, 317–324. https://doi.org/10.1155/2011/718694

Aoki, A., Fujitani, K., Takagi, K., Kimura, T., Nagase, H., Nakanishi, T., 2016. Male Hypogonadism Causes Obesity Associated with Impairment of Hepatic Gluconeogenesis in Mice. Biol. Pharm. Bull. 39, 587–592. https://doi.org/10.1248/bpb.b15-00942

Aponte, Y., Atasoy, D., Sternson, S.M., 2011. AGRP neurons are sufficient to orchestrate feeding behavior rapidly and without training. Nat. Neurosci. 14, 351–355. https://doi.org/10.1038/nn.2739

Arnold, C.S., Johnson, GailV.W., Cole, R.N., Dong, D.L.-Y., Lee, M., Hart, G.W., 1996. The Microtubule-associated Protein Tau Is Extensively Modified with O-linked N-acetylglucosamine. J. Biol. Chem. 271, 28741–28744. https://doi.org/10.1074/jbc.271.46.28741

Arriagada, P.V., Growdon, J.H., Hedley-Whyte, E.T., Hyman, B.T., 1992. Neurofibrillary tangles but not senile plaques parallel duration and severity of Alzheimer's disease. Neurology 42, 631–631. https://doi.org/10.1212/WNL.42.3.631

Ashford, M.L.J., Boden, P.R., Treherne, J.M., 1990. Glucose-induced excitation of hypothalamic neurones is mediated by ATP-sensitive K+ channels. Pfl□gers Arch. Eur. J. Physiol. 415, 479–483.

https://doi.org/10.1007/BF00373626
Atalayer, D., Robertson, K.L., Haskell-Luevano, C., Andreasen, A., Rowland, N.E., 2010. Food demand and meal size in mice with single or combined disruption of melanocortin type 3 and 4 receptors. Am. J. Physiol.-Regul. Integr. Comp. Physiol. 298, R1667–R1674. https://doi.org/10.1152/ajpregu.00562.2009
Atasoy, D., Betley, J.N., Su, H.H., Sternson, S.M., 2012. Deconstruction of a neural circuit for hunger. Nature 488, 172–177. https://doi.org/10.1038/nature11270

B

Bagnol, D., Lu, X.-Y., Kaelin, C.B., Day, H.E.W., Ollmann, M., Gantz, I., Akil, H., Barsh, G.S., Watson, S.J., 1999. Anatomy of an Endogenous Antagonist: Relationship between Agouti-Related Protein and Proopiomelanocortin in Brain. J. Neurosci. 19, RC26–RC26. https://doi.org/10.1523/JNEUROSCI.19-18-j0004.1999
Barbier, P., Zejneli, O., Martinho, M., Lasorsa, A., Belle, V., Smet-Nocca, C., Tsvetkov, P.O., Devred, F., Landrieu, I., 2019. Role of Tau as a Microtubule-Associated Protein: Structural and Functional Aspects. Front. Aging Neurosci. 11, 204. https://doi.org/10.3389/fnagi.2019.00204
Bear, M.H., Reddy, V., Bollu, P.C., 2022. Neuroanatomy, Hypothalamus, in: StatPearls. StatPearls Publishing, Treasure Island (FL).
Benderradji, H., Kraiem, S., Courty, E., Eddarkaoui, S., Bourouh, C., Faivre, E., Rolland, L., Caron, E., Besegher, M., Oger, F., Boschetti, T., Carvalho, K., Thiroux, B., Gauvrit, T., Nicolas, E., Gomez-Murcia, V., Bogdanova, A., Bongiovanni, A., Muhr-Tailleux, A., Lancel, S., Bantubungi, K., Sergeant, N., Annicotte, J.-S., Buée, L., Vieau, D., Blum, D., Buée-Scherrer, V., 2022. Impaired Glucose Homeostasis in a Tau Knock-In Mouse Model. Front. Mol. Neurosci. 15, 841892. https://doi.org/10.3389/fnmol.2022.841892
Berglund, E.D., Liu, T., Kong, X., Sohn, J.-W., Vong, L., Deng, Z., Lee, C.E., Lee, S., Williams, K.W., Olson, D.P., Scherer, P.E., Lowell, B.B., Elmquist, J.K., 2014. Melanocortin 4 receptors in autonomic neurons regulate thermogenesis and glycemia. Nat. Neurosci. 17, 911–913. https://doi.org/10.1038/nn.3737
Bhasin, S., Woodhouse, L., Casaburi, R., Singh, A.B., Bhasin, D., Berman, N., Chen, X., Yarasheski, K.E., Magliano, L., Dzekov, C., Dzekov, J., Bross, R., Phillips, J., Sinha-Hikim, I., Shen, R., Storer, T.W., 2001. Testosterone dose-response relationships in healthy young men. Am. J. Physiol.-Endocrinol. Metab. 281, E1172–E1181. https://doi.org/10.1152/ajpendo.2001.281.6.E1172
Bhasin, S., Woodhouse, L., Casaburi, R., Singh, A.B., Mac, R.P., Lee, M., Yarasheski, K.E., Sinha-Hikim, I., Dzekov, C., Dzekov, J., Magliano, L., Storer, T.W., 2005. Older Men Are as Responsive as Young Men to the Anabolic Effects of Graded Doses of Testosterone on the Skeletal Muscle. J. Clin. Endocrinol. Metab. 90, 678–688. https://doi.org/10.1210/jc.2004-1184
Bingham, N.C., Anderson, K.K., Reuter, A.L., Stallings, N.R., Parker, K.L., 2008. Selective Loss of Leptin Receptors in the Ventromedial Hypothalamic Nucleus Results in Increased Adiposity and a Metabolic Syndrome. Endocrinology 149, 2138–2148. https://doi.org/10.1210/en.2007-1200
Black, M.M., 2016. Axonal transport, in: Methods in Cell Biology. Elsevier, pp. 1–19. https://doi.org/10.1016/bs.mcb.2015.06.001
Bonora, E., Zavaroni, I., Coscelli, C., Butturini, U., 1983. Decreased hepatic insulin extraction in subjects with mild glucose intolerance. Metabolism 32, 438–446. https://doi.org/10.1016/0026-

0495(83)90004-5
Borg, M.A., Sherwin, R.S., Borg, W.P., Tamborlane, W.V., Shulman, G.I., 1997. Local ventromedial hypothalamus glucose perfusion blocks counterregulation during systemic hypoglycemia in awake rats. J. Clin. Invest. 99, 361–365. https://doi.org/10.1172/JCI119165
Borg, W.P., During, M.J., Sherwin, R.S., Borg, M.A., Brines, M.L., Shulman, G.I., 1994. Ventromedial hypothalamic lesions in rats suppress counterregulatory responses to hypoglycemia. J. Clin. Invest. 93, 1677–1682. https://doi.org/10.1172/JCI117150
Borg, W.P., Sherwin, R.S., During, M.J., Borg, M.A., Shulman, G.I., 1995. Local Ventromedial Hypothalamus Glucopenia Triggers Counterregulatory Hormone Release. Diabetes 44, 180–184. https://doi.org/10.2337/diab.44.2.180
Braak, H., Braak, E., 1991. Neuropathological stageing of Alzheimer-related changes. Acta Neuropathol. (Berl.) 82, 239–259. https://doi.org/10.1007/BF00308809
Braak, H., Thal, D.R., Ghebremedhin, E., Del Tredici, K., 2011. Stages of the Pathologic Process in Alzheimer Disease: Age Categories From 1 to 100 Years. J. Neuropathol. Exp. Neurol. 70, 960–969. https://doi.org/10.1097/NEN.0b013e318232a379
Breitling, J., Aebi, M., 2013. N-Linked Protein Glycosylation in the Endoplasmic Reticulum. Cold Spring Harb. Perspect. Biol. 5, a013359–a013359. https://doi.org/10.1101/cshperspect.a013359
Broadwell, R.D., Brightman, M.W., 1976. Entry of peroxidase into neurons of the central and peripheral nervous systems from extracerebral and cerebral blood. J. Comp. Neurol. 166, 257–283. https://doi.org/10.1002/cne.901660302
Brüning, J.C., Gautam, D., Burks, D.J., Gillette, J., Schubert, M., Orban, P.C., Klein, R., Krone, W., Müller-Wieland, D., Kahn, C.R., 2000. Role of Brain Insulin Receptor in Control of Body Weight and Reproduction. Science 289, 2122–2125. https://doi.org/10.1126/science.289.5487.2122
Bucht, G., Adolfsson, R., Lithner, F., Winblad, B., 1983. Changes in blood glucose and insulin secretion in patients with senile dementia of Alzheimer type. Acta Med. Scand. 213, 387–392. https://doi.org/10.1111/j.0954-6820.1983.tb03756.x
Burcelin, R., Dolci, W., Thorens, B., 2000a. Portal glucose infusion in the mouse induces hypoglycemia: evidence that the hepatoportal glucose sensor stimulates glucose utilization. Diabetes 49, 1635–1642. https://doi.org/10.2337/diabetes.49.10.1635
Burcelin, R., Dolci, W., Thorens, B., 2000b. Glucose sensing by the hepatoportal sensor is GLUT2-dependent: in vivo analysis in GLUT2-null mice. Diabetes 49, 1643–1648. https://doi.org/10.2337/diabetes.49.10.1643
Burcelin, R., Thorens, B., Glauser, M., Gaillard, R.C., Pralong, F.P., 2003. Gonadotropin-Releasing Hormone Secretion from Hypothalamic Neurons: Stimulation by Insulin and Potentiation by Leptin. Endocrinology 144, 4484–4491. https://doi.org/10.1210/en.2003-0457

C

Calsolaro, V., Edison, P., 2016. Alterations in Glucose Metabolism in Alzheimer's Disease. Recent Pat. Endocr. Metab. Immune Drug Discov. 10, 31–39. https://doi.org/10.2174/1872214810666160615102809
Carboneau, B.A., Le, T.D.V., Dunn, J.C., Gannon, M., 2016. Unexpected effects of the MIP-Cre ^{ER} transgene and tamoxifen on β -cell growth in C57Bl6/J male mice. Physiol. Rep. 4, e12863. https://doi.org/10.14814/phy2.12863

Carneiro, L., Allard, C., Guissard, C., Fioramonti, X., Tourrel-Cuzin, C., Bailbé, D., Barreau, C., Offer, G., Nédelec, E., Salin, B., Rigoulet, M., Belenguer, P., Pénicaud, L., Leloup, C., 2012. Importance of Mitochondrial Dynamin-Related Protein 1 in Hypothalamic Glucose Sensitivity in Rats. Antioxid. Redox Signal. 17, 433–444. https://doi.org/10.1089/ars.2011.4254
Chari, M., Yang, C.S., Lam, C.K.L., Lee, K., Mighiu, P., Kokorovic, A., Cheung, G.W.C., Lai, T.Y.Y., Wang, P.Y.T., Lam, T.K.T., 2011. Glucose Transporter-1 in the Hypothalamic Glial Cells Mediates Glucose Sensing to Regulate Glucose Production In Vivo. Diabetes 60, 1901–1906. https://doi.org/10.2337/db11-0120
Chasseigneaux, S., Allinquant, B., 2012. Functions of Aβ, sAPPα and sAPPβ : similarities and differences. J. Neurochem. 120, 99–108. https://doi.org/10.1111/j.1471-4159.2011.07584.x
Chaudhary, A.R., Berger, F., Berger, C.L., Hendricks, A.G., 2018. Tau directs intracellular trafficking by regulating the forces exerted by kinesin and dynein teams. Traffic 19, 111–121. https://doi.org/10.1111/tra.12537
Cheung, C.C., Kurrasch, D.M., Liang, J.K., Ingraham, H.A., 2013. Genetic labeling of steroidogenic factor-1 (SF-1) neurons in mice reveals ventromedial nucleus of the hypothalamus (VMH) circuitry beginning at neurogenesis and development of a separate non-SF-1 neuronal cluster in the ventrolateral VMH. J. Comp. Neurol. 521, 1268–1288. https://doi.org/10.1002/cne.23226
Choi, J.H., Kim, M.-S., 2022. Homeostatic Regulation of Glucose Metabolism by the Central Nervous System. Endocrinol. Metab. 37, 9–25. https://doi.org/10.3803/EnM.2021.1364
Choi, K., Kim, Y.-B., 2010. Molecular Mechanism of Insulin Resistance in Obesity and Type 2 Diabetes. Korean J. Intern. Med. 25, 119. https://doi.org/10.3904/kjim.2010.25.2.119
Chou, C.F., Omary, M.B., 1993. Mitotic arrest-associated enhancement of O-linked glycosylation and phosphorylation of human keratins 8 and 18. J. Biol. Chem. 268, 4465–4472.
Chou, C.F., Smith, A.J., Omary, M.B., 1992. Characterization and dynamics of O-linked glycosylation of human cytokeratin 8 and 18. J. Biol. Chem. 267, 3901–3906.
Clementi, A.H., Gaudy, A.M., Zimmers, T.A., Koniaris, L.G., Mooney, R.A., 2011. Deletion of interleukin-6 improves pyruvate tolerance without altering hepatic insulin signaling in the leptin receptor–deficient mouse. Metabolism 60, 1610–1619. https://doi.org/10.1016/j.metabol.2011.04.004
Cleveland, D.W., Hwo, S.-Y., Kirschner, M.W., 1977. Purification of tau, a microtubule-associated protein that induces assembly of microtubules from purified tubulin. J. Mol. Biol. 116, 207–225. https://doi.org/10.1016/0022-2836(77)90213-3
Cohen, T.J., Friedmann, D., Hwang, A.W., Marmorstein, R., Lee, V.M.Y., 2013. The microtubule-associated tau protein has intrinsic acetyltransferase activity. Nat. Struct. Mol. Biol. 20, 756–762. https://doi.org/10.1038/nsmb.2555
Combs, T.P., Berg, A.H., Rajala, M.W., Klebanov, S., Iyengar, P., Jimenez-Chillaron, J.C., Patti, M.E., Klein, S.L., Weinstein, R.S., Scherer, P.E., 2003. Sexual Differentiation, Pregnancy, Calorie Restriction, and Aging Affect the Adipocyte-Specific Secretory Protein Adiponectin. Diabetes 52, 268–276. https://doi.org/10.2337/diabetes.52.2.268
Comer, F., 1999. O-GlcNAc and the control of gene expression. Biochim. Biophys. Acta BBA - Gen. Subj. 1473, 161–171. https://doi.org/10.1016/S0304-4165(99)00176-2
Conde, C., Cáceres, A., 2009. Microtubule assembly, organization and dynamics in axons and dendrites. Nat. Rev. Neurosci. 10, 319–332. https://doi.org/10.1038/nrn2631
Considine, R.V., Sinha, M.K., Heiman, M.L., Kriauciunas, A., Stephens, T.W., Nyce, M.R., Ohannesian, J.P., Marco, C.C., McKee, L.J., Bauer, T.L., Caro, J.F., 1996. Serum Immunoreactive-Leptin Concentrations in Normal-Weight and Obese Humans. N. Engl. J. Med. 334, 292–295.

https://doi.org/10.1056/NEJM199602013340503
Cook, C., Carlomagno, Y., Gendron, T.F., Dunmore, J., Scheffel, K., Stetler, C., Davis, M., Dickson, D., Jarpe, M., DeTure, M., Petrucelli, L., 2014. Acetylation of the KXGS motifs in tau is a critical determinant in modulation of tau aggregation and clearance. Hum. Mol. Genet. 23, 104–116. https://doi.org/10.1093/hmg/ddt402
Coppari, R., Ichinose, M., Lee, C.E., Pullen, A.E., Kenny, C.D., McGovern, R.A., Tang, V., Liu, S.M., Ludwig, T., Chua, S.C., Lowell, B.B., Elmquist, J.K., 2005. The hypothalamic arcuate nucleus: A key site for mediating leptin's effects on glucose homeostasis and locomotor activity. Cell Metab. 1, 63–72. https://doi.org/10.1016/j.cmet.2004.12.004
Cowley, M.A., Smart, J.L., Rubinstein, M., Cerdán, M.G., Diano, S., Horvath, T.L., Cone, R.D., Low, M.J., 2001. Leptin activates anorexigenic POMC neurons through a neural network in the arcuate nucleus. Nature 411, 480–484. https://doi.org/10.1038/35078085
Craft, S., Peskind, E., Schwartz, M.W., Schellenberg, G.D., Raskind, M., Porte, D., 1998. Cerebrospinal fluid and plasma insulin levels in Alzheimer's disease: relationship to severity of dementia and apolipoprotein E genotype. Neurology 50, 164–168. https://doi.org/10.1212/wnl.50.1.164
Craft, S., Zallen, G., Baker, L.D., 1992. Glucose and memory in mild senile dementia of the Alzheimer type. J. Clin. Exp. Neuropsychol. 14, 253–267. https://doi.org/10.1080/01688639208402827
Crane, P.K., Walker, R., Hubbard, R.A., Li, G., Nathan, D.M., Zheng, H., Haneuse, S., Craft, S., Montine, T.J., Kahn, S.E., McCormick, W., McCurry, S.M., Bowen, J.D., Larson, E.B., 2013. Glucose Levels and Risk of Dementia. N. Engl. J. Med. 369, 540–548. https://doi.org/10.1056/NEJMoa1215740

D

da Silva, A.A., Hall, J.E., do Carmo, J.M., 2017. Leptin reverses hyperglycemia and hyperphagia in insulin deficient diabetic rats by pituitary-independent central nervous system actions. PLOS ONE 12, e0184805. https://doi.org/10.1371/journal.pone.0184805
Dallaporta, M., Himmi, T., Perrin, J., Orsini, J.-C., 1999. Solitary tract nucleus sensitivity to moderate changes in glucose level: NeuroReport 10, 2657–2660. https://doi.org/10.1097/00001756-199908200-00040
Davis, A.M., Seney, M.L., Stallings, N.R., Zhao, L., Parker, K.L., Tobet, S.A., 2004. Loss of steroidogenic factor 1 alters cellular topography in the mouse ventromedial nucleus of the hypothalamus. J. Neurobiol. 60, 424–436. https://doi.org/10.1002/neu.20030
de Backer, M.W., Fitzsimons, C.P., Brans, M.A., Luijendijk, M.C., Garner, K.M., Vreugdenhil, E., Adan, R.A., 2010. An adeno-associated viral vector transduces the rat hypothalamus and amygdala more efficient than a lentiviral vector. BMC Neurosci. 11, 81. https://doi.org/10.1186/1471-2202-11-81
DeFronzo, R.A., Ferrannini, E., Groop, L., Henry, R.R., Herman, W.H., Holst, J.J., Hu, F.B., Kahn, C.R., Raz, I., Shulman, G.I., Simonson, D.C., Testa, M.A., Weiss, R., 2015. Type 2 diabetes mellitus. Nat. Rev. Dis. Primer 1, 15019. https://doi.org/10.1038/nrdp.2015.19
Delacourte, A., David, J.P., Sergeant, N., Buee, L., Wattez, A., Vermersch, P., Ghozali, F., Fallet-

Bianco, C., Pasquier, F., Lebert, F., Petit, H., Di Menza, C., 1999. The biochemical pathway of neurofibrillary degeneration in aging and Alzheimer's disease. Neurology 52, 1158–1158. https://doi.org/10.1212/WNL.52.6.1158
Delaere, F., Duchampt, A., Mounien, L., Seyer, P., Duraffourd, C., Zitoun, C., Thorens, B., Mithieux, G., 2013. The role of sodium-coupled glucose co-transporter 3 in the satiety effect of portal glucose sensing. Mol. Metab. 2, 47–53. https://doi.org/10.1016/j.molmet.2012.11.003
Delaere, F., Magnan, C., Mithieux, G., 2010. Hypothalamic integration of portal glucose signals and control of food intake and insulin sensitivity. Diabetes Metab. 36, 257–262. https://doi.org/10.1016/j.diabet.2010.05.001
Delobel, P., Flament, S., Hamdane, M., Jakes, R., Rousseau, A., Delacourte, A., Vilain, J.-P., Goedert, M., Buée, L., 2002. Functional Characterization of FTDP-17 tau Gene Mutations through Their Effects on Xenopus Oocyte Maturation. J. Biol. Chem. 277, 9199–9205. https://doi.org/10.1074/jbc.M107716200
DeTure, M.A., Dickson, D.W., 2019. The neuropathological diagnosis of Alzheimer's disease. Mol. Neurodegener. 14, 32. https://doi.org/10.1186/s13024-019-0333-5
Ding, M., Vandré, D.D., 1996. High Molecular Weight Microtubule-associated Proteins Contain O-Linked N-Acetylglucosamine. J. Biol. Chem. 271, 12555–12561. https://doi.org/10.1074/jbc.271.21.12555
Dixit, R., Ross, J.L., Goldman, Y.E., Holzbaur, E.L.F., 2008. Differential Regulation of Dynein and Kinesin Motor Proteins by Tau. Science 319, 1086–1089. https://doi.org/10.1126/science.1152993
Dong, D.L.-Y., Xu, Z.-S., Hart, G.W., Cleveland, D.W., 1996. Cytoplasmic O-GlcNAc Modification of the Head Domain and the KSP Repeat Motif of the Neurofilament Protein Neurofilament-H. J. Biol. Chem. 271, 20845–20852. https://doi.org/10.1074/jbc.271.34.20845
Donovan, C.M., Hamilton-Wessler, M., Halter, J.B., Bergman, R.N., 1994. Primacy of liver glucosensors in the sympathetic response to progressive hypoglycemia. Proc. Natl. Acad. Sci. 91, 2863–2867. https://doi.org/10.1073/pnas.91.7.2863
Drechsel, D.N., Hyman, A.A., Cobb, M.H., Kirschner, M.W., 1992. Modulation of the dynamic instability of tubulin assembly by the microtubule-associated protein tau. Mol. Biol. Cell 3, 1141–1154. https://doi.org/10.1091/mbc.3.10.1141
Drubin, D.G., Feinstein, S.C., Shooter, E.M., Kirschner, M.W., 1985. Nerve growth factor-induced neurite outgrowth in PC12 cells involves the coordinate induction of microtubule assembly and assembly-promoting factors. J. Cell Biol. 101, 1799–1807. https://doi.org/10.1083/jcb.101.5.1799
Drubin, D.G., Kirschner, M.W., 1986. Tau protein function in living cells. J. Cell Biol. 103, 2739–2746. https://doi.org/10.1083/jcb.103.6.2739
Dubois, V., Laurent, M.R., Jardi, F., Antonio, L., Lemaire, K., Goyvaerts, L., Deldicque, L., Carmeliet, G., Decallonne, B., Vanderschueren, D., Claessens, F., 2016. Androgen Deficiency Exacerbates High-Fat Diet-Induced Metabolic Alterations in Male Mice. Endocrinology 157, 648–665. https://doi.org/10.1210/en.2015-1713
Dunn-Meynell, A.A., Rawson, N.E., Levin, B.E., 1998. Distribution and phenotype of neurons containing the ATP-sensitive K+ channel in rat brain. Brain Res. 814, 41–54. https://doi.org/10.1016/S0006-8993(98)00956-1
Duyckaerts, C., Uchihara, T., Seilhean, D., He, Y., Hauw, J.-J., 1997. Dissociation of Alzheimer type pathology in a disconnected piece of cortex. Acta Neuropathol. (Berl.) 93, 501–507. https://doi.org/10.1007/s004010050645

E

Edwards, C.M.B., Abbott, C.R., Sunter, D., Kim, M.-S., Dakin, C.L., Murphy, K.G., Abusnana, S., Taheri, S., Rossi, M., Bloom, S.R., 2000. Cocaine- and amphetamine-regulated transcript, glucagon-like peptide-1 and corticotrophin releasing factor inhibit feeding via agouti-related protein independent pathways in the rat. Brain Res. 866, 128–134. https://doi.org/10.1016/S0006-8993(00)02257-5

Elmquist, J.K., Elias, C.F., Saper, C.B., 1999. From Lesions to Leptin. Neuron 22, 221–232. https://doi.org/10.1016/S0896-6273(00)81084-3

Emoto, M., Langille, S.E., Czech, M.P., 2001. A Role for Kinesin in Insulin-stimulated GLUT4 Glucose Transporter Translocation in 3T3-L1 Adipocytes. J. Biol. Chem. 276, 10677–10682. https://doi.org/10.1074/jbc.M010785200

Ernst, A., Sharma, A.N., Elased, K.M., Guest, P.C., Rahmoune, H., Bahn, S., 2013. Diabetic db/db mice exhibit central nervous system and peripheral molecular alterations as seen in neurological disorders. Transl. Psychiatry 3, e263–e263. https://doi.org/10.1038/tp.2013.42

F

Fourriere, L., Jimenez, A.J., Perez, F., Boncompain, G., 2020. The role of microtubules in secretory protein transport. J. Cell Sci. 133, jcs237016. https://doi.org/10.1242/jcs.237016

Freire-Regatillo, A., Argente-Arizón, P., Argente, J., García-Segura, L.M., Chowen, J.A., 2017. Non-Neuronal Cells in the Hypothalamic Adaptation to Metabolic Signals. Front. Endocrinol. 8. https://doi.org/10.3389/fendo.2017.00051

Fujisawa, Y., Sasaki, K., Akiyama, K., 1991. Increased insulin levels after OGTT load in peripheral blood and cerebrospinal fluid of patients with dementia of Alzheimer type. Biol. Psychiatry 30, 1219–1228. https://doi.org/10.1016/0006-3223(91)90158-i

Fujita, S., Bohland, M., Sanchez-Watts, G., Watts, A.G., Donovan, C.M., 2007. Hypoglycemic detection at the portal vein is mediated by capsaicin-sensitive primary sensory neurons. Am. J. Physiol.-Endocrinol. Metab. 293, E96–E101. https://doi.org/10.1152/ajpendo.00415.2006

G

Galas, M.-C., Bonnefoy, E., Buee, L., Lefebvre, B., 2019. Emerging Connections Between Tau and Nucleic Acids, in: Takashima, A., Wolozin, B., Buee, L. (Eds.), Tau Biology, Advances in Experimental Medicine and Biology. Springer Singapore, Singapore, pp. 135–143. https://doi.org/10.1007/978-981-32-9358-8_12

Gallou-Kabani, C., Vigé, A., Gross, M.-S., Rabès, J.-P., Boileau, C., Larue-Achagiotis, C., Tomé, D., Jais, J.-P., Junien, C., 2007. C57BL/6J and A/J Mice Fed a High-Fat Diet Delineate Components of Metabolic Syndrome*. Obesity 15, 1996–2005. https://doi.org/10.1038/oby.2007.238

Gannon, M., 2010. High Fat Diet Regulation of β-Cell Proliferation and β-Cell Mass. Open Endocrinol. J. 4, 66–77. https://doi.org/10.2174/1874216501004010066
Gao, L., Ortega-SÃ¡enz, P., GarcÃ-a-FernÃ¡ndez, M., GonzÃ¡lez-RodrÃ-guez, P., Caballero-Eraso, C., LÃ³pez-Barneo, J., 2014. Glucose sensing by carotid body glomus cells: potential implications in disease. Front. Physiol. 5. https://doi.org/10.3389/fphys.2014.00398
Georgescu, T., Lyons, D., Doslikova, B., Garcia, A.P., Marston, O., Burke, L.K., Chianese, R., Lam, B.Y.H., Yeo, G.S.H., Rochford, J.J., Garfield, A.S., Heisler, L.K., 2020. Neurochemical Characterization of Brainstem Pro-Opiomelanocortin Cells. Endocrinology 161, bqaa032. https://doi.org/10.1210/endocr/bqaa032
Georgieff, I.S., Liem, R.K., Couchie, D., Mavilia, C., Nunez, J., Shelanski, M.L., 1993. Expression of high molecular weight tau in the central and peripheral nervous systems. J. Cell Sci. 105, 729–737. https://doi.org/10.1242/jcs.105.3.729
Goedert, M., Spillantini, M.G., Jakes, R., Rutherford, D., Crowther, R.A., 1989. Multiple isoforms of human microtubule-associated protein tau: sequences and localization in neurofibrillary tangles of Alzheimer's disease. Neuron 3, 519–526. https://doi.org/10.1016/0896-6273(89)90210-9
Golimstok, A., Cámpora, N., Rojas, J.I., Fernandez, M.C., Elizondo, C., Soriano, E., Cristiano, E., 2014. Cardiovascular risk factors and frontotemporal dementia: a case–control study. Transl. Neurodegener. 3, 13. https://doi.org/10.1186/2047-9158-3-13
Goode, B.L., Denis, P.E., Panda, D., Radeke, M.J., Miller, H.P., Wilson, L., Feinstein, S.C., 1997. Functional interactions between the proline-rich and repeat regions of tau enhance microtubule binding and assembly. Mol. Biol. Cell 8, 353–365. https://doi.org/10.1091/mbc.8.2.353
Goren, H.J., Kulkarni, R.N., Kahn, C.R., 2004. Glucose Homeostasis and Tissue Transcript Content of Insulin Signaling Intermediates in Four Inbred Strains of Mice: C57BL/6, C57BLKS/6, DBA/2, and 129X1. Endocrinology 145, 3307–3323. https://doi.org/10.1210/en.2003-1400
Graham, D.L., Gray, A.J., Joyce, J.A., Yu, D., O'Moore, J., Carlson, G.A., Shearman, M.S., Dellovade, T.L., Hering, H., 2014. Increased O-GlcNAcylation reduces pathological tau without affecting its normal phosphorylation in a mouse model of tauopathy. Neuropharmacology 79, 307–313. https://doi.org/10.1016/j.neuropharm.2013.11.025
Graham, W.V., Bonito-Oliva, A., Sakmar, T.P., 2017. Update on Alzheimer's Disease Therapy and Prevention Strategies. Annu. Rev. Med. 68, 413–430. https://doi.org/10.1146/annurev-med-042915-103753
Gratuze, M., Joly-Amado, A., Vieau, D., Buée, L., Blum, D., 2018. Mutual Relationship between Tau and Central Insulin Signalling: Consequences for AD and Tauopathies? Neuroendocrinology 107, 181–195. https://doi.org/10.1159/000487641
Grill, H.J., Hayes, M.R., 2012. Hindbrain Neurons as an Essential Hub in the Neuroanatomically Distributed Control of Energy Balance. Cell Metab. 16, 296–309. https://doi.org/10.1016/j.cmet.2012.06.015
Gromada, J., Franklin, I., Wollheim, C.B., 2007. α-Cells of the Endocrine Pancreas: 35 Years of Research but the Enigma Remains. Endocr. Rev. 28, 84–116. https://doi.org/10.1210/er.2006-0007
Gu, Y., Oyama, F., Ihara, Y., 1996. Tau is widely expressed in rat tissues. J. Neurochem. 67, 1235–1244. https://doi.org/10.1046/j.1471-4159.1996.67031235.x
Guillozet-Bongaarts, A.L., Cahill, M.E., Cryns, V.L., Reynolds, M.R., Berry, R.W., Binder, L.I., 2006. Pseudophosphorylation of tau at serine 422 inhibits caspase cleavage: in vitro evidence and implications for tangle formation in vivo. J. Neurochem. 97, 1005–1014. https://doi.org/10.1111/j.1471-4159.2006.03784.x
Gurka, M.J., Vishnu, A., Santen, R.J., DeBoer, M.D., 2016. Progression of Metabolic Syndrome

Severity During the Menopausal Transition. J. Am. Heart Assoc. 5, e003609. https://doi.org/10.1161/JAHA.116.003609

H

Han, I., Kudlow, J.E., 1997. Reduced O glycosylation of Sp1 is associated with increased proteasome susceptibility. Mol. Cell. Biol. 17, 2550–2558. https://doi.org/10.1128/MCB.17.5.2550

Hanover, J.A., 2001. Glycan-dependent signaling: O-linked N-acetylglucosamine. FASEB J. 15, 1865–1876. https://doi.org/10.1096/fj.01-0094rev

Hanover, J.A., Cohen, C.K., Willingham, M.C., Park, M.K., 1987. O-linked N-acetylglucosamine is attached to proteins of the nuclear pore. Evidence for cytoplasmic and nucleoplasmic glycoproteins. J. Biol. Chem. 262, 9887–9894.

Hashimoto, S., Matsuba, Y., Kamano, N., Mihira, N., Sahara, N., Takano, J., Muramatsu, S., Saido, T.C., Saito, T., 2019. Tau binding protein CAPON induces tau aggregation and neurodegeneration. Nat. Commun. 10, 2394. https://doi.org/10.1038/s41467-019-10278-x

Hatsell, S., Medina, L., Merola, J., Haltiwanger, R., Cowin, P., 2003. Plakoglobin Is O-Glycosylated Close to the N-terminal Destruction Box. J. Biol. Chem. 278, 37745–37752. https://doi.org/10.1074/jbc.M301346200

Herrera, A.C., Prince, M., Knapp, M., Karagiannidou, M., Maelenn Guerchet, 2016. World Alzheimer Report 2016: Improving healthcare for people with dementia. Coverage, quality and costs now and in the future. https://doi.org/10.13140/RG.2.2.22580.04483

Hill, J.W., Elias, C.F., Fukuda, M., Williams, K.W., Berglund, E.D., Holland, W.L., Cho, Y.-R., Chuang, J.-C., Xu, Y., Choi, M., Lauzon, D., Lee, C.E., Coppari, R., Richardson, J.A., Zigman, J.M., Chua, S., Scherer, P.E., Lowell, B.B., Brüning, J.C., Elmquist, J.K., 2010. Direct Insulin and Leptin Action on Pro-opiomelanocortin Neurons Is Required for Normal Glucose Homeostasis and Fertility. Cell Metab. 11, 286–297. https://doi.org/10.1016/j.cmet.2010.03.002

Hiltunen, M., Khandelwal, V.K.M., Yaluri, N., Tiilikainen, T., Tusa, M., Koivisto, H., Krzisch, M., Vepsäläinen, S., Mäkinen, P., Kemppainen, S., Miettinen, P., Haapasalo, A., Soininen, H., Laakso, M., Tanila, H., 2012. Contribution of genetic and dietary insulin resistance to Alzheimer phenotype in APP/PS1 transgenic mice. J. Cell. Mol. Med. 16, 1206–1222. https://doi.org/10.1111/j.1582-4934.2011.01384.x

Hinrichs, M.H., Jalal, A., Brenner, B., Mandelkow, E., Kumar, S., Scholz, T., 2012. Tau Protein Diffuses along the Microtubule Lattice. J. Biol. Chem. 287, 38559–38568. https://doi.org/10.1074/jbc.M112.369785

Ho, K.-H., Yang, X., Osipovich, A.B., Cabrera, O., Hayashi, M.L., Magnuson, M.A., Gu, G., Kaverina, I., 2020. Glucose Regulates Microtubule Disassembly and the Dose of Insulin Secretion via Tau Phosphorylation. Diabetes 69, 1936–1947. https://doi.org/10.2337/db19-1186

Ho, L., Qin, W., Pompl, P.N., Xiang, Z., Wang, J., Zhao, Z., Peng, Y., Cambareri, G., Rocher, A., Mobbs, C.V., Hof, P.R., Pasinetti, G.M., 2004. Diet-induced insulin resistance promotes amyloidosis in a transgenic mouse model of Alzheimer's disease. FASEB J. 18, 902–904. https://doi.org/10.1096/fj.03-0978fje

Holman, G.D., 2020. Structure, function and regulation of mammalian glucose transporters of the SLC2 family. Pflüg. Arch. - Eur. J. Physiol. 472, 1155–1175. https://doi.org/10.1007/s00424-020-02411-3

Holt, G.D., Snow, C.M., Senior, A., Haltiwanger, R.S., Gerace, L., Hart, G.W., 1987. Nuclear pore complex glycoproteins contain cytoplasmically disposed O-linked N-acetylglucosamine. J. Cell Biol. 104, 1157–1164. https://doi.org/10.1083/jcb.104.5.1157
Hooper, C., Killick, R., Lovestone, S., 2008. The GSK3 hypothesis of Alzheimer's disease: GSK3 and Alzheimer's disease. J. Neurochem. 104, 1433–1439. https://doi.org/10.1111/j.1471-4159.2007.05194.x
Hoover, B.R., Reed, M.N., Su, J., Penrod, R.D., Kotilinek, L.A., Grant, M.K., Pitstick, R., Carlson, G.A., Lanier, L.M., Yuan, L.-L., Ashe, K.H., Liao, D., 2010. Tau Mislocalization to Dendritic Spines Mediates Synaptic Dysfunction Independently of Neurodegeneration. Neuron 68, 1067–1081. https://doi.org/10.1016/j.neuron.2010.11.030
Hou, J.C., Min, L., Pessin, J.E., 2009. Chapter 16 Insulin Granule Biogenesis, Trafficking and Exocytosis, in: Vitamins & Hormones. Elsevier, pp. 473–506. https://doi.org/10.1016/S0083-6729(08)00616-X
Huang, J., Imamura, T., Olefsky, J.M., 2001. Insulin can regulate GLUT4 internalization by signaling to Rab5 and the motor protein dynein. Proc. Natl. Acad. Sci. 98, 13084–13089. https://doi.org/10.1073/pnas.241368698
Huang, X., Liu, G., Guo, J., Su, Z., 2018. The PI3K/AKT pathway in obesity and type 2 diabetes. Int. J. Biol. Sci. 14, 1483–1496. https://doi.org/10.7150/ijbs.27173
Hull, C., Dekeryte, R., Koss, D.J., Crouch, B., Buchanan, H., Delibegovic, M., Platt, B., 2020. Knock-in of Mutated hTAU Causes Insulin Resistance, Inflammation and Proteostasis Disturbance in a Mouse Model of Frontotemporal Dementia. Mol. Neurobiol. 57, 539–550. https://doi.org/10.1007/s12035-019-01722-6
Humphrey, S.J., James, D.E., Mann, M., 2015. Protein Phosphorylation: A Major Switch Mechanism for Metabolic Regulation. Trends Endocrinol. Metab. 26, 676–687. https://doi.org/10.1016/j.tem.2015.09.013
Huszar, D., Lynch, C.A., Fairchild-Huntress, V., Dunmore, J.H., Fang, Q., Berkemeier, L.R., Gu, W., Kesterson, R.A., Boston, B.A., Cone, R.D., Smith, F.J., Campfield, L.A., Burn, P., Lee, F., 1997. Targeted Disruption of the Melanocortin-4 Receptor Results in Obesity in Mice. Cell 88, 131–141. https://doi.org/10.1016/S0092-8674(00)81865-6

I

Ishihara, H., Maechler, P., Gjinovci, A., Herrera, P.-L., Wollheim, C.B., 2003. Islet β-cell secretion determines glucagon release from neighbouring α-cells. Nat. Cell Biol. 5, 330–335. https://doi.org/10.1038/ncb951
Ishii, M., Iadecola, C., 2015. Metabolic and Non-Cognitive Manifestations of Alzheimer's Disease: The Hypothalamus as Both Culprit and Target of Pathology. Cell Metab. 22, 761–776. https://doi.org/10.1016/j.cmet.2015.08.016
Ittner, L.M., Ke, Y.D., Götz, J., 2009. Phosphorylated Tau Interacts with c-Jun N-terminal Kinase-interacting Protein 1 (JIP1) in Alzheimer Disease. J. Biol. Chem. 284, 20909–20916. https://doi.org/10.1074/jbc.M109.014472

J

Janson, J., Laedtke, T., Parisi, J.E., O'Brien, P., Petersen, R.C., Butler, P.C., 2004. Increased Risk of Type 2 Diabetes in Alzheimer Disease. Diabetes 53, 474–481. https://doi.org/10.2337/diabetes.53.2.474

Jiang, H., Pierce, G.F., Ozelo, M.C., de Paula, E.V., Vargas, J.A., Smith, P., Sommer, J., Luk, A., Manno, C.S., High, K.A., Arruda, V.R., 2006. Evidence of Multiyear Factor IX Expression by AAV-Mediated Gene Transfer to Skeletal Muscle in an Individual with Severe Hemophilia B. Mol. Ther. 14, 452–455. https://doi.org/10.1016/j.ymthe.2006.05.004

Jiménez-Palomares, M., Ramos-Rodríguez, J.J., López-Acosta, J.F., Pacheco-Herrero, M., Lechuga-Sancho, A.M., Perdomo, G., García-Alloza, M., Cózar-Castellano, I., 2012. Increased Aβ production prompts the onset of glucose intolerance and insulin resistance. Am. J. Physiol.-Endocrinol. Metab. 302, E1373–E1380. https://doi.org/10.1152/ajpendo.00500.2011

K

Kahn, S.E., 2003. The relative contributions of insulin resistance and beta-cell dysfunction to the pathophysiology of Type 2 diabetes. Diabetologia 46, 3–19. https://doi.org/10.1007/s00125-002-1009-0

Kanaan, N.M., Morfini, G.A., LaPointe, N.E., Pigino, G.F., Patterson, K.R., Song, Y., Andreadis, A., Fu, Y., Brady, S.T., Binder, L.I., 2011. Pathogenic Forms of Tau Inhibit Kinesin-Dependent Axonal Transport through a Mechanism Involving Activation of Axonal Phosphotransferases. J. Neurosci. 31, 9858–9868. https://doi.org/10.1523/JNEUROSCI.0560-11.2011

Kanaan, N.M., Pigino, G.F., Brady, S.T., Lazarov, O., Binder, L.I., Morfini, G.A., 2013. Axonal degeneration in Alzheimer's disease: When signaling abnormalities meet the axonal transport system. Exp. Neurol. 246, 44–53. https://doi.org/10.1016/j.expneurol.2012.06.003

Kanai, Y., Takemura, R., Oshima, T., Mori, H., Ihara, Y., Yanagisawa, M., Masaki, T., Hirokawa, N., 1989. Expression of multiple tau isoforms and microtubule bundle formation in fibroblasts transfected with a single tau cDNA. J. Cell Biol. 109, 1173–1184. https://doi.org/10.1083/jcb.109.3.1173

Kang, L., Routh, V.H., Kuzhikandathil, E.V., Gaspers, L.D., Levin, B.E., 2004. Physiological and Molecular Characteristics of Rat Hypothalamic Ventromedial Nucleus Glucosensing Neurons. Diabetes 53, 549–559. https://doi.org/10.2337/diabetes.53.3.549

Kautzky-Willer, A., Harreiter, J., Pacini, G., 2016. Sex and Gender Differences in Risk, Pathophysiology and Complications of Type 2 Diabetes Mellitus. Endocr. Rev. 37, 278–316. https://doi.org/10.1210/er.2015-1137

Khachaturian, Z.S., 1985. Diagnosis of Alzheimer's Disease. Arch. Neurol. 42, 1097–1105. https://doi.org/10.1001/archneur.1985.04060100083029

Kim, K.W., Zhao, L., Donato, J., Kohno, D., Xu, Y., Elias, C.F., Lee, C., Parker, K.L., Elmquist, J.K., 2011. Steroidogenic factor 1 directs programs regulating diet-induced thermogenesis and leptin action in the ventral medial hypothalamic nucleus. Proc. Natl. Acad. Sci. 108, 10673–10678.

https://doi.org/10.1073/pnas.1102364108
Kim, S.P., Ellmerer, M., Kirkman, E.L., Bergman, R.N., 2007. β-Cell "rest" accompanies reduced first-pass hepatic insulin extraction in the insulin-resistant, fat-fed canine model. Am. J. Physiol.-Endocrinol. Metab. 292, E1581–E1589. https://doi.org/10.1152/ajpendo.00351.2006
Kim, W.J., Lee, S.J., Lee, E., Lee, E.Y., Han, K., 2022. Risk of Incident Dementia According to Glycemic Status and Comorbidities of Hyperglycemia: A Nationwide Population-Based Cohort Study. Diabetes Care 45, 134–141. https://doi.org/10.2337/dc21-0957
Kimura, K., Tanida, M., Nagata, N., Inaba, Y., Watanabe, H., Nagashimada, M., Ota, T., Asahara, S., Kido, Y., Matsumoto, M., Toshinai, K., Nakazato, M., Shibamoto, T., Kaneko, S., Kasuga, M., Inoue, H., 2016. Central Insulin Action Activates Kupffer Cells by Suppressing Hepatic Vagal Activation via the Nicotinic Alpha 7 Acetylcholine Receptor. Cell Rep. 14, 2362–2374. https://doi.org/10.1016/j.celrep.2016.02.032
Kleinridders, A., Ferris, H.A., Cai, W., Kahn, C.R., 2014. Insulin Action in Brain Regulates Systemic Metabolism and Brain Function. Diabetes 63, 2232–2243. https://doi.org/10.2337/db14-0568
Ko, L., Ko, E.C., Nacharaju, P., Liu, W.-K., Chang, E., Kenessey, A., Yen, S.-H.C., 1999. An immunochemical study on tau glycation in paired helical filaments. Brain Res. 830, 301–313. https://doi.org/10.1016/S0006-8993(99)01415-8
Kohjima, M., Sun, Y., Chan, L., 2010. Increased Food Intake Leads to Obesity and Insulin Resistance in the Tg2576 Alzheimer's Disease Mouse Model. Endocrinology 151, 1532–1540. https://doi.org/10.1210/en.2009-1196
Kolarova, M., García-Sierra, F., Bartos, A., Ricny, J., Ripova, D., 2012. Structure and Pathology of Tau Protein in Alzheimer Disease. Int. J. Alzheimers Dis. 2012, 1–13. https://doi.org/10.1155/2012/731526
Könner, A.C., Janoschek, R., Plum, L., Jordan, S.D., Rother, E., Ma, X., Xu, C., Enriori, P., Hampel, B., Barsh, G.S., Kahn, C.R., Cowley, M.A., Ashcroft, F.M., Brüning, J.C., 2007. Insulin Action in AgRP-Expressing Neurons Is Required for Suppression of Hepatic Glucose Production. Cell Metab. 5, 438–449. https://doi.org/10.1016/j.cmet.2007.05.004
Kotin, R.M., Siniscalco, M., Samulski, R.J., Zhu, X.D., Hunter, L., Laughlin, C.A., McLaughlin, S., Muzyczka, N., Rocchi, M., Berns, K.I., 1990. Site-specific integration by adeno-associated virus. Proc. Natl. Acad. Sci. 87, 2211–2215. https://doi.org/10.1073/pnas.87.6.2211
Koyama, Y., Coker, R.H., Stone, E.E., Lacy, D.B., Jabbour, K., Williams, P.E., Wasserman, D.H., 2000. Evidence that carotid bodies play an important role in glucoregulation in vivo. Diabetes 49, 1434–1442. https://doi.org/10.2337/diabetes.49.9.1434
Krashes, M.J., Koda, S., Ye, C., Rogan, S.C., Adams, A.C., Cusher, D.S., Maratos-Flier, E., Roth, B.L., Lowell, B.B., 2011. Rapid, reversible activation of AgRP neurons drives feeding behavior in mice. J. Clin. Invest. 121, 1424–1428. https://doi.org/10.1172/JCI46229
Krashes, M.J., Shah, B.P., Koda, S., Lowell, B.B., 2013. Rapid versus Delayed Stimulation of Feeding by the Endogenously Released AgRP Neuron Mediators GABA, NPY, and AgRP. Cell Metab. 18, 588–595. https://doi.org/10.1016/j.cmet.2013.09.009
Krebs, E.G., Fischer, E.H., 1955. Phosphorylase activity of skeletal muscle extracts. J. Biol. Chem. 216, 113–120.
Kuhla, B., Haase, C., Flach, K., Lüth, H.-J., Arendt, T., Münch, G., 2007. Effect of pseudophosphorylation and cross-linking by lipid peroxidation and advanced glycation end product precursors on tau aggregation and filament formation. J. Biol. Chem. 282, 6984–6991. https://doi.org/10.1074/jbc.M609521200

L

LaFerla, F.M., Green, K.N., Oddo, S., 2007. Intracellular amyloid-β in Alzheimer's disease. Nat. Rev. Neurosci. 8, 499–509. https://doi.org/10.1038/nrn2168

Leboucher, A., Ahmed, T., Caron, E., Tailleux, A., Raison, S., Joly-Amado, A., Marciniak, E., Carvalho, K., Hamdane, M., Bantubungi, K., Lancel, S., Eddarkaoui, S., Caillierez, R., Vallez, E., Staels, B., Vieau, D., Balschun, D., Buee, L., Blum, D., 2019. Brain insulin response and peripheral metabolic changes in a Tau transgenic mouse model. Neurobiol. Dis. 125, 14–22. https://doi.org/10.1016/j.nbd.2019.01.008

Leboucher, A., Laurent, C., Fernandez-Gomez, F.-J., Burnouf, S., Troquier, L., Eddarkaoui, S., Demeyer, D., Caillierez, R., Zommer, N., Vallez, E., Bantubungi, K., Breton, C., Pigny, P., Buée-Scherrer, V., Staels, B., Hamdane, M., Tailleux, A., Buée, L., Blum, D., 2013. Detrimental Effects of Diet-Induced Obesity on τ Pathology Are Independent of Insulin Resistance in τ Transgenic Mice. Diabetes 62, 1681–1688. https://doi.org/10.2337/db12-0866

Ledesma, M.D., Bonay, P., Avila, J., 1995. Tau protein from Alzheimer's disease patients is glycated at its tubulin-binding domain. J. Neurochem. 65, 1658–1664. https://doi.org/10.1046/j.1471-4159.1995.65041658.x

Ledesma, M.D., Bonay, P., Colaço, C., Avila, J., 1994. Analysis of microtubule-associated protein tau glycation in paired helical filaments. J. Biol. Chem. 269, 21614–21619.

Lee, G., Neve, R.L., Kosik, K.S., 1989. The microtubule binding domain of tau protein. Neuron 2, 1615–1624. https://doi.org/10.1016/0896-6273(89)90050-0

Lee, G., Newman, S.T., Gard, D.L., Band, H., Panchamoorthy, G., 1998. Tau interacts with src-family non-receptor tyrosine kinases. J. Cell Sci. 111, 3167–3177. https://doi.org/10.1242/jcs.111.21.3167

Leloup, C., Tourrel-Cuzin, C., Magnan, C., Karaca, M., Castel, J., Carneiro, L., Colombani, A.-L., Ktorza, A., Casteilla, L., Pénicaud, L., 2009. Mitochondrial Reactive Oxygen Species Are Obligatory Signals for Glucose-Induced Insulin Secretion. Diabetes 58, 673–681. https://doi.org/10.2337/db07-1056

Lhomme, T., Clasadonte, J., Imbernon, M., Fernandois, D., Sauve, F., Caron, E., da Silva Lima, N., Heras, V., Martinez-Corral, I., Mueller-Fielitz, H., Rasika, S., Schwaninger, M., Nogueiras, R., Prevot, V., 2021. Tanycytic networks mediate energy balance by feeding lactate to glucose-insensitive POMC neurons. J. Clin. Invest. 131, e140521. https://doi.org/10.1172/JCI140521

Li, C., Liu, C., Nissim, Itzhak, Chen, J., Chen, P., Doliba, N., Zhang, T., Nissim, Ilana, Daikhin, Y., Stokes, D., Yudkoff, M., Bennett, M.J., Stanley, C.A., Matschinsky, F.M., Naji, A., 2013. Regulation of Glucagon Secretion in Normal and Diabetic Human Islets by γ-Hydroxybutyrate and Glycine. J. Biol. Chem. 288, 3938–3951. https://doi.org/10.1074/jbc.M112.385682

Li, X., Wu, X., Camacho, R., Schwartz, G.J., LeRoith, D., 2011. Intracerebroventricular Leptin Infusion Improves Glucose Homeostasis in Lean Type 2 Diabetic MKR Mice via Hepatic Vagal and Non-Vagal Mechanisms. PLoS ONE 6, e17058. https://doi.org/10.1371/journal.pone.0017058

Lin, S., Boey, D., Herzog, H., 2004. NPY and Y receptors: lessons from transgenic and knockout models. Neuropeptides 38, 189–200. https://doi.org/10.1016/j.npep.2004.05.005

Liu, F., Iqbal, K., Grundke-Iqbal, I., Hart, G.W., Gong, C.-X., 2004. O-GlcNAcylation regulates phosphorylation of tau: A mechanism involved in Alzheimer's disease. Proc. Natl. Acad. Sci. 101,

10804–10809. https://doi.org/10.1073/pnas.0400348101
Liu, L.-Z., Cheung, S.C.K., Lan, L.-L., Ho, S.K.S., Chan, J.C.N., Tong, P.C.Y., 2013. Microtubule network is required for insulin-induced signal transduction and actin remodeling. Mol. Cell. Endocrinol. 365, 64–74. https://doi.org/10.1016/j.mce.2012.09.005
Liu, S., Mauvais-Jarvis, F., 2010. Minireview: Estrogenic Protection of β-Cell Failure in Metabolic Diseases. Endocrinology 151, 859–864. https://doi.org/10.1210/en.2009-1107
Liu, Y., Liu, F., Iqbal, K., Grundke-Iqbal, I., Gong, C.-X., 2008. Decreased glucose transporters correlate to abnormal hyperphosphorylation of tau in Alzheimer disease. FEBS Lett. 582, 359–364. https://doi.org/10.1016/j.febslet.2007.12.035
Livingston, G., Sommerlad, A., Orgeta, V., Costafreda, S.G., Huntley, J., Ames, D., Ballard, C., Banerjee, S., Burns, A., Cohen-Mansfield, J., Cooper, C., Fox, N., Gitlin, L.N., Howard, R., Kales, H.C., Larson, E.B., Ritchie, K., Rockwood, K., Sampson, E.L., Samus, Q., Schneider, L.S., Selbæk, G., Teri, L., Mukadam, N., 2017. Dementia prevention, intervention, and care. The Lancet 390, 2673–2734. https://doi.org/10.1016/S0140-6736(17)31363-6
Loomis, P.A., Howard, T.H., Castleberry, R.P., Binder, L.I., 1990. Identification of nuclear tau isoforms in human neuroblastoma cells. Proc. Natl. Acad. Sci. 87, 8422–8426. https://doi.org/10.1073/pnas.87.21.8422
López, M., Varela, L., Vázquez, M.J., Rodríguez-Cuenca, S., González, C.R., Velagapudi, V.R., Morgan, D.A., Schoenmakers, E., Agassandian, K., Lage, R., de Morentin, P.B.M., Tovar, S., Nogueiras, R., Carling, D., Lelliott, C., Gallego, R., Orešič, M., Chatterjee, K., Saha, A.K., Rahmouni, K., Diéguez, C., Vidal-Puig, A., 2010. Hypothalamic AMPK and fatty acid metabolism mediate thyroid regulation of energy balance. Nat. Med. 16, 1001–1008. https://doi.org/10.1038/nm.2207
Lu, D., Willard, D., Patel, I.R., Kadwell, S., Overton, L., Kost, T., Luther, M., Chen, W., Woychik, R.P., Wilkison, W.O., Cone, R.D., 1994. Agouti protein is an antagonist of the melanocyte-stimulating-hormone receptor. Nature 371, 799–802. https://doi.org/10.1038/371799a0
Lu, P.-J., Wulf, G., Zhou, X.Z., Davies, P., Lu, K.P., 1999. The prolyl isomerase Pin1 restores the function of Alzheimer-associated phosphorylated tau protein. Nature 399, 784–788. https://doi.org/10.1038/21650
Lührs, T., Ritter, C., Adrian, M., Riek-Loher, D., Bohrmann, B., Döbeli, H., Schubert, D., Riek, R., 2005. 3D structure of Alzheimer's amyloid-β(1–42) fibrils. Proc. Natl. Acad. Sci. 102, 17342–17347. https://doi.org/10.1073/pnas.0506723102
Luo, M., Tse, S.-W., Memmott, J., Andreadis, A., 2004. Novel isoforms of tau that lack the microtubule-binding domain. J. Neurochem. 90, 340–351. https://doi.org/10.1111/j.1471-4159.2004.02508.x
Luquet, S., Perez, F.A., Hnasko, T.S., Palmiter, R.D., 2005. NPY/AgRP Neurons Are Essential for Feeding in Adult Mice but Can Be Ablated in Neonates. Science 310, 683–685. https://doi.org/10.1126/science.1115524
Lyons, W.E., Mamounas, L.A., Ricaurte, G.A., Coppola, V., Reid, S.W., Bora, S.H., Wihler, C., Koliatsos, V.E., Tessarollo, L., 1999. Brain-derived neurotrophic factor-deficient mice develop aggressiveness and hyperphagia in conjunction with brain serotonergic abnormalities. Proc. Natl. Acad. Sci. 96, 15239–15244. https://doi.org/10.1073/pnas.96.26.15239

M

Maesako, M., Uemura, K., Kubota, M., Kuzuya, A., Sasaki, K., Asada, M., Watanabe, K., Hayashida, N., Ihara, M., Ito, H., Shimohama, S., Kihara, T., Kinoshita, A., 2012. Environmental enrichment ameliorated high-fat diet-induced Aβ deposition and memory deficit in APP transgenic mice. Neurobiol. Aging 33, 1011.e11-1011.e23. https://doi.org/10.1016/j.neurobiolaging.2011.10.028

Maj, M., Hoermann, G., Rasul, S., Base, W., Wagner, L., Attems, J., 2016a. The Microtubule-Associated Protein Tau and Its Relevance for Pancreatic Beta Cells. J. Diabetes Res. 2016, 1–12. https://doi.org/10.1155/2016/1964634

Maj, M., Hoermann, G., Rasul, S., Base, W., Wagner, L., Attems, J., 2016b. The Microtubule-Associated Protein Tau and Its Relevance for Pancreatic Beta Cells. J. Diabetes Res. 2016, 1–12. https://doi.org/10.1155/2016/1964634

Marciniak, E., Leboucher, A., Caron, E., Ahmed, T., Tailleux, A., Dumont, J., Issad, T., Gerhardt, E., Pagesy, P., Vileno, M., Bournonville, C., Hamdane, M., Bantubungi, K., Lancel, S., Demeyer, D., Eddarkaoui, S., Vallez, E., Vieau, D., Humez, S., Faivre, E., Grenier-Boley, B., Outeiro, T.F., Staels, B., Amouyel, P., Balschun, D., Buee, L., Blum, D., 2017. Tau deletion promotes brain insulin resistance. J. Exp. Med. 214, 2257–2269. https://doi.org/10.1084/jem.20161731

Martínez de Morentin, P.B., Whittle, A.J., Fernø, J., Nogueiras, R., Diéguez, C., Vidal-Puig, A., López, M., 2012. Nicotine Induces Negative Energy Balance Through Hypothalamic AMP-Activated Protein Kinase. Diabetes 61, 807–817. https://doi.org/10.2337/db11-1079

Martinez-Valbuena, I., Valenti-Azcarate, R., Amat-Villegas, I., Marcilla, I., Marti-Andres, G., Caballero, M.-C., Riverol, M., Tuñon, M.-T., Fraser, P.E., Luquin, M.-R., 2021. Mixed pathologies in pancreatic β cells from subjects with neurodegenerative diseases and their interaction with prion protein. Acta Neuropathol. Commun. 9, 64. https://doi.org/10.1186/s40478-021-01171-0

Martinez-Valbuena, I., Valenti-Azcarate, R., Amat-Villegas, I., Riverol, M., Marcilla, I., Andrea, C.E., Sánchez-Arias, J.A., Mar Carmona-Abellan, M., Marti, G., Erro, M., Martínez-Vila, E., Tuñon, M., Luquin, M., 2019a. Amylin as a potential link between type 2 diabetes and alzheimer disease. Ann. Neurol. 86, 539–551. https://doi.org/10.1002/ana.25570

Martinez-Valbuena, I., Valenti-Azcarate, R., Amat-Villegas, I., Riverol, M., Marcilla, I., Andrea, C.E., Sánchez-Arias, J.A., Mar Carmona-Abellan, M., Marti, G., Erro, M., Martínez-Vila, E., Tuñon, M., Luquin, M., 2019b. Amylin as a potential link between type 2 diabetes and alzheimer disease. Ann. Neurol. 86, 539–551. https://doi.org/10.1002/ana.25570

Marty, N., Dallaporta, M., Thorens, B., 2007. Brain Glucose Sensing, Counterregulation, and Energy Homeostasis. Physiology 22, 241–251. https://doi.org/10.1152/physiol.00010.2007

Matsuzaki, T., Sasaki, K., Tanizaki, Y., Hata, J., Fujimi, K., Matsui, Y., Sekita, A., Suzuki, S.O., Kanba, S., Kiyohara, Y., Iwaki, T., 2010a. Insulin resistance is associated with the pathology of Alzheimer disease: The Hisayama Study. Neurology 75, 764–770. https://doi.org/10.1212/WNL.0b013e3181eee25f

Matsuzaki, T., Sasaki, K., Tanizaki, Y., Hata, J., Fujimi, K., Matsui, Y., Sekita, A., Suzuki, S.O., Kanba, S., Kiyohara, Y., Iwaki, T., 2010b. Insulin resistance is associated with the pathology of Alzheimer disease: The Hisayama Study. Neurology 75, 764–770. https://doi.org/10.1212/WNL.0b013e3181eee25f

Mehla, J., Chauhan, B.C., Chauhan, N.B., 2014. Experimental Induction of Type 2 Diabetes in Aging-Accelerated Mice Triggered Alzheimer-Like Pathology and Memory Deficits. J. Alzheimers Dis. 39,

145–162. https://doi.org/10.3233/JAD-131238
Mercer, J.G., Moar, K.M., Findlay, P.A., Hoggard, N., Adam, C.L., 1998. Association of leptin receptor (OB-Rb), NPY and GLP-1 gene expression in the ovine and murine brainstem. Regul. Pept. 75–76, 271–278. https://doi.org/10.1016/S0167-0115(98)00078-0
Mighiu, P.I., Yue, J.T.Y., Filippi, B.M., Abraham, M.A., Chari, M., Lam, C.K.L., Yang, C.S., Christian, N.R., Charron, M.J., Lam, T.K.T., 2013. Hypothalamic glucagon signaling inhibits hepatic glucose production. Nat. Med. 19, 766–772. https://doi.org/10.1038/nm.3115
Miklossy, J., Qing, H., Radenovic, A., Kis, A., Vileno, B., Làszló, F., Miller, L., Martins, R.N., Waeber, G., Mooser, V., Bosman, F., Khalili, K., Darbinian, N., McGeer, P.L., 2010a. Beta amyloid and hyperphosphorylated tau deposits in the pancreas in type 2 diabetes. Neurobiol. Aging 31, 1503–1515. https://doi.org/10.1016/j.neurobiolaging.2008.08.019
Miklossy, J., Qing, H., Radenovic, A., Kis, A., Vileno, B., Làszló, F., Miller, L., Martins, R.N., Waeber, G., Mooser, V., Bosman, F., Khalili, K., Darbinian, N., McGeer, P.L., 2010b. Beta amyloid and hyperphosphorylated tau deposits in the pancreas in type 2 diabetes. Neurobiol. Aging 31, 1503–1515. https://doi.org/10.1016/j.neurobiolaging.2008.08.019
Mimee, A., Ferguson, A.V., 2015. Glycemic state regulates melanocortin, but not nesfatin-1, responsiveness of glucose-sensing neurons in the nucleus of the solitary tract. Am. J. Physiol.-Regul. Integr. Comp. Physiol. 308, R690–R699. https://doi.org/10.1152/ajpregu.00477.2014
Min, S.-W., Cho, S.-H., Zhou, Y., Schroeder, S., Haroutunian, V., Seeley, W.W., Huang, E.J., Shen, Y., Masliah, E., Mukherjee, C., Meyers, D., Cole, P.A., Ott, M., Gan, L., 2010. Acetylation of Tau Inhibits Its Degradation and Contributes to Tauopathy. Neuron 67, 953–966. https://doi.org/10.1016/j.neuron.2010.08.044
Mingozzi, F., High, K., 2007. Immune Responses to AAV in Clinical Trials. Curr. Gene Ther. 7, 316–324. https://doi.org/10.2174/156652307782151425
Mody, N., Agouni, A., Mcilroy, G.D., Platt, B., Delibegovic, M., 2011. Susceptibility to diet-induced obesity and glucose intolerance in the APP SWE/PSEN1 A246E mouse model of Alzheimer's disease is associated with increased brain levels of protein tyrosine phosphatase 1B (PTP1B) and retinol-binding protein 4 (RBP4), and basal phosphorylation of S6 ribosomal protein. Diabetologia 54, 2143–2151. https://doi.org/10.1007/s00125-011-2160-2
Morris, M., Knudsen, G.M., Maeda, S., Trinidad, J.C., Ioanoviciu, A., Burlingame, A.L., Mucke, L., 2015. Tau post-translational modifications in wild-type and human amyloid precursor protein transgenic mice. Nat. Neurosci. 18, 1183–1189. https://doi.org/10.1038/nn.4067
Mosleh, E., Ou, K., Haemmerle, M.W., Tembo, T., Yuhas, A., Carboneau, B.A., Townsend, S.E., Bosma, K.J., Gannon, M., O'Brien, R.M., Stoffers, D.A., Golson, M.L., 2020. Ins1-Cre and Ins1-CreER Gene Replacement Alleles Are Susceptible To Silencing By DNA Hypermethylation. Endocrinology 161, bqaa054. https://doi.org/10.1210/endocr/bqaa054
Mourad, N.I., Nenquin, M., Henquin, J.-C., 2011. Metabolic amplification of insulin secretion by glucose is independent of β-cell microtubules. Am. J. Physiol.-Cell Physiol. 300, C697–C706. https://doi.org/10.1152/ajpcell.00329.2010
Mukrasch, M.D., von Bergen, M., Biernat, J., Fischer, D., Griesinger, C., Mandelkow, E., Zweckstetter, M., 2007. The "Jaws" of the Tau-Microtubule Interaction. J. Biol. Chem. 282, 12230–12239. https://doi.org/10.1074/jbc.M607159200
Müller, A., Schmidt, D., Xu, C.S., Pang, S., D'Costa, J.V., Kretschmar, S., Münster, C., Kurth, T., Jug, F., Weigert, M., Hess, H.F., Solimena, M., 2021. 3D FIB-SEM reconstruction of microtubule–organelle interaction in whole primary mouse β cells. J. Cell Biol. 220, e202010039. https://doi.org/10.1083/jcb.202010039

Muller, U.C., Zheng, H., 2012. Physiological Functions of APP Family Proteins. Cold Spring Harb. Perspect. Med. 2, a006288–a006288. https://doi.org/10.1101/cshperspect.a006288
Munari, F., Barracchia, C.G., Parolini, F., Tira, R., Bubacco, L., Assfalg, M., D'Onofrio, M., 2020. Semisynthetic Modification of Tau Protein with Di-Ubiquitin Chains for Aggregation Studies. Int. J. Mol. Sci. 21, 4400. https://doi.org/10.3390/ijms21124400

N

Nacharaju, P., Ko, L., Yen, S.-H.C., 1997. Characterization of In Vitro Glycation Sites of Tau. J. Neurochem. 69, 1709–1719. https://doi.org/10.1046/j.1471-4159.1997.69041709.x
Ng, Y., Ramm, G., James, D.E., 2010. Dissecting the Mechanism of Insulin Resistance Using a Novel Heterodimerization Strategy to Activate Akt. J. Biol. Chem. 285, 5232–5239. https://doi.org/10.1074/jbc.M109.060632
Nguyen, A.D., Mitchell, N.F., Lin, S., Macia, L., Yulyaningsih, E., Baldock, P.A., Enriquez, R.F., Zhang, L., Shi, Y.-C., Zolotukhin, S., Herzog, H., Sainsbury, A., 2012. Y1 and Y5 Receptors Are Both Required for the Regulation of Food Intake and Energy Homeostasis in Mice. PLoS ONE 7, e40191. https://doi.org/10.1371/journal.pone.0040191
Nurse, C.A., Piskuric, N.A., 2013. Signal processing at mammalian carotid body chemoreceptors. Semin. Cell Dev. Biol. 24, 22–30. https://doi.org/10.1016/j.semcdb.2012.09.006

O

Obici, S., Zhang, B.B., Karkanias, G., Rossetti, L., 2002. Hypothalamic insulin signaling is required for inhibition of glucose production. Nat. Med. 8, 1376–1382. https://doi.org/10.1038/nm1202-798
Oliveira, R.B., Maschio, D.A., Carvalho, C.P.F., Collares-Buzato, C.B., 2015. Influence of gender and time diet exposure on endocrine pancreas remodeling in response to high fat diet-induced metabolic disturbances in mice. Ann. Anat. - Anat. Anz. 200, 88–97. https://doi.org/10.1016/j.aanat.2015.01.007
Olson, A.L., Trumbly, A.R., Gibson, G.V., 2001. Insulin-mediated GLUT4 Translocation Is Dependent on the Microtubule Network. J. Biol. Chem. 276, 10706–10714. https://doi.org/10.1074/jbc.M007610200
Oomura, Y., Ono, T., Ooyama, H., Wayner, M.J., 1969. Glucose and Osmosensitive Neurones of the Rat Hypothalamus. Nature 222, 282–284. https://doi.org/10.1038/222282a0
Oomura, Y., Ooyama, H., Sugimori, M., Nakamura, T., Yamada, Y., 1974. Glucose Inhibition of the Glucose-sensitive Neurone in the Rat Lateral Hypothalamus. Nature 247, 284–286. https://doi.org/10.1038/247284a0
Orellana, J.A., Sáez, P.J., Cortés-campos, C., Elizondo, R.J., Shoji, K.F., Contreras-Duarte, S., Figueroa, V., Velarde, V., Jiang, J.X., Nualart, F., Sáez, J.C., García, M.A., 2012. Glucose increases intracellular free Ca2+ in tanycytes via ATP released through connexin 43 hemichannels. Glia 60, 53–68. https://doi.org/10.1002/glia.21246
Osipovich, A.B., Stancill, J.S., Cartailler, J.-P., Dudek, K.D., Magnuson, M.A., 2020. Excitotoxicity

and Overnutrition Additively Impair Metabolic Function and Identity of Pancreatic β-Cells. Diabetes 69, 1476–1491. https://doi.org/10.2337/db19-1145
Östenson, C.-G., 1979. Regulation of glucagon release: Effects of insulin on the pancreatic A2-cell of the guinea pig. Diabetologia 17, 325–330. https://doi.org/10.1007/BF01235889

P

Parker, K.L., 2002. Steroidogenic Factor 1: an Essential Mediator of Endocrine Development. Recent Prog. Horm. Res. 57, 19–36. https://doi.org/10.1210/rp.57.1.19
Peruzzo, B., Pastor, F.E., Blázquez, J.L., Schöbitz, K., Peláez, B., Amat, P., Rodríguez, E.M., 2000. A second look at the barriers of the medial basal hypothalamus. Exp. Brain Res. 132, 10–26. https://doi.org/10.1007/s002219900289
Pooja Naik, L.C., 2014. Diabetes Mellitus and Blood-Brain Barrier Dysfunction: An Overview. J. Pharmacovigil. 02. https://doi.org/10.4172/2329-6887.1000125
Pottier, C., Ravenscroft, T.A., Sanchez-Contreras, M., Rademakers, R., 2016. Genetics of FTLD: overview and what else we can expect from genetic studies. J. Neurochem. 138, 32–53. https://doi.org/10.1111/jnc.13622
Prentki, M., 2006. Islet cell failure in type 2 diabetes. J. Clin. Invest. 116, 1802–1812. https://doi.org/10.1172/JCI29103
Prevot, V., Nogueiras, R., Schwaninger, M., 2021. Tanycytes in the infundibular nucleus and median eminence and their role in the blood–brain barrier, in: Handbook of Clinical Neurology. Elsevier, pp. 253–273. https://doi.org/10.1016/B978-0-12-820107-7.00016-1

Q/R

Qu, M., Li, H., Tian, R., Nie, C., Liu, Y., Han, B., He, R., 2004. Neuronal tau induces DNA conformational changes observed by atomic force microscopy. Neuroreport 15, 2723–2727.
Rabhi, N., Denechaud, P.-D., Gromada, X., Hannou, S.A., Zhang, H., Rashid, T., Salas, E., Durand, E., Sand, O., Bonnefond, A., Yengo, L., Chavey, C., Bonner, C., Kerr-Conte, J., Abderrahmani, A., Auwerx, J., Fajas, L., Froguel, P., Annicotte, J.-S., 2016. KAT2B Is Required for Pancreatic Beta Cell Adaptation to Metabolic Stress by Controlling the Unfolded Protein Response. Cell Rep. 15, 1051–1061. https://doi.org/10.1016/j.celrep.2016.03.079
Ramos-Rodriguez, J.J., Ortiz, O., Jimenez-Palomares, M., Kay, K.R., Berrocoso, E., Murillo-Carretero, M.I., Perdomo, G., Spires-Jones, T., Cozar-Castellano, I., Lechuga-Sancho, A.M., Garcia-Alloza, M., 2013. Differential central pathology and cognitive impairment in pre-diabetic and diabetic mice. Psychoneuroendocrinology 38, 2462–2475. https://doi.org/10.1016/j.psyneuen.2013.05.010
Ravid, T., Hochstrasser, M., 2008. Diversity of degradation signals in the ubiquitin–proteasome system. Nat. Rev. Mol. Cell Biol. 9, 679–689. https://doi.org/10.1038/nrm2468
Reinert, R.B., Kantz, J., Misfeldt, A.A., Poffenberger, G., Gannon, M., Brissova, M., Powers, A.C., 2012. Tamoxifen-Induced Cre-loxP Recombination Is Prolonged in Pancreatic Islets of Adult Mice. PLoS ONE 7, e33529. https://doi.org/10.1371/journal.pone.0033529

Reitz, C., Brayne, C., Mayeux, R., 2011. Epidemiology of Alzheimer disease. Nat. Rev. Neurol. 7, 137–152. https://doi.org/10.1038/nrneurol.2011.2
Reynolds, C.H., Garwood, C.J., Wray, S., Price, C., Kellie, S., Perera, T., Zvelebil, M., Yang, A., Sheppard, P.W., Varndell, I.M., Hanger, D.P., Anderton, B.H., 2008. Phosphorylation Regulates Tau Interactions with Src Homology 3 Domains of Phosphatidylinositol 3-Kinase, Phospholipase Cγ1, Grb2, and Src Family Kinases. J. Biol. Chem. 283, 18177–18186. https://doi.org/10.1074/jbc.M709715200
Ritter, S., Li, A.-J., Wang, Q., Dinh, T.T., 2011. Minireview: The Value of Looking Backward: The Essential Role of the Hindbrain in Counterregulatory Responses to Glucose Deficit. Endocrinology 152, 4019–4032. https://doi.org/10.1210/en.2010-1458
Rorsman, P., Ashcroft, F.M., 2018. Pancreatic β-Cell Electrical Activity and Insulin Secretion: Of Mice and Men. Physiol. Rev. 98, 117–214. https://doi.org/10.1152/physrev.00008.2017
Rossi, J., Balthasar, N., Olson, D., Scott, M., Berglund, E., Lee, C.E., Choi, M.J., Lauzon, D., Lowell, B.B., Elmquist, J.K., 2011. Melanocortin-4 Receptors Expressed by Cholinergic Neurons Regulate Energy Balance and Glucose Homeostasis. Cell Metab. 13, 195–204. https://doi.org/10.1016/j.cmet.2011.01.010
Routh, V.H., Hao, L., Santiago, A.M., Sheng, Z., Zhou, C., 2014. Hypothalamic glucose sensing: making ends meet. Front. Syst. Neurosci. 8. https://doi.org/10.3389/fnsys.2014.00236
Ruiz, H.H., Chi, T., Shin, A.C., Lindtner, C., Hsieh, W., Ehrlich, M., Gandy, S., Buettner, C., 2016. Increased susceptibility to metabolic dysregulation in a mouse model of Alzheimer's disease is associated with impaired hypothalamic insulin signaling and elevated BCAA levels. Alzheimers Dement. 12, 851–861. https://doi.org/10.1016/j.jalz.2016.01.008

S

Saberi, M., Bohland, M., Donovan, C.M., 2008. The Locus for Hypoglycemic Detection Shifts With the Rate of Fall in Glycemia. Diabetes 57, 1380–1386. https://doi.org/10.2337/db07-1528
Saito, T., Mihira, N., Matsuba, Y., Sasaguri, H., Hashimoto, S., Narasimhan, S., Zhang, B., Murayama, S., Higuchi, M., Lee, V.M.Y., Trojanowski, J.Q., Saido, T.C., 2019. Humanization of the entire murine Mapt gene provides a murine model of pathological human tau propagation. J. Biol. Chem. 294, 12754–12765. https://doi.org/10.1074/jbc.RA119.009487
Sakaguchi, T., Bray, G.A., 1987. The effect of intrahypothalamic injections of glucose on sympathetic efferent firing rate. Brain Res. Bull. 18, 591–595. https://doi.org/10.1016/0361-9230(87)90128-6
Sánchez-Lasheras, C., Christine Könner, A., Brüning, J.C., 2010. Integrative neurobiology of energy homeostasis-neurocircuits, signals and mediators. Front. Neuroendocrinol. 31, 4–15. https://doi.org/10.1016/j.yfrne.2009.08.002
Sanders, N.M., Dunn-Meynell, A.A., Levin, B.E., 2004. Third Ventricular Alloxan Reversibly Impairs Glucose Counterregulatory Responses. Diabetes 53, 1230–1236. https://doi.org/10.2337/diabetes.53.5.1230
Sandoval, D.A., Bagnol, D., Woods, S.C., D'Alessio, D.A., Seeley, R.J., 2008. Arcuate Glucagon-Like Peptide 1 Receptors Regulate Glucose Homeostasis but Not Food Intake. Diabetes 57, 2046–2054. https://doi.org/10.2337/db07-1824
Schellenberg, G.D., Montine, T.J., 2012. The genetics and neuropathology of Alzheimer's disease.

Acta Neuropathol. (Berl.) 124, 305–323. https://doi.org/10.1007/s00401-012-0996-2
Schneeberger, M., Gomis, R., Claret, M., 2014. Hypothalamic and brainstem neuronal circuits controlling homeostatic energy balance. J. Endocrinol. 220, T25–T46. https://doi.org/10.1530/JOE-13-0398
Schnütgen, F., Doerflinger, N., Calléja, C., Wendling, O., Chambon, P., Ghyselinck, N.B., 2003. A directional strategy for monitoring Cre-mediated recombination at the cellular level in the mouse. Nat. Biotechnol. 21, 562–565. https://doi.org/10.1038/nbt811
Schultz, C., Ghebremedhin, E., Braak, E., Braak, H., 1999. Sex-dependent cytoskeletal changes of the human hypothalamus develop independently of Alzheimer's disease. Exp. Neurol. 160, 186–193. https://doi.org/10.1006/exnr.1999.7185
Schwartz, G.J., 2000. The role of gastrointestinal vagal afferents in the control of food intake: current prospects. Nutrition 16, 866–873. https://doi.org/10.1016/S0899-9007(00)00464-0
Segerstolpe, Å., Palasantza, A., Eliasson, P., Andersson, E.-M., Andréasson, A.-C., Sun, X., Picelli, S., Sabirsh, A., Clausen, M., Bjursell, M.K., Smith, D.M., Kasper, M., Ämmälä, C., Sandberg, R., 2016. Single-Cell Transcriptome Profiling of Human Pancreatic Islets in Health and Type 2 Diabetes. Cell Metab. 24, 593–607. https://doi.org/10.1016/j.cmet.2016.08.020
Seitz-Tutter, D., Langford, G.M., Weiss, D.G., 1988. Dynamic instability of native microtubules from squid axons is rare and independent of gliding and vesicle transport. Exp. Cell Res. 178, 504–512. https://doi.org/10.1016/0014-4827(88)90418-1
Seoane, L.M., Tovar, S., Dieguez, C., 2018. Physiology of the Hypothalamus Pituitary Unit, in: Casanueva, F.F., Ghigo, E. (Eds.), Hypothalamic-Pituitary Diseases, Endocrinology. Springer International Publishing, Cham, pp. 1–33. https://doi.org/10.1007/978-3-319-44444-4_1
Sergeant, N., Bretteville, A., Hamdane, M., Caillet-Boudin, M.-L., Grognet, P., Bombois, S., Blum, D., Delacourte, A., Pasquier, F., Vanmechelen, E., Schraen-Maschke, S., Buée, L., 2008a. Biochemistry of Tau in Alzheimer's disease and related neurological disorders. Expert Rev. Proteomics 5, 207–224. https://doi.org/10.1586/14789450.5.2.207
Sergeant, N., Bretteville, A., Hamdane, M., Caillet-Boudin, M.-L., Grognet, P., Bombois, S., Blum, D., Delacourte, A., Pasquier, F., Vanmechelen, E., Schraen-Maschke, S., Buée, L., 2008b. Biochemistry of Tau in Alzheimer's disease and related neurological disorders. Expert Rev. Proteomics 5, 207–224. https://doi.org/10.1586/14789450.5.2.207
Sillen, A., Barbier, P., Landrieu, I., Lefebvre, S., Wieruszeski, J.-M., Leroy, A., Peyrot, V., Lippens, G., 2007. NMR Investigation of the Interaction between the Neuronal Protein Tau and the Microtubules. Biochemistry 46, 3055–3064. https://doi.org/10.1021/bi061920i
Silva Rosa, S.C., Nayak, N., Caymo, A.M., Gordon, J.W., 2020. Mechanisms of muscle insulin resistance and the cross-talk with liver and adipose tissue. Physiol. Rep. 8. https://doi.org/10.14814/phy2.14607
Silver, I., Erecinska, M., 1994. Extracellular glucose concentration in mammalian brain: continuous monitoring of changes during increased neuronal activity and upon limitation in oxygen supply in normo-, hypo-, and hyperglycemic animals. J. Neurosci. 14, 5068–5076. https://doi.org/10.1523/JNEUROSCI.14-08-05068.1994
Simpson, I.A., Dwyer, D., Malide, D., Moley, K.H., Travis, A., Vannucci, S.J., 2008. The facilitative glucose transporter GLUT3: 20 years of distinction. Am. J. Physiol.-Endocrinol. Metab. 295, E242–E253. https://doi.org/10.1152/ajpendo.90388.2008
Sjöberg, M.K., Shestakova, E., Mansuroglu, Z., Maccioni, R.B., Bonnefoy, E., 2006. Tau protein binds to pericentromeric DNA: a putative role for nuclear tau in nucleolar organization. J. Cell Sci. 119, 2025–2034. https://doi.org/10.1242/jcs.02907

Sotiropoulos, I., Galas, M.-C., Silva, J.M., Skoulakis, E., Wegmann, S., Maina, M.B., Blum, D., Sayas, C.L., Mandelkow, E.-M., Mandelkow, E., Spillantini, M.G., Sousa, N., Avila, J., Medina, M., Mudher, A., Buee, L., 2017. Atypical, non-standard functions of the microtubule associated Tau protein. Acta Neuropathol. Commun. 5, 91. https://doi.org/10.1186/s40478-017-0489-6

Soto, M., Cai, W., Konishi, M., Kahn, C.R., 2019. Insulin signaling in the hippocampus and amygdala regulates metabolism and neurobehavior. Proc. Natl. Acad. Sci. 116, 6379–6384. https://doi.org/10.1073/pnas.1817391116

Stanley, B.G., Leibowitz, S.F., 1984. Neuroreptide Y: Stimulation of feeding and drinking by injection into the paraventricular nucleus. Life Sci. 35, 2635–2642. https://doi.org/10.1016/0024-3205(84)90032-8

Stelzmann, R.A., Norman Schnitzlein, H., Reed Murtagh, F., 1995. An english translation of alzheimer's 1907 paper, Über eine eigenartige Erkankung der Hirnrinde. Clin. Anat. 8, 429–431. https://doi.org/10.1002/ca.980080612

Strömblad, G., Björntorp, P., 1986. Reduced hepatic insulin clearance in rats with dietary-induced obesity. Metabolism 35, 323–327. https://doi.org/10.1016/0026-0495(86)90148-4

Sue Kirkman, M., Briscoe, V.J., Clark, N., Florez, H., Haas, L.B., Halter, J.B., Huang, E.S., Korytkowski, M.T., Munshi, M.N., Odegard, P.S., Pratley, R.E., Swift, C.S., 2012. Diabetes in Older Adults: A Consensus Report. J. Am. Geriatr. Soc. 60, 2342–2356. https://doi.org/10.1111/jgs.12035

Sultan, A., Nesslany, F., Violet, M., Bégard, S., Loyens, A., Talahari, S., Mansuroglu, Z., Marzin, D., Sergeant, N., Humez, S., Colin, M., Bonnefoy, E., Buée, L., Galas, M.-C., 2011. Nuclear Tau, a Key Player in Neuronal DNA Protection. J. Biol. Chem. 286, 4566–4575. https://doi.org/10.1074/jbc.M110.199976

Takeda, S., Sato, N., Uchio-Yamada, K., Sawada, K., Kunieda, T., Takeuchi, D., Kurinami, H., Shinohara, M., Rakugi, H., Morishita, R., 2010. Diabetes-accelerated memory dysfunction via cerebrovascular inflammation and Aβ deposition in an Alzheimer mouse model with diabetes. Proc. Natl. Acad. Sci. 107, 7036–7041. https://doi.org/10.1073/pnas.1000645107

T

Thies, E., Mandelkow, E.-M., 2007. Missorting of Tau in Neurons Causes Degeneration of Synapses That Can Be Rescued by the Kinase MARK2/Par-1. J. Neurosci. 27, 2896–2907. https://doi.org/10.1523/JNEUROSCI.4674-06.2007

Thorens, B., 2015. GLUT2, glucose sensing and glucose homeostasis. Diabetologia 58, 221–232. https://doi.org/10.1007/s00125-014-3451-1

Thorens, B., 2011. Brain glucose sensing and neural regulation of insulin and glucagon secretion. Diabetes Obes. Metab. 13 Suppl 1, 82–88. https://doi.org/10.1111/j.1463-1326.2011.01453.x

Thurmond, D.C., Gaisano, H.Y., 2020. Recent Insights into Beta-cell Exocytosis in Type 2 Diabetes. J. Mol. Biol. 432, 1310–1325. https://doi.org/10.1016/j.jmb.2019.12.012

Tomic, D., Shaw, J.E., Magliano, D.J., 2022. The burden and risks of emerging complications of diabetes mellitus. Nat. Rev. Endocrinol. https://doi.org/10.1038/s41574-022-00690-7

Tong, Q., Ye, C.-P., Jones, J.E., Elmquist, J.K., Lowell, B.B., 2008. Synaptic release of GABA by AgRP neurons is required for normal regulation of energy balance. Nat. Neurosci. 11, 998–1000. https://doi.org/10.1038/nn.2167

Torres, C.R., Hart, G.W., 1984. Topography and polypeptide distribution of terminal N-acetylglucosamine residues on the surfaces of intact lymphocytes. Evidence for O-linked GlcNAc. J. Biol. Chem. 259, 3308–3317.
Tortelli, R., Lozupone, M., Guerra, V., Barulli, M.R., Imbimbo, B.P., Capozzo, R., Grasso, A., Tursi, M., Di Dio, C., Sardone, R., Giannelli, G., Seripa, D., Misciagna, G., Panza, F., Logroscino, G., 2017. Midlife Metabolic Profile and the Risk of Late-Life Cognitive Decline. J. Alzheimers Dis. JAD 59, 121–130. https://doi.org/10.3233/JAD-170153
Trabzuni, D., Wray, S., Vandrovcova, J., Ramasamy, A., Walker, R., Smith, C., Luk, C., Gibbs, J.R., Dillman, A., Hernandez, D.G., Arepalli, S., Singleton, A.B., Cookson, M.R., Pittman, A.M., de Silva, R., Weale, M.E., Hardy, J., Ryten, M., 2012. MAPT expression and splicing is differentially regulated by brain region: relation to genotype and implication for tauopathies. Hum. Mol. Genet. 21, 4094–4103. https://doi.org/10.1093/hmg/dds238

V

Vandal, M., White, P.J., Tremblay, C., St-Amour, I., Chevrier, G., Emond, V., Lefrançois, D., Virgili, J., Planel, E., Giguere, Y., Marette, A., Calon, F., 2014. Insulin Reverses the High-Fat Diet–Induced Increase in Brain Aβ and Improves Memory in an Animal Model of Alzheimer Disease. Diabetes 63, 4291–4301. https://doi.org/10.2337/db14-0375
Vanier, M.T., Neuville, P., Michalik, L., Launay, J.F., 1998. Expression of specific tau exons in normal and tumoral pancreatic acinar cells. J. Cell Sci. 111, 1419–1432. https://doi.org/10.1242/jcs.111.10.1419
Vercruysse, P., Vieau, D., Blum, D., Petersén, Å., Dupuis, L., 2018. Hypothalamic Alterations in Neurodegenerative Diseases and Their Relation to Abnormal Energy Metabolism. Front. Mol. Neurosci. 11, 2. https://doi.org/10.3389/fnmol.2018.00002
Vieira, E., Salehi, A., Gylfe, E., 2007. Glucose inhibits glucagon secretion by a direct effect on mouse pancreatic alpha cells. Diabetologia 50, 370–379. https://doi.org/10.1007/s00125-006-0511-1
Vinters, H.V., 2015. Emerging Concepts in Alzheimer's Disease. Annu. Rev. Pathol. Mech. Dis. 10, 291–319. https://doi.org/10.1146/annurev-pathol-020712-163927
Violet, M., Delattre, L., Tardivel, M., Sultan, A., Chauderlier, A., Caillierez, R., Talahari, S., Nesslany, F., Lefebvre, B., Bonnefoy, E., BuÃ©e, L., Galas, M.-C., 2014. A major role for Tau in neuronal DNA and RNA protection in vivo under physiological and hyperthermic conditions. Front. Cell. Neurosci. 8. https://doi.org/10.3389/fncel.2014.00084

W

Wang, J.-Z., Grundke-Iqbal, I., Iqbal, K., 1996. Glycosylation of microtubule–associated protein tau: An abnormal posttranslational modification in Alzheimer's disease. Nat. Med. 2, 871–875. https://doi.org/10.1038/nm0896-871
Wang, Y., Mandelkow, E., 2016. Tau in physiology and pathology. Nat. Rev. Neurosci. 17, 22–35. https://doi.org/10.1038/nrn.2015.1

Wegmann, S., Biernat, J., Mandelkow, E., 2021. A current view on Tau protein phosphorylation in Alzheimer's disease. Curr. Opin. Neurobiol. 69, 131–138. https://doi.org/10.1016/j.conb.2021.03.003
Wei, M.-L., Andreadis, A., 2002. Splicing of a Regulated Exon Reveals Additional Complexity in the Axonal Microtubule-Associated Protein Tau. J. Neurochem. 70, 1346–1356. https://doi.org/10.1046/j.1471-4159.1998.70041346.x
Wei, Y., Qu, M.-H., Wang, X.-S., Chen, L., Wang, D.-L., Liu, Y., Hua, Q., He, R.-Q., 2008. Binding to the Minor Groove of the Double-Strand, Tau Protein Prevents DNA from Damage by Peroxidation. PLoS ONE 3, e2600. https://doi.org/10.1371/journal.pone.0002600
Weingarten, M.D., Lockwood, A.H., Hwo, S.Y., Kirschner, M.W., 1975. A protein factor essential for microtubule assembly. Proc. Natl. Acad. Sci. 72, 1858–1862. https://doi.org/10.1073/pnas.72.5.1858
Weir, G.C., Bonner-Weir, S., 2004. Five Stages of Evolving Beta-Cell Dysfunction During Progression to Diabetes. Diabetes 53, S16–S21. https://doi.org/10.2337/diabetes.53.suppl_3.S16
Wendt, A., Birnir, B., Buschard, K., Gromada, J., Salehi, A., Sewing, S., Rorsman, P., Braun, M., 2004. Glucose Inhibition of Glucagon Secretion From Rat α-Cells Is Mediated by GABA Released From Neighboring β-Cells. Diabetes 53, 1038–1045. https://doi.org/10.2337/diabetes.53.4.1038
Whittle, A.J., Carobbio, S., Martins, L., Slawik, M., Hondares, E., Vázquez, M.J., Morgan, D., Csikasz, R.I., Gallego, R., Rodriguez-Cuenca, S., Dale, M., Virtue, S., Villarroya, F., Cannon, B., Rahmouni, K., López, M., Vidal-Puig, A., 2012. BMP8B Increases Brown Adipose Tissue Thermogenesis through Both Central and Peripheral Actions. Cell 149, 871–885. https://doi.org/10.1016/j.cell.2012.02.066
Wicksteed, B., Brissova, M., Yan, W., Opland, D.M., Plank, J.L., Reinert, R.B., Dickson, L.M., Tamarina, N.A., Philipson, L.H., Shostak, A., Bernal-Mizrachi, E., Elghazi, L., Roe, M.W., Labosky, P.A., Myers, M.G., Gannon, M., Powers, A.C., Dempsey, P.J., 2010. Conditional gene targeting in mouse pancreatic ß-Cells: analysis of ectopic Cre transgene expression in the brain. Diabetes 59, 3090–3098. https://doi.org/10.2337/db10-0624
Wijesekara, N., Ahrens, R., Sabale, M., Wu, L., Ha, K., Verdile, G., Fraser, P.E., 2017. Amyloid-β and islet amyloid pathologies link Alzheimer's disease and type 2 diabetes in a transgenic model. FASEB J. 31, 5409–5418. https://doi.org/10.1096/fj.201700431R
Wijesekara, N., Gonçalves, R.A., Ahrens, R., De Felice, F.G., Fraser, P.E., 2018a. Tau ablation in mice leads to pancreatic β cell dysfunction and glucose intolerance. FASEB J. 32, 3166–3173. https://doi.org/10.1096/fj.201701352
Wijesekara, N., Gonçalves, R.A., Ahrens, R., De Felice, F.G., Fraser, P.E., 2018b. Tau ablation in mice leads to pancreatic β cell dysfunction and glucose intolerance. FASEB J. 32, 3166–3173. https://doi.org/10.1096/fj.201701352
Wijesekara, N., Gonçalves, R.A., Ahrens, R., Ha, K., De Felice, F.G., Fraser, P.E., 2021. Combination of human tau and islet amyloid polypeptide exacerbates metabolic dysfunction in transgenic mice. J. Pathol. 254, 244–253. https://doi.org/10.1002/path.5674
Williams, K.W., Margatho, L.O., Lee, C.E., Choi, M., Lee, S., Scott, M.M., Elias, C.F., Elmquist, J.K., 2010. Segregation of Acute Leptin and Insulin Effects in Distinct Populations of Arcuate Proopiomelanocortin Neurons. J. Neurosci. 30, 2472–2479. https://doi.org/10.1523/JNEUROSCI.3118-09.2010
Winzell, M.S., Ahren, B., 2004. The High-Fat Diet-Fed Mouse: A Model for Studying Mechanisms and Treatment of Impaired Glucose Tolerance and Type 2 Diabetes. Diabetes 53, S215–S219. https://doi.org/10.2337/diabetes.53.suppl_3.S215

Witman, G.B., Cleveland, D.W., Weingarten, M.D., Kirschner, M.W., 1976. Tubulin requires tau for growth onto microtubule initiating sites. Proc. Natl. Acad. Sci. 73, 4070–4074. https://doi.org/10.1073/pnas.73.11.4070
World Health Organization, 2019. Classification of diabetes mellitus. World Health Organization, Geneva.
Wu, Q., Boyle, M.P., Palmiter, R.D., 2009. Loss of GABAergic Signaling by AgRP Neurons to the Parabrachial Nucleus Leads to Starvation. Cell 137, 1225–1234. https://doi.org/10.1016/j.cell.2009.04.022

X

Xu, A.W., Kaelin, C.B., Morton, G.J., Ogimoto, K., Stanhope, K., Graham, J., Baskin, D.G., Havel, P., Schwartz, M.W., Barsh, G.S., 2005. Effects of Hypothalamic Neurodegeneration on Energy Balance. PLoS Biol. 3, e415. https://doi.org/10.1371/journal.pbio.0030415
Xu, B., Goulding, E.H., Zang, K., Cepoi, D., Cone, R.D., Jones, K.R., Tecott, L.H., Reichardt, L.F., 2003. Brain-derived neurotrophic factor regulates energy balance downstream of melanocortin-4 receptor. Nat. Neurosci. 6, 736–742. https://doi.org/10.1038/nn1073
Xu, H., Zhang, M., Zhang, H., Alpadi, K., Wang, L., Li, R., Qiao, J., 2021. Clinical Applications of Serum Anti-Müllerian Hormone Measurements in Both Males and Females: An Update. The Innovation 2, 100091. https://doi.org/10.1016/j.xinn.2021.100091

Y

Yanase, T., Fan, W., Kyoya, K., Min, L., Takayanagi, R., Kato, S., Nawata, H., 2008. Androgens and metabolic syndrome: Lessons from androgen receptor knock out (ARKO) mice. J. Steroid Biochem. Mol. Biol. 109, 254–257. https://doi.org/10.1016/j.jsbmb.2008.03.017
Yeo, G.S.H., Connie Hung, C.-C., Rochford, J., Keogh, J., Gray, J., Sivaramakrishnan, S., O'Rahilly, S., Farooqi, I.S., 2004. A de novo mutation affecting human TrkB associated with severe obesity and developmental delay. Nat. Neurosci. 7, 1187–1189. https://doi.org/10.1038/nn1336
Yu, C.-H., Si, T., Wu, W.-H., Hu, J., Du, J.-T., Zhao, Y.-F., Li, Y.-M., 2008. O-GlcNAcylation modulates the self-aggregation ability of the fourth microtubule-binding repeat of tau. Biochem. Biophys. Res. Commun. 375, 59–62. https://doi.org/10.1016/j.bbrc.2008.07.101
Yuzwa, S.A., Macauley, M.S., Heinonen, J.E., Shan, X., Dennis, R.J., He, Y., Whitworth, G.E., Stubbs, K.A., McEachern, E.J., Davies, G.J., Vocadlo, D.J., 2008. A potent mechanism-inspired O-GlcNAcase inhibitor that blocks phosphorylation of tau in vivo. Nat. Chem. Biol. 4, 483–490. https://doi.org/10.1038/nchembio.96
Yuzwa, S.A., Shan, X., Macauley, M.S., Clark, T., Skorobogatko, Y., Vosseller, K., Vocadlo, D.J., 2012. Increasing O-GlcNAc slows neurodegeneration and stabilizes tau against aggregation. Nat. Chem. Biol. 8, 393–399. https://doi.org/10.1038/nchembio.797

Z

Zempel, H., Thies, E., Mandelkow, E., Mandelkow, E.-M., 2010. A Oligomers Cause Localized Ca2+ Elevation, Missorting of Endogenous Tau into Dendrites, Tau Phosphorylation, and Destruction of Microtubules and Spines. J. Neurosci. 30, 11938–11950. https://doi.org/10.1523/JNEUROSCI.2357-10.2010

Zhan, C., Zhou, J., Feng, Q., Zhang, J. -e., Lin, S., Bao, J., Wu, P., Luo, M., 2013. Acute and Long-Term Suppression of Feeding Behavior by POMC Neurons in the Brainstem and Hypothalamus, Respectively. J. Neurosci. 33, 3624–3632. https://doi.org/10.1523/JNEUROSCI.2742-12.2013

Zhang, M., Buttigieg, J., Nurse, C.A., 2007. Neurotransmitter mechanisms mediating low-glucose signalling in cocultures and fresh tissue slices of rat carotid body: Low glucose sensing by carotid body cells. J. Physiol. 578, 735–750. https://doi.org/10.1113/jphysiol.2006.121871

Zhang, Q., Ramracheya, R., Lahmann, C., Tarasov, A., Bengtsson, M., Braha, O., Braun, M., Brereton, M., Collins, S., Galvanovskis, J., Gonzalez, A., Groschner, L.N., Rorsman, N.J.G., Salehi, A., Travers, M.E., Walker, J.N., Gloyn, A.L., Gribble, F., Johnson, P.R.V., Reimann, F., Ashcroft, F.M., Rorsman, P., 2013. Role of KATP Channels in Glucose-Regulated Glucagon Secretion and Impaired Counterregulation in Type 2 Diabetes. Cell Metab. 18, 871–882. https://doi.org/10.1016/j.cmet.2013.10.014

Zhang, R., Dhillon, H., Yin, H., Yoshimura, A., Lowell, B.B., Maratos-Flier, E., Flier, J.S., 2008. Selective Inactivation of Socs3 in SF1 Neurons Improves Glucose Homeostasis without Affecting Body Weight. Endocrinology 149, 5654–5661. https://doi.org/10.1210/en.2008-0805

Zhang, X., Tong, T., Chang, A., Ang, T.F.A., Tao, Q., Auerbach, S., Devine, S., Qiu, W.Q., Mez, J., Massaro, J., Lunetta, K.L., Au, R., Farrer, L.A., 2022. Midlife lipid and glucose levels are associated with Alzheimer's disease. Alzheimers Dement. alz.12641. https://doi.org/10.1002/alz.12641

Zhou, R., Hu, W., Dai, C.-L., Gong, C.-X., Iqbal, K., Zhu, D., Liu, F., 2020. Expression of Microtubule Associated Protein Tau in Mouse Pancreatic Islets Is Restricted to Autonomic Nerve Fibers. J. Alzheimers Dis. 75, 1339–1349. https://doi.org/10.3233/JAD-200101

Zhu, X., Hu, R., Brissova, M., Stein, R.W., Powers, A.C., Gu, G., Kaverina, I., 2015. Microtubules Negatively Regulate Insulin Secretion in Pancreatic β Cells. Dev. Cell 34, 656–668. https://doi.org/10.1016/j.devcel.2015.08.020

Ziemke, F., Mantzoros, C.S., 2010. Adiponectin in insulin resistance: lessons from translational research. Am. J. Clin. Nutr. 91, 258S-261S. https://doi.org/10.3945/ajcn.2009.28449C

Appendices

Publications 2019-2022

Benderradji, H., Kraiem, S., Courty, E., Eddarkaoui, S., Bourouh, C., Faivre, E., Rolland, L., Caron, E., Besegher, M., Oger, F., Boschetti, T., Carvalho, K., Thiroux, B., Gauvrit, T., Nicolas, E., Gomez-Murcia, V., Bogdanova, A., Bongiovanni, A., Muhr-Tailleux, A., Lancel, S., Bantubungi, K., Sergeant, N., Annicotte, J.-S., Buée, L., Vieau, D., Blum, D., Buée-Scherrer, V., 2022. ***Impaired Glucose Homeostasis in a Tau Knock-In Mouse Model***. Front. Mol. Neurosci. 15, 841892. https://doi.org/10.3389/fnmol.2022.841892

Hamza Benderradji, Anne-Laure Barbotin, Maryse Leroy-Billiard, Julie Prasivoravong, François Marcelli, Christine Decanter, Geoffroy Robin, Valérie Mitchell, Jean-Marc Rigot, Antonino Bongiovanni, Florent Sauve, Luc Buée, Claude-Alain Maurage, Maryse Cartigny, Arnauld Villers, Vincent Prevot, Sophie Catteau-Jonard, Nicolas Sergeant, Paolo Giacobini, Pascal Pigny, Clara Leroy, ***Defining Reference Ranges for Serum Anti-Müllerian Hormone on a Large Cohort of Normozoospermic Adult Men Highlights New Potential Physiological Functions of AMH on FSH Secretion and Sperm Motility***, The Journal of Clinical Endocrinology & Metabolism, Volume 107, Issue 7, July 2022, Pages 1878–1887, https://doi.org/10.1210/clinem/dgac218

Hamza Benderradji, Elise Vernotte, Gustave Soto Ares, Jean Philippe Woillez, Arnaud Jannin, , Romain Perbet, Mélodie-Anne Karnoub, Benoît Soudan, Richard Assaker, Luc Buée, Vincent Prevot, Claude-Alain Maurage, Pascal Pigny, Marie-Christine Vantyghem, Emilie Merlen, Christine Cortet , ***Efficacy of lanreotide 120 mg primary therapy on tumour shrinkage and ophthalmologic symptoms in acromegaly after 1 month*****,** Volume97, Issue1, July 2022, Pages 52-63, https://doi.org/10.1111/cen.14748

Gauvrit T, **Benderradji H,** Buée L, Blum D, Vieau D. ***Early-Life Environment Influence on Late-Onset Alzheimer's Disease.*** Front Cell Dev Biol. 2022 Feb 17;10:834661. doi: 10.3389/fcell.2022.834661.

Benderradji H, Prasivoravong J, Marcelli F, Barbotin AL, Catteau-Jonard S, Marchetti C, Guittard C, Puech P, Mitchell V, Rigot JM, Villers A, Pigny P, Leroy C. ***Contribution of serum anti-Müllerian hormone in the management of azoospermia and the prediction of testicular sperm retrieval outcomes: a study of 155 adult men.*** Basic Clin Androl. 2021 Jun 17;31(1):15. doi: 10.1186/s12610-021-00133-9. PMID: 34134632; PMCID: PMC8210365.

Hamza Benderradji, Amandine Beron, Jean-Louis Wémeau, Bruno Carnaille, Laurent Delcroix, Christine Do Cao, Clio Baillet, Damien Huglo, Georges Lion, Samuel Boury, Jean-Félix Cussac, Robert Caiazzo, François Pattou, Emmanuelle Leteurtre, Marie-Christine Vantyghem, Miriam Ladsous, ***Quantitative dual isotope 123iodine/99mTc-MIBI scintigraphy: A new approach to rule out malignancy in thyroid nodules***, Annales d'Endocrinologie, Volume 82, Issue 2, 2021, Pages 83-91, ISSN 0003-4266, https://doi.org/10.1016/j.ando.2021.03.003.

Titre : Exploration du rôle de la protéine Tau dans la régulation de l'homéostasie du glucose

Title: Uncovering the role of Tau protein in the regulation of glucose homeostasis

Mots clés : Hypothalamus, pancréas, tau, homéostasie glucidique, et modèles murins.

Keywords: Hypothalamus, pancreas, tau, glucose homeostasis, and mouse models.

Résumé :

Tau est une protéine associée au microtubule, bien caractérisée pour son rôle dans le trafic neuronal. Ses modifications (hyperphosphorylation, agrégation) sont impliquées dans la physiopathologie de la Maladie d'Alzheimer (MA). En effet, une altération de l'homéostasie glucidique est connue pour augmenter le risque de MA. Cependant, il a été rapporté que des lésions de MA pourraient favoriser l'émergence de perturbations de l'homéostasie glucidique.

Une étude du laboratoire a montré que les souris tau-knock-out (tau KO) présentaient des altérations de l'homéostasie glucidique. Inversement, la surexpression neuronale d'une protéine tau humaine mutée a été associée à une meilleure tolérance au glucose. Néanmoins, les liens entre la perte de fonction de tau et l'homéostasie du glucose restent flous.

Dans ce contexte, le premier objectif de ma thèse de science est d'évaluer le phénotype métabolique d'un modèle original de souris tau Knock-in (KI) exprimant, sous le contrôle du promoteur tau murin, une protéine tau humaine mutée. Ce modèle de souris a permis d'évaluer l'impact de l'expression d'une protéine tau dysfonctionnelle à un niveau physiologique, dans les mêmes tissus que la protéine tau native, sans biais de surexpression. Bien que les souris tau KI sous un régime contrôle ne présentent pas de troubles métaboliques significatifs, les évaluations métaboliques ont révélé qu'uniquement les animaux tau KI mâles nourris par un régime riche en graisses (HFD) présentaient une intolérance au glucose, une augmentation de la prise alimentaire, et de la masse pondérale par rapport aux témoins.

De plus, des îlots isolés de souris tau KI et tau KO présentaient une altération de la sécrétion d'insuline en réponse à une stimulation par du glucose, un effet reproduit par la réduction de l'expression de tau dans une lignée de cellules β pancréatiques à l'aide d'un tau siRNA. Sur la base de ces données, la perte de fonction de tau est associée à une altération de l'homéostasie du glucose, qui correspond au phénotype métabolique observé chez les souris tau KO. Cependant, deux mécanismes mutuellement non exclusifs pourraient expliquer les altérations métaboliques observées chez les souris tau KO et tau KI : tau pourrait contrôler la régulation périphérique du glucose via une action centrale, en particulier hypothalamique ; ou bien, elle pourrait contrôler directement la fonction de la cellule ß pancréatique.

Le deuxième objectif de mon projet thèse est donc de comprendre la base de la régulation de l'homéostasie glucidique par tau en étudiant les mécanismes centraux et périphériques. Pour atteindre cet objectif, une souris transgénique innovante tau floxée combinée avec différents modèles/virus exprimant la CRE recombinase, a été caractérisée et utilisée. La caractérisation initiale a révélé une réduction de l'expression de tau dans les souris tau flox homozygotes en l'absence de CRE. Nous avons donc utilisé des animaux tau flox hétérozygotes qui ont été combinés avec des approches CRE pour réduire l'expression de tau dans l'hypothalamus médiobasal (cKO-Tau^{hyp}) ou les cellules ß pancréatiques (cKO-Tau$^{\beta}$).

Dans ces modèles, un phénotypage métabolique complet a été réalisé sous un régime contrôle et un HFD. Sous les deux régimes, les animaux cKO-Tau^{hyp} présentaient des altérations métaboliques importantes en comparaison aux animaux témoins. La délétion conditionnelle de tau chez les cKO-Tau$^{\beta}$ n'a toutefois pas été associée à l'apparition d'altérations métaboliques significatives.

En résumé, malgré certaines limites, mon projet de thèse souligne que la perte de fonction de tau favorise le développement de perturbations de l'homéostasie glucidique et aussi l'altération du fonctionnement des cellules ß, fournissant ainsi de nouvelles informations sur le rôle physiologique de tau dans le contrôle du métabolisme périphérique en agissant dans les cellules ß pancréatiques et l'hypothalamus.